VYSOKÉ UČENÍ TECHNICKÉ V BRNĚ

Fakulta strojního inženýrství

Ústav procesního inženýrství

Zpracování odpadní biomasy pomocí termochemických procesů

Habilitační práce

Ostrava 2024

Ing. Pavel Leštinský, Ph.D.

Prohlášení

Prohlašuji na svou čest, že jsem předloženou habilitační práci vypracoval samostatně a použil jsem jen pramenů a vlastních publikací, které cituji a uvádím v seznamu použité literatury či v přílohách.

Ve Vřesině dne 28. 9. 2024 Pavel Leštinský

Souhrn

Předložená habilitační práce stručně shrnuje nejdůležitější výsledky vědecko-výzkumné činnosti uchazeče v oblasti zpracování odpadní biomasy pomocí termochemických procesů, zejména pomocí pyrolýzy. Práce se zaměřuje zejména na pyrolýzu a přípravu uhlíkatých materiálů s definovanými vlastnostmi jako je výhřevnost, porozita apod. Vzhledem k rozsahu práce byly vybrány a podrobně popsány jen klíčové procesy, mezi něž patří nízkoteplotní torefikace, konvenční a mikrovlnná pyrolýza, a vysokoteplotní karbonizace včetně aktivace. Součástí práce je také kapitola věnovaná katalytické transformaci pyrolýzních par a plynů. Samostatnou kapitolou jsou pak zařízení pro zpracování odpadní biomasy, která byla v laboratoři používána. Dosažené výsledky jsou prezentovány formou komentářů k vybraným odborným publikacím uchazeče.

Klíčová slova

Biomasa, pyrolýza, torefikace, mikrovlnná pyrolýza, karbonizace, aktivace, biouhel, katalyzátor, krakování, poloprovoz

Poděkování

Děkuji prof. Petru Stehlíkovi a Pavlu Skryjovi za příležitost pracovat v inspirativním prostředí Vysokého učení technického v Brně, plném dobrých myšlenek a přátel. Tato neocenitelná zkušenost mi pomohla růst, jak osobně, tak profesně.

Rád bych využil příležitosti a poděkoval ředitelce Institutu environmentálních technologií, prof. Lucii Obalové, že mne před 9 lety po návratu z Brna do Ostravy oslovila, dala mi důvěru, a hlavně volné ruce při budování laboratoře termochemických procesů. Děkuji Lucie, snad jsem tě nezklamal.

Děkuji také kolegyním a kolegům jak z mého týmu, tak i těm, kteří se mnou na projektech spolupracují, či u ranní kávy jen diskutují. Vytváříte na našem institutu kreativní a přátelský kolektiv a je radost být toho součástí. Děkuji také svým výborným studentům – Janě, Zdeňkovi, Denise ale i dalším, jejichž závěrečné práce jsem vedl. Musím přiznat, že při jejich vedení jsem se místy učil více od nich, než oni ode mne.

Děkuji své ženě a dětem, … za vše.

Na závěr bych slovy ostravského herce Norberta Lichého poděkoval Ostravě za to, co mi dala, ale i vzala.

Seznam zkratek

ASTM	Americká společnost pro testování a materiály
C	Označení uhlíkatého absorbentu mikrovlnného záření
Co-C	Označení uhlíkatého absorbentu mikrovlnného záření, uhlík dopovaný kobaltem
ČOV	Čistírna odpadních vod
EBC	ang. „European Biochar Certificate“
Fe-C	Označení uhlíkatého absorbentu mikrovlnného záření, uhlík dopovaný železem
FID	Plamenově ionizační detektor
GC	Plynový chromatograf/plynová chromatografie
GC-MS	Plynová chromatografie s hmotnostním spektrometrem
IBI	ang. „International Biochar Initiative“
IČ	Infračervený
LMDT	ang. „Logarithmic mean temperature difference“
MW	ang. „Microwave“
Ni-C	Označení uhlíkatého absorbentu mikrovlnného záření, uhlík dopovaný niklem
PAU	Polycyklické aromatické uhlovodíky
PCB	Polychlorované bifenyly
PFAS	Perfluorované a polyfluorované látky
S	Síra
TGA	Termogravimetrická analýza
ÚKZÚZ	Ústřední kontrolní a zkušební ústav zemědělský

Seznam symbolů

C^d	Obsah uhlíku v sušině, hmot. %
FC^d	Neprchavá hořlavina v sušině, hmot. %
H^d	Obsah vodíku v sušině, hmot. %
HHV	Výhřevnost, MJ/kg
CHSK	Chemická spotřeba kyslíku, mg/l
$i_{biomasa}$	Entalpie vstupní biomasy, J/kg
$i_{pyr.plyn}$	Entalpie pyrolýzního plynu včetně inertního plynu, J/kg
$i_{kap.kondenzát}$	Entalpie kapalného kondenzátu (bio-olej + pyrolýzní voda), J/kg

$i_{pyr.par}$	Entalpie organických par a pyrolýzních plynů, J/kg
$m_{biomasa}$	Hmotnostní tok vstupní biomasy, kg/h
$m_{biouhel}$	Hmotnostní tok vznikajícího biouhlu, kg/h
$m_{kap.kondenzát}$	Hmotnostní tok vznikajícího kapalného kondenzátu, kg/h
$m_{pyr.plyn}$	Hmotnostní tok vznikajícího pyrolýzního plynu, kg/h
N^d	Obsah dusíku v sušině, hmot. %
O^d	Obsah kyslíku v sušině, hmot. %
Q_{kond}	Teplo odebrané při kondenzaci, W
Q_{pyr}	Teplo dodané do pyrolýzního reaktoru, W
$Q_{z,pyr}$	Tepelné ztráty pyrolýzního reaktoru, W
$Q_{z,kon}$	Tepelné ztráty při kondenzaci a separaci pyrolýzního plynu od kapalného kondenzátu, W
S_{BET}	Specifický povrch dle Brunauer, Emmett a Teller, m^2/g
S_{meso}	Specifický povrch mezopórů, m^2/g
V^d	Obsah prchavé hořlaviny v sušině, hmot. %
V_{mikro}	Objem mikropórů, mm^3_{liq}/g
V_{net}	Celkový objem pórů, mm^3_{liq}/g
T	Teplota, °C

Obsah

1 Úvod

Výzkum termochemického zpracování odpadní biomasy popsaný v této habilitační práci lze shrnout do následujících bodů:

- torefikace (nízkoteplotní pyrolýza),
- pyrolýza s konvenčním ohřevem,
- pyrolýza s mikrovlnným ohřevem,
- karbonizace (vysokoteplotní pyrolýza) a aktivace,
- katalytické krakování par z pyrolýzy biomasy.

V následujícím textu bude rozepsán nejen význam odpadu, jakož to suroviny, ale také způsoby jeho termochemického zpracování. Výzkum byl zejména zaměřen na zpracovaní odpadní biomasy procesem pyrolýzy.

1.1 Zpracování odpadu

Základní pravidla pro nakládání s odpady jsou stanovena zákonem č. 541/2020 Sb., o odpadech a jeho prováděcími právními předpisy. Zákon definuje, že: „Odpadem je každá movitá věc, které se osoba zbavuje, má úmysl nebo povinnost se jí zbavit“. Můžeme tedy říct, že odpady vznikají prakticky při veškeré lidské činnosti. Vznikají v průmyslu, ve stavebnictví, v zemědělství, v dopravě i při běžném životě člověka ve společnosti. Komunální odpady jsou pak produktem všech obyvatel.

Budeme-li se bavit o komunálních odpadech, tak v podmínkách ČR v roce 2020 bylo stále 48 % tohoto odpadu skládkováno, 39 % materiálové recyklováno a pouze 12 % energeticky využito (zdroj: www.mpz.cz [1]). Od 1. ledna 2030 by se mělo recyklovat více něž 60 % komunálního odpadu a současně by se na skládku neměly ukládat odpady jejichž výhřevnost v sušině je vyšší než 6,5 MJ/kg [2]. To vytváří tlak na separaci a opětovné využití některých komodit, jakými jsou např. odpadní plasty, které lze recyklovat materiálově nebo chemicky. Poslední možností je pak energetické využití.

Kromě komunálního odpadu (který obsahuje 30 až 35 % biosložky) a odpadních plastů, je nutné se zamyslet i nad zpracováním zemědělských a potravinářských odpadů, odpadů

[1] Ministerstvo životního prostřední, Tisková zpráva – Odpadová data 2020: https://www.mzp.cz/cz/news_20211103-odpadova-data-2020-K-narustu-mnozstvi-komunalnich-odpadu-v-dobe-covidove-v-CR-nedoslo

[2] Zákon o odpadech 541/2020 Sb., aktualizovaný 1.1.2024, https://www.e-sbirka.cz/sb/2020/541?zalozka=text

z dřevozpracujícího průmyslu či kaly z čistíren odpadních vod. Všechny tyto odpady obsahují vysoký podíl uhlíku a je v nich uložena energie. To dává do budoucna příležitost termochemickým a biologickým procesům pro zpracování těchto typů odpadů.

1.2 Zpracování biomasy

Zpracování biomasy provází lidstvo od pradávna. Nejznámějším zpracováním je chemická přeměna organické hmoty pomocí oxidace, nejčastěji doprovázená světelnými efekty a tepelnými procesy, kterou hovorově nazýváme hoření. Kromě spalování a výroby tepla se dřevní biomasa transformovala i pomocí pyrolýzy na dřevěné uhlí, které pak hrálo důležitou roli v počátcích metalurgie v době bronzové a železné. Proces spalování i proces pyrolýzy řadíme mezi tzv. termochemické procesy. Kromě nich byla historicky důležitá i biologická přeměna organické části biomasy, jako např. alkoholové kvašení, které sloužilo k přeměně jednoduchých cukrů na ethanol. V dnešní době je z biologického zpracování také důležitý proces anaerobní digesce (tzv. methanové kvašení), který se uplatňuje v bioplynových stanicích při zpracování odpadní zemědělské biomasy. Chemickým zpracováním biomasy je také výroba papíru, nebo esterifikace řepkového oleje pro přípravu methylesteru řepkového oleje, tedy bionafty.

1.3 Termochemické procesy

Termochemické procesy jsou procesy, které využívají teplo pro chemickou přeměnu materiálů na produkty s vyšším užitným potenciálem a/nebo užitnou hodnotou (v podobě energie či chemických sloučenin). Při všech těchto procesech vznikají různá množství tří hlavních produktů: pevných (uhlíkatý materiál a/nebo popel), kapalných (pyrolýzní voda, bio-olej a/nebo dehet) a plynných (pyrolýzní nebo syntézní plyn, nebo spaliny). Každý proces používá různé reakční podmínky (teplota, tlak, rychlost ohřevu, doba zdržení, oxidační nebo inertní atmosféra, průtok inertního plynu atd.) k optimalizaci výroby a/nebo kvality jednoho nebo více konkrétních produktů.

Velmi obecné rozdělení těchto procesních parametrů je vypsáno níže v tab. 1. Tabulka nezahrnuje všechny podmínky, neboť ty můžou být u jednotlivých procesů specifické, přesto pro obecnou představu je postačující. Z termochemických procesů bude pro potřeby zpracování odpadní biomasy použit proces pyrolýzy.

Tab. 1 Procesní parametry jednotlivých termochemických procesů (Helsen and Bosmans, 2010)

	Pyrolýza	**Zplyňování**	**Spalování**	**Plazmové zpracování**
Teplota (°C)	200–1200	700–1500	> 300	> 1000
Tlak (MPa)	0,1	0,1–5	0,1	0,1
Atmosféra	Inertní: N_2 Mírně oxidační: spaliny	Zplyňovací médium: O_2, H_2O	Vzduch	Zplyňovací médium: O_2, H_2O Ionizovaný plyn: O_2, N_2, Ar
Hlavní produkty:				
- v plynné fázi	H_2, CO, H_2O, N_2, CO_2, uhlovodíky	H_2, CO, CO_2, CH_4, H_2O, N_2	CO_2, H_2O, O_2, N_2	H_2, CO, CO_2, CH_4, H_2O, N_2
- v kapalné fázi	Pyrolýzní voda, pyrolýzní olej	-	-	-
- v pevné fázi	Uhlíkatý materiál, popel	Škvára, popel	Popel, škvára	Škvára, popel

1.4 Pyrolýza

Pyrolýza je termický rozklad materiálu za nepřístupu vzduchu, popř. jen s nízkou koncentrací oxidující složky. Materiál je při procesu pyrolýzy ohříván nad rozkladnou teplotu. Ze vstupního materiálu, např. biomasy nám vznikají tři produkty – tuhý zbytek, tedy uhlíkatý materiál obecně označovaný jako biouhel, kapalný kondenzát složený z bio-oleje a pyrolýzní vody, a nakonec pyrolýzní plyn. Množství jednotlivých produktů lze ovlivnit rychlostí ohřevu materiálu a konečnou teplotou pyrolýzy. U inertního plynu (např. N_2) předpokládáme, že se pyrolýzy neúčastní a beze změny hmoty systémem protéká. Materiálovou bilanci pyrolýzy biomasy můžeme tedy napsat jako:

$$m_{biomasa} = m_{biouhel} + m_{kap.kondenzát} + m_{pyr.plyn} \quad (1)$$

Teplo dodané do pyrolýzního reaktoru Q_{pyr} je dáno součtem tepla potřebného na ohřev materiálu na finální pyrolýzní teplotu a tepla spotřebovaného na endotermní rozkladné reakce samotné biomasy. Výsledné teplo dodané do pyrolýzního reaktoru musí být vždy o něco vyšší, aby se kompenzovaly tepelné ztráty, jak v pyrolýzního reaktoru, tak i v následné kondenzaci a separaci pyrolýzního plynu od kapalného kondenzátu.

Z energetické bilance pyrolýzy biomasy můžeme vyjádřit množství tepla, které je nutné do procesu pyrolýzy dodat:

$$Q_{pyr} = m_{biouhel} \cdot i_{biouhel} + m_{kap.kondenzát} \cdot i_{kap.kondenzát} + m_{pyr.plyn} \cdot i_{pyr.plyn} + \\ + Q_{kond} + Q_{z,pyr} + Q_{z,kond} - m_{biomasa} \cdot i_{biomasa} - m_{N2} \cdot i_{N2} \quad (2)$$

Ačkoliv v materiálové bilanci inertní plyn zanedbáváme, do energetické bilanci jej zahrnou musíme, neboť jeho přítomnost a ohřev zvyšuje spotřebu tepla na pyrolýzu. V případě, že směs plynů a par přímo za pyrolýzním reaktorem spalujeme, lze rovnici (2) zjednodušit na tvar:

$$Q_{pyr} = m_{biouhel} \cdot i_{biouhel} + m_{pyr.par} \cdot i_{pyr.par} + Q_{z,pyr} - m_{biomasa} \cdot i_{biomasa} - \\ - m_{N2} \cdot i_{N2} \quad (3)$$

Teplo dodané do pyrolýzního reaktoru lze pak kompenzovat teplem vytvořeným spálením organických par a pyrolýzního plynu. Záleží pak už pouze na účinnosti přenosu tepla ze spalin do pyrolýzního reaktoru, kolik nakonec musíme do pyrolýzního reaktoru dodat tepla, aby pyrolýza materiálu proběhla dle požadavků na kvalitu výstupního produktu – např. biouhlu. Zjednodušené blokové schéma procesu pyrolýzy je zobrazeno na obr. 1.

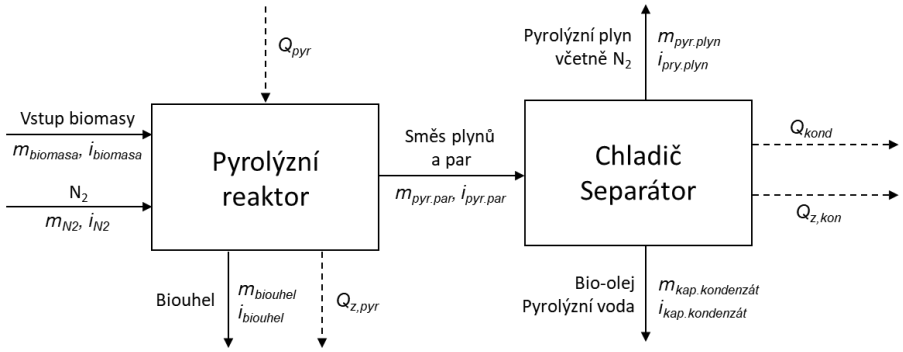

Obr. 1 Zjednodušené blokové schéma procesu pyrolýzy

1.5 Využití produktů pyrolýzy

Zpracování odpadní biomasy procesem pyrolýzy se provádí zejména za účelem získání uhlíkatého materiálu. Tyto uhlíkaté materiály mají široké uplatnění a jejich vlastnosti závisejí na zvolených podmínkách pyrolýzy, zejména teplotě. Při nižších teplotách do 340 °C lze připravovat z biomasy torefikovaný materiál (v případě pelet označovaný jako „black pellets“), které lze využít pro energetické účely, neboť se vlastnostmi velice podobají hnědému uhlí. Při vyšších teplotách okolo 400–700 °C připravujeme z biomasy tzv. biouhel, který má potenciál využití v zemědělství jako substrát, který může zvyšovat zádrž vody v půdě apod. Při teplotách

nad 800 °C již produkujeme uhlíkaté materiály s vysokým obsahem uhlíku a rozvinutou porézní strukturou, kterou navíc můžeme modifikovat různými způsoby aktivace. Tyto materiály nachází uplatnění zejména jako adsorbenty pro záchyt polutantů z ovzduší a vod a nazýváme je jako tzv. „aktivní“ či „aktivovaná uhlí“. Kromě těchto běžných aplikací se v nedávné době začaly testovat uhlíkaté materiály připravené karbonizací pro ukládání energie jako tzv. superkapacitory.

Kromě uhlíkatého materiálu vzniká během procesu pyrolýzy pyrolýzní voda a bio-olej. Na jejich získávání se zaměřuje mžiková pyrolýza. Využití těchto kapalin je však stále předmětem výzkumu a poloprovozních zkoušek, které obnáší složitou separaci látek, různé typy katalyzovaných reakcí (např. hydrodeoxygenace) a další rafinační procesy. V budoucnu by se touto problematikou měly zabývat bio-rafinerie. Pyrolýzní plyn je nejjednodušší využít energeticky, a tím část energie vrátit zpět do procesu, protože pyrolýza je silně endotermický proces. V případě, že bývá používán elektrický ohřev, je nutné se zabývat i zušlechťováním plynů a par vznikajících při pyrolýze.

Podíl jednotlivých produktů pyrolýzy je dán zejména vlastnostmi vstupního materiálu (biomasy), ale také teplotou a dobou zdržení v termické zóně pyrolýzního reaktoru. I tyto hlediska byla hodnocena v rámci výzkumu a jsou rozepsána dále v textu a v přiložených přílohách.

2 Pyrolýzní zpracování biomasy

Cílem výzkumu, který je uveden v předložené habilitační práci, bylo termochemické zpracování odpadní biomasy – zejména procesem pyrolýzy, a to za účelem získání uhlíkatého materiálu. Bylo snahou, aby vyrobený uhlíkatý materiál měl vyšší užitný potenciál (energetický nebo chemický), než původní odpadní biomasa. Získané výsledky jsou rozepsány a prezentovány v této kapitole.

2.1 Biomasa

Biomasou se obecně rozumí organický materiál pocházející z živých nebo nedávno živých organismů, který lze využít jako obnovitelný zdroj energie (Adina-Elena et al., 2013). Pro energetické či chemické účely je biomasa k dispozici v široké škále zdrojů, jako jsou dřevnaté a travnaté materiály, energetické plodiny či odpadní toky v zemědělství a potravinářství. Dřevo-vláknité materiály jsou upřednostňovány před potravinářskými plodinami, a to z několika důvodů. Materiály na bázi dřeva obsahují mnohem více energie než potravinářské plodiny. Množství hnojiv a pesticidů potřebných pro růst dřeva je také mnohem nižší a na jednotku hmotnosti je využito menší plochy půdy. Další charakteristikou biomasy je její klimaticky neutrální chování. Pokud je biomasa pěstována udržitelným způsobem, její výroba a aplikace nevytváří žádné další množství CO_2 v atmosféře. CO_2 uvolněné spálením či zpracováním biomasy je právě ten oxid uhličitý, který byl během fotosyntézy v biomase přeměněn a byl absorbován právě z atmosféry. To představuje přirozený cyklus CO_2, který je z hlediska globálního klimatu neutrální.

Biomasu lze rozdělit na tři typy:

- Dendromasa se představuje dřevní biomasu ze stromů, která zahrnuje větve, kmeny nebo další dřevnaté (ligninové) rostlinné materiály, včetně odpadů z dřevozpracujícího průmyslu (Stolarski et al., 2022).
- Fytomasou se rozumí rostlinná biomasa, vznikající v přírodě v průběhu fotosyntézy. Zahrnuje nadzemní a podzemní rostlinnou hmotu jako listy, stonky a kořeny (Nebeská et al., 2021).
- Zoomasa označuje živočišnou biomasu a zahrnuje veškerou živočišnou hmotu na planetě zemi včetně exkrementů. Jedná se také o organický podíl ve směsném komunálním odpadu nebo čistírenského kalu (Mosko et al., 2021).

Pokud chceme zpracovávat biomasu pomocí procesu pyrolýzy, je nutné mít alespoň základní povědomí o tom, jak se chovají tři základní stavební složky energeticky využívané biomasy – tedy hemicelulóza, celulóza a lignin při termickém zpracování. Nejjednodušším způsobem je využití termogravimetrické analýzy (zkráceně TGA). Termogravimetrické křivky těchto tří složek jsou zobrazeny níže na obr. 2. Z průběhu termogravimetrických křivek je zřejmé, že jako první dochází k rozkladu hemicelulózy, a to v teplotním rozmezí 200 až 350 °C. Celulóza se rozkládá v úzkém teplotním rozmezí 300 až 400 °C. Naopak lignin se rozkládá pozvolna od 240 °C až do více než 800 °C a tvoří pak hlavní část skeletu vznikajícího uhlíkatého materiálu.

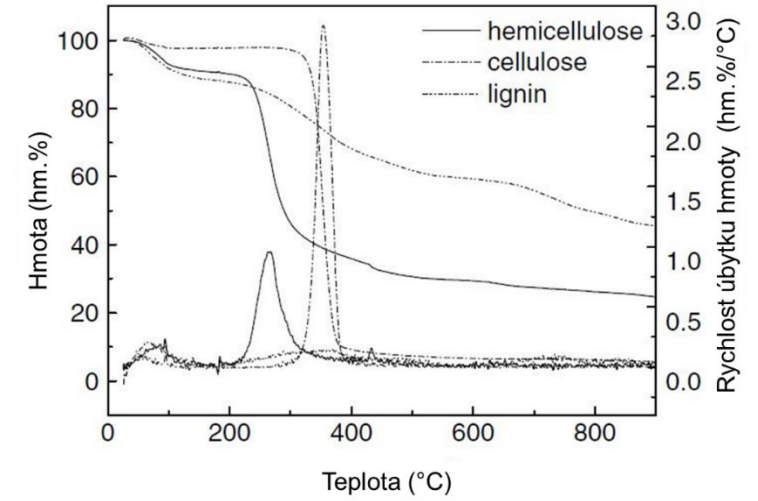

Obr. 2 Termogravimetrická analýza základních stavebních prvků biomasy (Yang et al., 2007)

2.2 Torefikace

Torefikace je řízený proces nízkoteplotní pyrolýzy, při kterém je biomasa zahřívána v rozmezí teplot 200 až 340 °C v bezkyslíkatém prostředí nebo za přítomnosti pouze malého množství kyslíku. Tento proces vede ke snížení vlhkosti biomasy a přeměně biomasy na produkt s podobnými vlastnostmi jaké má uhlí. Torefikované dřevní pelety jsou často označovány jako tzv. „black pellets“. Tuhý zbytek po torefikace příliš často neoznačujeme slovem biouhel, což je dáno nízkými teplotami zpracování biomasy, přesto se to označení nevylučuje.

Torefikovaná biomasa má oproti tradiční biomase tři hlavní výhody, kterými jsou: vyšší výhřevnost (množství energie na jednotku hmotnosti), větší energetická hustota (množství energie na jednotku objemu) a zlepšení řady fyzikálních vlastností, jako je tvarová stálost a

hydrofobní chování. To vše má za následek celkové snížení nákladů na výrobu a dopravu, snížení kapacity skladovacích prostor, menší nároky na vybavení výrobních závodů a zvýšení bezpečnosti při manipulaci ve skladovacích zařízeních. Na druhou stranu torefikací ztrácí biomasa část energie v podobě prchavé hořlaviny, která se zahřátím na teploty nad 200 °C uvolňuje. Tato nevýhoda je však bohatě kompenzována výše popsanými přednostmi.

2.2.1 Popis procesu torefikace

Celkový proces torefikace lze rozdělit na několik kroků, jako je ohřev, sušení, pyrolýza a chlazení. Průběh jednotlivých kroků lze pozorovat i na obr. 3. V první fázi do 200 °C dochází k pozvolnému ohřevu materiálu a tím dochází k odpaření vody, v tomto případě okolo 10 hm. %. Při finální teplotě 200 °C můžeme vidět, že k ustálení hmotnosti dochází během 10 nebo 20 minut. Při vyšších teplotách již začíná docházet k rozkladu zejména hemicelulózy, což se projevuje uvolňováním organických par a poklesem hmoty.

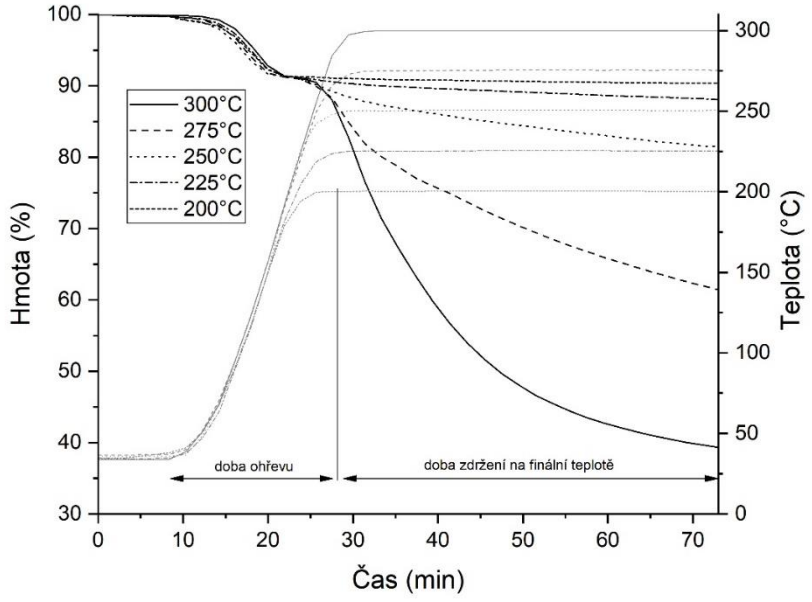

Obr. 3 Termogravimetrické křivky smrkových pilin při různých teplotách torefikace a době zdržení 45 min (šedá čára představuje teplotu) (Grycova et al., 2021)

Na obrázku vidíme, že doba zdržení 45 minut je pro ustálení hmoty nedostatečná a stále probíhají rozkladné reakce. Až při teplotě 300 °C při úbytku 60 % hmoty pozorujeme pozvolné narovnávání termogravimetrické křivky. Průběhy těchto křivek jsou velice důležité pro nastavení doby zdržení biomasy v termické zóně, viz příloha [P1].

2.2.2 Vliv teploty torefikace na kvalitu pevného uhlíkatého materiálu

Kromě torefikační teploty velikost úbytku hmoty závisí také na typu vstupní biomasy. Dřevní biomasa, která obsahuje vysokým podíl celulózy a ligninu, má vyšší teplotní stabilitu a k výraznému úbytku hmoty dochází až okolo 300 °C. Na opačné straně je zemědělská biomasa (traviny, sláma apod.), která již při 250 °C má téměř 50 % úbytek hmotnosti, což je dáno vysokým obsahem hemicelulózy. Srovnání chemického složení torefikované biomasy je možné vyčíst níže z tab. 2.

Tab. 2 Vliv teploty torefikace na složení uhlíkatého materiálu (Grycova et al., 2021)

	T (°C)	C^d (hm.%)	O^d (hm.%)	V^d (hm.%)	FC^d (hm.%)	HHV (MJ/kg)
Smrkové piliny	200	50,3	42,9	80,9	18,9	19,9
	225	50,6	42,4	79,7	19,9	20,0
	250	52,2	41,2	77,6	22,1	20,2
	275	56,2	37,9	65,0	34,5	20,7
	300	67,9	27,4	47,0	52,1	24,3
Sláma	200	46,3	41,6	75,8	19,1	17,2
	225	48,6	38,7	71,5	22,9	17,5
	250	58,0	27,6	44,6	46,8	20,7
	275	60,9	22,1	34,6	54,0	21,9
	300	65,2	17,8	31,3	56,8	23,2
Tráva Čirok	200	46,2	41,7	76,8	18,2	17,0
	225	48,9	38,1	73,2	21,3	17,9
	250	54,9	31,8	57,5	35,9	19,7
	275	61,4	23,4	44,1	46,9	22,3
	300	63,2	14,4	33,5	49,4	23,2
Rýžové slupky	200	41,7	38,1	65,7	19,9	16,5
	225	43,5	35,7	63,1	21,6	16,7
	250	45,8	29,6	51,0	29,8	16,9
	275	49,6	21,3	35,5	40,1	17,7
	300	51,6	15,9	27,6	44,1	18,6

T – teplota torefikace, C – obsah uhlíku, O – obsah kyslíku, V – prchavá hořlavina, FC – neprchavá hořlavina, HHV – výhřevnost, ^{d} – v sušině

Vyneseme-li data z elementární analýzy do Van Krevelenova diagramu zjistíme, že biomasa torefikovaná při 300 °C má již parametry jako uhlí, viz obr. 4.

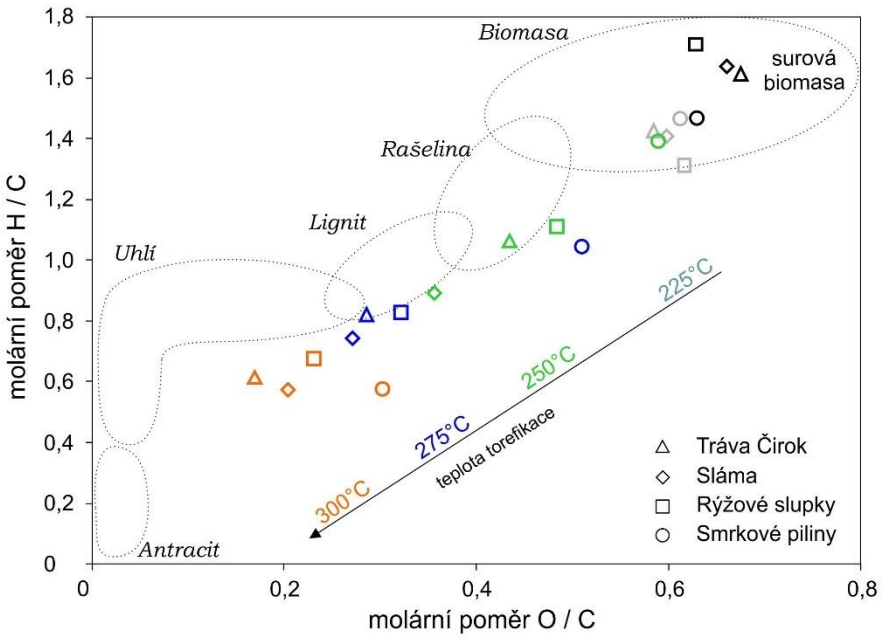

Obr. 4 Van Krevelenův diagram torefikovaných vzorků biomasy (Grycova et al., 2021)

Energetická hustota je definována jako hmotnost získaného uhlíkatého materiálu násobená jeho výhřevností a podělená původní hmotností surové biomasy. Podíváme-li se na hodnoty energetické hustoty, můžeme posoudit, při jaké teplotě se ještě vyplatí provádět torefikaci. Obdobně lze výhřevnost uhlíkatého materiálu přepočítat skrz sypnou hustotu, kdy dostaneme údaj o energii na jednotku objemu (GJ/m^3). Z výsledků torefikace smrkových pelet zobrazených na obr. 5 můžeme usuzovat, že doporučená teplota pro torefikaci je 260 °C.

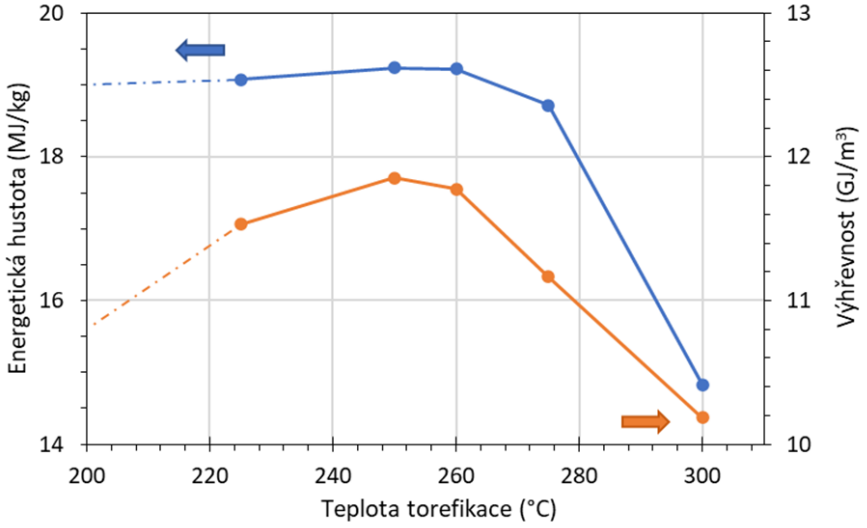

Obr. 5 Vliv teploty torefikace na energetickou hustotu a výhřevnost smrkových pelet (nepublikovaná data)

Kromě samotné torefikace pelet byly provedeny i testy se sypkým materiálem, který byl následně peletizován. Pro testy byla použita směs lignocelulózové biomasy – zahradního odpadu (ořezy z ovocných stromů a keřů, větve túji, smrkové větve včetně jehličí). Schéma experimentů je zobrazeno níže na obr. 6. Takto vyrobené pelety byly podrobeny běžným testům kvality jako je otěruvzdornost, tvrdost, index smáčivosti, objemová hustota, specifická hustota a bylo analyzováno elementární a chemické složení. Bylo zjištěno, že torefikovaná a následně peletizovaná biomasa měla vyšší obsah uhlíku a vyšší výhřevnost, než biomasa peletizovaná a následně torefikovaná. Za předpokladu stejná teploty a stejné doby zdržení probíhá přestup tepla skrz malou částici rychleji než skrz celý objem pelety. Na druhou stranu torefikované pelety vykazovaly lepší vlastnosti z hlediska tvrdosti a otěruvzdornosti. V průběhu torefikace dochází k rozkladu hemicelulózy na jednodušší cukry a k tvorbě par organických látek. Tyto látky pak procházejí skrz hmotu pelety až na její okraj, ale část v peletách zůstává a působí pravděpodobně jako pojidlo. Problematika je podrobněji rozepsána v příloze [P2].

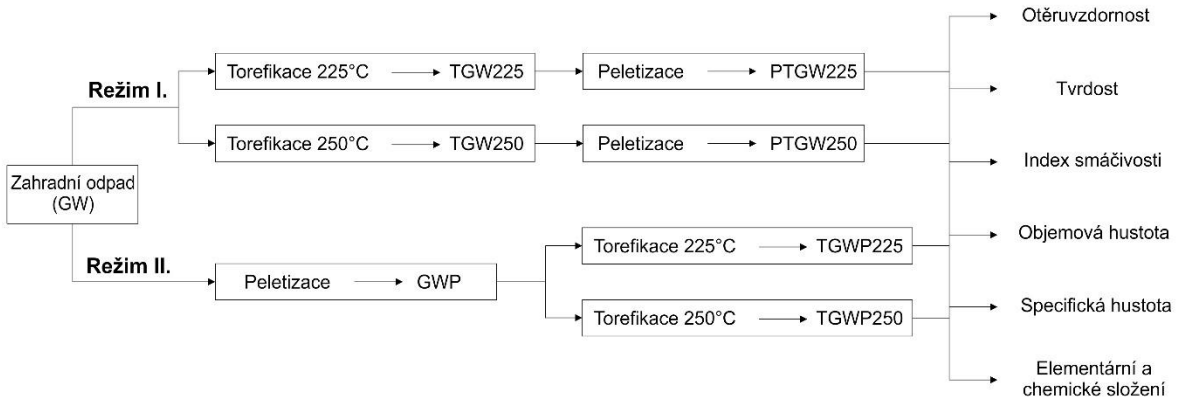

Obr. 6 Popis zpracování zahradního odpadu (Grycova et al., 2022), Zkratky: GW – Garden waste/Zahradní odpad, TGW225/250 – Torefikovaný zahradní odpad při teplotě 225 a 250 °C, PTGW – Peletizace torefikovaného zahradního odpadu, GWP – peletizovaný zahradní odpad, TGWP – Torefikace peletizovaného zahradního odpadu

2.2.3 Bilance procesu torefikace

Hlavním produktem torefikace je pevný uhlíkatý materiál. Se zvyšující se teplotou torefikace vzrůstá množství kapalného kondenzátu a mírně narůstá i množství plynu, jak můžeme vidět z bilance procesu torefikace na obr. 7. Znatelný nárůst produkce kapaliny u 300 °C souvisí se začínajícím rozkladem celulózy.

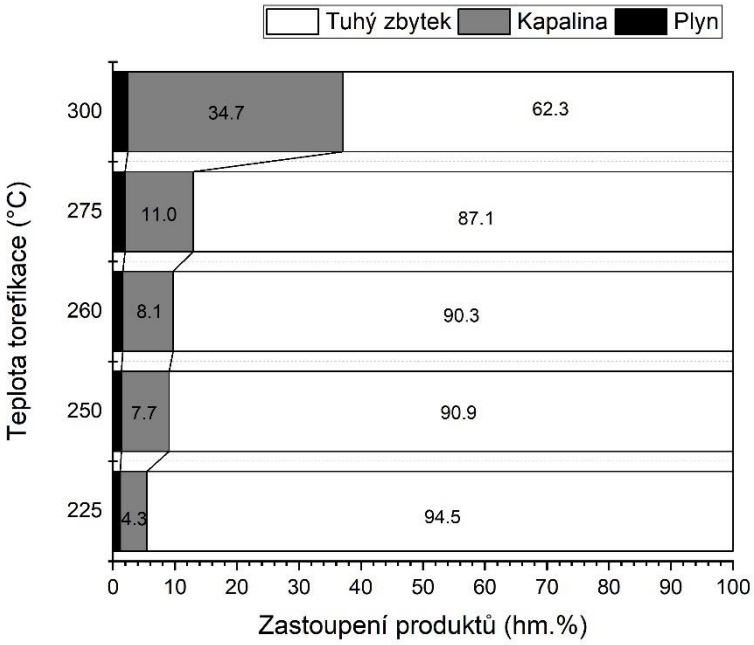

Obr. 7 Rozložení produktů torefikace smrkových pelet v závislosti na teplotě (nepublikovaná data)

2.2.4 Analýza pyrolýzní vody a plynu

Jednou z výhod torefikace je, že kapalný kondenzát obsahuje zejména pyrolýzní vodu. Kapalný kondenzát může obsahovat i olejovou fázi, ale většinou až od teplot 275–300 °C, kdy již dochází k rozkladu celulózy a také ligninu, díky čemuž vznikají ve vodě nerozpustné látky jako fenoly, kresoly apod.

Množství organických látek v pyrolýzní vodě lze vyjádřit pomocí chemické spotřeby kyslíku. S rostoucí teplotou podíl těchto organických látek ve vodě stoupá, viz tab. 3.

Tab. 3 Obsah organických látek v kapalném kondenzátu z torefikace smrkových pelet (nepublikovaná data)

	CHSK (mg/l)
Surové pelety	0
225 °C	28 785
250 °C	33 532
260 °C	51 914
275 °C	139 885
300 °C	359 762

CHSK – chemická spotřeba kyslíku

Do teploty torefikace 275–300 °C obsahuje kapalný kondenzát pouze pyrolýzní vodu a ta může být zpracována v čistírnách odpadních vod, protože hodnoty CHSK jsou na úrovni silně

znečištěných průmyslových vod. Kapalný kondenzát s olejovou fází už představuje problém. Kromě zpracování pyrolýzní vody na ČOV, je další variantou extrakce a získání důležitých chemických sloučenin jako jsou kyselina octová, furfural či hydroxymethylfurfural. Pro účely analýzy složení pyrolýzní vody pomocí plynové chromatografie s hmotnostním spektrometrem (GC-MS) byly vzorky pyrolýzních vod vytřepány s diethyletherem v poměru 1:1. Diethyether byl poté odpařen v proudu dusíku. Kapalný film s organickými látkami byl poté pro účely analýzy rozpuštěn v acetonu. Chromatografické záznamy pro pyrolýzní vody vzniklé při různých teplotách torefikace smrkových pelet jsou zobrazeny na obr. 8. Hlavními složkami, které můžeme pozorovat jsou kyselina octová (retenční čas 13 min.) a furfural (14 min.), které představují více než 30 % z celkové plochy všech píků. Ostatní sloučeniny, jejichž intenzity píků vzrůstaly s rostoucí teplotou, byly acetol (10 min.), furfurylalkohol (18 min.), 2-methoxyfenol (23 min.), kreosol (26 min.) a 5-hydroxymethylfurfural (34 min.). Tyto sloučeniny vznikají termickým rozkladem hemicelulózy a ligninu.

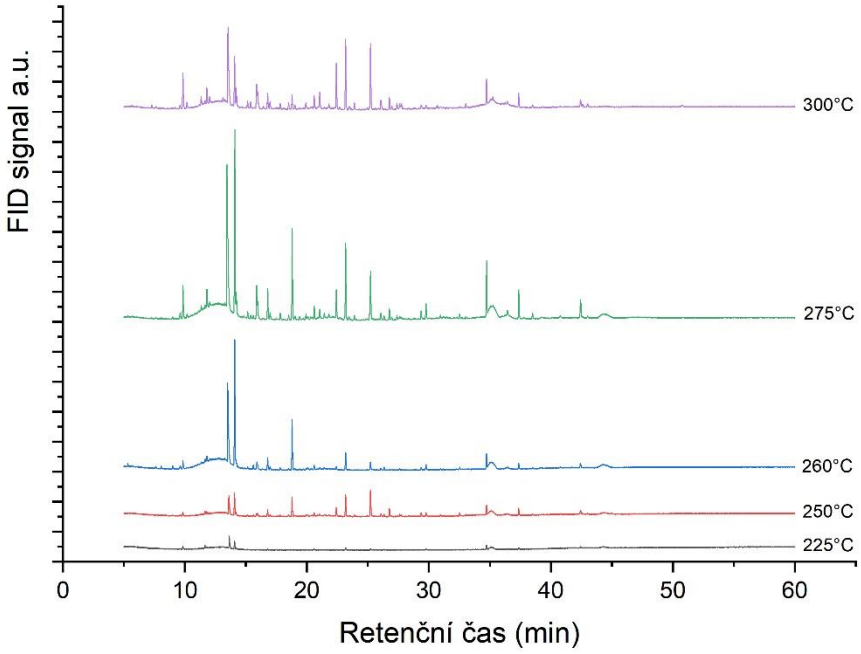

Obr. 8 Chromatogramy z analýzy vzorků pyrolýzních vod z torefikace smrkových pelet (nepublikovaná data)

U kondenzátu z torefikace smrkových pelet při 300 °C již vznikají viditelně obě fáze – pyrolýzní voda a bio-olej. Olejová fáze představuje zhruba 10 % z celkového objemu kapalného kondenzátu a obsahuje hlavně fenolické sloučeniny jako např. pyrokatechol. Tvorba olejové

fáze znamená komplikaci pro torefikační proces, protože kapalný kondenzát již není možné zpracovávat pomocí čistírny odpadních vod. Proto doporučujeme pro zpracování dřevní biomasy pomocí torefikace teplotu do 275 °C. Je nutné poznamenat, že i při teplotách 250-275 °C dochází díky rozkladu ligninu k tvorbě fenolických látek, ale jejich tvorba nevytváří samostatnou s vodou nemísitelnou vrstvu. Toto teplotní okno se v současnosti s oblibou používá pro tvorbu studeného kouře z bukových hoblin při uzení, neboť právě fenolické látky pocházející z ligninu (např. 2-methoxyfenol, tzv. Guajakol) dávají masu charakteristickou vůni.

Množství vzniklého pyrolýzního plynu se při torefikaci pohybovalo v rozmezí od 1,2 do 2,4 hmot.%. Tyto plyny obsahovaly především CO_2 a CO v poměru přibližně 2:1 (v obj.%).

2.2.5 Využití torefikace k hygienizaci čistírenského kalu

Použití čistírenských kalů na zemědělské půdě je definováno vyhláškou č. 273/2021 Sb. (Vyhláška o podrobnostech nakládání s odpady). Kaly lze aplikovat v množství nejvýše 5 t sušiny na 1 ha (v případě, že použité kaly obsahují méně než polovinu limitního množství každé ze sledovaných rizikových látek a prvků, může množství kalů dosáhnout 10 t sušiny). Před aplikací na zemědělské půdě je nutné kal upravit – podrobit biologické, chemické nebo tepelné úpravě tak, že se významně sníží obsah patogenních organismů v kalech, a tím zdravotní riziko spojené s jeho aplikací.

Čistírenský kal byl torefikován při různých teplotách – 150, 200 a 250 °C. Testy hygienizace a stability byly provedeny pomocí „Paddle“ testerů, na kterých se sleduje růst bakterií a plísní na živné půdě. Testery byly kontaminovány kalem torefikovaným při různých teplotách a poté byly vloženy do inkubátoru a několik dní se sledoval vývin jednotlivých skupin bakterií a plísní. Výsledky pozorování jsou uvedeny níže v tab. 4. Z výsledků je zřejmé, že proces torefikace již při teplotě 200 °C hygienizuje kal od koliformních bakterií a plísní, nicméně tento kal nadále podléhal hnilobným procesům, což není příliš vhodné pro skladování (nebezpečí tvorby methanu apod.). Kal torefikovaný při teplotě 250 °C lze již označit za hygienizovaný a stabilní, a takto hygienizovaný kal lze bez problému skladovat a použít např. jako půdní substrát (po splnění zákonných podmínek dle vyhlášky 273/2021 Sb.).

Tab. 4 Výsledky růstu bakterií a plísní na živné půdě kontaminované čistírenským kalem torefikovaném při různých teplotách

	Surový kal	150 °C	200 °C	250 °C
Koliformní bakterie	+	+	-	-
Aerobní bakterie celkově	+	+	+	-
Plísně a kvasinky	+	+	-	-

+ pozitivní výsledek testu, došlo k množení, - negativní výsledek testu, nedošlo k množení

Vzhledem k přítomnosti mnoha rizikových látek (PAU, PCB a PFAS), včetně mikroplastů bude aplikace kalů do půdy v budoucnu výrazně složitější, a termochemické procesy budou hrát důležitou roli při jejich utilizaci pyrolýzou či likvidaci spalováním.

2.3 Konvenční pyrolýza

Pod pojmem konvenční pyrolýza se rozumí zpracování materiálu v rozmezí teplot 340 až 700 °C při relativně pomalé rychlosti ohřevu (několik stupňů za minutu) v interní atmosféře. Doba zdržení materiálu v pyrolýzní zóně se pohybuje od desítek minut po hodiny. V tomto rozmezí teplot se již rozkládají všechny složky biomasy a vznikají nám tři produkty – pyrolýzní plyn, kapalný kondenzát složený z pyrolýzní vody a bio-oleje, a uhlíkatý materiál, který označujeme jako biouhel (anglicky „Biochars“).

Vlastnosti biouhlu vyrobeného z biomasy v pyrolýzních reaktorech lze shrnout do několika bodů (Pohořelý et al., 2019):

- Biouhel obsahuje cca 10–40 % hmotnosti sušiny původní biomasy.
- Hlavní stavební složkou biouhlu je chemicky stabilní uhlík (50–96 hm. %).
- Biouhel je porézní materiál, specifický povrch může být od 0,1 do více jak 1000 m^2/g.

Největší vliv na kvalitu biouhlu má kromě samotného typu zařízení, také teplota v pyrolýzní zóně reaktoru, rychlost ohřevu vstupního materiálu, čas zdržení v pyrolýzní zóně reaktoru a typ použité biomasy. S rostoucí teplotou pyrolýzy se snižuje výtěžek – tzn. produkce samotného biouhlu. Zvyšování teploty pyrolýzy má též silný vliv na rozklad a těkavost organických látek vzniklých procesem pyrolýzy a organických látek přítomných v biomase (Pohořelý et al., 2019).

2.3.1 Kvalita biouhlu

Kvalitu biouhlu, který se používá jako půdní aditivum, sleduje mnoho národních i nadnárodních institucí. V České republice registruje biouhel Ústřední kontrolní a zkušební ústav zemědělský (ÚKZÚZ). Dále existují organizace, od kterých může výrobce biouhlu po splnění určitých podmínek získat certifikát. Tyto certifikáty bývají náročnější na splnění, protože kontrolují více oblastí než v případě národní legislativy. Jedná se o „*European Biochar Certificate*“ (EBC) a „*International Biochar Initiative*“ (IBI). Cílem těchto iniciativ je zajistit bezpečný produkt pro životní prostředí a vytvořit jednotný soupis vlastností jako znak spolehlivosti a kvality pro spotřebitele.

Kvalita biouhlu vyrobeného pyrolýzou biomasy se dle doporučení „*IBI Biochar Standard*“[3] určuje pomocí tří kategorií testů:

- Testy kategorie A – Základní vlastnosti (anglicky „*Basic Utility Properties*“) – Tato sada testů analyzuje nejzákladnější vlastnosti potřebné k posouzení užitečnosti biouhlu pro použití v půdě (např. obsah uhlíku, dusíku, vodíku, obsah popela, pH a vodivost vodného výluhu, granulometrie atd.)
- Testy kategorie B – Hodnocení toxicity (anglicky „*Toxicant Assessment*“) – Tato sada testů posuzuje možnou toxicitu biouhlu v půdě. Toxické látky lze rozdělit do dvou kategorií:
    - na ty, které mohou být přítomny v použitých surovinách (např. těžké kovy),
    - a na ty, které mohou být při výrobě biouhlu vytvořeny procesem pyrolýzy (např. PAU – polycyklické aromatické uhlovodíky).
- Testy kategorie C – Pokročilé analýzy a zlepšení vlastností půdy (anglicky „*Advanced Analysis and Soil Enhancement Properties*“) – Tato sada testů analyzuje jak specifický povrch biouhlu, tak i obsah látek, které mohou sloužit jako živiny pro rostliny v půdě (např. vyluhovatelný fosfor, vápník, hořčík, síra ve formě síranů, dusík ve formě dusičnanů).

2.3.2 Bilance procesu pyrolýzy

Praktickým příkladem konvenční pyrolýzy byla příprava biouhlu z oddenků Miscanthu. *Miscanthus Giganteus* neboli Ozdobnice obrovská, je travina s bambusovými stonky, která dorůstá výšky 3 až 4 metrů. Je nenáročná na podmínky, proto je možné ji pěstovat i na místech,

[3] International Biochar Initiative, https://biochar-international.org/biochar-standards/

kde není zaručena vysoká bonita půdy, např. post-těžební lokality, brownfieldy apod. Kromě pěstování pro energetické účely v podobě Agro-pelet, lze ze stonků získávat i vlákna. Během zimy rostlina přesune všechny živiny do svých oddenků (rizomů) a suché stonky se v průběhu února/března sklízejí kombajnem. Na jaře pak z oddenků vyraší nová tráva. Tento cyklus lze opakovat 5-10 let, dokud nezačne klesat výtěžnost biomasy na plochu. Poté je nutné oddenky vyorat. A zde se právě nabízí zpracování oddenků pomocí pyrolýzy. Vzniklý biouhel lze pak vrátit na pole, kde se Miscanthus pěstuje a zlepšit tím tak půdní vlastnosti. Postup přípravy biouhlu (viz obr. 9) při různých teplotách (400, 500, 600 a 700 °C) při době zdržení 2 hodiny, ale i různých dobách zdržení (15 min, 1 h a 2 h) při 600 °C je rozepsán v příloze [P5].

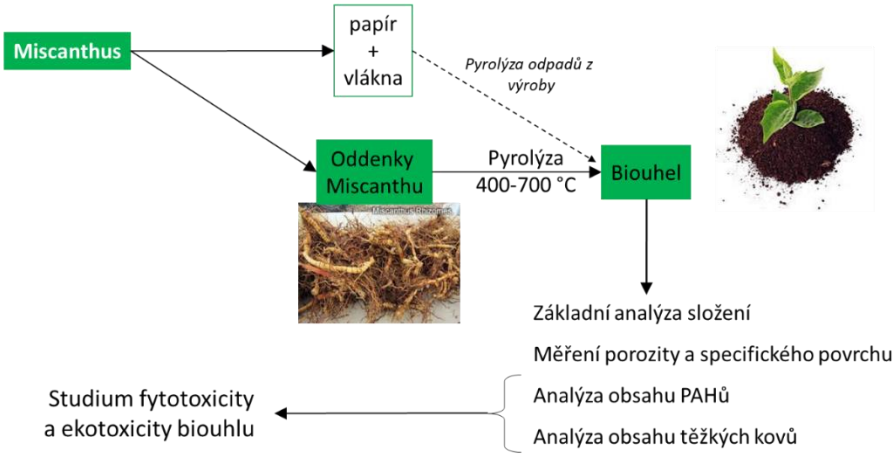

Obr. 9 Schéma postupu prací s oddenky Miscanthu

Z rozložení produktů oddenků Miscanthu pomocí konvenční pyrolýzy můžeme říci, že tyto výsledky kopírují obecné trendy, kdy s rostoucí teplotou pyrolýzy klesá množství vyrobeného biouhlu (viz obr. 10). Kromě teploty ovlivňuje výtěžek biouhlu i doba zdržení při konečné teplotě pyrolýzy. Vliv těchto podmínek na výsledné vlastnosti biouhlu je popsán v příloze [P5].

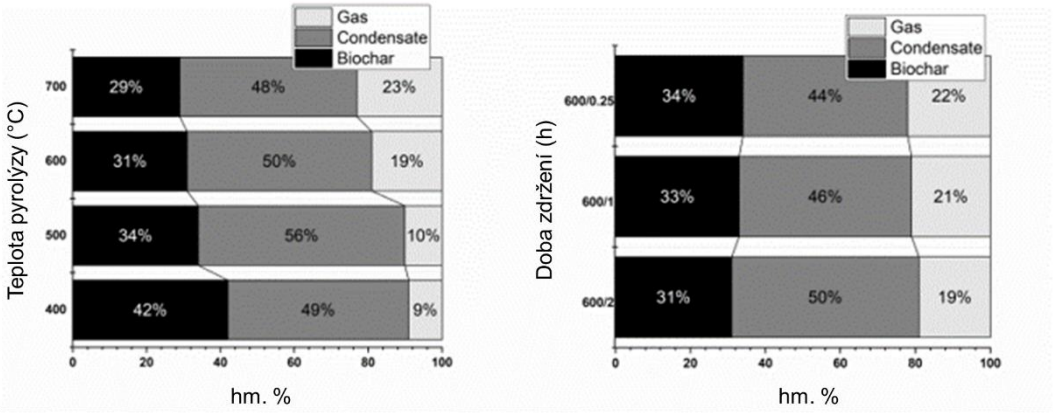

Obr. 10 Rozložení produktů pyrolýzy Miscanthu v závislosti na teplotě pyrolýzy (vlevo) a době zdržení při teplotě pyrolýze 600 °C (vpravo) (Klemencova et al., 2022)

Dle doporučení IBI byly hodnoceny i další parametry, zejména pak pórovitost biouhlu a jeho toxicita. Výsledky fyzisorpčního měření jsou uvedeny v tab. 5. Z výsledků vyplývá, že s rostoucí teplotou docházelo ke zvyšování specifického povrchu. Teplota pyrolýzy a doba zdržení měla vliv jak na specifický povrch, tak na objem mikropórů. Biouhel připravený při teplotě 700 °C měl nejvyšší specifický povrch. Při teplotách nižších než 500 °C nebo při krátké době zdržení v pyrolýzním reaktoru nevzniká téměř žádná porézní struktura.

Tab. 5 Texturní vlastnosti biouhlů připravených pyrolýzou Miscanthu (Klemencova et al., 2022)

Vzorek	S_{BET} (m^2/g)	S_{meso} (m^2/g)	V_{mikro} (mm^3_{liq}/g)	V_{net} (mm^3_{liq}/g)
Miscanthus	0,7	-	-	-
400	5	-	-	-
500	47	-	-	-
600/0,25	16	6	4	10
600/1	193	19	87	113
600/2	217	22	106	132
700	273	18	123	146

Pozn.: Vzorky jsou označeny dle podmínek pyrolýzy (teplota a dobou zdržení)

Pro stanovení obsahu polycyklických aromatických uhlovodíků (PAU) byla v laboratoři zavedena nová metoda dle literatury (Hilber et al., 2012), neboť nejnovější studie ukazují, že metoda ISO 13877:1998 používaná pro stanovení PAU v půdách a bioodpadech není vhodná pro stanovení PAU v biouhlech (uhlíkaté materiály s porézní strukturou). Obsahy PAU v biouhlech připravených při různých podmínkách jsou uvedeny v tab. 6. Dle „*European Biochar Certificate*“ (EBC) by obsah PAU v biouhlu v prémiové kvalitě neměl být

vyšší než 4 mg/kg sušiny, a u základní kvality je maximální hodnota obsahu PAU v biouhlu 12 mg/kg sušiny. Obsah těžkých kovů byl u vzorků biouhlů minimální.

Tab. 6 Výsledky stanovení obsahu polycyklických aromatických uhlovodíků (Klemencova et al., 2022)

Teplota (°C)	Obsah PAU (mg/kg sušiny)
400	6,8
500	17,4
600/0,25	5,0
600/1	5,8
600/2	5,6
700	4,1

Pozn.: Vzorky jsou označeny dle podmínek pyrolýzy (teplota a dobou zdržení)

Na základě výše uvedených dat byla pro poloprovozní výrobu biouhlu zvolena teplota 600 °C s dobou zdržení 2 hodina. Tímto způsobem bylo zpracováno více než 140 kg biomasy a vyrobeno téměř 40 kg biouhlu, který byl použit pro výzkum vlivu biouhlu na remediaci post těžebních lokalit.

Kromě těchto parametrů je vhodné kontrolovat u biouhlů i pH vodných výluhů, neboť obsah popelovin může významně ovlivnit toto pH. Právě biouhel připravený pyrolýzou oddenků Miscanthu při 600 °C má obsah popelovin okolo 13 hm.% v sušině. Vodný výluh tohoto biouhlu má pH okolo 10-11, tedy silně zásadité. Přídavek takto zásaditého biouhlu může výrazně ovlivnit výsledné pH půdy, do které bude aplikován. Další zkoumané parametry jsou uvedeny v příloze [P5].

2.3.3 Analýza pyrolýzní vody, bio-oleje a plynu

Vzhledem ke vzniku dvou fází (vodné a olejové vrstvy) kapalného kondenzátu, je nutné tyto fáze pro potřeby chromatografické analýzy odseparovat. Pro separaci se využívá extrakce do nepolárního rozpouštědla (např. dichlormethanu) a do polárního rozpouštědla (např. diethyletheru). Tyto rozpouštědla s vysokou tenzí par se pak z obou extraktů odpaří v proudu dusíku při teplotě cca 30 °C. Organické látky, které ve vialce tvoří tenký film se rozpustí v acetonu a vzorky jsou analyzovány pomocí GC-MS. Při chromatografické analýze je vhodné kvůli lepší separaci a identifikaci všech skupin látek použít dva různé typy kolon – HP5 pro nepolární látky vyextrahované dichlormethanem, a WAX pro polární látky vyextrahované diethyletherem. Majoritní složky nalezené v pyrolýzní vodě a bio-oleji jsou vypsány níže v tab. 7. Z porovnání je zřejmé, že ve vodné fázi se nacházejí zejména organické

kyseliny, ketony či alkoholy. Hlavní složky bio-oleje jsou zejména fenolické látky. Můžeme ale pozorovat, že např. furfural nebo furfurylalkohol jsou součástí obou fází.

Tab. 7 Složení kapalného kondenzátu rozděleného pomocí extrakce do dichlormethanu a diethyletheru

Sloučeniny rozpuštěné v dichlormethanu	Plocha píku (%)
Guajakol	9,3
Fenol	8,8
3-Furaldehyde	6,8
Furfural	5,9
2,3-Dihydrobenzofuran	5,7
4-Ethylfenol	4,9
Furfurylalkohol	3,9
2,6-Dimethoxyfenol	3,8
4-Ethylguajakol	3,1

Sloučeniny rozpuštěné v diethyletheru	Plocha píku (%)
Kyselina octová	28,2
1-Hydroxy-2-propanone	11,7
Furfurylalkohol	4,6
Hydrochinon	4,4
Kyselina propionová	3,8
1-Hydroxy-2-butanone	3,6
Furfural	2,7
Diacetyl	2,6
1,2-Cyclopentanedione	2,0

Bez ohledu na teplotu pyrolýzy, pyrolýzní plyn z pyrolýzy oddenků Miscanthu obsahoval zejména CO_2, asi 57-68 obj.%. Obsah CO se pohyboval mezi 23 až 31 obj.%. S rostoucí teplotou pyrolýzy rostl obsah methanu, z 2 obj.% při 400 °C až po 11 obj.% CH_4 při 700 °C. Kromě obsahu methanu roste i obsah vodíku, z 1,5 obj.% na 5 obj.%. Podrobnější výsledky včetně výhřevnosti pyrolýzního plynu jsou uvedeny v příloze [P5].

2.3.4 Modelování konvenční pyrolýzy

Zdánlivě jednoduchý proces konvenční pyrolýzy vybízí k vytvoření matematického modelu, který by predikoval množství produktů a jejich složení. Dle literatury (Fan et al., 2015) byl vytvořen výpočetní model konvenční pyrolýzy v prostředí AspenPlus®. Model vycházel z elementárního složení smrkových pilin, které byly rozloženy na jednotlivé prvky a poté bylo vypočteno rovnovážné složení plynných produktů s ohledem na danou teplotu pyrolýzy na základě minimalizace Gibbsových energií. Blokové schéma modelu je zobrazeno na obr. 11. Výsledky této simulace jsou k vidění v příloze [P8]. Složení pyrolýzního plynu, korespondovalo s reálnými experimenty.

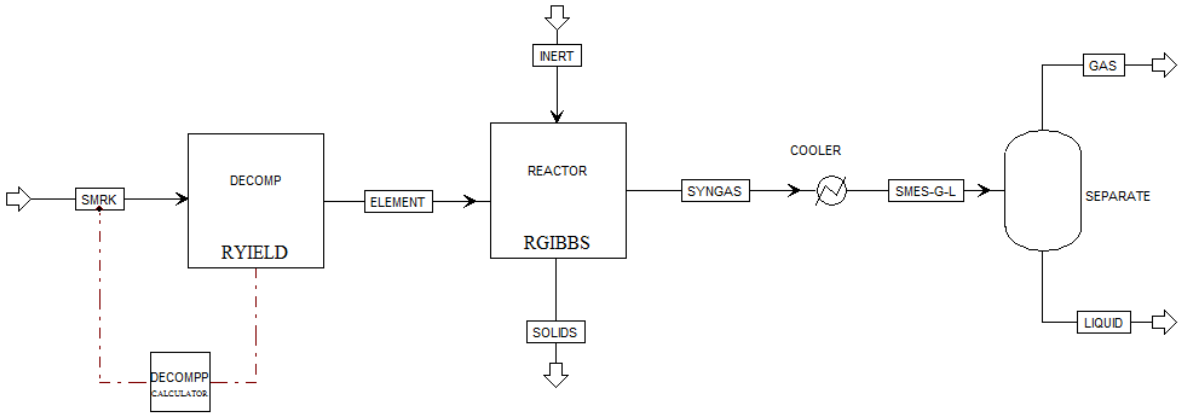

Obr. 11 Blokové schéma procesu pyrolýzy smrkových pilin modelované v AspenPlus® (Lestinsky and Palit, 2016)

Bohužel v modelu vystupuje jako kondenzát pouze voda. Aby mohl model predikovat i vznik organických látek jako jsou organické kyseliny, ketony apod., musel by obsahovat složité rozkladné reakce hemicelulózy, celulózy a ligninu na meziprodukty a další látky, které by byly podpořené kinetickými daty. Tento model je tak spíše vhodný pro modelování zplyňování biomasy než pro konvenční pyrolýzu.

2.4 Mikrovlnná pyrolýza

2.4.1 Princip mikrovlnné pyrolýzy

Komerční mikrovlnný ohřev využívá elektromagnetického záření (vlnění) k polarizaci molekul vody. Vlivem oscilací elektrického pole (při frekvenci 2,45 GHz se elektrického pole mění přibližně $2{,}45.10^9$ krát za sekundu) se rozkmitá molekula vody. Tato pohybová energie se poté přemění na tepelnou. Obecně se dá říci, že absorbovaný výkon závisí na frekvenci, permitivitě materiálu a intenzitě elektrického pole. Ovšem polarizace molekul je možná zejména u polárních kapalných látek. Experimenty ukázaly, že pokud vložíme odpadní surovou biomasu do MW reaktoru, došlo pouze k jejímu vysušení a po odparu vody již samotná hmota mikrovlnné záření příliš neabsorbovala a k pyrolýze vsázky nedošlo. Proto je nutné k biomase přidat vhodný absorbent mikrovlnného záření. Takovým absorbentem může být grafit či uhlíkatý materiál (tuhý zbytek z pyrolýzy) s vysokým obsahem uhlíku. Ve vrstvě grafitu je každý uhlík pevně vázán třemi dalšími atomy uhlíky (hybridizace sp^2), zbývající π-elektron (jeden na jeden uhlík) je delokalizovaný. To způsobuje dobrou elektrickou vodivost grafitu. Dále pak vazby uhlík-uhlík jsou velice silné a vytváří tzv. hexagonální struktury. Naproti tomu vazby mezi jednotlivými vrstvami grafitu jsou slabé, což umožňuje pohyb těchto vrstev (proto lze grafit použít jako mazivo). Elektromagnetickým zářením lze dosáhnout vibrací mezi

vrstvami a tím v kombinaci s dobrou vodivostí dosáhnout teploty více než 1000 °C během jedné minuty (Stuerga, 2006). U uhlíkatých materiálů připravených pyrolýzou biomasy může být oproti grafitu tato schopnost snížena vlivem různých funkčních skupin (např. -C=O) (Hashisho et al., 2009), přesto jsou biouhly také vhodnými absorbenty mikrovlnného záření.

Z laboratorních experimentů vyplynulo, že uhlíkatý materiál (vyrobený konvenční pyrolýzou) by měl být přidán k surové biomase v hmotnostním poměru 1:5 (Lestinsky et al., 2017). Pro účely experimentů byl používán uhlíkatý materiál připravený konvenční vsádkovou pyrolýzou a ze stejného materiálu (biomasy), který má být zpracován mikrovlnou pyrolýzou. Uhlíkatý materiál s obsahem uhlíku více jak 60 hm. % absorbuje mikrovlny stejně dobře, ne-li lépe jako voda, dokáže se během několika minut ohřát až na teploty 700-800 °C. Částice uhlíkatého materiálu rozptýleného ve vzorku biomasy předají teplo vedením a zářením biomase, která se začne pyrolyzovat. Zjednodušený princip mikrovlnné pyrolýzy je zobrazen na obr. 12. Vysoké teploty a uhlíkatý povrch navíc přispívají ke krakování par organických látek, díky čemuž se při mikrovlnné pyrolýze produkuje více pyrolýzního plynu a s vyšším obsahem vodíku než u konvenční pyrolýzy (Lestinsky et al., 2016).

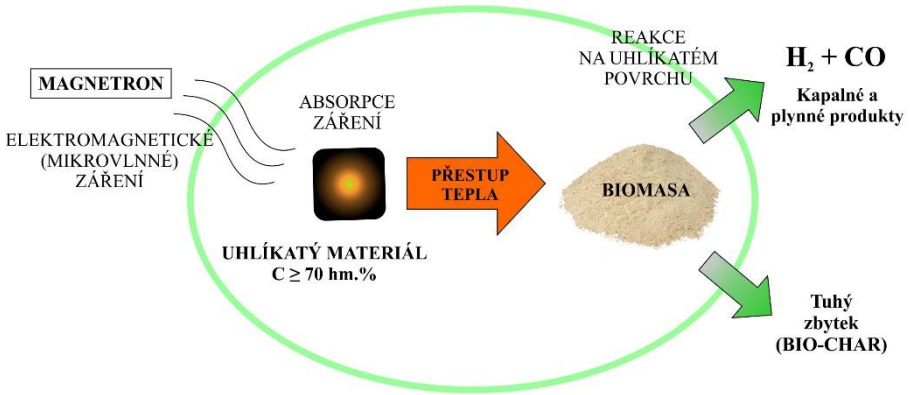

Obr. 12 Zjednodušený princip mikrovlnné pyrolýzy (Lestinsky et al., 2016)

2.4.2 Katalytická mikrovlnná pyrolýza

Uhlíkatý materiál při mikrovlnné pyrolýze neplní pouze funkci absorbentu mikrovlnného záření, ale samotný uhlík může fungovat jako katalyzátor, jak bylo zmíněno v předešlé podkapitole. Zvýšení účinnosti krakování a reformování par organických sloučenin vznikajících při mikrovlnné pyrolýze lze dosáhnout dopováním tohoto uhlíku (absorbentu MW záření) katalyticky aktivními kovy – zejména niklem, kobaltem nebo železem. V příloze [P3] je popsán postup přípravy takových absorbentů – katalyzátorů. Přídavkem absorbentu – katalyzátoru bylo při mikrovlnné pyrolýze smrkových pilin získáno téměř 2x více pyrolýzního

plynu, než při mikrovlnné pyrolýze pouze s absorbentem – uhlíkatým materiálem. Hmotnostní bilance je vypsána níže v tab. 8.

Tab. 8 Hmotnostní bilance mikrovlnné pyrolýzy smrkovým pilin s přídavkem katalyzátoru (Lestinsky et al., 2017)

Hmot.%	C	Fe-C	Co-C	Ni-C
Pyrolýzní plyn	31,21	47,74	52,72	51,59
Kapalný kondenzát	46,18	32,68	29,42	27,89
Uhlíkatý materiál	22,61	19,58	17,86	20,52

Vliv katalyticky aktivních kovů můžeme lépe vidět na složení pyrolýzního plynu, které je vypsáno níže v tab. 9. Při použití uhlíkatého materiálu dopovaného katalyticky aktivními kovy (Fe-C, Co-C, Ni-C) došlo k výraznému navýšení obsahu vodíku a oxidu uhelnatého v pyrolýzním plynu. Současně s tím došlo k poklesu oxidu uhličitého a lehkých uhlovodíků. Množství lehkých uhlovodíků včetně methanu bylo dokonce 2x nižší.

Tab. 9 Složení pyrolýzního plynu z mikrovlnné pyrolýzy smrkových pilin s přídavkem katalyzátoru (Lestinsky et al., 2017)

Obj.%	C	Fe-C	Co-C	Ni-C
H_2	28,37	40,24	43,22	41,00
CO	32,27	41,74	40,81	42,25
CO_2	21,30	9,05	9,03	9,42
CH_4	12,34	8,22	5,42	6,85
C_2H_2	0,164	0,029	0,015	0,016
C_2H_4	2,110	0,620	0,263	0,415
C_2H_6	0,700	0,377	0,267	0,342
C_3H_6	0,182	0,107	0,071	0,090
C_3H_8	0,078	0,047	0,039	0,049
H_2 + CO	60,63	82,44	83,95	83,25
$CH_4 + C_xH_y$	15,72	9,35	6,08	7,81

Tyto změny naznačují, že katalyticky aktivní kovy působí jako katalyzátory pro reakci suchého reformování:

$$CH_4 + CO_2 = 2\ H_2 + 2\ CO \quad (4)$$

$$C_xH_y + x\ CO_2 = y/2\ H_2 + 2x\ CO \quad (5)$$

Zároveň na uhlíkatém povrchu (jak na absorbentu, tak i na nově vznikajícím uhlíkatém materiálu) probíhá také Boudouardova reakce:

$$C\ (s) + CO_2 = 2\ CO \qquad (6)$$

díky čemuž je o něco nižší výtěžek tuhého zbytku po katalytické pyrolýze než u běžné MW pyrolýzy bez přídavku katalyzátoru, viz tab. 8.

Vzhledem k tomu, že uhlíkatý materiál dopovaný katalyticky aktivními kovy byl smíchán v baňce se smrkovými pilinami, takže ne všechny páry organických sloučenin se při mikrovlnné pyrolýze (rychlá generace par a vysoký průtok) dostaly do styku s katalyticky aktivním povrchem, jako tomu bývá např. v reaktoru s pevným ložem. Právě při použití reaktoru s pevným lože může být dosahováno vyšších konverzí, proto byl katalyzátor Ni-C byl podroben dalším katalytickým testům, kterým se věnuje kapitola 2.6 dále v textu.

2.5 Karbonizace a aktivace

Karbonizace, jinak též vysokoteplotní pyrolýza je zpracování materiálu při teplotách okolo 800 °C a vyšších v inertní atmosféře. Současně se využívá dlouhých dob zdržení. Při těchto teplotách již dochází k tvorbě čistě uhlíkaté sktruktury bez výrazného podílu dalších prvků – zejména H a O, ale také N a S. Zároveň se již tvoří výrazná porézní struktura. Tuhý zbytek po pyrolýze označujeme jako karbonizát.

Kromě samotné karbonizace můžeme tvorbě porézní struktury napomoci využitím aktivace. Ta může být buď fyzikální nebo chemická. Fyzikální aktivace předpokládá vysokou teplotu a proudění zplyňovacího/částečně oxidujícího média v podobě vodní páry nebo CO_2, které narušují povrch vznikajícího uhlíkatého materiálu a vytvářejí jemnou porézní strukturu. Naproti tomu chemická aktivace probíhá za přítomnosti aktivačního činidla. To obvykle přidáváme k již vytvořenému uhlíkatému materiálu pomocí pyrolýzy při teplotách 300 až 600 °C, ale předešlá pyrolýza není podmínkou. Toto činidlo má za úkol dehydratovat uhlíkatý materiál (odstranit z něj zejména kyslík a vodík). Nejběžněji se používají hydroxidy v podobě KOH nebo NaOH, dále pak uhličitany nebo chloridy (Xia et al., 2016). Literatura rozděluje aktivační činidla do tří skupin – kdy právě pro rozšíření mikroporézní struktury povrchu jsou používány hydroxid, např. KOH, pro rozšíření mezoporézní struktury povrchu můžeme použít chloridy, např. $FeCl_3$, a nakonec k vytvoření heterogenní směsi všech typů pórů se používají kyseliny, např. H_3PO_4 (Molina-Sabio and Rodríguez-Reinoso, 2004). Aktivovaný uhlíkatý materiál pak nazýváme „aktivní“ nebo „aktivované uhlí“ (anglicky „Activated Carbon“).

Chemickou aktivaci také používáme pro úpravu uhlíkatých materiálů, které nemají téměř žádnou porézní strukturu a vznikly pyrolýzou např. odpadů ze zemědělské nebo potravinářské

výroby, jak je rozepsáno v příloze [P4] a [P6]. Bylo prokázáno, že použitím chemické aktivace pomocí KOH se specifický povrch uhlíkatého materiálu připraveného ze zbytků pomleté vyextrahované kávy zvýšil z původní hodnoty v řádu jednotek až desítek m^2/g na konečných 1794 m^2/g. Vzorek byl nejdříve karbonizován při 800 °C s dobou zdržení 1 h. Poté byl smíchán s roztokem KOH v poměru 1:4, vysušen a znova karbonizován na 800 °C s dobou zdržení 1 h. Obdobným způsobem s pomocí KOH bylo připravováno aktivované uhlí ze zahradního odpadu a kukuřičné siláže. Kromě konvenčního ohřevu byl použit také mikrovlnný ohřev, tedy mikrovlnná pyrolýza. Uhlíkatý materiál bez aktivace opět vykazoval nižší specifický povrch než uhlíkatý materiál aktivovaný (Grycova et al., 2018, Grycova et al., 2017).

2.6 Katalytické zušlechťování par z pyrolýzy biomasy

Vzhledem k tomu, že biomasa obsahuje vysoký podíl kyslíku, dochází při pyrolýze nejen ke vzniku CO_2 a CO, ale také kyslíkatých organických sloučenin, které po kondenzaci vytvářejí kapalný kondenzát – pyrolýzní vodu a bio-olej. Jedná se typicky o organické kyseliny, estery, ketony a aldehydy nebo heterocyklické sloučeniny např. furfural. Tyto sloučeniny si na trhu postupně hledají své místo, přesto je snaha transformovat tyto kyslíkaté sloučeniny do podoby alifatických či aromatických uhlovodíků např. pomocí nikelnatých katalyzátorů či kyselých zeolitů (Grams et al., 2015).

Mikrovlnou pyrolýzou impregnované biomasy byl připraven nikelnatý katalyzátor na nosiči na uhlíkatém materiálu, viz postup v příloze [P3] a [P7]. Vzniklý katalyzátor obsahoval zhruba 20 hm.% niklu hlavně v kovové formě Ni^0, a částečně NiO. Přítomnost kovové formy je dána přítomností vodíku, který vzniká při MW pyrolýze biomasy, kdy se NiO redukuje na Ni^0.

Velkovu výhodou katalyzátoru připraveného z biomasy je tvar jeho částic – uhlíkatý skelet smrkových pilin, který připomíná voštinový katalyzátor (viz obr. 13). Kromě viditelné voštinové struktury má katalyzátor specifický povrch až 120 m^2/g, kdy 2/3 zaujímají mezopóry, které jsou svou velikostí pro krakování organických par velice vhodné.

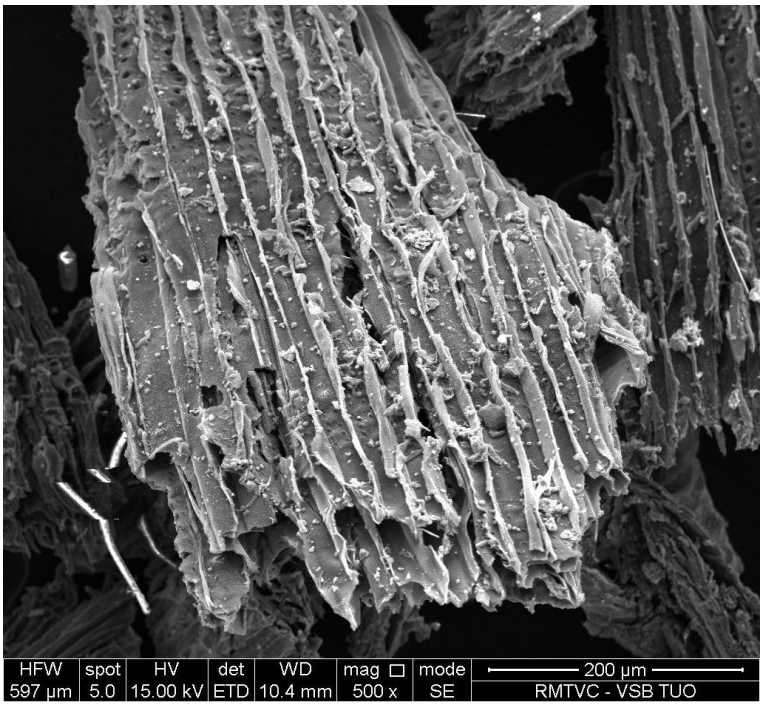

Obr. 13 Obrázek částice Ni-C katalyzátoru ze skenovacího elektronového mikroskopu (Lestinsky et al., 2020)

Zušlechťování organických par probíhalo v aparatuře zobrazené na obr. 14. Katalyzátor Ni-C byl umístěn v samostatně vyhřívaném reaktoru a byl vyhřát na 700 °C. Poté byl spuštěn ohřev vzorku biomasy na 500 °C. Páry organických látek z pyrolýzy vzorku biomasy proudily skrz katalyzátor, kde došlo ke krakování. Výsledný produkt byl analyzován na plynovém chromatografu.

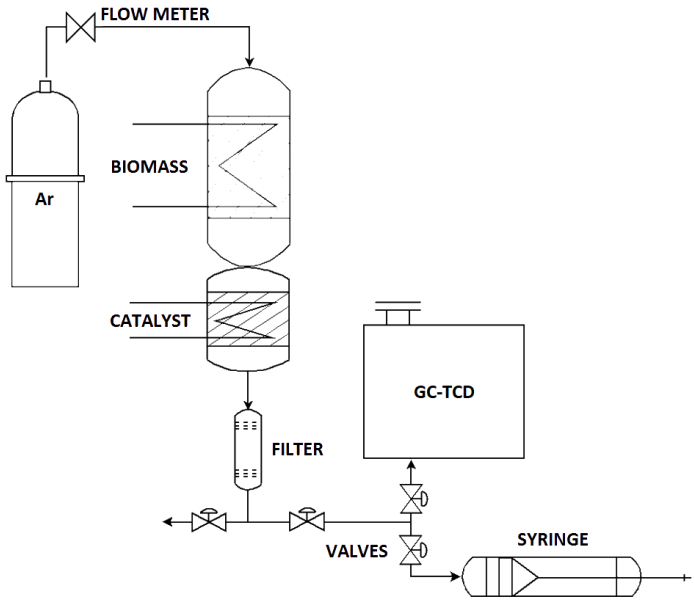

Obr. 14 Schéma testovací jednotky pro katalytické zušlechťování par z pyrolýzy biomasy (Lestinsky et al., 2020)

Porovnání výtěžnosti zejména vodíku je vypsáno níže v tab. 10. Při použití katalyzátoru Ni-C byl výtěžek vodíku 12x vyšší než z běžné pyrolýzy biomasy.

Tab. 10 Hlavní plynné produkty zušlechťování organických par z pyrolýzy biomasy (Lestinsky et al., 2020)

Biomasa/Katalyzátor	Výtěžek (mmol/g)			
	H_2	CO	CH_4	CO_2
Celulóza	1,3	1,2	0,9	6,2
Smrkové piliny	1,2	0,9	1,2	6,3
Celulóza/Ni-C	17,1	3,1	1,1	11,9
Smrkové piliny/Ni-C	14,1	2,6	1,3	10,2

Kromě krakování organických par a reakce suchého reformování probíhala při teplotě 700 °C pravděpodobně také konverze vodního plynu (tzv. „water-gas shift reaction“, rovnice (7)), kterou můžeme vysvětlit nízký obsah oxidu uhelnatého.

$$CO + H_2O = CO_2 + 2\ H \qquad (7)$$

3 Zařízení pro pyrolýzní zpracování biomasy

V této kapitole jsou uvedena a popsána zařízení od mikroměřítka v podobě TGA až po makroměřítko v podobě poloprovozní kontinuální pyrolýzní jednotky, která byla pro potřeby pyrolýzy biomasy využita. Jedná se buď o komerční zařízení, nebo běžné laboratorní aparatury, které využívají pracoviště věnující se pyrolýze. Posledním jmenovaným zařízením, které je uvedeno v podkapitole 3.3 je poloprovozní pyrolýzní jednotka. Tato jednotka byla námi navržena při řešení projektu OP PIK Aplikace III (*Technologie torrefikace pro malé a mobilní jednotky*). Z důvodu poptávky po větším množství biouhlu pro vědecké účely ze stran přírodovědně zaměřených univerzit či soukromých subjektů, byla jednotka upravena tak, aby zvládla i teplotu pyrolýzy 600 °C a bylo schopna zpracovat různé typy materiálů s rozdílnou objemovou hustotou.

3.1 Termogravimetrický analyzátor

Základní přístroj pro termické zpracování vzorků včetně biomasy je termogravimetrický analyzátor (TGA). Principem měření je vážení vzorku při termickém ohřevu vzorku ať už v inertní (N_2, Ar, He), tak i v oxidační (O_2 nebo vzduch) atmosféře. Je možné nastavit různou rychlost ohřevu materiálu, finální teplotu až do 1100 °C, různou dobu zdržení na finální teplotě a tyto kroky opakovat. Některé přístroje jsou schopny i řízeně chladit. Navážky vzorku jsou do 1 g, proto je nutné dbát na dobrou homogenizaci vzorku. Pokud TGA disponuje karuselem s více kelímky, je možné při jednom teplotním programu měřit více vzorků najednou ať už kvůli srovnání různých typů biomasy, nebo jeden typ kvůli získání průměrných hodnot a ověření homogenity vzorku.

Tím způsobem byly např. torefikovány vzorky biomasy. Po skončení torefikace a vychladnutí pece byly vzorky opět vloženy do TGA a byla spuštěna metoda dle ASTM D121, která slouží ke stanovení vlhkosti, prchavé hořlaviny, neprchavé hořlaviny a popela. V kombinaci s elementární analýzou C, H, N, S, jsme rychle získali základní představu o chování biomasy při termickém zpracování procesem torefikace, a nahradili tak zdlouhavé laboratorní vsázkové pyrolýzní experimenty, viz příloha [P1].

3.2 Vsádkový pyrolýzní reaktor

Nevýhodou TGA měření je fakt, že získáme jen údaj o zůstatkové hmotě tuhého zbytku uhlíkatého materiálu při dané teplotě a rychlost úbytku hmoty při ohřevu, ale nevíme, kolik

plynu či kapaliny při termickém rozkladu vzniklo. Pro tyto účely je nutné zvětšit měřítko, a používat vsádkové pyrolýzní reaktory, kde se navážka vzorku biomasy pohybuje řádově v desítkách až stovkách gramů.

3.2.1 Vsádkový pyrolýzní reaktor s konvenčním ohřevem

Vsádkový pyrolýzní reaktor slouží pro určení hmotnostní bilance procesu pyrolýzy při daných podmínkách (rychlost ohřevu, konečná teplota pyrolýzy, doba zdržení na konečné teplotě). Slovo konvenční znamená, že teplo přestupuje z otopného tělesa (většinou otopné spirály elektrické pece) skrz stěnu pyrolýzního reaktoru do ohřívaného materiálu. Typické schéma zapojení laboratorní vsázkové pyrolýzní aparatury je zobrazeno níže na obr. 15. Elektrické pece jsou velice dobře programovatelné z hlediska podmínek pyrolýzy. Před experimenty se vzorek biomasy propláchnut proudem dusíku. Za pyrolýzním reaktorem (nerezová retorta nebo skleněná baňka) následuje chladič a nádoba na kondenzát. Část organických par je nasycena v pyrolýzním plynu a tento aerosol obtížně kondenzuje. Proto je nutné pro vyčištění pyrolýzního plynu před vstupem do plynoměru použít promývačky s acetonem a vodou. Vyčištěný plyn je jímán do Tedlarových vaků a je analyzován na plynovém chromatografu. Pro kontrolu teploty pyrolýzy je vhodné do reaktoru poblíž vzorku zasunout další termočlánek. Podrobnější experimenty v této aparatuře jsou popsány v přílohách [P4] a [P5].

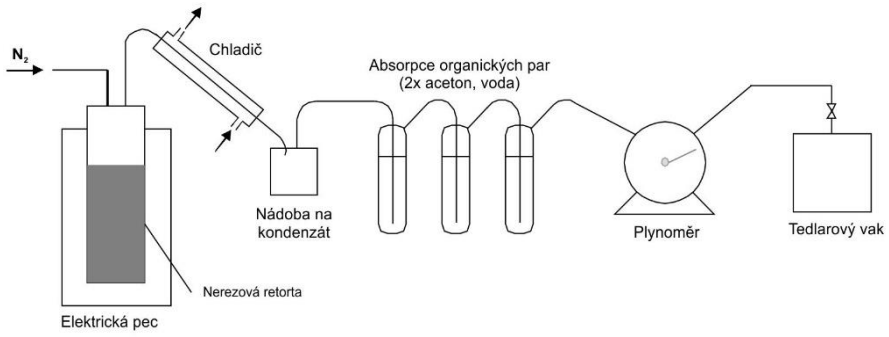

Obr. 15 Schéma aparatury vsádkového pyrolýzního reaktoru s konvenčním ohřevem (Grycova et al., 2017)

3.2.2 Vsádkový pyrolýzní reaktor s mikrovlnným ohřevem

Aparatura s mikrovlnným ohřevem (viz obr. 16) je obdobou aparatury vsádkové pyrolýzy s konvenčním ohřevem. Rozdíl je pouze ve způsobu ohřevu, kdy u mikrovlnného ohřevu je nutné využít vhodný absorbent mikrovlnného (elektromagnetického) záření, který se rychle ohřeje a který poté předá teplo vzorku biomasy ve svém okolí. Díky vysokým teplotám a

lokálním hot-spotům je vhodné používat křemenné sklo. Pro experimenty byla použita běžná domácí mikrovlnná trouba, do jejíž vrchní části byl vyvrtán otvor o průměru 3 cm, a do kterého byla vložena kovová trubka, která byla uzemněna ke kavitě (vnitřní prostor MW trouby), aby kov neabsorboval MW záření a nevytvářel se elektrický oblouk. Délka kovové trubky by měla být alespoň 13 cm, aby nedošlo k úniku mikrovlnného záření ven ze zařízení, protože domácí MW trouby pracují s elektromagnetickým zářením o frekvenci 2,45 GHz a jejich vlnová délka je přibližně 12,2 cm. Do trubky se umisťovala skleněná trubice s normalizovanými zábrusy na obou koncích tak, aby na ni bylo možné napojovat běžné laboratorní či křemenné sklo se zábrusem. Pro měření teploty vzorku odpadní biomasy během mikrovlnné pyrolýzy bylo nutné ke kavitě uzemnit i termočlánek typu K. Během mikrovlnné pyrolýzy dosahuje teplota vzorku odpadní biomasy 700 až 800 °C. Při experimentech bylo zjištěno, že pro rovnoměrnou pyrolýzu v celém objemu vsádky je vhodné připravovat homogenní směs, kdy distribuce velikosti částic biomasy a uhlíkatého materiálu (absorbentu záření) jsou řádově podobné. Vzhledem k velmi rychlému ohřevu bývá při mikrovlnné pyrolýzy produkováno více permanentních plynů, které s sebou nesou páry organických látek. Díky tomu je funkce primárního chladiče-kondenzátoru při vysoké rychlosti proudění velice omezená. Z toho důvodu je nutné v laboratoři využít alespoň 5 promývaček k záchytu všech par, tak aby v Tedlarovém vaku byly jen permanentní plyny a lehké uhlovodíky, které lze poté analyzovat na plynovém chromatografu. Podrobnější experimenty v této aparatuře jsou popsány v přílohách [P3], [P4], [P6] a [P7].

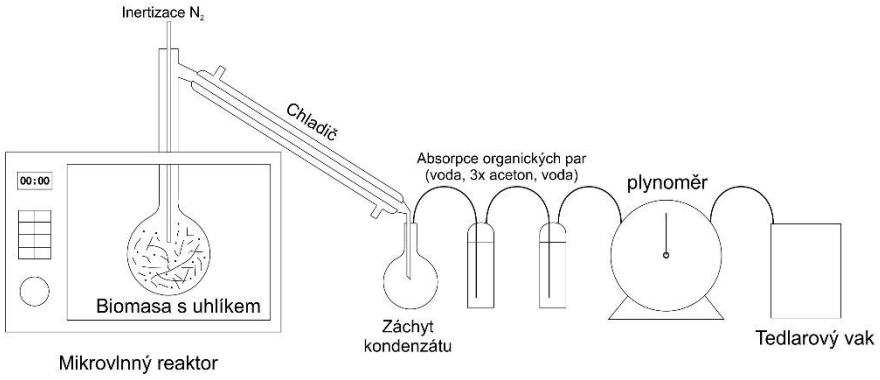

Obr. 16 Schéma aparatury vsádkového pyrolýzního reaktoru s mikrovlnným ohřevem (Lestinsky et al., 2016)

3.3 Poloprovozní kontinuální pyrolýzní jednotka

Poloprovozní kontinuální pyrolýzní jednotka je zařízení, které se skládá z několika součástí: z násypky se šnekovým podavačem pro sypké materiály a/nebo šnekovým podavačem na pelety a zásobníkem na pelety, z pyrolýzního reaktoru se šnekovým dopravníkem, z

rozdělovače, výsypky a kondenzátoru. Násypka dávkuje do pece sypký materiál a je vybavena šnekovým podavačem. Násypka pojme na jedno naplněné až 20 kg materiálu, který lze postupně doplňovat skrz plnicí otvor ve víku. Podavač disponuje pojistkou proti ucpání. Násypku s podavačem na sypké materiály lze odmontovat a nahradit šnekovým podavačem na pelety včetně zásobníku na zhruba 80 kg pelet. Z podavače je materiál dávkován do pyrolýzního reaktoru. Pyrolýzní reaktor má vnitřní průměr 200 mm, délku 1500 mm a je vytápěn elektricky. Uvnitř reaktoru je šnekový dopravník, který posunuje materiál od místa, kde je materiál dávkován podavačem na pelety nebo na sypký materiál až po konec reaktoru, za nímž je umístěn rozdělovač. V rozdělovači dochází k oddělení vyrobeného uhlíkatého materiálu, který padá do výsypky a pyrolýzní plyn spolu s vodní párou a parami organických látek odchází vrchním otvorem do kondenzátoru. Výsypka slouží k uložení a vychladnutí výsledného uhlíkatého materiálu, je odnímatelná a je napojena na přívod inertního plynu, aby se zabránilo zahoření žhavého uhlíkatého materiálu. Objem výsypky je 30 dm^3. Konstrukční část poloprovozní jednotky včetně motoru, převodovky byla vyrobena firmou SMS CZ s.r.o. na základě našich požadavků a doporučených rozměrů. Poloprovozní jednotka je dále osazena několika termočlánky pro měření teploty a barometry pro měření relativního tlaku, jak je zobrazeno na obr. 17. Data z termočlánků jsou snímány pomocí měřícího modulu Papouch 2TC doplněným o Wi-Fi vysílač. Teploty pak lze zobrazovat na jakémkoliv zařízení, které se na Wi-Fi připojí a obsahuje free software Wix firmy Papouch pro zobrazování dat. Poloprovozní jednotka byla navržena jako mobilní, hlavní část jednotky – pyrolýzní pec je umístěna na kolečkách, neboť se předpokládá její využití i mimo prostory laboratoře.

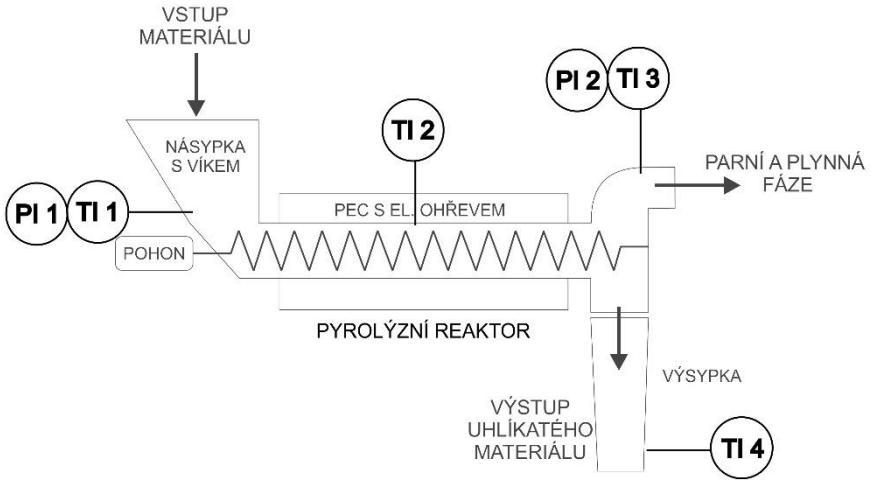

Obr. 17 Umístění měřených veličin na pilotní jednotce

K této pyrolýzní peci byl navržen kondenzátor v podobě výměníku trubka v trubce (tzv. „shell-and-tube“) s teplosměnnou plochou 2 m^2, kde jsou páry odcházející z rozdělovače chlazeny studenou chladící vodou. Délka trubek kondenzátoru je cca 1000 mm, průtok chladící vody (o teplotě 12 °C) je v rozmezí 5-10 dm^3/minutu. Návrh výměníku byl proveden pomocí střední logaritmické teplotní diference (metoda LMDT).

Za kondenzátorem následuje skrubr (pračka plynů), kde dochází k rozstřiku cirkulující vody a záchytu aerosolu (kapiček organických par v plynu). Plyny jsou pak odsávány ventilátorem, případně mohou být spalovány na fléře. Za skrubrem se také nachází odběrné místo pro pyrolýzní plyn, který je buď analyzován pomocí IČ analyzátoru CO_2 a elektrochemicky O_2, díky kterému je možné včas rozpoznat přisávání kyslíku netěsnostmi do poloprovozní jednotky. Pyrolýzní plyn může být také odebírán do Tedlarových vaků a analyzován pomocí plynové chromatografie.

Schematicky je poloprovozní jednotka znázorněna níže na obr. 18. Podrobnější experimenty v této aparatuře jsou popsány v příloze [P2].

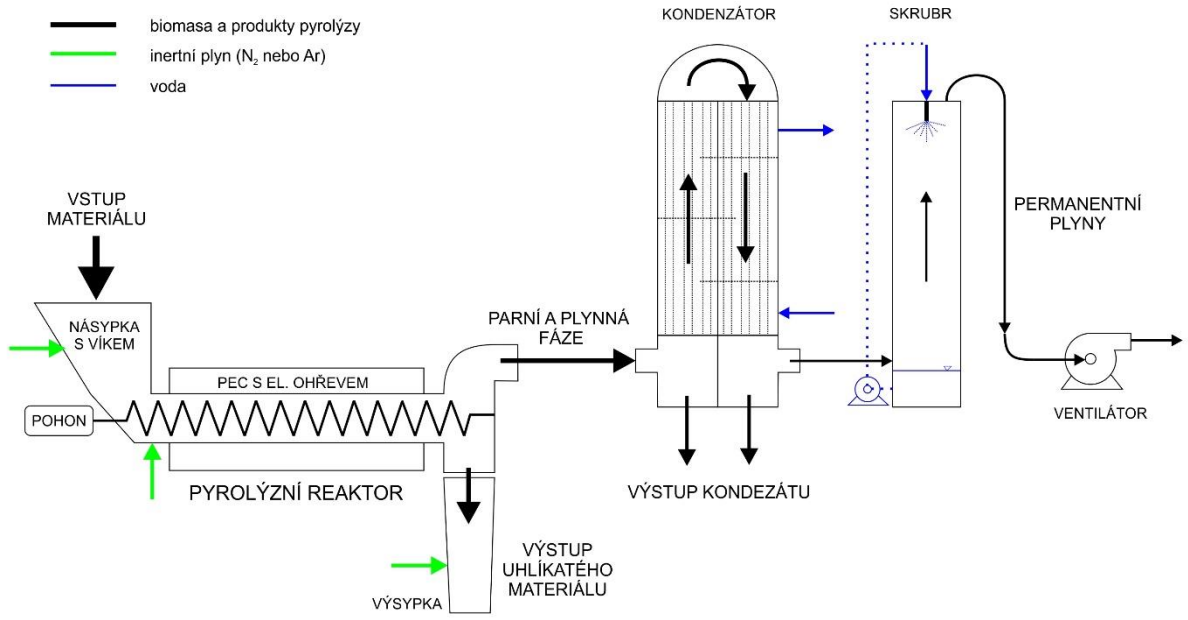

Obr. 18 Schéma poloprovozní kontinuální pyrolýzní jednotky (Grycova et al., 2022)

Jak již bylo zmíněno, zpracovatelská kapacita jednotky úzce souvisí s nastavením šnekového podavače a šnekového dopravníku v pyrolýzním reaktoru. Podavač je spínán pomocí multifunkčního časového relé (nastavení doby chodu a doby prodlevy, cyklovač), jehož pomocí lze dávkování materiálu regulovat od 0,1 do 5 kg/h. Dále se pomocí časového relé

nastavuje také šnekový dopravník uvnitř pyrolýzního reaktoru tak, aby bylo dosaženo požadované doby zdržení biomasy uvnitř pyrolýzního reaktoru (od 10 do 120 minut v závislosti na typu odpadní biomasy). Sladěním obou časovačů se docílí optimální doby zdržení a zároveň dostatečného zaplnění pyrolýzního reaktoru. Toto nastavení je individuálně a závisí na granulometrii materiálu. Nastavení časových relé se provádí na základě zkušeností obsluhy a hmotnostní průtok se ověřuje testem za studena před spuštěním ohřevu pyrolýzního reaktoru. Fotografie jednotky jsou k náhledu na obr. 19.

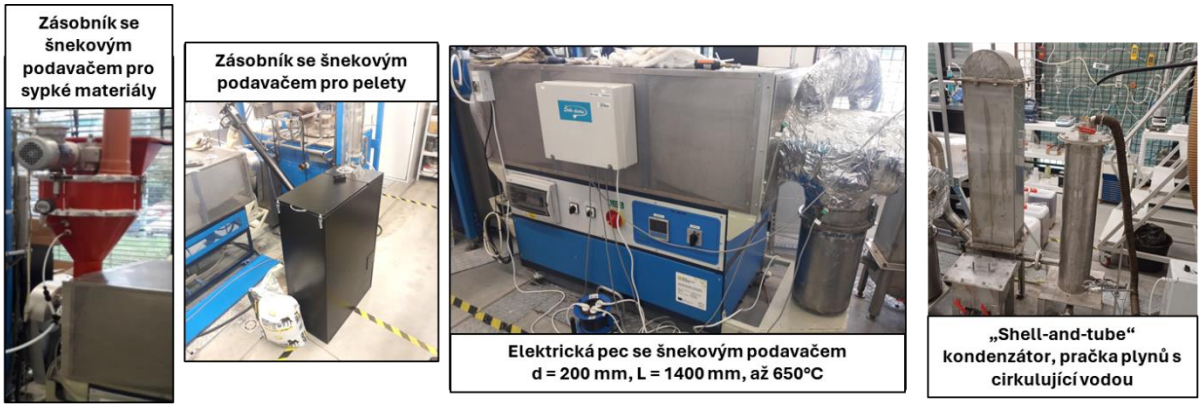

Obr. 19 Fotografie poloprovozní kontinuální pyrolýzní jednotky

4 Závěr

Termochemické procesy, zvláště pak pyrolýza je důležitým procesem v oblasti zpracování odpadní biomasy a výroby uhlíkatých materiálů, které lidstvo provázejí již od doby bronzové. Díky stále se zvyšujícímu tlaku na snižování používání fosilních paliv, a posilující roli obnovitelných zdrojů energie bude i v budoucnu proces pyrolýzy hrát důležitou roli.

Předložená habilitační práce ukazuje výsledky výzkumu z oblasti termochemického zpracování odpadní biomasy procesem pyrolýzy. V rámci výzkumné problematiky pyrolýzy a přípravy uhlíkatých materiálů bylo již publikováno 8 článků; z toho 3 jsou v nejvyšším kvartilu Q1 a 3 jsou v kvartilu Q2. Všechny tyto články jsou uvedeny v příloze. Další články jsou nyní v recenzním řízení.

Výzkum v oblasti nízkoteplotní pyrolýzy, tzv. torefikace prokázal, že upravená biomasa má lepší energetické parametry než surová biomasa. Nepopiratelným přínosem je zejména hydrofobita torefikované biomasy, protože se tím výrazně zlepšují možnosti dlouhodobého skladování bez rizika navlhnutí a rozpadu pelet. Je ovšem důležité u každého materiálu experimentálně ověřit energetickou hustotu, která do sebe promítá úbytek hmoty, ke kterému při torefikaci dochází. Prvotní testy ukázaly, že pro torefikaci je vhodnější používat biomasu v podobě pelet než peletizovat torefikovaný materiál. Tato oblast si však i do budoucna zaslouží pozornost, neboť při naši práci nebyly použity žádná pojiva, které se při výrobě pelet s nízkým obsahem ligninu (tedy z nedřevní biomasy) musí používat, aby byly dodrženy kvalitativní vlastnosti pelet. Vhodné bude také podrobit torefikované pelety i palivovým zkouškám, zejména jak tato úprava ovlivňuje emisní parametry při spalování.

Naproti tomu konvenční pyrolýza se již pomalu dostává do průmyslových aplikací. Aplikačně zajímavý je zejména tuhý zbytek po pyrolýze, tzv. biouhel, který může být využit jako půdní aditivum, které může zvyšovat bonitu půdy. Zbylé produkty pyrolýzy mohou být spáleny a produkovaná energie využita pro otápění pyrolýzního reaktoru. První takovou aplikací na území ČR je čistírna odpadních vod Bohuslavice – Trutnov, kde se pyrolyzuje čistírenský kal a produkovaný biouhel se prodává jak certifikované půdní aditivum. Výzkum v oblasti však nadále pokračuje zejména se zaměřením na přípravu biouhlu se specifickými vlastnosti, neboť se ukazuje, že pro některé látky, jakou jsou residua léčiv a pesticidů ve vodách můžou hrát funkční skupiny na povrchu biouhlu důležitou roli při jejich sorpci. Použití mikrovlnné pyrolýzy přináší benefit zejména v rychlosti ohřevu. Již nyní jsou na trhu průmyslové magnetrony s regulovaným výkonem dle teploty v prostoru kavity. V naší

laboratoři tak dokončujeme větší měřítko MW pyrolýzního reaktoru, které bude využívat skupina zaměřující se na fyzikálně-chemické vlastnosti biouhlů zejména pro aplikace v oblasti sorpce výše zmíněných residuí.

Karbonizace (vysokoteplotní pyrolýza) a aktivace odpadní biomasy je jedním z nejrozšířenějších pyrolýzních procesů v průmyslovém měřítku, protože se používá pro výrobu aktivovaného uhlí, a to jak pro medicínské použití, tak i pro přípravu adsorbentů pro záchyt polutantů z ovzduší, při čištění spalin na spalovnách odpadů (záchyt rtuti a dioxinů), nebo při čištění pitné vody od residuí pesticidů a léčiv[4]. Pestrost odpadní biomasy je velká, a tak je zde stále potenciál pro hledání vhodných materiálů a aktivačních činidel pro tvorbu nových sorpčních materiálů.

Výzkum katalytického zušlechťování par vznikajících při pyrolýze přinesl mnoho užitečných poznatků v oblasti krakování a suchého reformování, které jsou dále rozvíjeny např. při krakování dehtových látek při čistění syntézního plynu ze zplyňování biomasy. Tyto znalosti byly přeneseny na další výzkumná témata týkající se např. zpracování odpadních plastů, suché reformování pyrolýzních par a plynů. Výzkum v této oblasti dále pokračuje i ve spolupráci se zahraničními pracovišti.

Nedílnou součástí výzkumných aktivit a prací s odpadní biomasou jsou laboratorní přístroje a experimentální aparatury. Soustavným výzkumem jsme se od mikroměřítka dostali až do poloprovozního měřítka. Přesto právě menší aparatury hrají důležitou roli v přípravě na poloprovozní testy. Dokážeme na nich ověřit chování biomasy při různých teplotních podmínkách a získat hmotnostní bilanci. Znalost hmotnostní bilance pyrolýzy je základní předpoklad pro bezpečný provoz poloprovozní jednotky. Důležitá je i zpětná vazba, kdy produkt pyrolýz – uhlíkatý zbytek je analyzován a srovnán se stejným uhlíkatým materiálem vyrobeným vsádkovou pyrolýzou. Poloprovozní pyrolýzní jednotka je v současnosti zařazena do Velký výzkumné infrastruktury ENREGAT, kde ji využívají pro produkci biouhlu či torefikovaných pelet jak lidé z akademické, tak i komerční sféry.

[4] Pražské vodovody a kanalizace, Úpravna vody Želivka, https://cistavoda.pvk.cz/upravna-vody-zelivka/uprava-vody/

5 Literatura

ADINA-ELENA, S., FLORENTINA, C., PAULINA, V., PAULA, S., IOAN, G. & VASILE DANIEL, G. 2013. Biomass Extraction Methods. *In:* MIODRAG DARKO, M. (ed.) *Biomass Now*. Rijeka: IntechOpen.

FAN, Y., YI, Q., LI, F., YI, L. & LI, W. 2015. Tech-economic assessment of a coproduction system integrated with lignite pyrolysis and Fischer–Tropsch synthesis to produce liquid fuels and electricity. *Fuel Processing Technology,* 135**,** 180-186.

GRAMS, J., NIEWIADOMSKI, M., RUPPERT, A. M. & KWAPINSKI, W. 2015. Influence of Ni catalyst support on the product distribution of cellulose fast pyrolysis vapors upgrading. *Journal of Analytical and Applied Pyrolysis,* 113**,** 557-563.

GRYCOVA, B., KLEMENCOVA, K., JEZERSKA, L., ZIDEK, M. & LESTINSKY, P. 2022. Effect of torrefaction on pellet quality parameters. *Biomass Conversion and Biorefinery*.

GRYCOVA, B., PRYSZCZ, A., KRZACK, S., KLINGER, M. & LESTINSKY, P. 2021. Torrefaction of biomass pellets using the thermogravimetric analyser. *Biomass Conversion and Biorefinery,* 11**,** 2837-2842.

GRYCOVA, B., PRYSZCZ, A., LESTINSKY, P. & CHAMRADOVA, K. 2017. Preparation and characterization of sorbents from food waste. *Green Processing and Synthesis,* 6**,** 287-293.

GRYCOVA, B., PRYSZCZ, A., LESTINSKY, P. & CHAMRADOVA, K. 2018. Influence of potassium hydroxide and method of carbonization treatment in garden and corn waste microwave pyrolysis. *Biomass & Bioenergy,* 118**,** 40-45.

HASHISHO, Z., ROOD, M. J., BAROT, S. & BERNHARD, J. 2009. Role of functional groups on the microwave attenuation and electric resistivity of activated carbon fiber cloth. *Carbon,* 47**,** 1814-1823.

HELSEN, L. & BOSMANS, A. 2010. Waste-to-Energy through thermochemical processes: matching waste with process.

HILBER, I., BLUM, F., LEIFELD, J., SCHMIDT, H. P. & BUCHELI, T. D. 2012. Quantitative Determination of PAHs in Biochar: A Prerequisite To Ensure Its Quality and Safe Application. *Journal of Agricultural and Food Chemistry,* 60**,** 3042-3050.

KLEMENCOVA, K., GRYCOVA, B. & LESTINSKY, P. 2022. Influence of Miscanthus Rhizome Pyrolysis Operating Conditions on Products Properties. *Sustainability,* 14.

LESTINSKY, P., GRYCOVA, B., KOUTNIK, I. & PRYSZCZ, A. 2016. Microwave Pyrolysis of the Spruce Sawdust for Producing High Quality Syngas. 19th International Conference on Process Integration, Modeling and Optimization for Energy Savings and Pollution Reduction (PRES), Aug 27-31 2016 Prague, CZECH REPUBLIC. 307-312.

LESTINSKY, P., GRYCOVA, B., PRYSZCZ, A., MARTAUS, A. & MATEJOVA, L. 2017. Hydrogen production from microwave catalytic pyrolysis of spruce sawdust. *Journal of Analytical and Applied Pyrolysis,* 124**,** 175-179.

LESTINSKY, P. & PALIT, A. 2016. Wood Pyrolysis Using Aspen Plus Simulation and Industrially Applicable Model. *GeoScience Engineering,* 62**,** 11-16.

LESTINSKY, P., ZIKMUND, Z., GRYCOVA, B., RYCZKOWSKI, R., GRAMS, J. & INAYAT, A. 2020. Production of hydrogen over Ni/carbonaceous catalyst. *Fuel,* 278.

MOLINA-SABIO, M. & RODRíGUEZ-REINOSO, F. 2004. Role of chemical activation in the development of carbon porosity. *Colloids and Surfaces A: Physicochemical and Engineering Aspects,* 241**,** 15-25.

MOSKO, J., POHORELY, M., SKOBLIA, S., FAJGAR, R., STRAKA, P., SOUKUP, K., BENO, Z., FARTÁK, J., BICÁKOVÁ, O., JEREMIÁS, M., SYC, M. & MEERS, E. 2021. Structural and chemical changes of sludge derived pyrolysis char prepared under different process temperatures. *Journal of Analytical and Applied Pyrolysis,* 156.

NEBESKÁ, D., TRÖGL, J., SEVCU, A., SPÁNEK, R., MARKOVÁ, K., DAVIS, L., BURDOVÁ, H. & PIDLISNYUK, V. 2021. Miscanthus x giganteus role in phytodegradation and changes in bacterial community of soil contaminated by petroleum industry. *Ecotoxicology and Environmental Safety,* 224.

POHOŘELÝ, M., SEDMIHRADSKÁ, A., TRAKAL, L. & JEVIČ, P. 2019. Biochar – production, properties, certification, and utilization. *Waste Forum***,** 197-210.

STOLARSKI, M. J., DUDZIEC, P., OLBA-ZIĘTY, E., STACHOWICZ, P. & KRZYŻANIAK, M. 2022. Forest Dendromass as Energy Feedstock: Diversity of Properties and Composition Depending on Systematic Genus and Organ. *Energies,* 15**,** 1442.

STUERGA, D. 2006. Microwave-Material Interactions and Dielectric Properties, Key Ingredients for Mastery of Chemical Microwave Processes. *Microwaves in Organic Synthesis.*

XIA, H., CHENG, S., ZHANG, L. & PENG, J. 2016. Utilization of walnut shell as a feedstock for preparing high surface area activated carbon by microwave induced activation: Effect of activation agents. *Green Processing and Synthesis,* 5**,** 7-14.

YANG, H., YAN, R., CHEN, H., LEE, D. H. & ZHENG, C. 2007. Characteristics of hemicellulose, cellulose and lignin pyrolysis. *Fuel,* 86**,** 1781-1788.

Tisková zpráva – Odpadová data 2020. Online. Ministerstvo životního prostřední. 2020. Dostupné z: https://www.mzp.cz/cz/news_20211103-odpadova-data-2020-K-narustu-mnozstvi-komunalnich-odpadu-v-dobe-covidove-v-CR-nedoslo. [cit. 2024-10-02].

Zákon o odpadech 541/2020 Sb., aktualizovaný 1.1.2024. Online. Elektronická Sbírka zákonů a mezinárodních smluv. 2024. Dostupné z: https://www.e-sbirka.cz/sb/2020/541?zalozka=text. [cit. 2024-10-02].

Úpravna vody Želivka. Online. Pražské vodovody a kanalizace. 2021. Dostupné z: https://cistavoda.pvk.cz/upravna-vody-zelivka/uprava-vody/. [cit. 2024-10-02].

International Biochar Initiative. Online. International Biochar Initiative. 2024. Dostupné z: https://biochar-international.org/biochar-standards/. [cit. 2024-10-02].

6 Seznam příloh

[P1] GRYCOVA, B., PRYSZCZ, A., KRZACK, S., KLINGER, M. & **LESTINSKY, P.** 2021. Torrefaction of biomass pellets using the thermogravimetric analyser. *Biomass Conversion and Biorefinery*, 11**,** 2837-2842. IF_{2021} = 4,050. Autorský podíl 30 %. Počet citací dle WoS 16.

[P2] GRYCOVA, B., KLEMENCOVA, K., JEZERSKA, L., ZIDEK, M. & **LESTINSKY, P.** 2022. Effect of torrefaction on pellet quality parameters. *Biomass Conversion and Biorefinery*. IF_{2022} = 4,0. Autorský podíl 20 %. Počet citací dle WoS 6.

[P3] **LESTINSKY, P.**, GRYCOVA, B., PRYSZCZ, A., MARTAUS, A. & MATEJOVA, L. 2017. Hydrogen production from microwave catalytic pyrolysis of spruce sawdust. *Journal of Analytical and Applied Pyrolysis*, 124**,** 175-179. IF_{2017} = 3,468. Autorský podíl 50 %. Počet citací dle WoS 42.

[P4] GRYCOVA, B., PRYSZCZ, A., **LESTINSKY, P.** & CHAMRADOVA, K. 2017. Preparation and characterization of sorbents from food waste. *Green Processing and Synthesis*, 6, 287-293. IF_{2017} = 0,736. Autorský podíl 25 %. Počet citací dle WoS 5.

[P5] KLEMENCOVA, K., GRYCOVA, B. & **LESTINSKY, P.** 2022. Influence of Miscanthus Rhizome Pyrolysis Operating Conditions on Products Properties. *Sustainability*, 14. IF_{2022} = 3,9. Autorský podíl 30 %. Počet citací dle WoS 7.

[P6] GRYCOVA, B., PRYSZCZ, A., **LESTINSKY, P.** & CHAMRADOVA, K. 2018. Influence of potassium hydroxide and method of carbonization treatment in garden and corn waste microwave pyrolysis. *Biomass & Bioenergy*, 118, 40-45. IF_{2018} = 3,537. Autorský podíl 25 %. Počet citací dle WoS 15.

[P7] **LESTINSKY, P.**, ZIKMUND, Z., GRYCOVA, B., RYCZKOWSKI, R., GRAMS, J. & INAYAT, A. 2020. Production of hydrogen over Ni/carbonaceous catalyst. *Fuel*, 278. IF_{2020} = 6,609. Autorský podíl 45 %. Počet citací dle WoS 15.

[P8] **LESTINSKY, P.** & PALIT, A. 2016. Wood Pyrolysis Using Aspen Plus Simulation and Industrially Applicable Model. *GeoScience Engineering*, 62, 11-16. Bez IF. Autorský podíl 90 %. Počet citací dle Google Scholar 35.

Příloha [P1]

GRYCOVA, B., PRYSZCZ, A., KRZACK, S., KLINGER, M. & **LESTINSKY, P.** 2021. Torrefaction of biomass pellets using the thermogravimetric analyser. *Biomass Conversion and Biorefinery*, 11**,** 2837-2842. IF_{2021} = 4,050 (5 year IF 4.103). Autorský podíl 30 %. Počet citací dle WoS 16.

Role uchazeče:

- návrh tématu, návrh postupu prací, vyhodnocení výsledků, vyvození závěrů z dosažených výsledků

Biomass Conversion and Biorefinery (2021) 11:2837–2842
https://doi.org/10.1007/s13399-020-00621-4

ORIGINAL ARTICLE

Torrefaction of biomass pellets using the thermogravimetric analyser

B. Grycova[1] · A. Pryszcz[1] · S. Krzack[2] · M. Klinger[2] · P. Lestinsky[1]

Received: 27 November 2019 / Revised: 23 January 2020 / Accepted: 29 January 2020 / Published online: 11 February 2020

Abstract
Greater heating values, greater energy density and improved physical properties such as shape stability, homogeneity and hydrophobic behaviour are advantages of torrefied biomass. All this leads to an overall reduction in transport costs, storage capacity and to lower requirements for factory equipment. The properties of the different types of biomass used before and after torrefaction and the effect of torrefaction at the different process conditions were studied. For the laboratory tests of torrefaction, wood and grass waste biomass were used. For these selected materials, a number of measurements were performed to verify the most suitable torrefaction conditions (heating temperature and retention time). Experiments were carried out on a small scale on TGA 701 (LECO). Waste biomass was heated to a final temperature of 200, 225, 250, 275 and 300 °C with a retention time at these temperatures of 10, 20 and 45 min. The heating rate was set up to 15 °C min^{-1}. The determination of the appropriate temperature depended on the optimum ratio between mass loss and higher heating values (in case of grassy material from 200 to 225 °C and for woody material at 250 °C). From the results we can state that it is possible to do fast and exact test in TGA before the torrefaction process on the pilot unit to shorten the whole process.

Keywords Torrefaction · Biomass · Thermogravimetric analysis · Process conditions

1 Introduction

Commitments to reduce greenhouse gas emissions, the wide spreading identification on the need to replace coal and legally binding EU 20-20-20 targets are all strong inspiring reasons to prioritize the renewable energy. Low-cost preconditioning technologies of raw biomass that are able to transform and modify various sources of solid biomass into a bioenergy feedstock with similar or even better properties as coal could significantly improve trade and usage of biomass in the existing transport and conversion infrastructure.

Among numeral technologies that could be used to meet this goal, such as conventional pyrolysis, hydrothermal carbonisation or chemical treatment. Torrefaction is considered as a mild pyrolysis process, where the biomass is treated in a temperature range from 200 to 300 °C. It stands out as a very promising technological possibility, drawing attention and financial support for following development. Torrefaction is currently being greatly commercialized. Engineering initiatives focuses not only on a number of demonstration plants but now also first commercial plants are in operation respectively under construction. Several pilot scale torrefiers have been reported in the literature ranging in throughput from 3 to 274 kg h^{-1} [1]. After torrefaction, the bulk density of torrefied biomass is decreased, therefore pelletisation is proposed. This traditional approach has a main drawback. To pelletise torrefied biomass is a key challenge because of the degradation of bonding forces between biomass particles and the loss of natural lignin-binding features after torrefaction [1] and may require the use of binders, which are expensive and can be unsuited.

The number of publications on torrefaction is relatively small compared with another biomass processing methods but has increased significantly currently. Literature sources

Highlights
- Four types of biomass pellets were torrefied.
- Small scale laboratory torrefaction tests using TGA were performed.
- Different torrefaction temperatures and residence times in reactor were experimentally tested.
- It is more efficient to pelletise biomass material prior to torrefication.
- The Van Krevelen diagram was created.

✉ B. Grycova
barbora.grycova@vsb.cz

[1] Institute of Environmental Technology, VSB – Technical University of Ostrava, Ostrava, Czech Republic

[2] Institute of Energy Process Engineering and Chemical Engineering, TU Bergakademie Freiberg, Freiberg, Germany

about the torrefaction of bagasse [2], bamboo [3], wood briquette [4], oak [5] and others can be found [6–8].

Torrefaction is a controlled process of carbonisation in which the biomass is heated in the temperature range from 200 to 300 °C in an oxygen-free environment or in the presence of only a small amount of oxygen. To provide a non-oxidizing atmosphere, nitrogen is the most commonly used carrier gas. Thermal methods below 200 °C are used for wood preservation [9, 10], while higher temperatures in the torrefaction method are used for energy purposes. In addition to temperature, torrefaction time or duration is another important factor in determining the performance of torrefaction. Torrefaction can be carried out between several minutes [11] to several hours [12]. This process leads to the moisture reduction and the transformation of biomass into a product with properties comparable with coal. Torrefaction also increases the hydrophobicity of biomass. And therefore, biomass becomes more resistant to water adsorption, resulting in an improvement in the control of storage conditions [13]. Due to its low water content, it also becomes lighter and less predisposed to rot [14].

Combinations of the range of temperatures and retention times can be done in terms of reaching a given degree of torrefaction, as represented by the mass loss. The exposure of biomass to high temperatures leads to thermal degradation of its physical structure and, accordingly, to mass loss [15]. In contrast, the key properties of the torrefied product, such as higher heating value and saturated moisture uptake, are primarily determined by the mass loss [1, 16]. Retention time generally affects the decomposition of hemicellulose, whereas cellulose is decomposed in particular, depending on the reaction time [17]. The used heating rate throughout the torrefaction process has influence on the secondary degradation reactions, which affect the final solid, liquid and gas product distribution [18]. Kumer et al. noticed that by the rate increasing, there would be a reduction of the effects of heat and mass transfers between particles [19].

The mass loss of the biomass leads to an increase in the porosity. As a result, significant decrease in the volumetric density of the biomass has been observed, depending on the initial density [20]. Despite this decrease in bulk density, the energy density of the torrefied biomass increases after torrefaction by 30% approx. [21]. Factors, such as particle size distribution and specific surface area, are essential parameters with respect to behaviour during burning of the torrefied biomass [22]. The heating value of the torrefied biomass is higher than that of the non-torrefied biomass, since there is an increase of the fixed carbon, on the contrary to the release of the oxygen compounds, leaving more carbon available to be oxidized [23]. Recent results have shown that torrefied biomass particles were harder to pelletise. So it was found that it is more efficient to pelletise biomass material prior to torrefication [24].

This article aims to show a possibility of fast small-scale laboratory torrefication tests, which could be used for basic introduction of different types of biomass torrefaction. The properties of the different types of biomasses used before and after torrefaction, and the effect of torrefaction in the different process parameters were studied.

2 Materials and methods

Pellets from grass biomass (Sorghum), straw, rice husk and spruce were used as torrefaction materials. Size of the pellets was 20 mm with a diameter of 6 mm.

Raw materials as well torrefied samples were analysed with the thermogravimetric analyser, TGA 701 (LECO). For determination of moisture, ash, volatile and fixed carbon approximately 0.8–1 g of sample was used. Samples were first heated to 105 °C to constant weight in inert atmosphere to define water amount; further samples were covered and heated in inert atmosphere to 800 °C, and the last step was burning the samples in pure oxygen to 815 °C to constant weight. The measurement was done according to the ASTM D7582 MVA in Coal. Nitrogen was used as an inert medium.

Around 100 mg of sample was used for the determination of C, H, N and O; the measurement was done by the elementary analyser CHN 628 (LECO). This instrument utilises a combustion technique and provides a fast result for all the elements being determined. A weighed and encapsulated sample was placed in the loader and transferred to the purge chamber directly above the furnace. The sample was then introduced to the primary furnace resulting in a rapid sample oxidation. Non-dispersive infrared absorption was used to detect C/H. TCD was used for nitrogen detection.

Higher heating value was defined by isoperibol method with the calorimetric analyser, AC 600 (LECO) combined with the use of thermodynamic TruSpeed®. Approximately 200–300 mg of sample was placed into a combustion vessel, which was pressurized with oxygen. The combustion vessel was automatically lowered into a water bath. The sample was ignited, and the temperature was measured by an electrical thermometer. Compositions of inputs biomass pellets are listed in Table 1.

Small scale laboratory torrefaction tests were performed for the four biomass materials using a thermogravimetric analyser (TGA 701 - LECO). In an automated sample changer, a total of 19 crucibles could be loaded with biomass and placed inside the TGA, where the mass loss with increasing temperature was constantly measured. The weight used for all the experimental runs for TGA torrefaction was around 0.8–1 g (one pellet). The final temperature in TGA was 200, 225, 250, 275 and 300 °C with a heating rate of 15 °C min^{-1}. The retention times, when the biomass materials were exposed to final torrefaction temperatures, were 10, 20 and 45 min,

Table 1 Proximate and ultimate analysis of biomass pellets

	W_r (wt.%)	C_d (wt.%)	H_d (wt.%)	N_d (wt.%)	O_d (wt.%)	A_d (wt.%)	V_d (wt.%)	FC_d (wt.%)	HHV_d (MJ/kg)
Spruce	8.5 ± 0.2	50.7 ± 0.4	6.2 ± 0.2	0.3 ± 0.1	42.3 ± 0.3	0.5 ± 0.1	81.6 ± 0.5	17.9 ± 0.2	19.8 ± 0.4
Straw	7.8 ± 0.2	46.4 ± 0.4	6.3 ± 0.2	1.2 ± 0.1	40.9 ± 0.3	5.1 ± 0.2	77.2 ± 0.4	17.7 ± 0.2	17.2 ± 0.5
Grass	7.5 ± 0.3	46.4 ± 0.4	6.2 ± 0.2	1.3 ± 0.1	41.7 ± 0.3	4.4 ± 0.2	78.2 ± 0.5	17.4 ± 0.2	16.9 ± 0.4
Rise husk	5.2 ± 0.2	42.7 ± 0.3	6.1 ± 0.3	0.7 ± 0.1	35.8 ± 0.3	14.6 ± 0.2	66.1 ± 0.4	19.3 ± 0.2	16.4 ± 0.4

W Water content, *A* ash, *V* volatile matter, *FC* fixed carbon, *HHV* higher heating value, *d* dry

respectively. Inert atmosphere inside the TGA was archived by flow of 10 l min^{-1} of nitrogen. After the torrefaction tests were done, proximate, ultimate and calorimetric analyses with the same methods were again performed for the torrefied materials (Table 2). All measured data were finally evaluated.

3 Results and discussion

Several materials were treated by means of the thermogravimetric analyser used as small torrefaction reactor. Different torrefaction temperatures and retention times in reactor were experimentally tested. All torrefied samples were analysed by proximate and ultimate analysis. Dried and deoxygenated biomass was the main goal of torrefaction which was archived. The change of oxygen content during the torrefaction process for different temperatures is noticeable in Fig. 1.

The results of elemental composition of individual samples were put into the Van Krevelen diagram, as can be seen in Fig. 1. The increasing of torrefaction temperature leads to decreasing of the oxygen content. Of course, the hydrogen content decreases as well. The materials with lowest oxygen content can be classified as a subbituminous coal or alike. The highest oxygen content was in torrefied spruce, because spruce material has the higher content of lignin, and the degradation of lignin needs higher temperature than the degradation of cellulose. Dry materials are marked as full black. In the picture is missing materials after 200 °C torrefaction, because the difference between composition of dry biomass and torrefied biomass at 200 °C was insignificant.

The decrease of oxygen content had positive effect, but on the other side, it is connected with a decreasing of mass amount. The mass decreasing depends on the temperature and on the retention time in the reactor. The maximum retention time used for our experiments was 45 min. We tested

Table 2 Proximate and ultimate analysis of torrefied biomass pellets

	T (°C)	C_d (wt.%)	O_d (wt.%)	V_d (wt.%)	FC_d (wt.%)	HHV_d (MJ/kg)
Spruce	200	50.3 ± 0.4	42.9 ± 0.3	80.9 ± 0.6	18.9 ± 0.2	19.9 ± 0.5
	225	50.6 ± 0.5	42.4 ± 0.4	79.7 ± 0.5	19.9 ± 0.2	20.0 ± 0.6
	250	52.2 ± 0.4	41.2 ± 0.3	77.6 ± 0.5	22.1 ± 0.2	20.2 ± 0.5
	275	56.2 ± 0.4	37.9 ± 0.3	65.0 ± 0.4	34.5 ± 0.2	20.7 ± 0.4
	300	67.9 ± 0.5	27.4 ± 0.4	47.0 ± 0.4	52.1 ± 0.4	24.3 ± 0.5
Straw	200	46.3 ± 0.4	41.6 ± 0.3	75.8 ± 0.6	19.1 ± 0.2	17.2 ± 0.4
	225	48.6 ± 0.4	38.7 ± 0.3	71.5 ± 0.5	22.9 ± 0.2	17.5 ± 0.4
	250	58.0 ± 0.4	27.6 ± 0.3	44.6 ± 0.4	46.8 ± 0.3	20.7 ± 0.5
	275	60.9 ± 0.5	22.1 ± 0.3	34.6 ± 0.3	54.0 ± 0.4	21.9 ± 0.4
	300	65.2 ± 0.4	17.8 ± 0.4	31.3 ± 0.3	56.8 ± 0.4	23.2 ± 0.5
Grass	200	46.2 ± 0.4	41.7 ± 0.3	76.8 ± 0.5	18.2 ± 0.2	17.0 ± 0.4
	225	48.9 ± 0.5	38.1 ± 0.4	73.2 ± 0.6	21.3 ± 0.2	17.9 ± 0.4
	250	54.9 ± 0.4	31.8 ± 0.3	57.5 ± 0.4	35.9 ± 0.3	19.7 ± 0.4
	275	61.4 ± 0.5	23.4 ± 0.3	44.1 ± 0.4	46.9 ± 0.4	22.3 ± 0.5
	300	63.2 ± 0.5	14.4 ± 0.4	33.5 ± 0.3	49.4 ± 0.5	23.2 ± 0.5
Rise husk	200	41.7 ± 0.4	38.1 ± 0.3	65.7 ± 0.5	19.9 ± 0.2	16.5 ± 0.4
	225	43.5 ± 0.4	35.7 ± 0.3	63.1 ± 0.5	21.6 ± 0.2	16.7 ± 0.4
	250	45.8 ± 0.4	29.6 ± 0.3	51.0 ± 0.4	29.8 ± 0.3	16.9 ± 0.4
	275	49.6 ± 0.5	21.3 ± 0.4	35.5 ± 0.4	40.1 ± 0.3	17.7 ± 0.5
	300	51.6 ± 0.5	15.9 ± 0.4	27.6 ± 0.3	44.1 ± 0.4	18.6 ± 0.4

T Torrefaction temperatures, *V* volatile matter, *FC* fixed carbon, *HHV* higher heating value, *d* dry

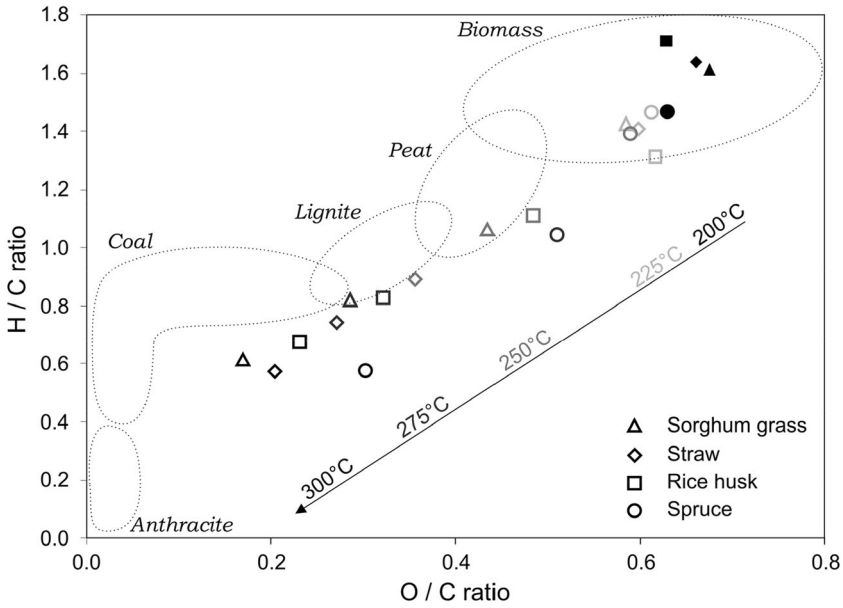

Fig. 1 Van Krevelen diagram of torrefied samples

shorter torrefaction retention times, e.g. 10 and 20 min for our biomass materials too, but these times were insufficient. Time for heating to the final temperature was not calculated to the retention time. Mass loss of spruce samples for different retention times is shown in Fig. 2. It can be seen that the vaporization of all water (free and bound) were already achieved during increasing of temperature up to 200 °C. Retention time to 10 or 20 min led to stable sample only for torrefaction temperature of 200 °C. Vaporization of organic compounds, mainly for the higher torrefaction temperature, led to higher slope of mass loss curve, and longer retention time was needed, because 10 or 20 min were insufficient. It is noticed that longer retention time has comparable effects as increased torrefaction temperature. The opposite effects can be seen when the particle size was increased. The torrefied pellets

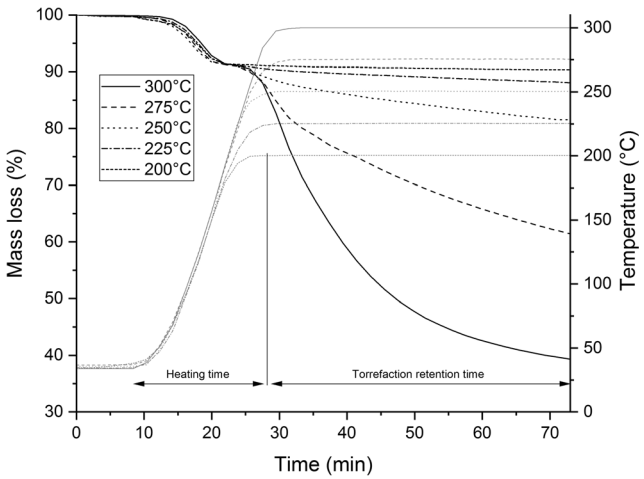

Fig. 2 TGA curves of spruce biomass for different torrefaction temperatures and residence time of 45 min (the grey line indicates the temperature)

obtained from the short-time tests were also tested by naked eye: pellets were cut, and the colour of the centre was different (with a lighter coloured core). This indicated that the material was not treated through the whole volume. Therefore, all subsequent experiments were done with a retention time of 45 min, which led to homogenous coloured pellets. At the first part (drying during heating time), the mass loss was connected to free and bound water removing. Reaching a temperature of 200 °C is sufficient for biomass drying; retention time on this temperature is not necessary. At the second part (torrefaction process), the significant decreasing of weight is caused by the decomposition of hemicellulose in spruce material. This is supported by the knowledge that cellulose and lignin are decomposed at 300 °C only very slow or not at all [25, 26]. The degradation of hemicellulose can be seen significantly for torrefaction temperatures of 275 and 300 °C. During sufficiently long retention times at these temperatures range, cellulose and lignin started decomposition too.

On the other side, mass loss is one of the important economic parameter, which decides about the feasibility of torrefaction process. Mass loss at different torrefaction temperatures for all examined biomass materials can be seen in Fig. 3. The biggest grass and straw mass loss had occurred between 225 and 250 °C. The decreasing of the weight was slower only for wood biomass. The weight of rice husk sample was stable to 250 °C; this means that rice husk is more stable then spruce sample. But looking at the proximate and ultimate analysis, it can be found that the rice husks have a very different composition than the remaining grassy biomass, i.e. higher content of ash, therefore lower content of volatile matter and lower content of oxygen.

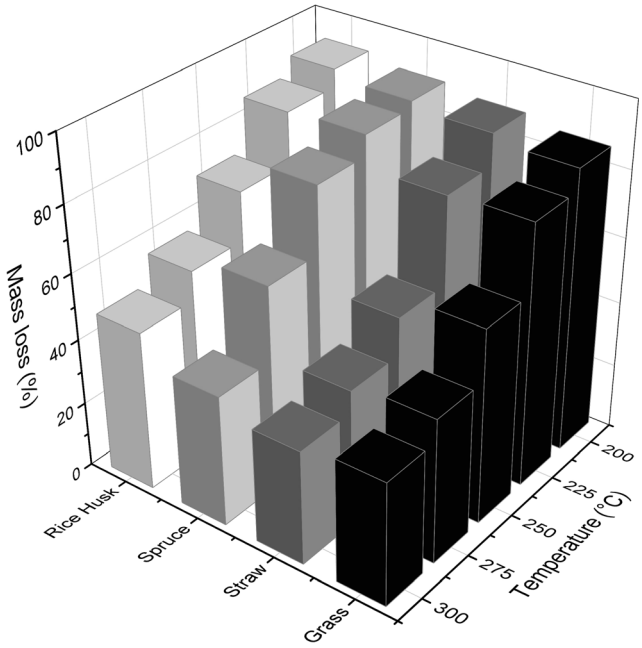

Fig. 3 Mass loss for different materials at different torrefication temperatures

Another important parameter for torrefied material is the higher heating value (HHV) which is one of the most important parameters for combustion technology. During the torrefaction process, the content of oxygen and part of volatile matter (mostly water of constitution, CO_2 and CO) decreased, which was accompanied by an increasing amount of carbon, and HHV (see Table 2). The biggest changes of material happened when torrefied to 300 °C, but on the other side, for this temperature, the mass loss of dried biomass was more than 50%.

So, for choosing the best parameters for torrefaction processes, it is necessary to balance the ideal ratio between mass loss and HHV. Energy yield, which is given in Fig. 4, was calculated as multiplication of HHV and the fraction of solid residues from torrefaction. The most economically worthy torrefaction temperatures for grassy material seems to be in the range from 200 to 225 °C and for woody material at 250 °C. But low torrefaction temperatures of 200 and 225 °C made just negligible changes to the raw biomass; it looks like it mostly just dried the material. From the comparison with other articles [27–29], it can be seen that mostly the amount of carbon and HHV correspond with our measurements. From the results, we can state that it is possible to do fast and exact test in TGA before the torrefaction process on the pilot unit. This significantly shortens the initial tests on a pilot unit and gives time to investigate products, including pyrolysis water and gases, investigate a heat and mass balance which cannot be studied on a small scale.

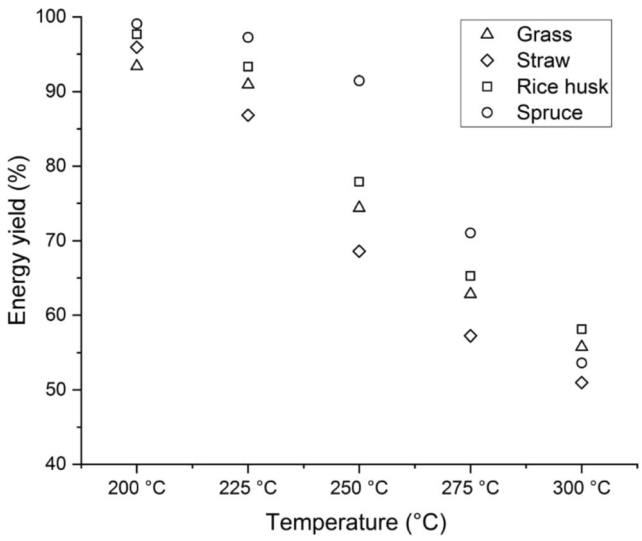

Fig. 4 Energy yields for torrefied biomass pellets for different temperatures and residence time 45 min

4 Conclusion

Torrefication is one of the technologies to use renewable energy sources such as biomass to supplement fossil fuels in the energy sector. It is probably not worth discussing the use of wood biomass, because it is the best. The potential in the production of black pellets is huge, but production of these pellets brings a big loss of mass, which is unreasonably reflected on value of energy yields. For example, spruce pellets torrefied to 300 °C (HHV ≈ 24 MJ/Kg, C ≈ 68 wt.%) resemble to brown coal (HHV ≈ 20 MJ/kg, C ≈ 50–80 wt.%), but the energy yields are half (52%) that of the raw state. So, the most economically worthy torrefaction temperatures for woody material is 250 °C with yield of 91% because loss of mass is only 11.1 wt.%, and this torrefied wood is totally waterproof, so it is great to store and transport. But even grass and agrobiomass can be processed with torrefaction process, mainly up to 225 °C to facilitate year-round storage. The use of a thermogravimetric analyser for biomass torrefication has proven to be very useful as it saves a lot of time for pilot plant optimization process. Minimal time for biomass treatment by torrefaction processes is 45 min, but it is necessary added time for preheating of materials.

Acknowledgements This work was supported by EU structural funding in Operational Programme Research, Development and Education, project No. CZ.02.1.01/0.0/0.0/16_019/0000853 „IET-ER“, and project No. CZ.01.1.02/0.0/0.0/16_084/0010290 “Torrefaction for small and mobile units”, and by using Large Research Infrastructure ENREGAT supported by the Ministry of Education, Youth and Sports of the Czech Republic under project No. LM2018098“.

References

1. Peng JH, Bi XT, Sokhansanj S, Lim CJ (2013) Torrefaction and densification of different species of softwood residues. Fuel 111: 411–421. https://doi.org/10.1016/j.fuel.2013.04.048
2. Pach M, Vigouroux R, Björnbom E (2002) Torrefied biomass a substitute for wood and charcoal
3. Gururaja Rao S, Subbukrishna N, Sridhar HV, Dasappa S, Paul PJ, Mukunda H (2007) Torrefaction of bamboo
4. Felfli FF, Luengo CA, Suárez JA, Beatón PA (2005) Wood briquette torrefaction. Energy Sustain Dev 9(3):19–22. https://doi.org/10.1016/S0973-0826(08)60519-0
5. Pierre F, Almeida G, José O, Brito PP (2011) Influence of torrefaction on some chemical and energy properties of maritime pine and pedunculate oak. BioRes 6(2):1204–1218
6. He Q, Ding L, Gong Y, Li W, Wei J, Yu G (2019) Effect of torrefaction on pinewood pyrolysis kinetics and thermal behavior using thermogravimetric analysis. Bioresour Technol 280:104–111. https://doi.org/10.1016/j.biortech.2019.01.138
7. Zhang S, Su Y, Ding K, Zhu S, Zhang H, Liu X, Xiong Y (2018) Effect of inorganic species on torrefaction process and product properties of rice husk. Bioresour Technol 265:450–455. https://doi.org/10.1016/j.biortech.2018.06.042
8. Zeng K, Yang Q, Zhang Y, Mei Y, Wang X, Yang H, Shao J, Li J, Chen H (2018) Influence of torrefaction with Mg-based additives on the pyrolysis of cotton stalk. Bioresour Technol 261:62–69. https://doi.org/10.1016/j.biortech.2018.03.094
9. Hakkou M, Pétrissans M, Gérardin P, Zoulalian A (2006) Investigations of the reasons for fungal durability of heat-treated beech wood. Polym Degrad Stab 91(2):393–397. https://doi.org/10.1016/j.polymdegradstab.2005.04.042
10. Windeisen E, Strobel C, Wegener G (2007) Chemical changes during the production of thermo-treated beech wood. Wood Sci Technol 41(6):523–536. https://doi.org/10.1007/s00226-007-0146-5
11. Peng JT, Bi H, Sokhansanj S, Lim J (2012) A study of particle size effect on biomass torrefaction and densification. Energy Fuel 26(6): 3826–3839. https://doi.org/10.1021/ef3004027
12. Wannapeera J, Fungtammasan B, Worasuwannarak N (2011) Effects of temperature and holding time during torrefaction on the pyrolysis behaviors of woody biomass. J Anal Appl Pyrolysis 92(1):99–105. https://doi.org/10.1016/j.jaap.2011.04.010
13. van der Stelt MJC, Gerhauser H, Kiel JHA, Ptasinski KJ (2011) Biomass upgrading by torrefaction for the production of biofuels: a review. Biomass Bioenergy 35(9):3748–3762. https://doi.org/10.1016/j.biombioe.2011.06.023
14. Pang S, Mujumdar A (2010) Drying of woody biomass for bioenergy: drying technologies and optimization for an integrated bioenergy plant. Dry Technol 28:690–701. https://doi.org/10.1080/07373931003799236
15. Miguel Carneiro Ribeiro J, Godina R, Matias J, Nunes L (2018) Future perspectives of biomass torrefaction: review of the current state-of-the-art and research development. Sustainability 10(7): 2323. https://doi.org/10.3390/su10072323
16. Peng JH, Bi HT, Lim CJ, Sokhansanj S (2013) Study on density, hardness, and moisture uptake of torrefied wood pellets. Energy Fuel 27(2):967–974. https://doi.org/10.1021/ef301928q
17. Bergman PCA, Boersma AR, Zwart RWR, Kiel JHA (2005) Torrefaction for biomass co-firing in existing coal-fired power stations. Report no. ECNC05013. Energy research Centre of the Netherlands (ECN): Petten, the Netherlands
18. Nunes LJR, De Oliveira Matias JC, Da Silva Catalão JP (2018) Chapter 3 - biomass torrefaction process. In: Nunes LJR, De Oliveira Matias JC, Da Silva Catalão JP (eds) Torrefaction of biomass for energy applications. Academic Press, pp 89–124. doi: https://doi.org/10.1016/B978-0-12-809462-4.00003-1
19. Kumar G, Panda AK, Singh RK (2010) Optimization of process for the production of bio-oil from eucalyptus wood. J Fuel Chem Technol 38(2):162–167. https://doi.org/10.1016/S1872-5813(10)60028-X
20. Chen W-H, Peng J, Bi XT (2015) A state-of-the-art review of biomass torrefaction, densification and applications. Renew Sust Energ Rev 44:847–866. https://doi.org/10.1016/j.rser.2014.12.039
21. Bergman CAP, Kiel J (2005) Torrefaction for biomass upgrading.
22. Acharya B, Sule I, Dutta A (2012) A review on advances of torrefaction technologies for biomass processing. Biomass Conversion Biorefinery 2(4):349–369. https://doi.org/10.1007/s13399-012-0058-y
23. Tumuluru JS, Sokhansanj S, Hess J, Wright C, Boardman R (2011) A review on biomass torrefaction process and product properties for energy applications. Ind Biotechnol 7:384–401. https://doi.org/10.1089/ind.2011.7.384
24. Ghiasi B, Kumar L, Furubayashi T, Lim CJ, Bi X, Kim CS, Sokhansanj S (2014) Densified biocoal from woodchips: is it better to do torrefaction before or after densification? Appl Energy 134: 133–142. https://doi.org/10.1016/j.apenergy.2014.07.076
25. Jiang G, Nowakowski DJ, Bridgwater AV (2010) A systematic study of the kinetics of lignin pyrolysis. Thermochim Acta 498(1–2):61–66. https://doi.org/10.1016/j.tca.2009.10.003
26. Ranzi E, Cuoci A, Faravelli T, Frassoldati A, Migliavacca G, Pierucci S, Sommariva S (2008) Chemical kinetics of biomass pyrolysis. Energy Fuel 22(6):4292–4300. https://doi.org/10.1021/ef800551t
27. Chen D, Gao A, Ma Z, Fei D, Chang Y, Shen C (2018) In-depth study of rice husk torrefaction: characterization of solid, liquid and gaseous products, oxygen migration and energy yield. Bioresour Technol 253:148–153. https://doi.org/10.1016/j.biortech.2018.01.009
28. Kai X, Meng Y, Yang T, Li B, Xing W (2019) Effect of torrefaction on rice straw physicochemical characteristics and particulate matter emission behavior during combustion. Bioresour Technol 278:1–8. https://doi.org/10.1016/j.biortech.2019.01.032
29. Chen Y, Yang H, Yang Q, Hao H, Zhu B, Chen H (2014) Torrefaction of agriculture straws and its application on biomass pyrolysis poly-generation. Bioresour Technol 156:70–77. https://doi.org/10.1016/j.biortech.2013.12.088

Příloha [P2]

GRYCOVA, B., KLEMENCOVA, K., JEZERSKA, L., ZIDEK, M. & **LESTINSKY, P.** 2022. Effect of torrefaction on pellet quality parameters. *Biomass Conversion and Biorefinery*. IF_{2022} = 4,0 (5 year IF 4.103). Autorský podíl 20 %. Počet citací dle WoS 6.

Role uchazeče:
- návrh tématu, návrh postupu prací, vyvození závěrů z dosažených výsledků

Biomass Conversion and Biorefinery
https://doi.org/10.1007/s13399-021-02164-8

ORIGINAL ARTICLE

Effect of torrefaction on pellet quality parameters

Barbora Grycova[1] · Katerina Klemencova[1] · Lucie Jezerska[2] · Martin Zidek[2] · Pavel Lestinsky[1]

Received: 20 August 2021 / Revised: 26 November 2021 / Accepted: 30 November 2021

Abstract
Torrefied biomass is characterized as a high-quality renewable energy commodity that can substitute fossil fuels. Combined torrefaction and pelletization are used to increase the value of biomass by improving its handling and fuel properties. The aim of this study is to present the influence of pelletization process on torrefaction in a pilot-scale unit. Above that, two process modes were assessed, and the properties of the torrefied and pelletized biomass and vice versa were studied. Mode I involved torrefaction prior pelletization. In mode II, on the contrary, the waste biomass was first pelletized and then torrefied. Analysis of mechanical parameters and chemical composition was therefore used to determine which of the modes was more advantageous. The results showed that within both modes it is evident that a higher torrefaction temperature caused wettability index decrease with a simultaneous higher heating value increase. Pellets produced in mode I showed better calorific values, however worse mechanical properties particularly durability.

Keywords Torrefaction · Biomass · Pelletization · Pilot-scale unit

1 Introduction

The world's interest in finding new sources of green energy reflects growing energy demands, the loss of fossil fuels, and environmental damage. There is a freely available amount of biomass for bioenergy production, and this amount is expected to increase in the next few decades. Various biomass pre-processing technologies has been introduced over the years, but only a small percentage of them (such as torrefaction) has been shifted into extensive demonstration [1].

During the torrefaction process, heat is transferred to the surface of the individual biomass particles and then passed through the surface of the particles to their center, where thermal decomposition occurs. Heat transfer is affected by the size and conductivity of the biomass, which is generally low, and therefore, the initial heating takes longer. The course of the exothermic reaction is greatly influenced by particle size. Unfortunately, it is generally not constant in an industrial environment, so it is necessary to consider this effect on the whole torrefaction process when designing the equipment [2].

Even though torrefaction is able to improve the biomass properties [3], it also has some operating challenges. By studying various operating conditions and reactor configurations is how researchers are increasingly trying to improve the operational feasibility of this process. There are numerous contributions explaining in detail the chemistry of biomass torrefaction, discussions about torrefaction kinetics, and reaction mechanisms as well. On the other hand, economic and environmental feasibility of torrefaction process has been reviewed the least in the literature [4]. Studies on the environmental feasibility of torrefaction process confirm that using torrefied pellets instead of wood pellets is highly recommendable because of lower emissions generation. However, the economic data shows that torrefied biomass is not yet competitive to wood pellets, mainly due to the additional investment for torrefaction reactor. The most influential factor on the overall economics of the torrefaction, the price of raw materials is playing [4].

Torrefied char has fuel properties similar to sub-bituminous coal, and therefore, it is able for co-firing with coal in already working coal-fired power plants [5]. Some large

✉ Barbora Grycova
barbora.grycova@vsb.cz

[1] VSB – Technical University of Ostrava, Energy and Environmental Technology Centre, Institute of Environmental Technology, 17. listopadu 15/2172, Ostrava–Poruba 708 00, Czech Republic

[2] VSB – Technical University of Ostrava, Energy and Environmental Technology Centre, Bulk Solid Centre - Czech Republic, ENET Centre, 17. listopadu 15/2172, Ostrava–Poruba 708 00, Czech Republic

Published online: 15 January 2022

dimensions' torrefaction units have been built around the world thanks to this possibility. Despite the fuel properties improvement, torrefied char has a lower energy density in comparison with coal [6]. However, to increase energy density and thus easy transport, it is possible by pelletizing torrefied biomass [7]. Biomass does not require additional binders for pelletization thanks to lignin and its binding properties [8, 9]. By torrefaction, the biomass loses its natural moisture, which then has an adverse effect on the pelletization process. Therefore, it is hardly possible to approach pelletization of already torrefied biomass in the same way [7]. The effect of changes in pelletization conditions has already been studied, as well as the use of external binders [10]. As already tested binders, it is possible to mention plastics, starch, molasses, phenolic resins, crude lignin, calcium hydroxide, and heavy oils [11]. However, these binders often significantly increase energy costs of torrefied char pellets [12], which is undesirable. The influence of moisture and additives such as pine, grape pomace, and glycerol on the core features of the obtained pellets were assessed and compared with pellets formed from raw pine with regard to international standard requirements [13]. Other biomass fuels (almond shell, cocoa shell, *Miscanthus*, and olive stone) were also evaluated as possible additives [14]. Various parameters, including torrefaction temperature, time, pressure, and water content during pelletization, can be modified to produce torrefied pellets of the required quality, i.e., with high-energy density, resilience, and hydrophobicity [15].

Some researchers observed higher HHV in torrefied pellets compared to non-torrefied one, and moreover lower the overall cost, including production and logistics costs [16, 17]. These days, combined pelletization and torrefaction, have been the subject of many studies [18]. As already mentioned, pelletization of torrefied biomass may not be easy because of hydroxyl groups elimination and lignin components breakage during the process [19]. Taking into account the overall energy and material balance, torrefaction of pellets is more advantageous than pelletization of torrefied biomass, as described by Ghiasi et al. [20]. It should be noted that although pellets after torrefaction lose some hardness and they are fragile, there is always an optimal balance between the benefits and weaknesses that can be achieved [21].

Relatively less often it is written about the process of torrefaction of already pelletized biomass [22]. Manouchehrinejad and Mani [23] dealt with torrefaction of wood pellets and concluded that improvements in the calorific value and water resistance have been achieved. On the other hand, properties such as density, hardness, and durability of pellets were aggravated. The bulk density remained stable up to a temperature of 270 °C; above this temperature there was a drastic fall. A similar trend is described by Siyal et al. [24]. In this case, torrefaction subsequent to pelletization improved the features of pellets and made them fit for other thermal processes used in industrial fields. A noticeable decline in mass and energy yields with increasing temperature was determined. The highest lower heating value 26.76 $MJ \bullet kg^{-1}$ and energy density ratio 1.46 for torrefied sawdust pellets were achieved at the following conditions (temperature of 300 °C and time of 120 min). The highest true density 2.40 and porosity 1.85 $g \bullet cm^{-3}$ were achieved during these conditions, much higher than those of non-torrefied pellets. Abedi and Dalai [25] came up with the comparable conclusions for oat-hull pellets.

Recently, many studies have been focused on pelletization of mostly single-species torrefied biomass. Torrefaction subsequent to pelletization has rarely been reported. However, the effect of both process modes and especially the choice of their sequence in the case of garden waste treatment has not yet been thoroughly investigated. Therefore, this study is addressed to a comparison of both modes with their advantages and conversely difficulties together with the detailed evaluation of the resulting pellets in terms of changes in the physical quality and fuel properties. Parameters optimization in order to prepare binder-free pellets was discussed.

2 Material and methods

2.1 Material characterization

The production of biowaste with Cat. No. 200201 recorded a change in the trend on the basis of Decree No. 321/2014 Coll. implementation. Thus, an obligation was imposed on municipalities to allow biowaste separation. This waste fraction includes biodegradable kitchen waste from households and garden waste. The theoretical potential of biowaste separation is significantly influenced by the type of the given area. In the case of rural and residential area, this was calculated at 140 kg per person and year. Garden waste used in this experimental part as a raw material was obtained from the maintenance of greenery in the city of Ostrava. This type of waste is often processed by biochemical processes or just landfilled. The biomass was composed of *picea abies* branches, *picea abies* needles, and *thuja*, including a tiny number of fruit trees and shrubs, simply spring pruning of trees. The randomly composed mixture was first crushed to 2–3 cm, then to 5 mm, and finally to 3 mm. The mixture of biomass was air dried to constant humidity for several days.

The proximate analysis was performed in accordance with the standard procedure of the American Society for Testing and Materials (ASTM E790, 830, 897). Moisture (W), volatile matter (VM), fixed carbon (FC), and ash (A) contents were determined with the use of LECO TGA701. The samples of raw garden waste and pellets from garden

waste were heated from 20 to 800 °C with a heating rate of 5 °C/min in an inert nitrogen atmosphere. Carbon (C), nitrogen (N), hydrogen (H), and sulfur (S) content of garden waste were determined by LECO CHSN628 elemental analyzer according to ASTM E775-8. The mass of oxygen (O) was calculated by difference (i.e., O = 100-C-H-N-S-A [%]). A bomb calorimeter LECO AC600 was used to determine the higher heating value (HHV) in accordance with ASTM E711. Initially, the calorimeter was calibrated using the benzoic acid tablets. The content of lignin, cellulose, and hemicellulose was determined according to the standard SOP 87.

2.2 Pre-treatment, pelletization process, and characterization of pellets

In order to pelletization, garden waste was ground with the use of a knife grinder LMN 180 to a powder and passed through a 3-mm sieve and further homogenized in a homogenizer Alba Re 22. During the homogenization, water was gradually added by spraying. The humidity of the mixture was adjusted to 15 wt. %. For pelletization, the laboratory rotary pelletizer KAHL 14–175 (Amandus Kahl GmbH & Co. KG) with a flat die of engine power 3 kW was used. The main parts are rollers and flat die. They are practically tools for making pellets. Rollers thicken and push the lying material carpet into the channels in the flat die. Rollers rotate freely on fixed axis. The garden waste samples were compressed in range 200–250 MPa and at frequency 52 Hz. Temperature was in the range 80–100 °C.

Mechanical resistance of the pellets, durability (D) was measured according to EN15210-1. (EN15210-1: Solid biofuels—Determination of Mechanical Durability of Pellets and Briquettes—Part 1: Pellets) on a Holmen NHP 1000 instrument. During the test, a sample of 100 g of pellets pneumatically circulated at 70 MBar in a chamber with perforated conical walls for 60 s. After the test, the sample was sieved through a 3-mm sieve. Durability was calculated according to Eq. (1), where m_1 is the pellet weight before the test and m_2 after the test:

$$D = \frac{m_2}{m_1} \times 100[\%] \tag{1}$$

The procedure was repeated ten times. The average value was calculated from the results [26]. Bulk density (BD) was determined according to standard ISO 17828:2015 [27]. Specific density (SD) was determined with the use of Mettler Toledo JEW-DNY-43. The values were taken from 10 measurements as the average value. The hardness test (H) was carried out using KAHL ac-14 hardness tester. Pellet hardness, defined as the force that is required to break it, was expressed as the mass load on the given pellet area in kilograms.

The resistance to moisture, the so-called wettability index (WI), was performed according to Eq. (2) defined by %:

$$\mathrm{WI} = \frac{m_2 - m_1}{m_1} \times 100[\%] \tag{2}$$

where m_1 is the weight of the pellet before the test and m_2 is the weight of the pellet after the test. The test consisted in immersing the pellet in distilled water for 30 s. The procedure was repeated ten times. The average value was subsequently calculated from the results.

Samples of pellets were also characterized by scanning electron microscope (SEM: Tescan Vega) with tungsten cathode and energy-dispersive X-ray spectroscopy (EDS: EDAX). Micrographs were obtained using secondary electrons (SE) and backscattered electrons (BSE) mode with an acceleration voltage of 30 keV. To ensure adequate electron conductivity, samples were gold sputtered before imaging.

The FT-IR spectra were measured by a Thermo Scientific Nicolet iS10 FTIR Spectrometer. The measurements were carried out in the range 500–4000 cm^{-1} with a resolution of 2 cm^{-1} using transmission mode. A small amount of sample (approx. 1 mg) was mixed and homogenized with KBr (approx. 200 mg) and pressed at a pressure of 10 MPa to obtain transmission tablet. The prepared sample was placed in the holder and then in the transmission attachment where the spectrum was collected. Each spectrum consisted of at least 64 scans lasting 1 s. Before each measurement, the background was collected to eliminate apparatus and environmental effects. Each sample spectrum was ratioed.

2.3 Torrefaction

Torrefaction tests are performed in a pilot-scale unit using an inert atmosphere of argon, the scheme of which is shown in Fig. 1. A reactor with a length of 155 cm, an inner diameter of 14.5 cm, and an outer diameter of 22 cm was used.

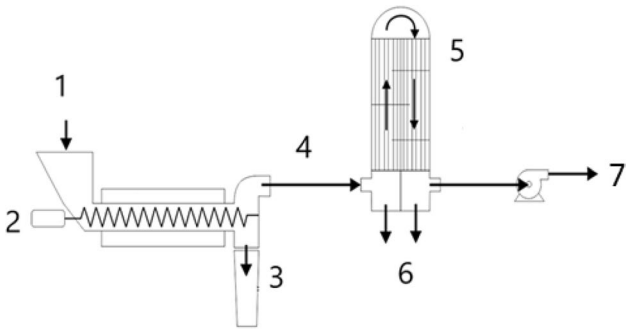

Fig. 1 Pilot-scale unit (1, tank with pelletized and non-pelletized input material; 2, oven with screw conveyor; 3, tank with solid residue; 4, organic vapors, steam, and gaseous products; 5, cooling; 6, tank with liquid residue; 7, ventilator)

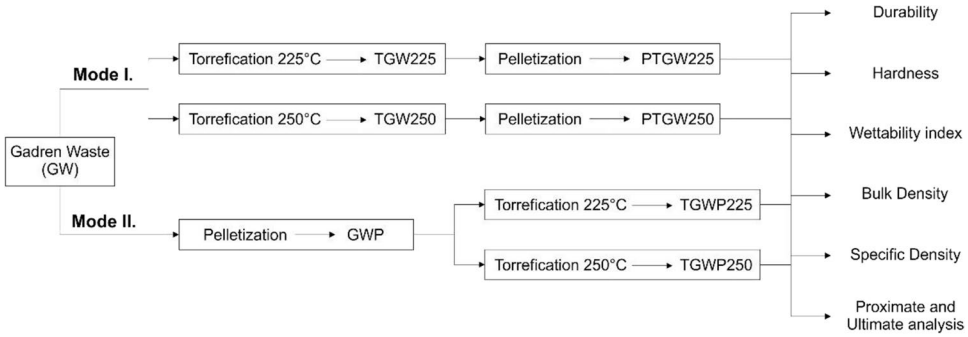

Fig. 2 Description of garden waste procedure and its evaluation (PTGW, pelletizied torrefied garden waste; TGWP, torrefied garden waste pellets)

Table 1 Biochemical composition of samples

	Lignin (%)	Cellulose (%)	Hemicellulose (%)
GW	28.10 ± 0.06	29.41 ± 1.57	15.92 ± 0.27
TGWP225	34.54 ± 1.97	28.29 ± 0.36	15.50 ± 0.18
TGW225	64.13 ± 0.28	13.70 ± 0.09	3.68 ± 0.61
TGWP250	53.24 ± 1.07	26.79 ± 0.48	6.62 ± 0.62
TGW250	74.61 ± 2.25	9.05 ± 0.61	0.15 ± 0.03

The garden waste (GW) and garden waste pellets (GWP) were torrefied at two different temperatures, i.e., 225 °C and 250 °C. These temperatures were selected on the basis of previous experiments [28]. The garden waste was poured into a tank; a certain amount of waste was continuously dosed into the furnace space. A different feeder type was selected for each material. The tube kiln was equipped with a screw conveyor. The residence time of garden waste in the oven was set up to 55 min. It was calculated on the basis of experience as the time when all the material in the apparatus was sufficiently torrefied. In case of pellets, 1.445 kg was processed per hour, while in case of bulk material, 0.780 kg was processed per hour. The total duration of one experiment was 3 h, including the residence time. The torrefied material was collected in a container. The generated gas flowed through the cooler. The condensate was collected in a tank under the cooler.

2.4 Pellets physical quality evaluation

The pellets produced during the torrefaction experiments at two different temperatures (225 and 250 °C), as well as pellets made from torrefied garden waste processed at the same temperature regime, are subjected to the analyses mentioned in Fig. 2. To clarify acronyms, TGWP means torrefaction after pelletization, while PTGW means torrefaction prior pelletization. Physical quality (durability, hardness, wettability index, bulk and specific density) of produced pellets was evaluated. Proximate and ultimate analyses were performed as well Table 1.

3 Results and discussion

3.1 Characterization of garden waste (GW)

The results of the evaluation of garden waste are shown in Table 2 and Table 3 together with the proximate and ultimate analysis results of all produced pellets. The volatile matter in

Table 3 Ultimate analysis of samples

	N (wt.%)	C (wt.%)	H (wt.%)	O (wt.%)
GW	0.83 ± 0.02	50,96 ± 0.22	6.78 ± 0.31	38.08 ± 0.04
TGWP225	0.82 ± 0.01	50.66 ± 0.07	6.35 ± 0.29	38.70 ± 0.08
PTGW225	1.15 ± 0.01	55.12 ± 0.21	5.81 ± 0.34	32.50 ± 0.14
TGWP250	0.96 ± 0.04	54.64 ± 0.56	6.08 ± 0.25	34.77 ± 0.55
PTGW250	1.17 ± 0.01	57.27 ± 0.21	5.82 ± 0.35	30.26 ± 0.15

Table 2 Proximate analysis of samples

	W (wt.%)	A^d (wt.%)	VM^d (wt.%)	FC^d (wt.%)	HHV (kJ kg^{-1})
GW	7.39 ± 0.11	3.35 ± 0.06	76.30 ± 0.63	20.35 ± 0.61	20,841 ± 49
TGWP225	2.51 ± 0.33	3.47 ± 0.16	75.04 ± 0.91	21.49 ± 0.79	21,098 ± 130
PTGW225	4.70 ± 0.06	5.42 ± 0.01	65.58 ± 0.31	29.00 ± 0.33	22,534 ± 180
TGWP250	1.98 ± 0.17	3.55 ± 0.04	74.08 ± 0.69	22.37 ± 0.65	22,244 ± 84
PTGW250	3.82 ± 0.02	5.48 ± 0.01	64.36 ± 0.05	30.16 ± 0.06	23,078 ± 26

A ash, *W* moisture, *VM* volatile matter, *FC* fixed carbon, *HHV* higher heating value

Fig. 3 Pellets

garden waste (76.30 wt.%) strongly influenced the thermal decomposition during torrefaction. The higher heating value was measured 20.9 MJ kg^{-1}, which was noticeably higher than the garden waste used by Pradhan et al. [9].

3.2 Torrefaction of garden waste

The samples were denoted according to the component acronym and final temperature. In total, four experiments in a pilot-scale unit were performed, namely torrefaction of garden waste pellets at temperature of 225 °C (TGWP225), of 250 °C (TGWP250), and torrefaction of garden waste (non-peletizied) at temperature of 225 °C (TGW225) and 250 °C (TGW250). The mass balance for each experiment was determined. A noticeable decline in mass yields with increasing temperature was noticed. The highest yield of solid residue was observed in the case of TGWP225 (93.5 wt.%), while the lowest yield was reached when processing the same sample at higher temperature (76.1 wt.%). In case of garden waste torrefaction, the solid yields were similar (TGW225 82.1 wt.%; TGW250 82.3 wt.%, respectively). The yields of energetically poor process gas did not exceed 10 wt.% (namely TGWP225 3.0 wt.%; TGWP250 5.7 wt.%; TGW225 4.5 wt.%; TGW250 8.8 wt.%). The yields of condensate ranged from 3.5 (TGWP225) to 18.2 wt.% (TGWP250).

3.3 Pelletization process

The produced pellets had a diameter of 6 mm. Garden waste pellets (GWP), torrefied garden waste pellets (TGWP), and pelletized torrefied garden waste (PTGW) are shown in Fig. 3.

3.4 Effect of torrefaction on biochemical composition

Hemicelluloses, cellulose, and lignin are three main constituents' part in lignocellulosic biomass. The number of individual components depends on the type of biomass. The garden waste sample contained 28.10 wt. % of lignin, 29.41 wt. % of cellulose, and 15.92 wt. % of hemicellulose.

During torrefaction, most of the oxygenated compounds (mainly hemicellulose) from biomass is decomposed to produce a torrefied biomass as already reported by Manouchehrinejad and Mani [23] and can be seen in Table 1. Both the temperature and the input material condition had a strong influence in terms of all components content due to their decomposition. Lignin generally increases the hardness and density of pellets. Lignin is hydrophobic, so pellets with higher lignin content show good water resistance, as can be confirmed in Table 4. Another undeniable role of lignin is that it acts as a binder at elevated temperatures; lignin softens and aids the binding process. However, the higher proportion of lignin is debatable, because it encounters the possibilities of this analytical method, which does not serve for the analysis of already partially thermally degraded (torrefied/pyrolyzed) material.

As expected, torrefaction noticeably reduced the hemicellulose content of the raw material representing volatilization and carbonization during the torrefaction process. This hemicellulose loss reduced the hydrogen bonding sites in the

Table 4 Physical properties of pellets

	BD ($kg.m^{-3}$)	H (kg)	WI (%)	SD ($g.cm^{-3}$)	D (%)
GWP	502.54 ± 14.77	21.10 ± 1.61	13.54 ± 4.30	1.27 ± 0.02	99.08 ± 0.20
TGWP225	585.87 ± 8.99	21.90 ± 1.97	9.35 ± 4.65	1.14 ± 0.02	99.32 ± 0.15
PTGW225	492.35 ± 14.15	30.30 ± 6.72	3.06 ± 2.21	1.29 ± 0.01	95.05 ± 1.07
TGWP250	516.73 ± 10.89	20.10 ± 1.92	0.59 ± 0.94	1.04 ± 0.02	97.60 ± 0.33
PTGW250	554.82 ± 15.92	22.90 ± 7.91	1.73 ± 0.73	1.06 ± 0.05	72.85 ± 6.43

BD bulk density, *H* hardness, *WI* wettability index, *SD* specific density, *D* durability

material which caused a poorer affinity to water. This also explains why torrefied material was more hydrophobic compared to the raw material as mentioned by Ghiasi et al. [20].

3.5 Effect of torrefaction in terms of fuel properties

The thermal decomposition of all samples is investigated through thermogravimetric and calorific analysis as can be seen below in Table 2.

By torrefaction, the biomass losts its natural moisture, which then had an adverse effect on the pelletization process, as stated by Kambo and Dutta [7]. With increasing temperature, the fixed carbon content increased, while volatile matter decreased; this was reflected in an increase in the value of HHV (20 841 to 23 078 kJ kg^{-1}). This trend is in line with literature sources [15, 18]. The increasing HHV tendency during torrefaction was similar as reported by other researchers [3, 17]. Thus, it can be concluded that torrefaction is very important to promote the fuel quality of biomass pellets. The ash content increased, especially for PTGW mode, compared to raw material. These results are correspond to Ramakrishna's findings [18]. When comparing the influence of pelletization on torrefaction, better properties regarding fuel qualities were reached in the mode of torrefaction prior pelletization (PTGW). The disadvantage of pellets is their mass (volume), through which the heat must pass while the products of pyrolysis go out in turn. The time of this process was significantly higher compared to the torrefaction of small biomass particles. However, this parameter must be compared with the production capacity, where thanks to the higher bulk density it was able to process up to 2 × more material in the same time. By extending the residence time, it would be possible to obtain pellets of the same composition as in case of small torrefied biomass. Oxygen contained in the material generally contributed to fuel combustion but reduced the heating values as was confirmed. The moisture content of the pellets which were subsequently torrefied (TGWP) was only 2.5% compared to 4.7% of the moisture presented in the torrefied and subsequently pelletized material (PTGW). This trend was also reported by Ghasi et al. [20]. Elemental composition is given in Table 3.

3.6 Effect of torrefaction on the physical quality of pellets

For all pellet samples, durability, bulk and specific density, wettability index, and hardness were determined. The results of the individual experiments are presented in Table 4, which gives the average values for individual samples. The results showed that the hardness of the pelletized torrefied garden waste, i.e., torrefaction prior pelletization, at 225 °C is greater than that of torrefied garden waste pellets, i.e., torrefaction after pelletization, which corresponds to Spîrchez et al. [21]. The torrefaction process contributed to the hardness of the pellets. However, as the torrefaction temperature increased, the hardness and durability of pellets decreased; this effect was particularly noticeable in case of torrefaction prior pelletization. The pellet hardness decreased at higher torrefaction temperatures as described elsewhere in the literature [22, 23]. However, torrefaction in these studies was performed for wood respectively furfural residue pellets, not for available garden waste.

Wettability index decreased with material modification. The lowest water absorption was indicated for the TGWP250 sample with a value of 0.59%. A significant decrease in WI with torrefaction temperature was evident, for both PTGW and TGWP samples. Water absorption affected the calorific value of the fuel (see Table 2). Within the individual modifications (PTGW/TGWP), it is evident that a higher torrefaction temperature caused the WI decrease with a simultaneous HHV increase. Moisture of the pellets is undesirable as it can cause swelling and clogging of transport systems. In addition, there is also a possible risk of mold creation during storage. All produced pellets showed a higher specific density than water. Both modified pellets prepared at temperature of 250 °C floated on water. The result again confirmed the increased hydrophobicity of these pellets. The mechanical resistance of the pellets was significantly affected by the torrefaction temperature. A significant decrease in this parameter was observed at the temperature of 250 °C.

Generally speaking, the mechanical resistance of composts starts from 90.0% [29, 30]. However, the *D* value of the PTGW250 sample (73%) was low and unsatisfactory; on the other hand, these pellets showed a slightly better value in terms of hardness. Since wettability index and hardness are not normative parameters, which could be evaluated by standard procedures, they were compared with hay pellets produced by our team, to make thorough evaluation possible [31]. Their durability reached 98.9%; wettability index was 17% and hardness 33.6 kg. These hay pellets with a moisture content of 6.3% and ash ≤ 6% normatively complied with the EN 17,225–6 standard. It can be seen that only GWP, TGWP225, and TGWP250 pellets would be suitable according to durability D, which can be considered as satisfactory according to the standard D ≥ 97.5%. Durability for PTGW225 and PTGW250 can be effectively increased by adding a suitable binder such as starch, lignosulfonate, bentonite, and modified cellulose [32]. The choice of binder should be considered with regard to its cost and environmental friendliness. From this point of view, using also waste as a binder in the production of PTGW225 and PTGW250 seems to be the only appropriate approach given their low cost and availability. For example, fallen pinecones could be added to garden waste as a binder. However, by how much durability would be raised is a question of further study.

The comparison also shows that the WI was significantly lower (better) for all samples except GWP. Again, it corresponds to the increasing hydrophobicity of the torrefaction-treated pellets. At the same time, a higher torrefaction temperature reduced the WI and increased the HHV (Table 2). The hardness (H) of the tested samples widely ranged. For hay and energy grass pellets, this range was measured from 33.6 to 47.7 kg. By processing garden waste by both modes, significant changes occurred in terms of hardness. The value of around 20 kg for TGWP250, TGWP225, and GWP was lower; therefore, the handling of these pellets could be more complicated. However, the value of this parameter can be influenced by the torrefaction process and the temperature setting. The durability of the torrefied pellets was also fairly close and comparable to that of the raw material pellets which also corresponds to data measured by Ghasi et al. [20].

Micro-structural analysis of all pellets is presented in Fig. 4. The preparation process had a significant influence on the morphological structure. The analysis clearly shows that pellets had large quantities of small flakes on the surface. Unlike the pellets from the torrefied material, only small cracks appeared on the surface. This is due to the fact that torrefied garden waste was dry and without any binders, making it possible to create strong pellets without cracks on their surface. The flakes on the surface of these pellets were bigger, in comparison with TGWP. Their quantity increased with growing temperature. The micro-structural analysis of torrefied pellets showed that the natural binders in these biomass materials created bonding between particles in the pellets. Activating the natural binding components through moisture and temperature is essential to produce highly durable pellets.

FTIR spectrum (Fig. 5) was measured for study of surface properties of torrefied material. Difference between TGWP and PTGW is invisible, but can be observed small effect of torrefaction temperature to change of surface function groups. With increasing temperature, we can see a decrease in the broad peak representing the O–H group at 3440 cm^{-1}. Another decrease to almost disappearance of the peak is at

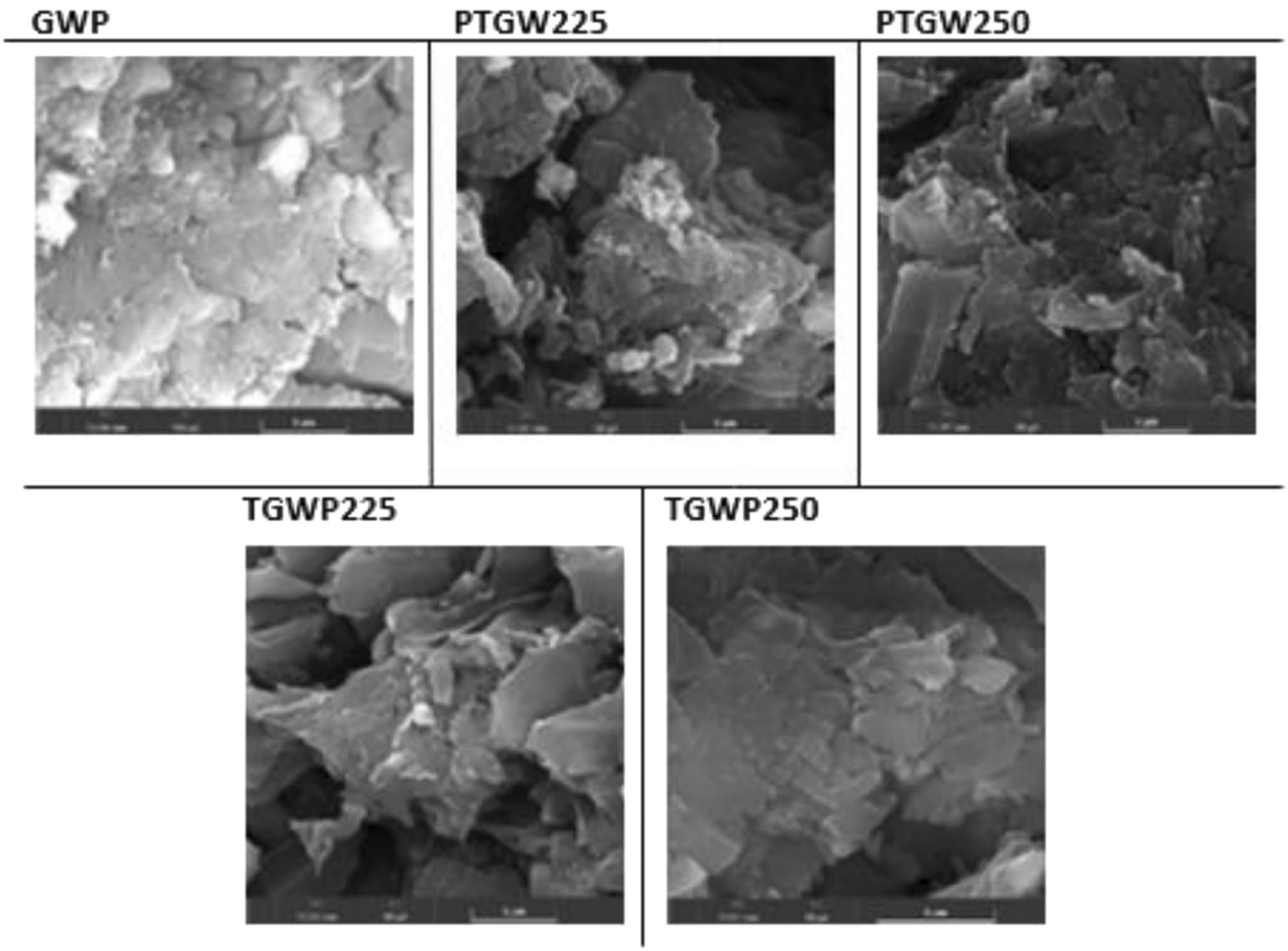

Fig. 4 Micrographs of GW, PTGW225, PTGW250, TGWP225, TGWP250 (SEM: SE-BSE)

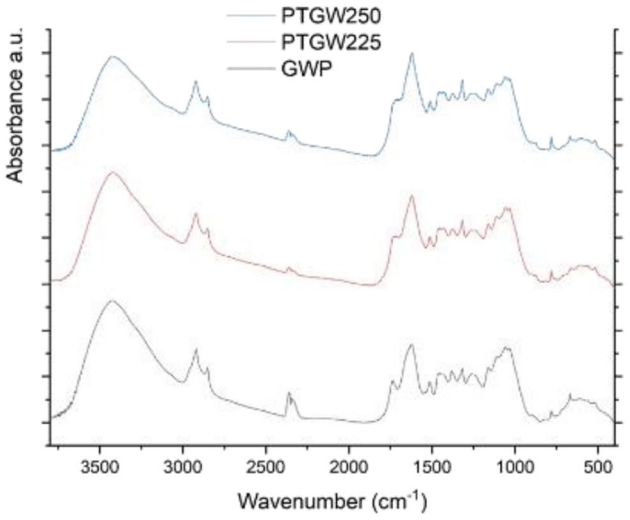

Fig. 5 FTIR spectrum of the pelletized torrefied garden waste

1740 cm^{-1} where the C = O group is associated with carboxylic acids. These disappearing carboxylic acid groups, in turn, appear in the liquid condensate-pyrolysis water. A certain decrease in peaks can be observed in the range from 1150 to 1030 cm^{-1} where the C-O group is located; the decrease in oxygen content is also observable from the elemental analysis. All these changes are related to the loss of oxygen and O–H group and the formation of hydrophobicity. However, it is necessary to mention a small increase of the peak at 1625 cm^{-1} representing the C = C group. It is the wide peak of the O–H group between 3400 and 3300 cm^{-1} in combination with C = C group and a small group of C-O peaks that indicates the presence of phenolic groups. Peak at 2350 cm^{-1} is probably due to adsorbed CO_2, created during torrefaction, and can be neglected.

4 Conclusions

This study compared two different process modes to convert garden waste into torrefied binder-free pellets as the final product. From the measured data, it can be stated that both modes have their advantages and they are also accompanied by some difficulties.

Pellets prepared in mode I (torrefaction prior pelletization) showed better fuel properties (calorific value, carbon content), but it is worth mentioning that after torrefaction, pellets of lower quality concerning mainly their durability were produced. In addition, the pelletization of torrefied garden waste was due to the mechanical and physical properties of the material (brittleness, friability, fluffiness) more complicated than pelletization of non-toredified garden waste. The torrefied material adhered to the walls of the hopper, layered, and had to be mechanically removed during pelletization. However, the selection of an optimal binder, which is not the subject of this study, might help to optimize the durability. Moreover, these binders often significantly increase demands in terms of costs and energy uses. For pellets prepared in mode II, it is necessary to strictly monitor the residence time in order to heat the entire volume of the pellet to the center, because fuel properties of torrefied pellet were worse at the same retention time in reactor than torrefied fine GW particles. On the other hand, during pellet torrefaction, organic vapors such as furfural or phenols, act as a natural binder, which improves the mechanical properties of the pellets. Further work would be appropriate to determine the optimum pelletizing conditions for the production of pellets with reasonable transportable properties and a high potential in different end product applications when charging costs associated with the binders.

Funding This work was supported by EU structural funding in Operational Programme Research, Development and Education, project No. CZ.02.1.01/0.0/0.0/16_019/0000853 "IET-ER", and project No. CZ.01.1.02/0.0/0.0/16_084/0010290 "Torrefaction for small and mobile units", and by using Large Research Infrastructure ENREGAT supported by the Ministry of Education, Youth and Sports of the Czech Republic under project No. LM2018098 and under OP RDE grant number CZ.02.1.01/0.0 /0.0 /16_019/0000753 "Research centre for low-carbon energy technologies".

Declarations

Ethics approval All authors approved the version to be published. All authors agree to be accountable for all aspects of the work in ensuring that questions related to the accuracy or integrity of any part of the work are appropriately investigated and resolved.

Competing interests The authors declare no competing interests.

References

1. Ribeiro JMC, Godina R, Matias JCO de, Nunes LJR (2018) Future perspectives of biomass torrefaction: review of the current state-of-the-art and research development. Sustainability Sustainability, MDPI 10(7):1–17
2. Turner I, Rousset P, Rémond R, Perré P (2010) An experimental and theoretical investigation of the thermal treatment of wood (Fagus sylvatica L.) in the range 200–260 °C. Int J Heat Mass Transf 53(4):715–725. https://doi.org/10.1016/j.ijheatmasstransfer.2009.10.020
3. Zhang Y, Chen F, Chen D, Cen K, Zhang J, Cao X (2020) Upgrading of biomass pellets by torrefaction and its influence on the hydrophobicity, mechanical property, and fuel quality. Biomass Convers Biorefin. https://doi.org/10.1007/s13399-020-00666-5
4. Cahyanti MN, Doddapaneni TRKC, Kikas T (2020) Biomass torrefaction: an overview on process parameters, economic and environmental aspects and recent advancements. Bioresour Technol 301:122737. https://doi.org/10.1016/j.biortech.2020.122737

5. Mun TY, Tumsa TZ, Lee U, Yang W (2016) Performance evaluation of co-firing various kinds of biomass with low rank coals in a 500 MWe coal-fired power plant. Energy 115:954–962. https://doi.org/10.1016/j.energy.2016.09.060
6. Toptas A, Yildirim Y, Duman G, Yanik J (2015) Combustion behavior of different kinds of torrefied biomass and their blends with lignite. Bioresour Technol 177:328–336. https://doi.org/10.1016/j.biortech.2014.11.072
7. Kambo HS, Dutta A (2014) Strength, storage, and combustion characteristics of densified lignocellulosic biomass produced via torrefaction and hydrothermal carbonization. Appl Energy 135:182–191. https://doi.org/10.1016/j.apenergy.2014.08.094
8. Kaliyan N, Morey RV (2010) Natural binders and solid bridge type binding mechanisms in briquettes and pellets made from corn stover and switchgrass. Bioresour Technol 101(3):1082–1090. https://doi.org/10.1016/j.biortech.2009.08.064
9. Pradhan P, Arora A, Mahajani SM (2018) Pilot scale evaluation of fuel pellets production from garden waste biomass. Energy Sustain Dev 43:1–14. https://doi.org/10.1016/j.esd.2017.11.005
10. Hu Q, Shao J, Yang H, Yao D, Wang X, Chen H (2015) Effects of binders on the properties of bio-char pellets. Appl Energy 157:508–516. https://doi.org/10.1016/j.apenergy.2015.05.019
11. Emadi B, Iroba KL, Tabil LG (2017) Effect of polymer plastic binder on mechanical, storage and combustion characteristics of torrefied and pelletized herbaceous biomass. Appl Energy 198:312–319. https://doi.org/10.1016/j.apenergy.2016.12.027
12. Agar DA (2017) A comparative economic analysis of torrefied pellet production based on state-of-the-art pellets. Biomass Bioenerg 97:155–161. https://doi.org/10.1016/j.biombioe.2016.12.019
13. García R, González-Vázquez MP, Martín AJ, Pevida C, Rubiera F (2020) Pelletization of torrefied biomass with solid and liquid bio-additives. Renew Energy 151:175–183. https://doi.org/10.1016/j.renene.2019.11.004
14. García R, González-Vázquez MP, Pevida C, Rubiera F (2018) Pelletization properties of raw and torrefied pine sawdust: effect of co-pelletization, temperature, moisture content and glycerol addition. Fuel 215:290–297. https://doi.org/10.1016/j.fuel.2017.11.027
15. Saba A, Saha N, Williams KC, Coronella CJ, Reza MT (2020) Binder-free torrefied biomass pellets: significance of torrefaction temperature and pelletization parameters by multivariate analysis. Biomass Convers Biorefi. https://doi.org/10.1007/s13399-020-00737-7
16. Chen WH, Peng J, Bi XT (2015) A state-of-the-art review of biomass torrefaction, densification and applications. Renew Sustain Energy Rev 44:847–866. https://doi.org/10.1016/j.rser.2014.12.039
17. Chen WH, Zhuang YQ, Liu SH, Juang TT, Tsai CM (2016) Product characteristics from the torrefaction of oil palm fiber pellets in inert and oxidative atmospheres. Bioresour Technol 199:367–374. https://doi.org/10.1016/j.biortech.2015.08.066
18. Ramakrishna V, Singh AK, Bayen GK et al (2021) "Torrefaction of agro-wastes (palmyra palm shell and redgram stalk): characterization of the physicochemical properties and mechanical strength of binderless pellets,". Biomass Conv Bioref. https://doi.org/10.1007/s13399-021-01720-6
19. Chew JJ, Doshi V (2011) Recent advances in biomass pretreatment - torrefaction fundamentals and technology. Renew Sustain Energy Rev 15(8):4212–4222. https://doi.org/10.1016/j.rser.2011.09.017
20. Ghiasi B et al (2014) Densified biocoal from woodchips: is it better to do torrefaction before or after densification? Appl Energy 134:133–142. https://doi.org/10.1016/j.apenergy.2014.07.076
21. Spîrchez C, Lunguleasa A, Antonaru C (2017) Experiments and modeling of the torrefaction of white wood fuel pellets. BioResources 12(4):8595–8611. https://doi.org/10.15376/biores.12.4.8595-8611
22. Brachi P, Chirone R, Miccio M, Ruoppolo G (2019) Fluidized bed torrefaction of biomass pellets: a comparison between oxidative and inert atmosphere. Powder Technol 357:97–107. https://doi.org/10.1016/j.powtec.2019.08.058
23. Manouchehrinejad M, Mani S (2018) Torrefaction after pelletization (TAP): Analysis of torrefied pellet quality and co-products. Biomass Bioenerg 118(March):93–104. https://doi.org/10.1016/j.biombioe.2018.08.015
24. Siyal AA et al (2020) Torrefaction subsequent to pelletization: characterization and analysis of furfural residue and sawdust pellets. Waste Manag 113:210–224. https://doi.org/10.1016/j.wasman.2020.05.037
25. Abedi A, Dalai AK (2017) Study on the quality of oat hull fuel pellets using bio-additives. Biomass Bioenerg 106:166–175. https://doi.org/10.1016/j.biombioe.2017.08.024
26. Kaliyan N, Vance Morey R (2009) Factors affecting strength and durability of densified biomass products. Biomass Bioenergy 33(3):337–359. https://doi.org/10.1016/j.biombioe.2008.08.005
27. ISO (2015) "ISO 17828:2015 Solid biofuels - Determination of bulk density," Int Organ Stand. Published 10-Dec-2015
28. Grycova B, Pryszcz A, Krzack S, Klinger M, Lestinsky P (2020) Torrefaction of biomass pellets using the thermogravimetric analyser. Biomass Convers Biorefin. https://doi.org/10.1007/s13399-020-00621-4
29. Ryu C, Finney K, Sharifi VN, Swithenbank J (2008) Pelletised fuel production from coal tailings and spent mushroom compost - Part I. Identification of pelletisation parameters. Fuel Process Technol 89(3):269–275. https://doi.org/10.1016/j.fuproc.2007.11.035
30. Zajonc O, Frydrych J, Jezerska L (2014) Pelletization of compost for energy utilization. IERI Procedia. https://doi.org/10.1016/j.ieri.2014.09.002
31. Jezerska L, Drozdova J, Rozbroj J, Zegzulka J, Frydrych J (2019) Pelletization of energy grasses: a study on the influence of process and material parameters on pellet quality. Int J Green Energy 16(14):1278–1286. https://doi.org/10.1080/15435075.2019.1671402
32. Ahn BJ et al (2014) Effect of binders on the durability of wood pellets fabricated from Larix kaemferi C. and Liriodendron tulipifera L. sawdust. Renew Energy 62:18–23. https://doi.org/10.1016/j.renene.2013.06.038

Příloha [P3]

LESTINSKY, P., GRYCOVA, B., PRYSZCZ, A., MARTAUS, A. & MATEJOVA, L. 2017. Hydrogen production from microwave catalytic pyrolysis of spruce sawdust. *Journal of Analytical and Applied Pyrolysis,* 124**,** 175-179. IF_{2017} = 3,468 (5 year IF 5.914). Autorský podíl 50 %. Počet citací dle WoS 42.

Role uchazeče:

- návrh tématu, návrh postupu prací, experimentální práce v laboratoři, vyhodnocení výsledků, vyvození závěrů z dosažených výsledků

Journal of Analytical and Applied Pyrolysis 124 (2017) 175–179

Contents lists available at ScienceDirect

Journal of Analytical and Applied Pyrolysis

journal homepage: www.elsevier.com/locate/jaap

Hydrogen production from microwave catalytic pyrolysis of spruce sawdust

Pavel Lestinsky*, Barbora Grycova, Adrian Pryszcz, Alexandr Martaus, Lenka Matejova

Institute of Environmental Technology, VSB – Technical University of Ostrava, 17. listopadu 15/2172, 708 33 Ostrava, Czechia

ARTICLE INFO

Article history:
Received 16 December 2016
Received in revised form 2 February 2017
Accepted 2 February 2017
Available online 3 February 2017

Keywords:
Hydrogen
Microwave
Catalysts
Pyrolysis
Biomass

ABSTRACT

The production of energy from wood biomass is as old as humanity itself. In the last 20 years there has been enormous progress in research of torrefaction, pyrolysis and mainly gasification of biomass. Products from conventional pyrolysis of biomass are gas known as pyrolysis gas, a liquid condensate known as bio-oil and char named bio-char. Most of the articles dealing with convectional pyrolysis of biomass are focused on the production of bio-oil. Only some works deal with the possibility of producing high-quality syngas (H_2 + CO) or hydrogen itself. For this purpose, the technology of microwave pyrolysis could be suitable. Microwaves can generate microplasma and hot spots, which promote heterogeneous catalytic reactions and produce a greater concentration of hydrogen in the resulting gas than convectional pyrolysis. In this work, an experimental study of spruce sawdust microwave pyrolysis was performed in the presence of catalysts to maximize the yield of hydrogen or syngas. Experiments were carried out in a microwave reactor with a power of 400 W. As catalysts char from sawdust, or sawdust char-doped with metal ions (Ni, Co, Fe) were used. Ions of metals were used to increase the yield of hydrogen (e.g. Nickel is widely used in the catalytic cracking of methane). The influence of the catalyst on the quantity of products (gas, liquid and solid) was studied, as well as the amount of hydrogen generated in the pyrolysis gas, or the amount of waste water in the liquid condensate.

1. Introduction

Hydrogen is the oldest and simplest element in the universe. Hydrogen can be produced in many ways. Most environmentally friendly method is electrolysis of water. The large consumption of electricity is main disadvantage of this method for industrial production. The thermal decomposition of hydrocarbons is another option to obtain hydrogen.

Declining supplies of fossil energy resources and adverse impacts of fossil energy uses on the worldwide environment have prompted a strong interest in renewable energy. Biomass can be used as a renewable energy source. There are already several possible industrial processing methods, such as combustion, gasification, pyrolysis, liquefaction or torrefaction [1,2]. The microwave technique is one of the most promising methods of enhancing and accelerating chemical reactions. Fast, selective, and uniform heating are the first advantages of this method which make the treatment and utilization of non-homogeneous wastes and large size biomass feasible. Process flexibility and equipment portability are the other advantages of this technique [3]. The choice of material for microwave radiation absorption is the most important parameter in the case of microwave heating. Materials such as activated carbon or charcoal absorb radiation more than distillate water. Carbon materials can be used as an effective absorbent of microwave radiation [4]. Microwave heating for treatment of various materials, such as biomass [5], coal [6] or waste oil [7] was done. The heating of material occurs when microwave radiation is absorb by carbon particles and this energy is converted to thermal energy by dipole reorientation (polarisation) and ionic conduction [8]. These mechanisms generate heat within the carbon particles. The accurate measurement of temperature is one of the most important challenges under microwave pyrolysis as it affects the reaction's conditions and efficiency. Choosing the correct temperature sensor seems critical to reduce measurement errors.

Microwave heating is often used for catalytic reaction. Fidalgo et al. [9] used microwave radiation for heating of catalytic bed for CO_2 and CH_4 reforming. As a catalyst mixture of carbon with Ni on Alumina was used. Conversion in microwave heating was higher, than during reforming in conventional oven at the same temperature. The using of microwave heating in the other scientific works [10,11] shows the great potential to catalyse. The effect of conventional and microwave-assisted methods for syngas production

* Corresponding author.
E-mail address: pavel.lestinsky@vsb.cz (P. Lestinsky).

http://dx.doi.org/10.1016/j.jaap.2017.02.008
0165-2370/

Table 1
Proximate and ultimate analysis of spruce sawdust.

Material	Spruce sawdust
Proximate analysis (wt.%)	
Moisture	0.64 ± 0.04
Volatiles	77.51 ± 0.65
Fixed Carbon	21.25 ± 0.24
Ash	0.60 ± 0.05
Ultimate analysis (wt.%)	
C	51.74 ± 0.38
N	0.96 ± 0.07
H	6.07 ± 0.11
O^{diff}	41.23 ± 0.47

from glycerol was compared within the three different processes, namely pyrolysis, steam reforming, and dry reforming by using commercial activated carbon as the catalyst [12]. The results proved that the microwave-assisted heating method produced higher gas yields in comparison with conventional heating methods. Additionally, it was observed that the use of a carbonaceous catalyst improved syngas production and produced the least amount of CO_2 emissions.

In this study, microwave pyrolysis of spruce sawdust was performed in the presence of catalysts to maximize the yield of hydrogen, or syngas. As catalysts char from sawdust or sawdust char-doped with metal ions (Ni, Co, Fe) were used. Ions of metals were used to increase the yield of hydrogen (e.g. Nickel is widely used in the catalytic cracking of methane). The influence of the catalyst on the quantity of products (gas, liquid and solid) was studied as well as the amount of hydrogen generated in the pyrolysis gas, and the amount of waste water in the liquid condensate.

2. Material and methods

2.1. Raw material

Spruce sawdust was used as a feed biomass material. The spruce sawdust was dried at 105 °C for 24 h before each experiment. The ultimate and proximate analyses of spruce sawdust (dry) were performed on analysers LECO TGA701 and LECO CHSN628 (Table 1).

2.2. Preparation of char and char-doped catalyst

The spruce sawdust was thermal treated in a microwave reactor for 20 min at 400 W. The prepared char was used as an absorber of microwave irradiation and the experiment was labelled as carbonaceous material, abbreviated as CM. The spruce sawdust was mixed with 0.1 M aqueous solution of $Ni(NO_3)_2{\cdot}6H_2O$, $Co(NO_3)_2{\cdot}6H_2O$ and $Fe(NO_3)_3.9H_2O$. Samples of sawdust were wet-impregnated for 24 h in these solutions. The impregnated sawdust was dried at a temperature of 110 °C in an oven for 48 h. These dried wet-impregnated samples were treated in the microwave reactor to obtain char (char-doped metallic catalyst) in the inert atmosphere. These experiments are labelled according to the metal element used – nickel as Ni, cobalt as Co and iron as Fe. The average content of metal on the carbon surface is 7 wt.%. The proximate analysis of char (CM) and char-doped metallic catalysts (Ni, Co, Fe) were performed on analyser LOCO TGA701 (Table 2).

2.3. Characterisation of catalysts

The textural properties of ACs were evaluated based on nitrogen physisorption. The nitrogen adsorption – desorption measurements at 77 K were performed using a 3Flex instrument (Micromeritics, USA). Prior to the nitrogen physisorption measurements, the ACs were degassed at 300 °C for 24 h under a vacuum

Table 2
Proximate analysis of char and char-doped catalysts.

	W^r (wt.%)	V^r (wt.%)	FC^r (wt.%)	A^r (wt.%)
CM	0.97 ± 0.02	10.59 ± 0.84	85.82 ± 0.84	2.62 ± 0.84
Ni	0.95 ± 0.03	14.11 ± 0.97	73.67 ± 0.84	11.27 ± 0.84
Co	0.71 ± 0.02	14.60 ± 0.82	73.88 ± 0.84	10.81 ± 0.84
Fe	0.94 ± 0.02	15.86 ± 0.93	71.06 ± 0.84	12.14 ± 0.84

of less than 1 Pa. The specific surface area, S_{BET}, was calculated according to the Brunauer–Emmett–Teller (BET) theory for the p/p_0 range = 0.05–0.25. Whereas S_{BET} is not appropriate parameter for characterisation of mesoporous solids containing micropores [13], the mesopore surface area, S_{meso}, and the micropore volume, V_{micro}, were also evaluated from the t-plot method [14], using Carbon Black STSA standard isotherm. The total pore volume, V_{net}, was determined from the nitrogen adsorption isotherm at p/p_0 (~0.988). The mesopore-size distribution was evaluated from the adsorption branch of the nitrogen adsorption-desorption isotherm by the Barrett–Joyner–Halenda (BJH) method [15], using the Carbon Black STSA standard isotherm with Faas correction. The micropore-size distribution was evaluated from the low-pressure part of the nitrogen adsorption isotherm ($10^{-7} < p/p_0 < 0.05$) by the application of the Horvath-Kawazoe solution for the slit-pore geometry of carbonaceous materials [16] using the Micromeritics software.

The phase composition was determined using X-ray powder diffraction. The XRD patterns were obtained using Rigaku SmartLab diffractometer (Rigaku, Japan) with the detector D/teX Ultra 250. The source of X-ray irradiation was a cobalt lamp (CoKα, 0.15418 nm), operated at 40 kV and 40 mA. The powder samples were pressed in a carousel holder and measured in the reflection mode. The XRD patterns were collected in a 2θ range from 5° to 90° with a step of 0.02° and speed of 1.5087° min. The registered XRD patterns were evaluated using the databases PDF 2 and COD.

2.4. Experimental apparatus

A 50 g of sawdust sample with 10 g of char/char-doped catalyst (the ratio of 5:1) was placed into the glass reactor. The gas-tight reactor was inserted into the microwave oven with a power of up to 1 kW and connected to the rest of the device components. The nitrogen was used as an inert medium for purging. The spruce samples with the catalyst were treated in the microwave reactor for 20 min at a power of 400 W and a frequency of 2450 MHz. Gaseous and vapours products of microwave catalytic pyrolysis were treated in the water cooler (the condensate was captured in a condensate flask) and were further purified in five gas bubblers with water and acetone. This purified pyrolysis gas flowed through the gasometer to the gas sample point. The gas samples were taken into 20 dm^3 gas sampling bags (Tedlar).

2.5. Characterization of products

The selected gaseous components were analysed by gas chromatography (methane, acetylene, ethylene, ethane, propane, hydrogen, carbon monoxide and carbon dioxide). Agilent 7890A gas chromatograph, with a flame ionization detector (FID) and a thermal conductivity detector (TCD), was used for analysis of the pyrolysis gas. The Micropacked column (2 m × 0.53 mm) was used for separation. Agilent 7890A gas chromatograph with MS detector Agilent 5975C was used for analysis of liquid products. A column of 30 m × 250 μm × 0.25 μm was used for separation. The water- and oil-phase were dissolved in methanol before chromatographic analysis. The content of water in the water- and oil-phase of condensate was analysed by Karl-Fischer titration on TitroLine 7500 KF.

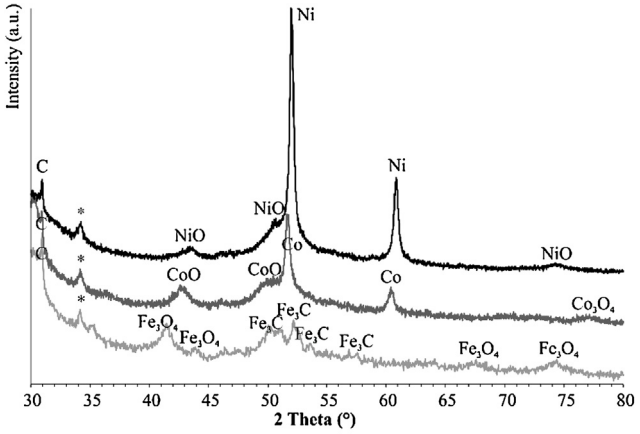

Fig. 1. XRD patterns of catalysts Ni-C and Co-C.

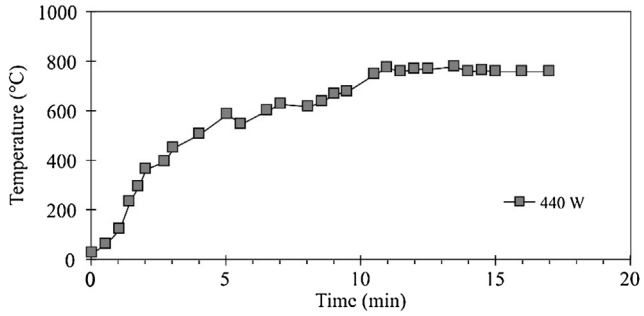

Fig. 2. Temperature profile inside bed of spruce sawdust.

Table 4
Comparison of product distribution for different catalysts.

	CM (wt.%)	Fe (wt.%)	Co (wt.%)	Ni (wt.%)
gas	31.21 ± 2.20	47.74 ± 2.33	52.72 ± 3.07	51.59 ± 2.30
liquid	46.18 ± 2.71	32.68 ± 2.21	29.42 ± 2.01	27.89 ± 2.38
solid	22.61 ± 1.13	19.58 ± 1.04	17.86 ± 1.30	20.52 ± 1.07

3. Results and discussion

3.1. Characterization of catalyst

Char and char-doped metallic catalysts were analysed using nitrogen physisorption. The results from this analysis are shown in Table 3. From the results of the surface area, it is clear that the preparation of the catalyst in the microwave reactor is very good, since the catalysts have nearly the same surfaces. This applies particularly to the CM itself, because these surface properties cannot be achieved by conventional thermal treatment without activating the surface. This relates to the fact that the microwave heats the material from the inside, thus creating a porous structure, in contrast to convectional heating, which heats the material from the surface. The cobalt and nickel catalysts have a bigger mesopores surface area, as we can see in the following table. These mesopores have a major effect on the cracking and dry/steam reforming reactions. This also explains the lowest amount of gas in the CM.

Char-doped Nickel and Cobalt catalysts were analysed using X-ray diffraction (XRD) to compare the catalyst's structure for each metallic ion (see Fig. 1). The main phases detected on the Ni-C catalyst surface included metallic nickel (Ni^0) (2*Theta* = 52.0° and 60.9°), a small amount of nickel oxide (NiO) (2*Theta* = 43.3°, 50.8° and 74.5°), and finally carbon (C^0) (2*Theta* = 30.9°). Similarly, the main phases detected on the Co-C catalyst surface were metallic cobalt (Co^0) (2*Theta* = 51.7° and 60.5°), a small amount of cobalt oxides (CoO) (2*Theta* = 42.8° and 50.5°) and (Co_3O_4) (2*Theta* = 77.1°), and finally carbon (C^0) (2*Theta* = 30.9°). The main phases detected on the Fe-C catalyst surface were iron carbide (Fe_3C) (2*Theta* = 50.5°, 52.3°, 56.9° and 57.7), a small amount of iron oxides (Fe_3O_4) (2*Theta* = 41.5°, 44.0°, 67.6° and 74.5°), and finally carbon (C^0) (2*Theta* = 30.8°). The Fe-C catalyst has not any content of metallic iron, which conflicts with literature [17].

The peak marked as (*) at 2*Theta* = 34.2° is magnesium calcite ($Mg_{0.03}Ca_{0.97}CO_3$). It is a common component of biomass ash.

This catalyst structure gives us some interesting information, because metallic nickel has a higher catalytic activity than nickel oxide for dry and stream reforming reactions.

The metallic nickel (Ni^0) as well as cobalt (Co^0) are generated by reducing hydrogen at a high temperature. The temperature inside the microwave reactor was measured using a K-type thermocouple, which has to be grounded and shielded. The increase of the temperature in the microwave reactor with power of 400 W is shown in Fig. 2. The temperature inside the bed was stabilized at 780 °C after 10 min. Shi et al. [18] found that metallic iron (Fe^0) can be created from iron oxides at the temperature above 800 °C, but the iron carbide (Fe_3C) was created too. The formation of iron carbide (Fe_3C) was observed at the 1000 °C. Iron carbide decomposed to the iron above 1600 °C, which corresponds with knowledge of the equilibrium iron-carbon phase diagram. On the other site, iron carbide together with iron oxide are used as catalyst too.

3.2. Mass balance

Three products of catalytic microwave pyrolysis were produced – pyrolysis gas as gas, liquid condensate as liquid and solid residue as char. The balance was calculated based on the weight of char and gas volume together with the composition of the pyrolysis gas. The amount of condensated liquid in the cooler was only 90 wt.% of the overall liquid, the rest of non-condensated liquid, such as tar-vapour dispersion, were absorbed in the water and the acetone bubblers. This weight was recalculated to 100 wt.%. The product distribution is listed in Table 4. It is obvious that the presence of catalysts has affected the gas production. The metallic catalysts,

Table 3
Textural properties of activated carbons determined from nitrogen physisorption.

	S_{BET} ($m^2\ g^{-1}$)	S_{meso} ($m^2\ g^{-1}$)	V_{micro} ($cm^3_{liq}\ g^{-1}$)	V_{net} ($cm^3_{liq}\ g^{-1}$)	V_{micro}/V_{net} (%)	L_{micro} (nm)
CM	341	35	0.150	0.192	78	0.43
Fe	342	73	0.132	0.244	54	0.45
Ni	343	104	0.118	0.267	44	0.43
Co	335	134	0.099	0.275	36	0.45

S_{BET} specific surface area.
S_{meso} mesopore surface area.
V_{micro} volume of micropores.
V_{net} total pore volume at relative pressure $p/p_0 = 0.988$.
L_{micro} median micropore width.

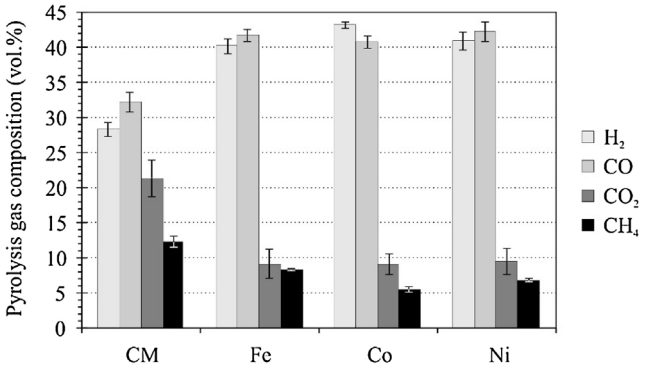

Fig. 3. Comparison of pyrolysis gas composition for different catalysts.

especially cobalt and nickel, reduced the amount of the liquid, specifically cracked more tars and hydrocarbons into gaseous products than the separate carbonaceous material (CM).

3.3. Pyrolysis gas composition

The pyrolysis gas composition was very dependent on the catalyst used; especially char vs. doped-char. The main components of gas are shown in Fig. 3.

We can see that the amount of hydrogen generated in the case of cobalt and nickel catalysts is almost double compared to the experiment only with CM. These results of gas composition can be explained by the dry and steam reforming reaction. The catalytic effect of metal in the char promoted several types of cracking and reforming reactions. Zhang et al. [17] published list of reactions which have big effect to the difference in syngas composition, such as tar cracking reactions, hydrocarbons and methane dry reforming reactions, hydrocarbons and methane steam reforming reaction and water gas-shift reactions. And finally, the reduction of carbon due to the Boudouard reaction. These reactions are promoted by metallic catalysts.

The change of pyrolysis gas composition due to the dry and steam reforming reaction is listed in Table 5. It is evident that the concentration of CH_4, C_xH_y and CO_2 decreased with the presence of cobalt and nickel catalysts. Hydrogen production in microwave pyrolysis with a Fe catalyst was high, as well as with nickel and cobalt. Due to higher water content in the liquid phase for Fe catalyst it is assumed, that the increase of hydrogen was not achieved through methane dry reforming reaction, but probably due to the decomposition of tar and tar reforming reaction (see Table 5).

3.4. Liquid condensates

The liquid condensate was a mixture of water and organic liquids. The composition of liquid condensate was analysed by Karl-Fisher titration to determine the water content in the water- and oil-phase and by gas chromatography (with a mass spectrometer) to determine organic compounds. The content of water in the water-phase is listed in Table 6. The content of water in the oil-phase (from pyrolysis with CM) was only 5.63 wt.%. The oil-phase was not observed in the condensate flask during the pyrolysis with metallic catalyst, but 10 wt.% of liquid condensate was absorbed in water and acetone bubblers. Therefore, it is possible to say that components from the oil-phase of the liquid condensate were cracked during the catalytic pyrolysis. The content of water in the water-phase was very high. This high content is caused by a reverse water gas-shift reaction, especially for the Fe catalyst.

The metallic catalysts have big effect on the amount of oil-phase in the liquid product. The amount of oil-phase created with metallic catalyst was lower than the amount obtained with pyrolysis without catalyst. On the other hand, the composition change in the liquid product was small.

The composition of organic species in the water phase of liquid condensate is a little bit more complicated. The composition in Table 7 is approximately similar. It can be estimated that the organic substances contained in the condensate are not involved in the catalytic cracking reactions. These substances are formed by thermal decomposition of wood or his part (cellulose, hemicellulose and lignin). The short residence time in the bed and minimal contact with a catalytically active surface is main reason, why these compounds are not decomposed to lighter hydrocarbons or gases and were captured after cooling as a condensate. It can be assumed that by modifying batch reactor to the tubular reactor with plug flow through the catalyst bed will improve the catalytic cracking reactions. A change of composition of the condensate was observed in some experiments, e.g. with furfural. But the overall catalytic effect on the oil-phase is much more complicated and requires further research in the field of bio-oils and catalysis.

Table 5
Pyrolysis gas composition for different catalysts.

	CM (vol.%)	Fe (vol.%)	Co (vol.%)	Ni (vol.%)
H_2	28.37 ± 1.03	40.24 ± 1.08	43.22 ± 0.50	41.00 ± 1.28
CO	32.27 ± 1.38	41.74 ± 0.83	40.81 ± 0.82	42.25 ± 1.41
CO_2	21.30 ± 2.69	9.05 ± 2.04	9.03 ± 1.46	9.42 ± 1.91
CH_4	12.34 ± 0.78	8.22 ± 0.13	5.42 ± 0.42	6.85 ± 0.24
C_2H_2	0.164 ± 0.009	0.029 ± 0.007	0.015 ± 0.007	0.016 ± 0.010
C_2H_4	2.110 ± 0.071	0.620 ± 0.031	0.263 ± 0.037	0.415 ± 0.066
C_2H_6	0.700 ± 0.075	0.377 ± 0.052	0.267 ± 0.029	0.342 ± 0.018
C_3H_6	0.182 ± 0.009	0.107 ± 0.015	0.071 ± 0.014	0.090 ± 0.009
C_3H_8	0.078 ± 0.009	0.047 ± 0.009	0.039 ± 0.012	0.049 ± 0.005
H_2 + CO	60.63 ± 2.41	82.44 ± 1.79	83.95 ± 1.24	83.25 ± 2.63
$CH_4 + C_xH_y$	15.72 ± 0.75	9.35 ± 0.15	6.08 ± 0.50	7.81 ± 0.26

Table 6
Content of water in water-phase condensate for different catalysts.

	Water content (wt.%)
CM	63.91 ± 1.22
Fe	77.79 ± 1.31
Co	67.98 ± 1.29
Ni	65.48 ± 1.28

Table 7
Composition of liquid condensate.

	CM (rel.%)	Fe (rel.%)	Co (rel.%)	Ni (rel.%)
Acetaldehyde, hydroxy-	7.93	3.60	4.01	2.78
Acetic acid	13.56	6.86	17.12	11.60
2-Propanone, 1-hydroxy-	8.17	1.70	5.49	4.33
Acetic acid, methyl ester	3.94	1.12	3.11	2.32
Furfural	–	1.67	6.33	5.52
2-Pentanone, 4-hydroxy-4-methyl-	2.30	–	0.95	1.04
2-Furancarboxaldehyde, 5-methyl-	1.06	1.11	1.72	1.70
Phenol	2.69	1.46	1.83	2.15
1,2-Cyclopentanedione, 3-methyl-	1.53	2.02	1.81	1.96
p-Cresol	1.60	1.01	1.02	1.11
Phenol, 2-methoxy-	1.81	0.47	1.26	1.09
Cyclohexanol, 4-methyl-	2.78	6.66	6.26	6.44
Creosol	2.22	0.53	1.12	1.11
Catechol	2.17	2.38	1.60	1.99
5-Hydroxymethylfurfural	1.21	1.96	1.97	2.23
Vanillin	0.78	1.72	0.98	1.12
d-Mannose	3.37	4.65	2.42	5.35
Apocynin	1.82	6.70	2.82	0.59
d-Allose	12.57	25.91	13.80	18.48
3:4 Altrosan	1.27	1.53	1.55	1.60

4. Conclusion

In this study, a microwave catalytic pyrolysis of wood waste biomass has been carried out. Spruce sawdust was mixed with char from a previous pyrolysis of spruce sawdust at the ratio of 5:1. Char from the woody biomass also contained small amounts of inorganic ash (up to 3 wt.%), which included alkali metals and alkaline earth metals. The presence of such char has a catalytic effect on the pyrolysis process, the cracking of tars and phenolic compounds to the simple gases (H_2 and CO). However, the addition of the catalytic active elements, such as a nickel, cobalt or iron to the char (metallic catalysts), has a strong effect on hydrogen production. It was also found that the most active phase of catalysts for heavy compounds cracking and reforming is the metallic phase, i.e., Co^0 and Ni^0. It corresponds to basic research in the area of these catalysts [19]. The preparation of a metallic catalyst in the microwave reactor was quick and easy, but due to lower temperature (around 800 °C) is a better for Ni catalyst then Fe catalyst. The catalytic surface also has suitable properties for cracking and reforming. Still, it will be necessary for these metals to add some promoters; because of the influence of reverse water-gas shift reaction was considerable. The overall efficiency of the process of hydrogen production was only around 40%. This means that from 1 kg of wood biomass (60.7 g H_2) only about 25 g of H_2 could be obtained. Distributing the reactor to pyrolysis and a catalyst bed would also help to increase the yield of hydrogen.

Acknowledgements

This work was financially supported by the Ministry of Education, Youth and Sports of the Czech Republic in the "National Feasibility Program I" project LO1208 "TEWEP" and EU structural funding Operational Programme Research and Development for Innovation, project No. CZ.1.05/2.1.00/19.0388.

References

[1] A. Dominguez, J. Menendez, M. Inguanzo, P. Bernad, J. Pis, J. Chromatogr. A 1012 (2003) 193.
[2] S.M. Liu, J.L. Zhu, M.Q. Chen, W.P. Xin, Z.L. Yang, L.H. Kong, Int. J. Hydrogen Energy 39 (2014) 13128.
[3] F. Motasemi, M.T. Afzal, Renew. Sustain. Energy Rev. 28 (2013) 317.
[4] J.A. Menendez, A. Arenillas, B. Fidalgo, Y. Fernandez, L. Zubizarreta, E.G. Calvo, J.M. Bermudez, Fuel Process. Technol. 91 (2010) 1.
[5] A. Domínguez, J.A. Menéndez, Y. Fernández, J.J. Pis, J.M.V. Nabais, P.J.M. Carrott, M.M.L.R. Carrott, J. Anal. Appl. Pyrolysis 79 (2007) 128.
[6] B.R. Reddy, R. Vinu, Fuel Process. Technol. 154 (2016) 96.
[7] S.S. Lam, R.K. Liew, C.K. Cheng, H.A. Chase, Appl. Catal. B: Environ. 176–177 (2015) 601.
[8] R.J. Meredith, Engineers' Handbook of Industrial Microwave Heating, Institution of Electrical Engineers, 1998, ISBN 9780852969168.
[9] B. Fidalgo, A. Arenillas, J.A. Menendez, Fuel Process. Technol. 92 (2011) 1531.
[10] B. Fidalgo, Y. Fernandez, A. Dominguez, J.J. Pis, J.A. Menendez, J. Anal. Appl. Pyrolysis 82 (2008) 158.
[11] M.-Q. Chen, J. Wang, M.-X. Zhang, M.-G. Chen, X.-F. Zhu, F.-F. Min, Z.-C. Tan, J. Anal. Appl. Pyrolysis 82 (2008) 145.
[12] Y. Fernandez, A. Arenillas, J.M. Bermudez, J.A. Menendez, J. Anal. Appl. Pyrolysis 88 (2010) 155.
[13] M.W. Roberts, Nature 215 (1967) 215.
[14] J.H. Deboer, B.C. Lippens, B.G. Linsen, J.C. Broekhof, A. Vandenhe, T.J. Osinga, J. Colloid Interface Sci. 21 (1966) 405.
[15] E.P. Barrett, L.G. Joyner, P.P. Halenda, J. Am. Chem. Soc. 73 (1951) 373.
[16] G. Horvath, K. Kawazoe, J. Chem. Eng. Jpn. 16 (1983) 470.
[17] S. Zhang, Q. Dong, L. Zhang, Y. Xiong, Bioresour. Technol. 191 (2015) 17.
[18] S.Q. Shi, W. Che, K.W. Liang, C.L. Xia, D.M. Zhang, J. Anal. Appl. Pyrolysis 115 (2015) 1.
[19] J.A. Torres, J. Llorca, A. Casanovas, M. Dominguez, J. Salvado, D. Montane, J. Power Sources 169 (2007) 158.

Příloha [P4]

GRYCOVA, B., PRYSZCZ, A., CHAMRADOVA, K. & **LESTINSKY, P.** 2017. Preparation and characterization of sorbents from food waste. *Green Processing and Synthesis*, 6, 287-293. IF_{2017} = 0,736 (5 year IF 3.0). Autorský podíl 25 %. Počet citací dle WoS 5.

Role uchazeče:

- vyvození závěrů z dosažených výsledků

Barbora Grycova*, Adrian Pryszcz, Pavel Lestinsky and Katerina Chamradova

Preparation and characterization of sorbents from food waste

DOI 10.1515/gps-2016-0182
Received October 27, 2016; accepted January 17, 2017; previously published online February 28, 2017

Abstract: Waste coffee was treated by pyrolysis in the conventional laboratory apparatus at 800°C. Afterwards, a mass balance of the final yields, gas chromatographic analysis and assessment of solid and liquid residues were done. The selected waste material was also subjected to microwave pyrolysis in terms of adsorbents preparation. The solid residues were further activated with potassium hydroxide. Final characterization of prepared sorbents was made by sorption of nitrogen at 77 K. Activated sorbents had much better sorption properties. The surface area according to Brunauer-Emmett-Teller (BET) theory of activated material (from conventional pyrolysis) was measured 1794 $m^2 \cdot g^{-1}$.

Keywords: activated carbon; food waste; pyrolysis.

1 Introduction

An enormous amount of food waste is produced in the world. These recyclable wastes threaten the localities due to depositing wastes in landfills, which are known to produce carbon dioxide, methane and other contaminated elements. In particular, methane is classified as the most plentiful greenhouse gas. Because of the Directive No. 1999/31/EC on the waste landfilling [1], pressure to decrease the quantity of recyclable waste placed in landfills until 2020 to 35 wt. % of the weight of this type of waste produced in 1995 is growing. Usually, wastes from food processing are constantly stereotypically placed in landfills; a trivial amount is utilized for fattening intents and for biogas performance [2, 3], or compost [4]. Lipid originating from these wastes could be transformed to biodiesel [5, 6]. Furthermore, a comprehensive carbohydrate such as cellulose plus starch may be hydrolyzed to glucose and fructose and these sugars may be converted to bioethanol by fermentation later on [7, 8].

Pyrolysis is demonstrably an original form of application technique related to waste that converts less valuable material to higher value outputs [9]. Pyrolysis has been utilized for production of charcoal from biomass for thousands of years. At present, a trendy approach is rising up in the manufacture of low-cost adsorbents from biomass and numerous food waste inputs on a commercial basis. Activated carbons (ACs) are extremely permeable substances with the required surface characteristics [10], which are widely used in various fields of purification and industrial processes [11]. For that reason, the demand for ACs is constantly growing. New invention methods and the use of low-priced raw materials have been considered [12]. Conventional heating is one of the most appropriate methods used for preparation. As a substitute heating method, microwave irradiation has created hopeful results recently in this area [13, 14]. Microwave heating provides many benefits in comparison with conventional heating, such as non-contact prompt heating, energy transmission instead of heat transmission, quick start-up and stopping, advanced level of protection and mechanization [15].

Basically, physical activation and chemical activation are used to obtain ACs. The enormous interest in the research area belongs to chemical activation due to a number of benefits equated to the so called physical activation, e.g. lower temperatures for process, extremely high surface area, etc. Between the weaknesses of this procedure, the process corrosiveness and the washing phase are to be noted. The chemicals mostly used are alkali (potassium hydroxide, sodium hydroxide), alkali earth metal salts (aluminum chloride and zinc chloride) and some acids (phosphoric acid and sulfuric acid). These chemicals are dehydrating representatives supporting pyrolytic decomposition and suppressing the tar creation. KOH and $ZnCl_2$ belong to among the most frequently used compounds for the production of sorbents [16]. Universally, physical activation covers a carbonization and activation stage. For activation, steam and carbon dioxide are the most shared elements, pronouncedly prompting the porosity of the resulting material [17]. Most predecessors which are practical for the production

***Corresponding author: Barbora Grycova,** Institute of Environmental Technology, VSB-Technical University of Ostrava, 17 Listopadu 15/2172, Ostrava-Poruba, 708 33, Czech Republic, e-mail: barbora.grycova@vsb.cz
Adrian Pryszcz, Pavel Lestinsky and Katerina Chamradova: Institute of Environmental Technology, VSB-Technical University of Ostrava, 17 Listopadu 15/2172, Ostrava-Poruba, 708 33, Czech Republic

of ACs are organic carbon-rich materials. Natural wastes can be taken into account to be a very meaningful feedstock for this production due to their availability and renewability. During the last several years, there has been growing interest in research with the use of renewable and lower priced precursors. A significant portion of research has been stated on ACs from agricultural and food wastes, such as walnut shell [18], coconut shell [19, 20], almond shell [21], acavia mangium wood [22], rice husk [23, 24], mung bean husk [25], buriti shell [26], edible fungi residue [27], coffee husk [28], coffee ground [29, 30], tea industry waste [31, 32], olive-waste cake [33], etc.

Authors of the study [34] assessed the pyrolysis process with regard to syngas and hydrogen flow rates, complete gas and hydrogen yields, and also apparent thermal effectiveness. The outcomes prove that food waste provides a worthy potential for compact waste thermal handling with the exact target of power generation. Energy generation based on the food waste by means of digestion with subsequent pyrolysis was also evaluated [35].

In this study waste coffee was pyrolyzed in the conventional pyrolysis apparatus at a maximum temperature of 800°C and also in the microwave reactor with power of 400 W. The solid residues were further activated with KOH. Final characterization of prepared sorbents was made by sorption of nitrogen at 77 K.

2 Materials and methods

2.1 Material

For the measurement, a sample of waste coffee was selected: WaCo (Cervus Inc.)

The production of this waste is counted in tonnes per week. Most of this waste is landfilled. WaCo was analyzed by thermogravimetry and differential scanning calorimetry with the use of the unit STA 409C (Netzsch, Selb, Germany) on 18-414/4 in an atmosphere of helium, with two heating rates of 10 $K \cdot min^{-1}$ and 20 $K \cdot min^{-1}$. Thermo-analytical techniques are specific methods to determine mass loss properties which are necessary for understanding the pyrolysis kinetics in an easy way [36, 37]. Elemental analysis was performed with the use of the LECO CHSN628 (LECO, Saint Joseph, USA). The higher heating value HHV was measured based on ISO 1928 with the use of the calorimeter LECO AC-350.

2.2 Laboratory devices

Laboratory apparatuses assembled for the purpose of experiments are shown in Figure 1. In the case of conventional pyrolysis, an appropriate quantity of sample (200 g) was weighed and placed into the prepared retort. The retort with length of 30 cm and inner diameter of 5.5 cm was tightly fastened, positioned into the furnace and connected to other components of the apparatus. A gasometer was placed at the end of the apparatus. The final temperature of 800°C was chosen. Nitrogen was used for inertization.

The sample was also treated in the microwave reactor for 20 min at a power of 400 W and frequency of 2450 MHz, which corresponds

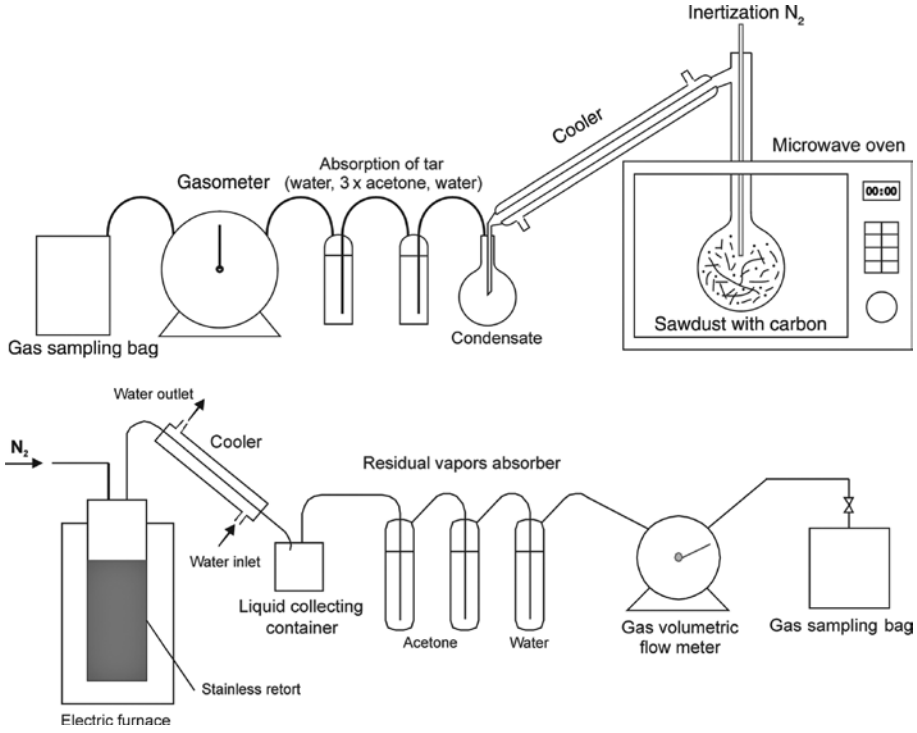

Figure 1: Microwave and conventional apparatus.

to a temperature of 800°C. A hole was cut out in the upper part of the PANASONIC NN-SD271 microwave for placing a flask with the sample into the microwave. The flask was connected with a glass tube with a cooler. After the cooler, there were washing bottles and a gasometer placed (same as in conventional pyrolysis). Microwave heating was used only in terms of adsorbents preparation (the gas and liquid products were not subjected to other determination).

2.3 KOH activation

The sample was treated in a two-stage process which was found to be very effective for preparation of porous carbons with high surface area from biodegradable waste materials [24, 32]. The residues from conventional and microwave pyrolysis were further activated with potassium hydroxide, which is described as the best activation agent. Different activation agents such as KOH (1835 $m^2 \cdot g^{-1}$), NaOH (1558 $m^2 \cdot g^{-1}$), K_2CO_3 (1579 $m^2 \cdot g^{-1}$) and Na_2CO_3 (660 $m^2 \cdot g^{-1}$) were utilized in the study [18] to identify a suitable activation agent. The result indicated that KOH was the most suitable activation agent among those agents, with the highest porosity and surface area of AC. Also the impregnation ratio of KOH has a strong effect on the characteristics of activated char, as is disclosed by Khezami et al. [38]. The char was mixed with KOH, in a ratio of 1 : 4, which is suggested in literature to be the optimum [24]. According to authors [30], higher KOH concentrations consistently produce a lower yield of product with a much larger surface area.

Such prepared mixtures were then thermally treated in an inert atmosphere of nitrogen at 800°C for 1 h. Authors [39] confirm that Brunauer-Emmett-Teller (BET) surface areas of carbons increase with activation temperature. After cooling, the activated samples were neutralized, filtered and finally washed. For neutralization, hydrochloric acid was applied. After drying, the activated samples were ready for subsequent surface analysis.

2.4 Characterization of solid residues

Basic determination of solid residues of pyrolyzed samples was done to define the sorption capacity. The true density was analyzed with the use of an automatic pycnometer PYCNOMATIC ATC (Thermo Fisher Scientific, Waltham, USA) by using helium as a carrier gas. The specific surface area of the samples was evaluated using two methods; the single point measurement at $P/P_0 = 0.2$ and the BET method. Final characterization of prepared sorbents was made by sorption of N_2 at 77 K. Measurement was carried out on a 3Flex Surface Characterization (Micromeritics Instrument Corporation, Norcross, USA) Analyzer (Micromeritics). Ahead of the nitrogen physisorption measurements, the activated samples were degassed at 300°C for 24 h under vacuum less than 1 Pa. The iodine adsorption number according to the standard DIN 53 582 was measured for further characterization of microporous structure.

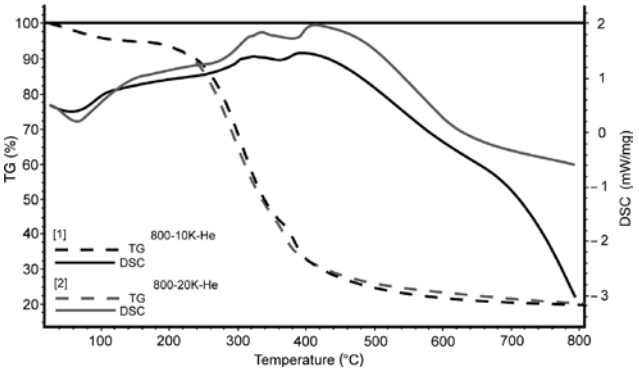

Figure 2: TG and DSC.

3 Results and discussion

For the sample, proximate and ultimate analyses were carried out (see Table 1); thermogravimetry (TG) and differential scanning calorimetry curves (DSC) curves are presented in Figure 2.

The mass balance of the pyrolysis experiment was done according to the weight of the resulting products (solid residue, liquid residue). The process temperature significantly affected the distribution of final products. Solid residue yield decreased with rising temperature; on the other side, desired properties were achieved at higher pyrolysis temperature. Solid residue yield (30 wt. %) was dependent on the working temperature and heating rate which corresponds with authors [40].

3.1 Analysis of gaseous products

The pyrolysis gas was analyzed with the use of the Agilent 7890A (Agilent Technologies, Santa Clara, USA) gas chromatograph equipped with flame ionization and thermal conductivity detector. A significant amount of publications are focused on hydrogen production [41]. Hydrogen evolution was strongly influenced by increasing temperature, as expected. The maximum concentration of measured hydrogen (56 vol. %) was analyzed during the third gas sampling at a temperature from 700°C to 800°C. The amounts of measured hydrocarbons and carbon monoxide reduced with the rising temperature, as disclosed by

Table 1: Proximate and ultimate analysis.

Sample	W(r) (wt. %)	A(r) (wt. %)	V(r) (wt. %)	C(r) (%)	H(r) (%)	N(r) (%)	S(r) (%)	O(r) (%)	HHV(r) ($MJ \cdot kg^{-1}$)	LHV(r) ($MJ \cdot kg^{-1}$)
WaCo	2.5	2.9	75.7	46.7	6.8	1.2	0.1	40.3	20.9	19.5

A, ash; C, carbon; H, hydrogen; HHV, higher heating value; LHV, lower heating value; N, nitrogen; O, oxygen; (r), original sample; S, sulfur; V, volatile matter; W, moisture.

Kalinci et al. [42]. The gas formation gradually increased and peaked in temperature around 500°C (see Figure 3).

3.2 Evaluation of solid residues in terms of adsorption properties

Table 2 demonstrates the values of ultimate and proximate analysis, S_{BET}, t-Plot Micropore Area, iodine adsorption number and true density of activated and non-activated samples after conventional and microwave pyrolysis. In the case of non-activated samples, a very low value of the surface area (below 10 $m^2 \cdot g^{-1}$) was achieved in comparison with commercial ACs. This conclusion conforms to Mohan et al. [43]. The iodine number of the pyrolyzed sample after conventional pyrolysis was 280 $mg \cdot g^{-1}$. This value suggests an opportunity for usage of this waste in "single-use sorbents" production. The surface area of the carbonisates was subsequently activated to improve its removal efficiency (see Figure 4).

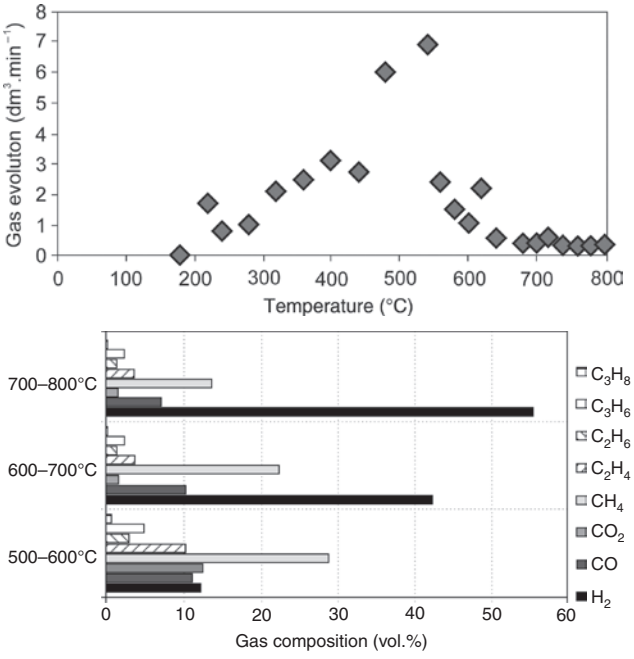

Figure 3: Gas evolution and composition.

3.3 Evaluation of activated solid residues

Activated samples had much better sorption properties. The surface area according to BET of activated material (from conventional pyrolysis) was measured 1794 $m^2 \cdot g^{-1}$ (see Table 2). Surface area of sorbents prepared by microwave pyrolysis was measured as much lower in comparison with conventional pyrolysis. This could be caused by two differences. The first is that the temperature could change throughout the entire volume; there could be spots with higher temperature (hot spots) and also with lower temperature. Secondly the activation time in a microwave is shorter than in a conventional furnace.

Table 3 compares the characteristics with respect to sorption capabilities of some commercial and food/vegetable based ACs mentioned in the literature.

These results show that WaCo could be a substitute precursor for the profitable AC production. It could be also engaged as an advantageous carbonaceous adsorbent for the removal cationic and anionic dyes from wastewater.

3.4 Rating condensates

The condensate from conventional pyrolysis (38 wt. %) was subjected to the determination of water content

Table 2: Proximate and ultimate analysis, S_{BET}, t-Plot microarea, iodine adsorption number and density of activated and non-activated samples after conventional and microwave pyrolysis.

Conventional pyrolysis						
C(d) (wt. %)	H(d) (wt. %)	N(d) (wt. %)	S(d) (wt. %)	O(d) (wt. %)	C_t(d) (wt. %)	A(d) (wt. %)
$83.3^n/82.5^a$	$0.4^n/0.3^a$	$1.4^n/2.9^a$	$0.1^n/0.1^a$	$2.8^n/2.2^a$	$88.0^n/88.0^a$	$12.0^n/12.0^a$
V(d) (wt. %)	FC(d) (wt. %)	Yield (wt. %)	S_{BET} ($m^2 \cdot g^{-1}$)	t-Plot ^{MicroArea} ($m^2 \cdot g^{-1}$)	I ($mg \cdot g^{-1}$)	ρ ($g \cdot cm^{-3}$)
$3.3^n/11.5^a$	$84.7^n/76.5^a$	$30.0^n/19.5$	$3.2^n/1794.0^a$	$9.4^n/1128.0^a$	$280.0^n/1437.0^a$	$1.8^n/2.5$
Microwave pyrolysis						
C(d) (wt. %)	H(d) (wt. %)	N(d) (wt. %)	S(d) (wt. %)	O(d) (wt. %)	C_t(d) (wt. %)	A(d) (wt. %)
$74.1^n/73.8^a$	$2.7^n/0.5^a$	$2.2^n/1.2^a$	$0.1^n/0.1^a$	$7.9^n/4.9^a$	$87.0^n/80.6^a$	$13.0^n/19.6^a$
V(d) (wt. %)	FC(d) (wt. %)	Yield (wt. %)	S_{BET} ($m^2 \cdot g^{-1}$)	t-Plot ^{MicroArea} ($m^2 \cdot g^{-1}$)	I ($mg \cdot g^{-1}$)	ρ ($g \cdot cm^{-3}$)
$15.3^n/13.5^a$	$71.7^n/67.1^a$	$41.0^n/26.7^a$	$2.9^n/1044.0^a$	$3.3^n/882.0^a$	$55.0^n/1335.0^a$	$1.8^n/2.4$

Index^n, non-activated sample/index^a activated sample; (d), anhydrous sample; C, carbon; H, hydrogen; N, nitrogen; S, sulfur; O, oxygen; C_t, total combustible; A, ash; V, volatile matter; FC, fixed carbon; S_{BET}, (Brunauer, Emmett and Teller) surface area; t-Plot^{MicroArea}, t-Plot micropore area; I, jodine adsorption number; ρ, density.

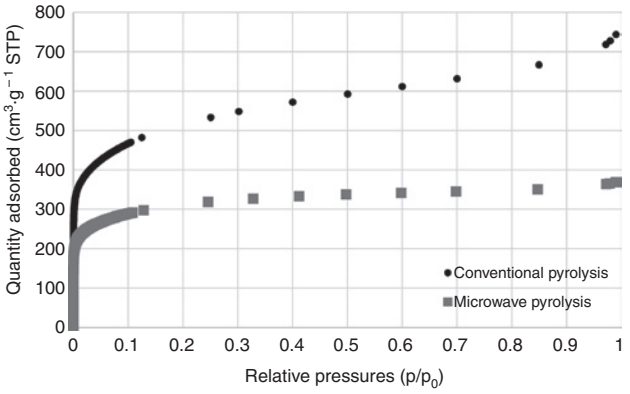

Figure 4: Adsorption isotherms of activated samples.

(76.8 wt. %) by the Karl-Fischer method on TitroLine 7500 KF (SI Analytics GmbH, Mainz, Germany). Among the most represented components analyzed in the condensate were lauric acid (29.5 rel. %), which could be used in the case of possible isolation in the manufacture of shampoos, liquid soaps and detergents, caprylic acid (9.2 rel. %), myristic acid (6.5 rel. %) and capric acid (6 rel. %). Caprylic acid could be used, for example in the treatment of bacterial infections, or in the production of esters for perfumery and myristic acid as an additive for cosmetic creams.

4 Conclusion

The selected food waste material was treated by pyrolysis in conventional laboratory apparatus at 800°C. Afterwards, a mass balance of the final yields, gas chromatographic analysis and assessment of solid and liquid residues were done. Waste coffee was also subjected to microwave pyrolysis in terms of adsorbents preparation. The final step of this work was by activation and sorption characterization on a 3Flex Surface Characterization Analyzer (Micromeritics). The measured data from BET and t-plot confirm that the surface area of activated materials had sorption properties close to higher quality AC. The non-activated samples had almost zero sorption properties. From the results, it could be concluded that waste coffee, which is a waste material that is mostly disposed of by landfilling, could be used for preparation of sorbents with surface area around 1800 $m^2 \cdot g^{-1}$. The surface area of sorbent prepared by microwave pyrolysis was measured as much lower in comparison with conventional pyrolysis. By contrast, it must be mentioned that the treatment time can be considerably reduced, which in many cases represents a reduction in the energy consumption as well. The

Table 3: Comparison of adsorptive characteristics of activated carbons (ACs) reported in literature.

AC	Commercial AC	Coffee ground AC	Coffee husk AC	Pine cone AC	Buriti shell AC	Coconut shell AC	Grape waste AC
S_{BET} ($m^2 \cdot g^{-1}$)	1440	925	1522	1806	843	500	1455
References	[44]	[29]	[28]	[44]	[26]	[20]	[44]
AC	**Walnut shell AC**	**Coconut husk AC**	**Acavia mangium wood AC**	**Olive-waste cake AC**	**Edible fungi residue AC**	**Almond shell AC**	**Rice husk AC**
S_{BET} ($m^2 \cdot g^{-1}$)	1835	1356	1040	1020	684	840	516
References	[18]	[19]	[22]	[33]	[27]	[21]	[23]

AC, activated carbon.

preparation took only 20 min compared to several hours in the case of conventional pyrolysis, and it could be an interesting way of sorbents preparation in the future.

Acknowledgments: This work was financially supported by the Ministry of Education, Youth and Sports of the Czech Republic in the "National Feasibility Program I", project LO1208 "TEWEP" and also by EU structural funding Operational Programme Research and Development for Innovation project no. CZ.1.05/2.1.00/19.0388.

References

[1] Council Directive 1999/31/EC of 26 April 1999 on the landfill of waste. Official Journal L 182, 16/07/1999, 1–19.
[2] Wu L-J, Kobayashi T, Hidetoshi Kuramochi, Yu-You Li, Kai-Qin Xu. *Bioresour. Technol.* 2016, 201, 237–244.
[3] Sydney EB, Larroche C, Novak AC, Nouaille R, Sarma SJ, Brar SK, Junior Letti LA, Soccol VT, Soccol CR. *Bioresour. Technol.* 2014, 159, 380–386.
[4] Tronina P, Bubel F. *Pol. J. Chem. Technol.* 2008, 10, 37–42.
[5] Karmee SK, Lin CSK. *Sustainable Chem. Processes* 2014, 2, 22.
[6] Karmee SK, Lin CSK. *Lipid Technol.* 2014, 26, 206–209.
[7] Pham TPT, Kaushik R, Parshetti GK, Russell M, Balasubramanian R. *Waste Manage.* 2015, 38, 399–408.
[8] Yang X, Lee JH, Yoo HY, Shin HY, Thapa LP, Park C, Kim SW. *Bioprocess Biosyst. Eng.* 2014, 2014, 1627–1635.
[9] Hocking MB. *Environ. Manage.* 1994, 18, 889–99.
[10] Kaouah F, Boumaza S, Berrama T, Trari M, Bendjama Z. *J. Cleaner Prod.* 2013, 54, 296–306.
[11] Sahin Ö, Baytar O, Saka C. *J. Anal. Appl. Pyrol.* 2013, 104, 378–383.
[12] Budinova T, Ekinci E, Yardim F, Grimm A, Björnbom E, Minkova V, Goranova M. *Fuel Process. Technol.* 2006, 87, 899–905.
[13] Hesas RH, Arami-Niya A, Daud WMAW, Sahu JN. *Bioresour.* 2013, 8, 2950–2966.
[14] Haili L, Xiaogian M, Longjun L, Zhifeng H, Pingsheng G, Juhui J. *Bioresour. Technol.* 2014, 166, 45–50.
[15] Menéndez JA, Arenillas A, Fidalgo B, Fernández Y, Zubizarreta L, Calvo EG, Bermúdez JM. *Fuel Process. Technol.* 2010, 91, 1–8.
[16] Özdemir IV, Sahin M, Orhan R, Erdem M. *Fuel Process. Technol.* 2014, 125, 200–206.
[17] Bae W, Kim J, Chung J. *J. Air Waste Manage. Assoc.* 2014, 64, 879–886.
[18] Hongying X, Song Ch, Libo Z, Jinnhui P. *Green Process. Synth.* 2016, 5, 7–14.
[19] Foo KY, Hameed BH *Chem. Eng. J.* 2012, 184, 57–65.
[20] Santra AK, Pal TK, Datta S. *Separ. Sci. Technol.* 2008, 43, 1434–1458.
[21] Chunfeng D, Hongbing Y, Zhansheng W, Xinyu G, Giancarlo C, Bang-Ce Y, Imdad K. *Green Process. Synth.* 2016, 5, 395–406.
[22] Danisha M, Hashim R, Mohamad Ibrahim MN, Sulaiman O. *J. Anal. Appl. Pyrol.* 2013, 104, 418–425.
[23] Malik PK. *Dyes Pigm.* 2003, 56, 239–249.
[24] Gyu Hwan Oh, Chong Rae Park. *Fuel* 81, 2002, 327–336.
[25] Mondal S, Sinha K, Aikat K, Halder G. *J. Environ. Chem. Eng.* 2015, 3, 187–195.
[26] Pezoti JO, Cazetta AL, Souza IPAF, Bedin KC, Martins AC, Silva TL, Almeida VC. *J. Ind. Eng. Chem.* 2014, 20, 4401–4407.
[27] Xiao H, Peng H, Deng SH, Yang XY, Zhang Z, Li YW. *Bioresour. Technol.* 2012, 111, 127–133.
[28] Oliveira LC, Pereira E, Guimaraes IR, Vallone A, Pereira M, Mesquita JP, Sapag K. *J. Hazard. Mater.* 2009, 165, 87–94.
[29] Reffas A, Bernardet V, David B, Reinert L, Lehocine MB, Dubois M, Batisse N, Duclaux L. *J. Hazard. Mater.* 2010, 175, 779–788.
[30] Evans MJB, Halliop E, MacDonald JAF. *Carbon* 37, 1999, 269–274.
[31] Kazmi M, Saleemi AR, Feroze N, Yaqoob A, Ahmad SW. *Pol. J. Chem. Technol.* 2013, 15, 1–6.
[32] Nowicki P, Kazmierczak-Razna J, Skibiszewska P, Wiśniewska M, Nosal-Wiercińska A, Pietrzak R. *Adsorption* 2016, 22, 489.
[33] Baccar R, Bouzid J, Feki M, Montiel A. *J. Hazard. Mater.* 2009, 162, 1522–1529.
[34] Ahmed II, Gupta AK. *Appl. Energy* 2010, 87, 101–108.
[35] Opatokun SA, Strezov V, Kan T. *Energy* 2015, 92. Special Issue: SI, 349–354.
[36] Janković B. *Energy Convers. Manage.* 2014, 85, 33–49.
[37] Duan HB, Li JH. *J Air Waste Manage. Assoc.* 2010, 60, 540–547.
[38] Khezami L, Chetouani A, Taouk B, Capart R. *Powder Technol.* 2005, 157, 48–56.
[39] Stavropoulos GG, Zabaniotou AA. *Microporous Mesoporous Mater.* 82, 2005, 79–85.
[40] Titiladunayo IF, McDonald AG, Fapetu OP. *Waste Biomass Valorization* 2012, 3, 311–318.
[41] Bičáková O, Straka P. *Int. J. Hydrogen Energy* 2012, 37, 11563–11578.
[42] Kalinci I, Hepbasli A, Dincer I. *Int. J. Hydrogen Energy* 2009, 34, 8799–8817.
[43] Mohan D, Pittman JCU, Bricka M, Smith F, Yancey B, Mohammad J, Steele PH, Alexandre-Franco MF, Gómez-Serrano V, Gong H. *J. Colloid Interface Sci.* 2007, 310, 57–73.
[44] Saygılı H, Güzel F, Önal Y. *J. Cleaner Prod.* 2015, 93, 84–93.

Bionotes

Barbora Grycova

Barbora Grycova studied Economics in Metallurgy and Metallurgy at VSB Technical University of Ostrava and obtained her PhD degree in 2012 at VSB Technical University of Ostrava (field of study: thermal technology and fuels in industry). She is a junior researcher and lecturer at the Institute of Environmental Technology, VSB Technical University of Ostrava and interested in the field of thermal engineering, e.g. new generation biofuels and activated carbon production by pyrolysis and gasification.

Adrian Pryszcz

Adrian Pryszcz MSc studied Environmental Technology at the Institute of Chemical Technology, Prague and obtained his MSc degree in 2007. He is a PhD student at the Institute of Environmental Technology, VSB Technical University of Ostrava and interested in the field of thermal engineering, e.g. new generation biofuels and activated carbon production by pyrolysis and gasification.

Pavel Lestinsky

Pavel Lestinsky studied Process Engineering at VSB Technical University and obtained his PhD in 2013. He is a senior researcher and lecturer at the Institute of Environmental Technology, VSB Technical University of Ostrava and interested in the field of chemical engineering, e.g. gas and flue gas cleaning, mathematical modeling of the transport phenomena (by Matlab, Comsol, Fluent), simulation of chemical processes (by Aspen Plus) or new generation biofuel production by pyrolysis.

Katerina Chamradova

Katerina Chamradova studied at the Faculty of Mining and Geology, VSB Technical University of Ostrava and obtained her PhD degree in 2012 from VSB Technical University of Ostrava (field of study: environmental protection within industry). She is a junior researcher and lecturer at the Institute of Environmental Technology, VSB Technical University of Ostrava and a member of the anaerobic digestion team. She is interested in the field of anaerobic digestion, in particular use of food waste by anaerobic treatment.

Příloha [P5]

KLEMENCOVA, K., GRYCOVA, B. & **LESTINSKY, P.** 2022. Influence of Miscanthus Rhizome Pyrolysis Operating Conditions on Products Properties. *Sustainability*, 14. IF_{2022} = 3,9 (5 year IF 4.089). Autorský podíl 30 %. Počet citací dle WoS 7.

Role uchazeče:

- návrh postupu prací, vyhodnocení výsledků, vyvození závěrů z dosažených výsledků

sustainability

MDPI

Article

Influence of Miscanthus Rhizome Pyrolysis Operating Conditions on Products Properties

Katerina Klemencova, Barbora Grycova * and Pavel Lestinsky

Institute of Environmental Technology, Centre of Energy and Environmental Technologies, VSB—Technical University of Ostrava, 17. listopadu 15/2172, Poruba, 708 00 Ostrava, Czech Republic; katerina.klemencova@vsb.cz (K.K.); pavel.lestinsky@vsb.cz (P.L.)

* Correspondence: barbora.grycova@vsb.cz; Tel.: +420-59-6997-331

Abstract: Waste from the Miscanthus production cycle may be a promising source of material for the pyrolysis and biochar production. The biochar can be used to enrich the soil on which the crop grows, thus increasing productivity. A sample of Miscanthus rhizomes was used as a raw material in a series of experiments in order to find the most suitable conditions for the preparation of biochar. Miscanthus biochar was prepared in a laboratory unit using four different temperatures (i.e., 400, 500, 600 and 700 °C). All pyrolysis products were subsequently evaluated in terms of their quality and product yields were determined. For a temperature of 600 °C and a residence time of 2 h, the appropriate properties of biochar were achieved and the process was still economical. The biochar contained a minimal number of polycyclic aromatic hydrocarbons and a high percentage of carbon. Surface area was measured to be 217 m^2/g. The aqueous extract of biochar was alkaline.

Keywords: Miscanthus rhizomes; biochar; pyrolysis

Citation: Klemencova, K.; Grycova, B.; Lestinsky, P. Influence of Miscanthus Rhizome Pyrolysis Operating Conditions on Products Properties. *Sustainability* **2022**, *14*, 6193. https://doi.org/10.3390/su14106193

Academic Editor: Salvatore Cataldo

Received: 4 April 2022
Accepted: 17 May 2022
Published: 19 May 2022

1. Introduction

Nowadays, biomass is one of the most promising renewable alternatives to fossil fuels. Due to many reasons, rapidly increasing utilization of lignocellulose feedstock for producing renewable energy and chemicals can be seen [1,2]. It currently represents the world's fourth largest energy source after coal, oil and natural gas [3,4]. *Miscanthus giganteus* is a fast-growing and high-yielding grass originally from East Asia, the result of a cross between *M. sinensis* and *M. sacchariflorus*. It grows up to a height of 4 m and can be cultivated for approx. 10 years in the same place. Its adaptability to different environments makes this novel crop suitable for production in European and North American climatic conditions [5]. This rhizomatous grass with the C_4 synthetic pathway has been reported as a high potential biomass [6]. Miscanthus is able to translocate minerals to its rhizomes in the winter, which makes it interesting [7]. Thus, Miscanthus is typically harvested during winter or early spring [8]. As the use of Miscanthus in different branches is growing continuously, so is the production of waste from processing it. Hand in hand with this, an important question about the possibilities of its further use arises.

Thermochemical methods offer a way of its processing. Pyrolysis can be highlighted among all the other techniques as a form of thermal decomposition without the presence of oxygen [9]. Biochar as one of the products is a carbon-rich porous material with a high specific surface area and special physicochemical properties. Biochar has been widely used in various applications reducing greenhouse gas emissions, improving soil fertility and crop yield, and remediating contaminated or degraded soils [10,11]. Biochar has been proposed to promote plant growth and improve plant productivity in saline-alkali soils [12].

The effect of biochar on soil fertility and its stability depends on the interactions of soil and climatic conditions with biochar physicochemical properties, mainly on feedstock and pyrolysis conditions. For example, Mimmo et al. reported that thermal and biological stability of biochar is affected by pyrolysis temperature in a nonlinear manner. Increased

resistance to biodegradation has been confirmed for biochar produced at temperatures above 360 °C [13]. Biochar is widely used as an additive in agriculture [14–17]. Biochar is characterized by significant surface area, porosity, high water retention capacity, and environmental persistence. It is also considered as a suitable material for soil amendment. Application of biochar into soil does not usually have a toxic effect. However, possible negative effects should be considered in order to prevent their occurrence. Contaminants can be distinguished as either by products of pyrolysis, formed during biochar production, or components of the feedstock (polycyclic aromatic hydrocarbons, polychlorinated dibenzo-p-dioxins and furans, volatile organic compounds, heavy metals) [18]. Biochar can also be used as bio stimulant for the remediation of hydrocarbon contamination [19].

A major problem with the presence of contaminants in biochar is their availability to organisms and thus their potential toxic effect. Polycyclic aromatic hydrocarbons are the most frequently occurring contaminants in biochar. PAHs are formed during pyrolysis and have carcinogenous, mutagenous, and teratogenous properties. The content of PAHs depends on the organic matter in biochar, the residence time, the heating rate and the pyrolysis temperature [20]. The mass of polychlorinated dibenzo-p-dioxins and furans (PCDD/Fs) in biochar is generally low, and they form in biochar during the pyrolysis of a chlorine-containing material [21]. The other contaminants are heavy metals present in the feedstock, which remain in biochar after pyrolysis, often more concentrated [18]. Biochar may induce a positive effect on the reproduction of microorganisms by providing both protection and a carbon source. However, biochar could have negative impacts on soil microorganisms [22]. The greatest toxic effect in this matter was observed in biochar produced at 300 °C. With increasing temperature, its toxicity decreased [23]. The effect of biochar on the plants is strictly determined by the kind of biomass and pyrolysis conditions. Electrical conductivity and pH play a considerable role as well [18].

The total amount of contaminants in biochar does not correspond to the number of contaminants causing toxic effects. Therefore, it is very important to determine the amount of contaminants with these harmful properties [24,25]. Miscanthus can be classified as a biomass tolerant to heavy metals. This makes it interesting for use in phytoremediation of areas previously contaminated by heavy metals and where energy production is possible [26]. Plants generally transfer metals from the soil through the roots to the shoots, but Miscanthus protects its photosynthetic system by regulating and limiting this transfer. It does not transfer metals to aboveground parts, but accumulates them mostly in rhizomes [27,28].

This study is focused on the possibilities of using waste from the Miscanthus production cycle (Miscanthus rhizomes) as an alternative source for material with a higher utility value, especially biochar. It follows the demand of EU Bioeconomy Strategy encouraging the production of renewable biological resources and processing to vital products and bio-energy. From that perspective, Miscanthus, a popular perennial non-food crop resistant to pests with a high lignocellulose content, looks like excellent feedstock for producing fibre-based materials. Its physiological characteristics and extensive root system allow the plant to adapt to various soils and environmental conditions. Moreover, this adaptation can be promoted with the use of its biochar. Unlike in previous studies, in which the authors deal with the production of biochar from the aboveground parts of Miscanthus, i.e., stems and leaves, the aim of this study is the processing of Miscanthus rhizomes and search for a suitable pyrolysis condition for Miscanthus rhizomes biochar production. Due to the long period of availability of Miscanthus rhizomes to produce aboveground biomass (10 years or even more), pyrolysis and processing of Miscanthus rhizomes has not been addressed so far. Besides, in contaminated postmining soils, repeated utilization of Miscanthus in the form of biochar will bring additional positive outcomes, including improving soil quality, in line with the "zero waste" approach. In addition, gaseous and liquid products were evaluated and dependencies were given.

2. Materials and Methods

2.1. Feedstock

For the series of experiments, Miscanthus rhizomes were used in order to find the suitable conditions for biochar preparation. Miscanthus was produced by S WHG Ltd. (Valasske Mezirici, Czech Republic in a local field. The sample was air-dried and adjusted to the required size with the use of knife grinder LMN 180 (Testchem Sp. z o.o. Pszów, Poland). The fraction rate of 3–5 mm was used.

Proximate and ultimate analysis of biochar was performed according to the standard procedure of the American Society for Testing and Materials. Thermogravimetric analysis was performed on a TGA 701 analyzer (LECO, US, St. Joseph, MI, USA) in an inert helium atmosphere at a heating rate of 5 °C/min in a temperature range from ambient temperature to 800 °C in accordance with ASTM D1762-84. Elemental analysis was performed on a CHSN 628 elemental analyser (LECO, US) according to ASTM D5373, and higher heating value was determined on an AC 600 calorimeter (LECO, US), and the standard ASTM E711 was used. The Miscanthus rhizomes were also subjected to chemical analysis based on standard operating procedure SOP 87 for the purpose of lignin, cellulose and hemicellulose determination.

2.2. Experimental Setup

The Miscanthus biochar was prepared in a laboratory unit [29] at different temperatures. Four different temperatures (i.e., 400, 500, 600 and 700 °C) were selected for experiments with a residence time of 2 h (marked 600/2). Based on the initial results of experiments with selected temperatures, for a temperature of 600 °C, two other residence times were chosen (15 min and 1 h; marked 600/0.25 and 600/1). The heating rate of 5 °C/min was used the same for all experiments. The pyrolysis experiments were performed using the fixed bed reactor. The reactor was externally heated by an electrical furnace, in which the temperature was measured by a thermocouple placed inside the oven. The laboratory unit was supplemented by a cooler and a flask for condensate collecting. A retort with an appropriate quantity of sample (100 g) was connected with other parts of apparatus and the whole system was inertized using nitrogen before starting the experiment. A gasometer Spektrum P 0.1 (Spektrum s.r.o., Skutec, Czech Republic) was placed at the end of the apparatus. The pyrolysis gas was captured into Teglar bags and subsequently analyzed as mentioned below.

2.3. Gas Characterization

For each experiment, three gas samples were gradually taken. Sample 1 was taken up to 350 °C, sample 2 was taken from 350 °C to a final temperature (400, 500, 600 or 700 °C) and the last sample 3 was taken throughout the residence time on the final temperature. All samples were analyzed by gas chromatography and the quantity of H_2, CO, CO_2, CH_4, and light hydrocarbons were determined by gas chromatograph YL 6100 (Young In Chromass, Anyang, Korea) with FID and TCD detectors and micropacked ShinCarbon column (2 m × 0.53 mm). Conditions for GC are given in Table 1. Higher heating value was calculated for each sample based on its gas composition.

2.4. Condensate Characterization

To identify all compounds and their percentages in the condensate, samples were prepared by mixing a 10 mL sample of condensate with 10 mL of dichlormethane. Dichlormethane phase was separated in a separatory funnel and the remaining phase was further mixed with 10 mL of diethyl ether. The ether phase was separated. The solvents from the dichloromethane and ether phases were evaporated by the sample concentrator with block heater (SBHCNC/1, SBH200D/3). After evaporation, a film was formed which was dissolved in 5 mL of acetone and evaluated by a gas chromatograph Agilent 7890b (Agilent, Santa Clara, CA, USA) with a mass spectrometer using a column HP-5 for non-polar substances and a column WAX for polar substances. MS—single quad, scan 20–650 m/z,

MS source 230 °C, MS Quad 150 °C were used. The water content in condensates was determined by the Karl-Fischer method on TitroLine 7500 KF (Xylem Analytics, Weilheim, Germany).

Table 1. Conditions for GC.

Oven (°C)	60	Run Time (min)	34.5
Value (°C)	70		
Injector			
Temperature (°C)	200		
Pressure (psi)	50		
Detector	**FID**		**TCD**
Temperature (°C)	250	Temperature (°C)	200
Air (mL/min)	350	Ref. (mL/min)	20
H_2 (mL/min)	40	Make up (ml/min)	25
Make up (mL/min)	5		

2.5. Biochar Characterization

Proximate and ultimate analyses were performed with the use of TGA 701, CHSN 628 and AC 600 analyzers. Biochar was evaluated in terms of its sorption properties using 3Flex commercial apparatus (Micromeritics, Norcross, GA, USA). The analysis of surface area follows the methodologies presented in ASTM D6556-10. Physisorption measurement of nitrogen at 77 K allows evaluation of textural properties of porous materials such as specific surface area, micropore volume, mesopore and macropore surface or pore size distribution from ~0.35 to ~200 nm. Prior to measurement, each sample was dried and degassed in a vacuum (~0.06 mbar) at 350 °C for 48–120 h. Samples prepared at less than 350 °C were dried at lower temperatures in order to prevent their oxidation. For pH and EC determination, samples of raw Miscanthus rhizomes and biochars were prepared by adjusting their size using a mortar first and then they were mixed with de-ionized water, in a ratio of 1:20. These samples were blended on a shaker for 90 min.

All biochars were subjected to soil toxicity assessment. Toxicants may be divided into two categories. The first category is toxic substances present in the used feedstock (i.e., heavy metals) and the second category is formed by products which are created during pyrolysis process (i.e., polycyclic aromatic hydrocarbons). The amount of heavy metals in biochar was determined by the S-METAXHB1 method for As, Cd Cr, Co, Cu Pb, Hg, Mo, Ni, Zn and for Se determination, the S-METAXHB2 method was used.

PAHs were extracted from 1 g biochar samples using 24 h Soxhlet extraction with 150 mL toluene as a solvent. Extracts were stabilized by adding a small amount of iso-octane and further were concentrated to 1 mL on vacuum vaporizer. These samples were analyzed on GC-MS with SIMs analysis for 12 basic PAHs.

The total and available content of Ca, K, Mg, S (sulphates), F (phosphates) and N (ammonium and nitrates) in biochar samples were determined as well. The total content of components was measured according to the ČSN EN ISO 11885 and ČSN EN 13657 standards. The amount of available content was determined in an aqueous extract according to the Flame Atomic Absorption Spectroscopy method in a ratio of 1:10. The aqueous extract was prepared based on the method Merlich III.

The morphology structure of the biochar was studied with the use of Scanning Electron Microscopy (SEM: Tescan Vega, TESCAN ORSAY HOLDING, a.s., Brno, Czech Republic) with Tungsten cathode and energy-dispersive X-ray spectroscopy (EDS: EDAX, Pleasanton, CA, USA). Micrographs were obtained using secondary electrons (SE) and backscattered electrons (BSE) mode with an acceleration voltage of 30 KeV. Samples were gold sputtered before imaging to ensure adequate electron conductivity.

3. Results and Discussion

3.1. Feedstock Characterization

The behaviour of Miscanthus during pyrolysis was strongly related to its composition. The ash content was 3.42 wt.%, which corresponds to ash content 3.52 wt.% reported by Lakshman et al. [30]. The basic components of biomass have several different chemical and physical properties, which affect the pyrolysis process and thus biochar production [31]. The material with HHV 19.8 MJ/kg had a moisture of 8.53 wt.%; this parameter is very important factor as it affects its thermal degradation. For the pyrolysis experiment, a water content of feedstock below 10 wt.% is recommended. Moisture then contributed to the water content in the condensate [30].

Thermal degradation of raw Miscanthus rhizomes can be seen in Figure 1. The first peak is connected with water evaporation and it is followed by thermal degradation, which started at 250 °C and ended at around 400 °C, with a 70 wt.% mass loss. This loss was mainly caused by cellulose and hemicellulose decomposition; at approximately 300 °C it was linked to the decomposition of hemicelluloses (second peak), and between 350 and 400 °C due to the decomposition of cellulose (third peak). Lignin reacted in the temperature range from 200 to 800 °C [32], and its decomposition was evident by a gradual decrease in mass, especially at higher temperatures as already reported [33,34].

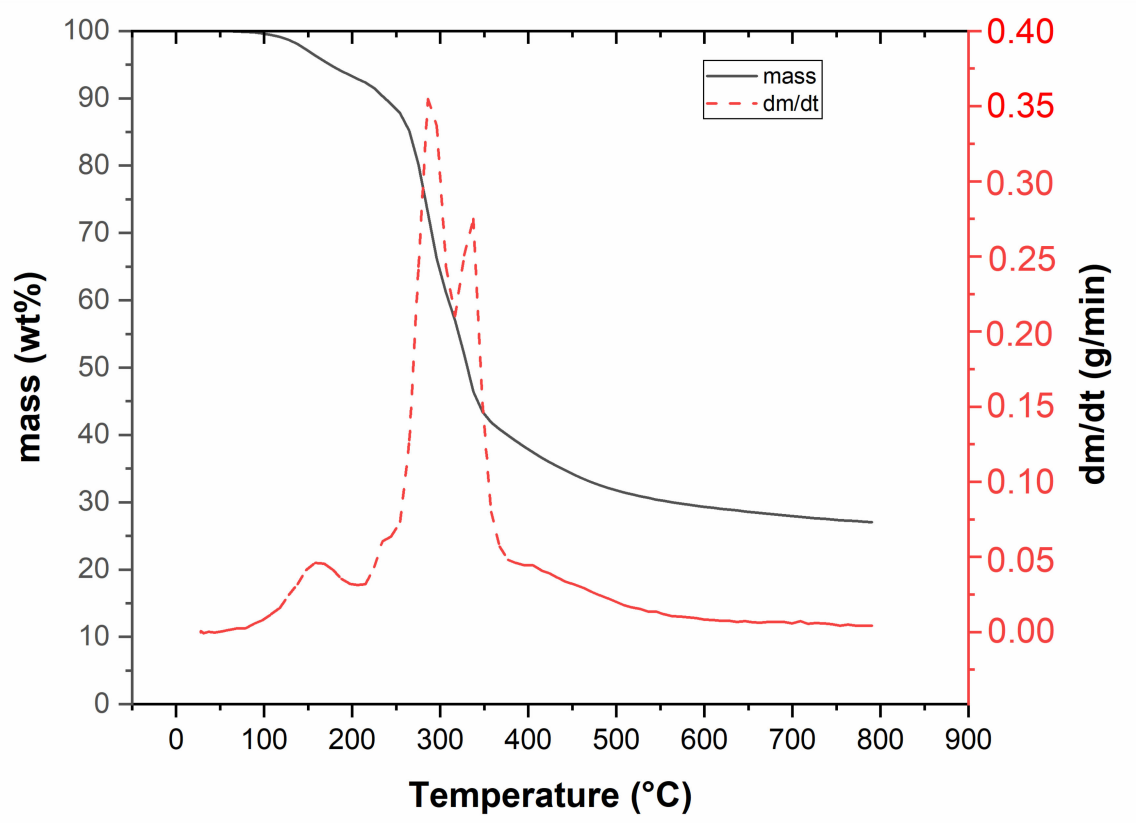

Figure 1. Thermogravimetric curve of Miscanthus rhizomes.

The lignocellulosic structure of a plant is also important because it forms a significant portion of dried biomass [35]. From the chemical composition it can be seen that the used Miscanthus rhizomes consisted mainly of lignin (approx. 65 wt.%), which is not unusual. The higher amount of lignin means slower decomposition and lower water mass in the condensate, as published by Lakshman et al. [30]. Product balance depends on the type of equipment, the temperature in the reactor, the heating rate, and residence time in the heating zone. The yields of biochar decreased with rising temperature, which is in contrast with Budai et al. [33]. The increasing pyrolysis temperature affected the decomposition and content of volatiles, as well as the content of organic substances present in the biomass.

Increasing residence time led to a decrease in biochar yield. A significant biochar decrease occurred at a temperature from 400 to 500 °C. The effect of temperature on the yields of biochar, gas and condensate is shown in Figure 2. The temperature effect is shown on the left, the residence time effect on the right. From the product balance it can be seen that with rising temperature the yield of generated gas increased.

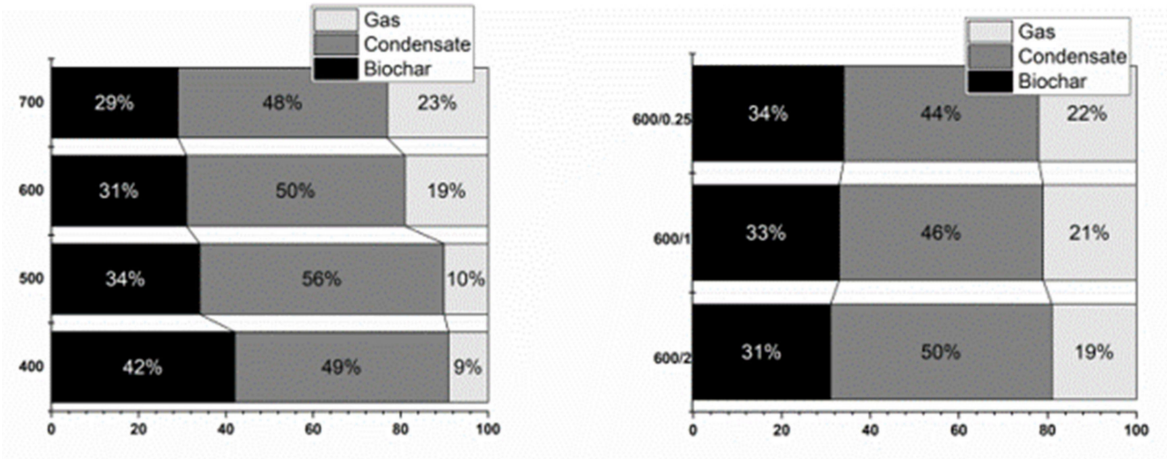

Figure 2. Product balance.

3.2. Gas Characterization

Three gas samples were taken for each experiment. The average quantity of H_2, CO, CO_2, CH_4, and light hydrocarbons is shown in Table 2. Higher heating value was calculated for each gas sample. Higher heating value (HHV) was chosen as a parameter for evaluating the quality of the pyrolysis gas created during the pyrolysis process. During the experiment, three samples were taken at different temperatures (see Section 2). HHVs of these samples are shown in Figure 3. It is clear from the results that the composition of Sample 1 was always the same, as all materials were heated to 350 °C at the same heating rate. The dominant component was CO_2, which was about 70% in the gas. The rest was mainly CO. For Sample 2, a change is already noticeable, where HHV of the gas increased with increasing final temperature. At 400 °C, the gas still had 63% CO_2, 35% CO and a small amount of light hydrocarbons. At 700 °C, the CO_2 content decreased to 45 vol.%, CO decreased to 25 vol.%, but there already were 20 vol.% CH_4 and about 5% light hydrocarbons. These hydrocarbons, including methane, significantly increased HHV. This can also be observed in the last Sample 3, where HHV increased up to values of 25 MJ/kg. In Sample 3, the proportions of hydrocarbons as well as hydrogen were already increasing, while the CO_2 content decreased significantly. The breaking temperature was between 500 and 600 °C, where at 500 °C CO_2 content was still 40 vol.%, while at 600 °C CO_2 content ranged from 20 to 28 vol.% (depending on residence time). The amount of hydrogen in Sample 3 at 700 °C was up to 40 vol.%, while at temperature of 400 °C it was barely 1 vol.%.

Table 2. Gas characterization.

	400	**500**	**600**	**700**	**600/1**	**600/0.25**
H_2 (vol.%)	1.81 ± 0.08	1.13 ± 0.05	4.52 ± 0.12	4.92 ± 0.16	2.21 ± 0.10	1.93 ± 0.04
CO (vol.%)	27.66 ± 0.18	31.39 ± 0.11	23.22 ± 0.13	25.00 ± 0.20	26.27 ± 0.21	29.64 ± 0.19
CO_2 (vol.%)	68.13 ± 0.77	59.88 ± 0.85	57.98 ± 0.74	56.49 ± 0.89	56.78 ± 0.70	56.70 ± 0.81
CH_4 (vol.%)	1.99 ± 0.01	5.82 ± 0.01	11.62 ± 0.01	11.09 ± 0.16	12.01 ± 0.01	9.57 ± 0.01
C_2H_4 (vol.%)	0.15 ± 0.01	0.51 ± 0.02	0.53 ± 0.02	0.49 ± 0.03	0.52 ± 0.01	0.43 ± 0.02
C_2H_6 (vol.%)	0.17 ± 0.01	0.89 ± 0.07	1.48 ± 0.08	1.38 ± 0.14	1.56 ± 0.08	1.23 ± 0.11
C_3H_6 (vol.%)	0.04 ± 0.01	0.15 ± 0.01	0.24 ± 0.01	0.26 ± 0.01	0.24 ± 0.01	0.18 ± 0.01
C_3H_8 (vol.%)	0.05 ± 0.01	0.24 ± 0.01	0.41 ± 0.02	0.37 ± 0.01	0.40 ± 0.01	0.32 ± 0.01

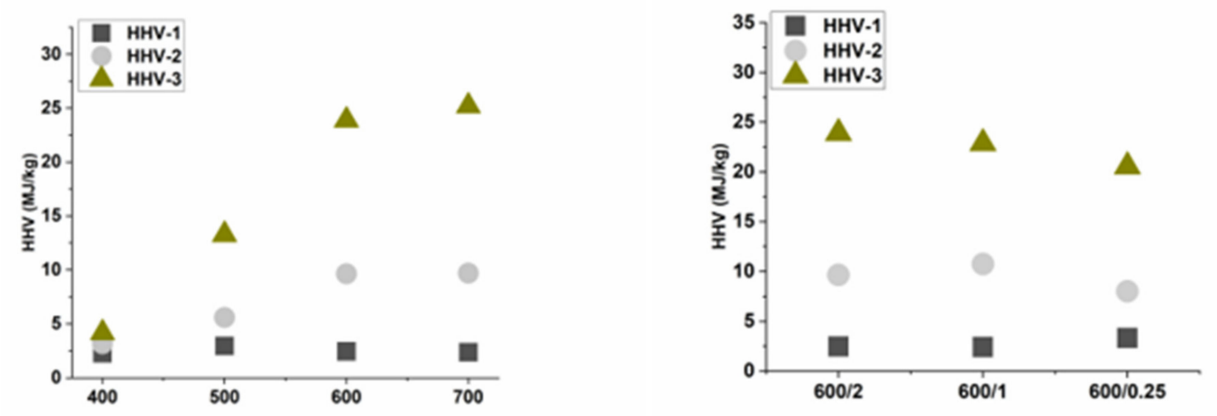

Figure 3. Higher heating value (HHV) for gaseous samples: Sample 1—gas created in temperature range 20–350 °C, Sample 2—gas created between 350 °C and final temperature, Sample 3—gas created at final temperature during residence time.

3.3. Condensate Characterization

The amount of resulting condensate ranged from 44 to 56 wt.%. In general, it is well known that maximum yields of condensate from biomass are obtained at reaction temperatures around 500 °C [36]. All condensates contained a huge amount of water, and the water content in the condensate was measured in the range from 27.7 to 29.8 wt.%. The water content was roughly the same within the measurement error. Determination of water content in the condensate was limited by the considerable inhomogeneity of pyrolysis oil, where part of the substances insoluble in water adhered to the walls of the containers, and even thorough shaking did not form a homogeneous solution, which was necessary for a correct determination. These results inform that the temperature of biochar preparation did not have a significant effect on the amount of water in the condensate. Higher heating value of condensate was insignificant, due to the high amount of water negligible (0.15 MJ/kg).

The results from GC-MS are shown in Table 3. Two samples were prepared for each experiment. The first sample contained water-soluble compounds and the second sample contained water-insoluble compounds. Water soluble compounds contained a huge amount of Acetic acid, 1-hydroxyl-2 Propanone and Phenol and the water-insoluble compounds contained 1-(acetyloxy)-2-Propanone, 2-methoxy-Phenol and Phenol. These results showed a similar tendency compared to Bergs et al. [34] focused on stem/leaf Miscanthus mixture pyrolysis. The temperature did not significantly affect the composition of the condensate. The reason is that the majority of condensate was formed until the temperature of 400 °C, as shown in the TGA curve (Figure 1).

3.4. Biochar Characterization

Thermogravimetric, elemental and calorific analyses were performed for raw Miscanthus rhizomes and all biochar samples. The results are presented in Table 4. The volatile and moisture content decreased with increasing temperature. Temperature had positive effect on HHV. The amount of carbon was higher for biochar compared to raw Miscanthus and its amount increased with rising temperature.

Proximate analysis confirms that moisture (W) and volatile matter (VM) decreased with the increase in the pyrolysis temperature, while the amount of the fixed carbon (FC) significantly increased with increasing temperature, which corresponds to Huang et al. [37]. As the pyrolysis temperature increased, the amount of hydrogen and oxygen atoms were released through dehydration and decarboxylation reactions. The HHV increased with the reaction temperature, and the yield of ash increased as well.

Table 3. Water-insoluble compounds and water-soluble compounds in condensate sample at pyrolysis of 600 °C and residence time of 2 h.

Condensate Compounds in Dichlormethane Extract	Peak Area/Total Area of All Peaks	Condensate Compounds in Diethyleether Extract	Peak Area/Total Area of All Peaks
2-Propanone, 1-(acetyloxy)-	10.58	Acetic acid	28.23
Phenol, 2-methoxy-	9.32	2-Propanone, 1-hydroxy-	11.74
Phenol	8.80	Phenol	4.94
3-Furaldehyde	6.75	2-Furanmethanol	4.57
Furfural	5.86	Hydroquinone	4.44
Benzofuran, 2,3-dihydro-	5.73	Propanoic acid	3.80
1-Hydroxy-2-butanone	5.10	1-Hydroxy-2-butanone	3.61
Phenol, 4-ethyl-	4.86	2-Propanone, 1-(acetyloxy)-	3.21
Butyrolactone	4.48	Phenol, 2-methoxy-	2.82
2-Furanmethanol	3.89	Furfural	2.65
Phenol, 2,6-dimethoxy-	3.82	2,3-Butanedione	2.63
Propanoic acid, 2-methyl-, anhydride	3.12	Benzofuran, 2,3-dihydro-	2.05
Phenol, 4-ethyl-2-methoxy-	3.08	1,2-Cyclopentanedione	1.96
2-Methoxy-4-vinylphenol	2.84	Phenol, 4-ethyl-	1.68
Propanoic acid	2.68	Phenol, 2,6-dimethoxy-	1.35
1,2-Cyclopentanedione, 3-methyl-	2.33	1,2-Cyclopentanedione, 3-methyl-	1.33

Table 4. Proximate and ultimate analysis.

	Raw Miscanthus	Biochar 400	Biochar 500	Biochar 600	Biochar 700	Biochar 600/1	Biochar 600/0.25
				Proximate analysis (wt.%)			
W	8.53 ± 0.08	2.05 ± 0.02	1.84 ± 0.01	1.55 ± 0.01	1.53 ± 0.03	1.74 ± 0.00	1.85 ± 0.04
VM [d]	76.00 ± 1.05	22.82 ± 0.31	15.78 ± 0.24	9.92 ± 0.08	7.30 ± 0.07	11.07 ± 0.46	13.13 ± 0.42
FC [d]	20.58 ± 0.32	67.33 ± 0.28	74.04 ± 0.42	77.82 ± 0.13	78.71 ± 0.04	76.79 ± 0.73	76.50 ± 0.38
A [d]	3.42 ± 0.01	9.86 ± 0.01	10.17 ± 0.21	12.26 ± 0.04	13.98 ± 0.14	12.14 ± 0.27	10.38 ± 0.84
				Ultimate analysis (wt.%)			
C [d]	55.33 ± 0.29	74.73 ± 0.22	80.63 ± 0.32	81.42 ± 0.42	81.30 ± 0.06	80.90 ± 0.27	80.98 ± 0.47
H [d]	12.51 ± 0.21	4.41 ± 0.08	4.18 ± 0.05	2.61 ± 0.04	1.59 ± 0.01	2.84 ± 0.11	2.87 ± 0.03
O [d]	27.53 ± 0.23	8.58 ± 0.07	2.22 ± 0.04	1.32 ± 0.03	1.08 ± 0.01	1.68 ± 0.10	3.23 ± 0.02
N [d]	0.87 ± 0.10	1.57 ± 0.01	1.69 ± 0.01	1.58 ± 0.00	1.48 ± 0.01	1.59 ± 0.00	1.58 ± 0.02
S [d]	0.34 ± 0.00	0.85 ± 0.00	1.11 ± 0.00	0.81 ± 0.01	0.57 ± 0.00	0.85 ± 0.01	0.96 ± 0.02
				Atomic ratio			
H/C	2.71 ± 0.02	0.71 ± 0.01	0.62 ± 0.01	0.39 ± 0.01	0.24 ± 0.01	0.42 ± 0.01	0.43 ± 0.01
O/C	0.38 ± 0.00	0.09 ± 0.00	0.02 ± 0.00	0.01 ± 0.00	0.01 ± 0.00	0.02 ± 0.00	0.03 ± 0.00
				Higher heating value (MJ/kg)			
HHV [d]	19.84 ± 0.01	30.00 ± 0.03	31.17 ± 0.02	30.37 ± 0.07	29.32 ± 0.03	30.70 ± 0.04	31.18 ± 0.10

A ash, W moisture content, VM volatile matter, FC fixed carbon, HHV higher heating value. [d] in dry matter.

Pyrolysis is primarily characterized by degradation of hemicellulose. Dehydration and decarboxylation are the main reactions in this degradation.

The purpose of the pyrolysis of biomass is to maximize energy and yields while reducing O/C and H/C ratio. The biochar yield during pyrolysis decreased with increasing temperature. While the O and H content significantly decreased with increasing pyrolysis temperature, the opposite happened to C and N content. The effect of temperature can be clearly described by the Van Krevelen diagram (see Figure 4). The O/C and H/C ratio decreased with increasing pyrolysis temperature. Nevertheless, according to the analysis of the effect of residence time on biochar characteristics, fuel characteristics did not significantly change. This finding implies that biochar characteristics were mainly influenced by the pyrolysis temperature rather than residence time, which corresponds to Huang et al. [37]. The Van Krevelen diagram shows the effect of the process parameters except pyrolysis temperature on the chemical reactions during the biochar preparation, as reported by Schimmelpfennig et al. [38].

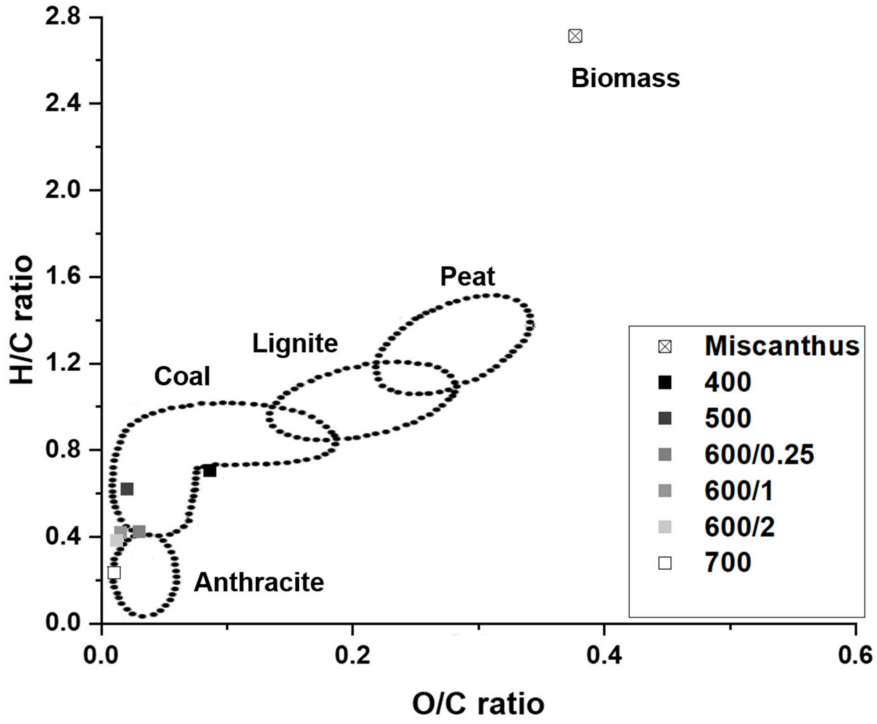

Figure 4. Van Krevelen diagram.

3.5. pH and Electrical Conductivity (EC)

pH and electrical conductivity are important properties of the soil. EC and pH were determined for raw Miscanthus rhizomes and all biochars using two grain sizes (<3.15 mm; <300 µm). Pyrolysis temperature affected both pH and EC. The aqueous extract of biochar was alkaline. As the temperature increased, the pH rose, which is in agreement with Skopas et al. [39]. pH values of the biochars increased from slightly alkaline to highly alkaline as carbonization temperature increased (Figure 5). As the temperature of pyrolysis rose, the EC of biochars increased (Figure 6). This phenomenon is due to the fact that during pyrolysis, the bonds of higher molecules were broken up and simpler inorganic compounds were formed, thus increasing electrical conductivity.

3.6. Surface Area

Macropores are relevant to vital soil functions. The presence of the larger amount of macropores, mesopores, and micropores in biochar may improve physical properties of soil [40]. Specific surface area was measured for raw Miscanthus rhizomes and all biochars. The results are presented in Table 5. The porosity of solid residues depends mainly on the final temperature. The results show that the pyrolysis temperature predominantly affected the specific surface area, porosity, and pore size distribution of biochar. Specific surface area increased with increasing temperature. The higher pyrolysis temperature resulted in a higher specific surface area, but the area of mesopores was lower. The higher pyrolysis temperature caused biochar yields to decrease whilst their quality in terms of sorption properties were improved [40]. The temperature of 700 °C led to the formation of large quantities of micropores. As temperature increased, the porosity grew too. Only for an experiment at 600/0.25 was the value lower, which was due to the fact that the pyrolysis time of this experiment was shorter than for the experiment at 500 °C.

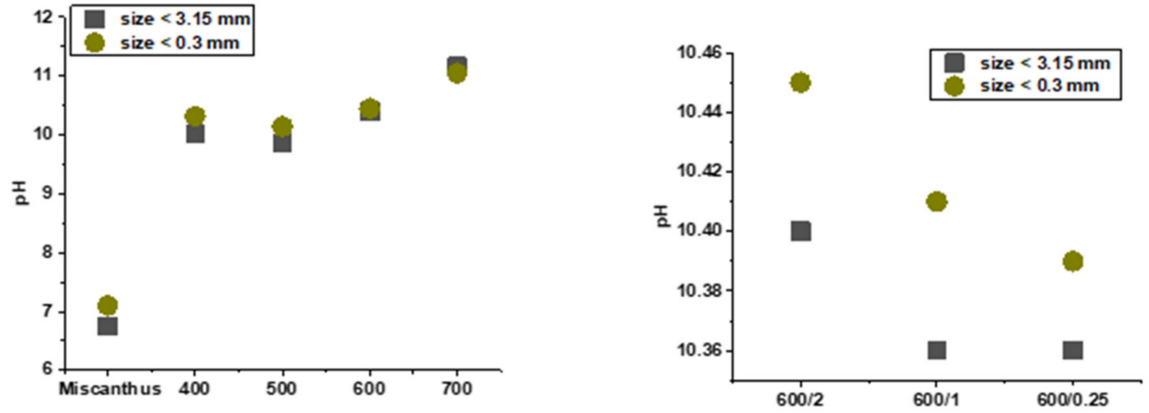

Figure 5. pH of raw Miscanthus rhizomes and biochars.

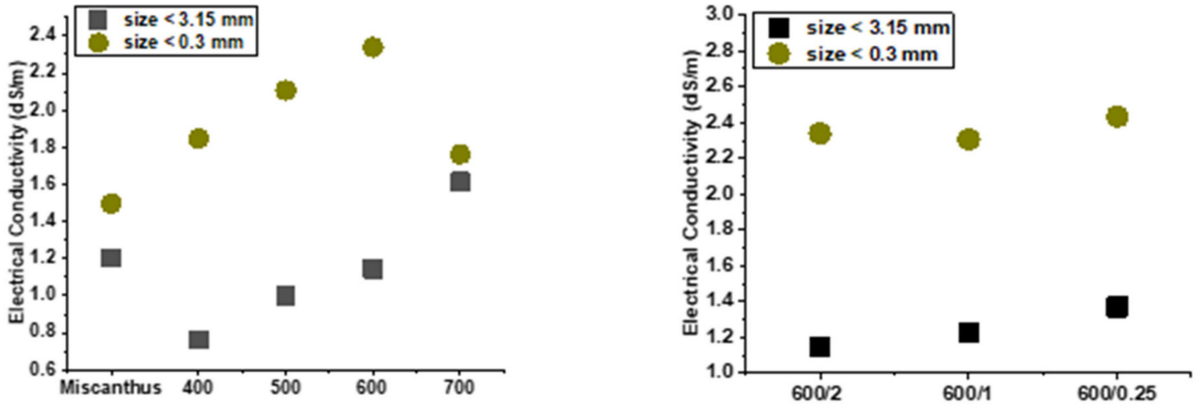

Figure 6. EC of raw Miscanthus rhizomes and biochars.

Table 5. Adsorption analysis for raw Miscanthus rhizomes and biochars.

Sample	S_{BET} (m^2/g)	S_{meso} (m^2/g)	V_{micro} (mm^3_{liq}/g)	V_{net} (mm^3_{liq}/g)
Miscanthus	0.7 ± 0.01	nd	nd	nd
400	5 ± 0.01	nd	nd	nd
500	47 ± 0.08	nd	nd	nd
600	217 ± 6.21	22 ± 0.08	106 ± 4.03	132 ± 2.87
700	273 ± 4.24	18 ± 0.06	123 ± 1.89	146 ± 1.04
600/1	193 ± 0.28	19 ± 0.45	87 ± 1.14	113 ± 3.40
600/0.25	16 ± 0.02	6 ± 0.01	4 ± 0.01	10 ± 0.01

3.7. PAHs and Heavy Metals

Polycyclic aromatic hydrocarbons are the most frequently occurring contaminants in biochar, because they are created during the pyrolysis process. The results of this special analysis are shown in Table 6. The quantity of PAHs was strongly influenced by the chemical composition of the feedstock and the pyrolysis conditions. This is in agreement with Quilliam et al., and Dutta et al. [41,42]. Among various pyrolysis conditions, the temperature played a critical role in determining the quantity and type of compounds released from biochar. During pyrolysis, the main components of biomass, lignin and cellulose undergo dehydrogenation, dealkylation, and aromatization. At a temperature of about 500 °C, carbonization and aromatization occurred to form biochar and PAHs. The biochar prepared at lower temperatures contained mainly low molecular weight PAHs (LMW-PAH). Naphthalene was the main PAH detected in biochar around 500 °C. Then at

higher pyrolysis temperatures, above 500 °C, the PAHs were formed into longer aromatic structures as mentioned by Odinga et al. [43]. However, in a temperature range from 600 to 700 °C PAH concentration with four aromatic rings was increased. The number of PAHs did not show a linear dependence on the temperature. All biochars prepared at the different temperatures met the soil toxicity assessment based on International Biochar Initiative Guidelines [44]. Lignin, cellulose and hemicellulose affected the number of PAHs formed during pyrolysis. The feedstock rich in lignin yielded biochar with lower PAHs as confirmed by Cho at al. [45]. Lignin promotes Miscanthus rhizomes to be a promising raw material for the production of biochar.

Table 6. Effect of temperature on PAH mass.

	Criteria (IBI) mg/kg Dry wt	400	500	600	700	600/1	600/0.25
PAHs	6–300	6.80 ± 0.02	17.40 ± 0.68	5.60 ± 0.13	4.10 ± 0.11	5.80 ± 0.08	5.00 ± 0.07

All biochars must comply with the soil toxicity assessment according to the IBI, which defines the standards for heavy metals in biochar [44]. The amount of heavy metals in the input sample was determined. The results are shown in Table 7. Miscanthus rhizomes were grown in uncontaminated soil. The input sample was not contaminated with any heavy metals, so rhizomes met all the criteria.

Table 7. Heavy metals in feedstock.

	Criteria (IBI) mg/kg Dry wt	Miscanthus
As	13–100	<0.5 ± 0.00
Cd	1.4–39	<0.4 ± 0.00
Cr	93–1200	9.57 ± 0.14
Co	34–100	1.26 ± 0.28
Cu	143–6000	10.6 ± 0.71
Pb	121–300	2.7 ± 0.08
Hg	1–17	<0.2 ± 0.00
Mo	5–75	0.44 ± 0.02
Ni	47–420	7.5 ± 0.93
Se	2–200	<2.0 ± 0.00
Zn	416–7400	102 ± 0.08

3.8. Concentration of Ca, K, Mg, S, N and P

Biochar has a significant effect on plant quality in terms of nutrient content. All nutrients were determined in the form of ions. The amount of available content of S was determined as SO_4^{2-}, available content of N as NH^{3+} and available content of P as PO_4^{3-}. The content of these nutrients (Ca, Mg and K) in biochar was significantly affected by the selected pyrolysis temperature and residence time at the final temperature. With increasing temperature and residence time, the concentration of the above-mentioned components increased. The concentrations of Ca, K, Mg, S, N and P are presented in Table 8. The plant macro nutrients in Miscanthus biochar were lower. The results show that most of the nutrients contained in biochar were extracted.

The results of morphology structure analysis are shown in Figure 7. The effect of the preparation temperature can be seen. As the preparation temperature and atmosphere changed, the surface structures of the biochar had different morphologies. The biochar prepared at 400 and 500 °C showed a macrostructure in the form of honey combs. The biochar prepared at 600 and 700 °C showed a rod-shaped structure with considerable cracks and small floccules on the surface. The corners of rod shapes remained relatively sharp and the edges were well defined, which is typical for graphene materials as defined by Yan [31].

Table 8. Concentration of Ca, Mg, K, S, N and P in biochars 600/2.

	600/2
Total Ca (mg/kg)	1910 ± 98.07
Available Ca (mg/kg)	1204 ± 37.44
Total Mg (mg/kg)	1190 ± 36.98
Available Mg (mg/kg)	272 ± 10.26
Total K (mg/kg)	25,400 ± 109.03
Available K (mg/kg)	7069 ± 13.91
Total S (mg/kg)	8100 ± 61.23
Available SO_4^{2-} (mg/kg)	2558 ± 79.54
Total N (mg/kg)	15,800 ± 102.01
Available NH^{3+} (mg/kg)	<2 ± 0.00
Total P (mg/kg)	2870 ± 75.08
Available PO_4^{3-} (mg/kg)	1983 ± 26.12

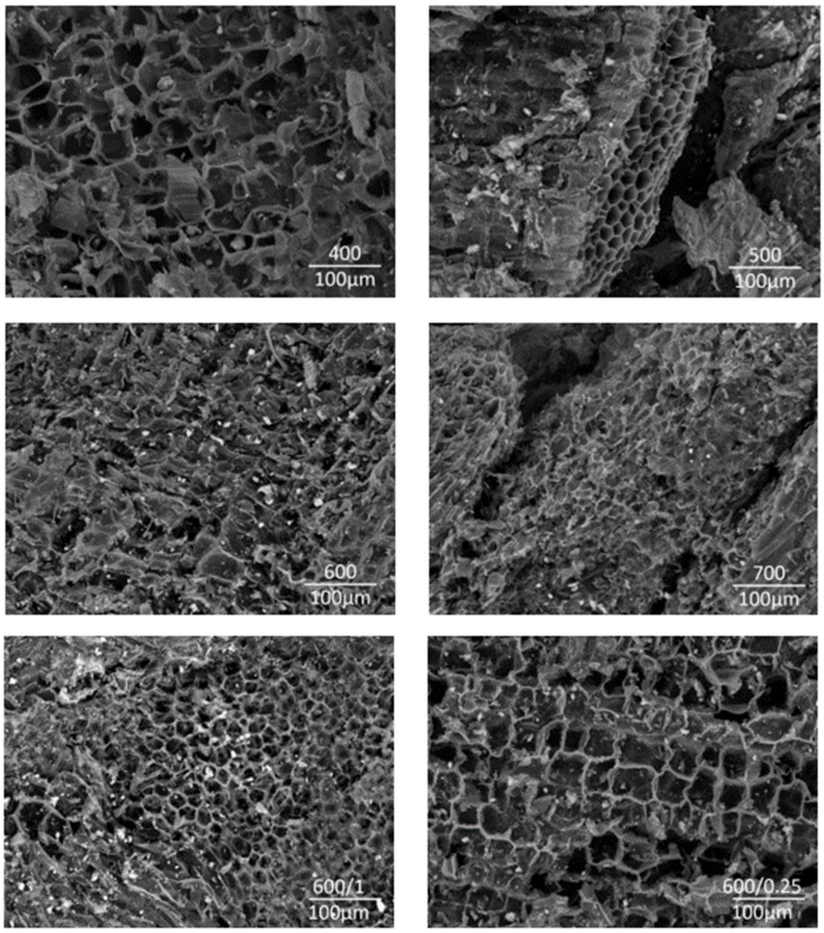

Figure 7. SEM images of biochar prepared at 400, 500, 600/2, 700, 600/0.1, 600/0.25.

The pyrolysis temperature affected the number of considerable cracks and flakes, which led to the gradual destruction of the surface structure as reported by Tian et al. [46]. The surface structure was also affected by the residence time of Miscanthus in the pyrolysis unit. As the residence time increased, the number of flakes on the surface also increased. It can be mentioned that destroying carbon structures at higher temperatures led to an increase in porosity, i.e., a porous structure was formed. The residence time for the experiments 600/0.25 and 600/1 was insufficient to break carbonaceous structures.

4. Conclusions

A series of experiments was performed in order to find the suitable conditions for the preparation of biochar. In this study, the effect of pyrolysis conditions on the properties of biochar produced by Miscanthus rhizome pyrolysis was studied. In addition to the type of plant itself, the temperature in the pyrolysis zone of the reactor and residence time in the reaction space had a great influence on both the quality and quantity of biochar. The resulting products were evaluated from several perspectives. However, the basic parameter was the content of polycyclic aromatic hydrocarbons. At 700 °C, PAH content was slightly less, while other parameters were comparable—i.e., carbon content, biogenic element content as well as specific surface area. Conversely, 500 °C led to the formation of biochar with a high PAH content. A temperature of 600 °C was chosen as a compromise between the achieved properties of biochar and its yield with respect to the economics of the process. Changes in residence time resulted in negligible differences in PAH concentrations, but a significant effect on the specific surface area was observed. Insufficient residence time caused an inefficiently developed porous structure. Chemical properties of biochar, especially pH and nutrient content, but also physical properties such as pore size, pore volume and specific surface area, played a key role in determining biochar quality and thus its effect on soil microorganisms that in turn affect plant growth. In line with the "zero waste" approach, the produced biochar was reused at the field and the results of its application together with phytotoxicity tests will be the subject of further study.

Author Contributions: Formal analysis, K.K. and B.G.; investigation, K.K. and B.G.; methodology, P.L.; supervision, P.L.; validation, P.L.; writing—original draft, K.K. and B.G. All authors have read and agreed to the published version of the manuscript.

Funding: This work was supported by the Czech Ministry of Industry and Trade by MiscanValue—Cornet project No. CZ.01.1.02/0.0/0.0/19_263/0018837, and by using Large Research Infrastructure ENREGAT supported by the Ministry of Education, Youth and Sports of the Czech Republic under project No. LM2018098.

Institutional Review Board Statement: Not applicable.

Informed Consent Statement: Not applicable.

Data Availability Statement: Not applicable.

Conflicts of Interest: The authors declare no conflict of interest.

References

1. Ghalibaf, M.; Ullah, S.; Alén, R. Fast pyrolysis of hot-water-extracted and soda-AQ-delignified okra (Abelmoschus esculentus) and miscanthus (miscanthus x giganteus) stalks by Py-GC/MS. *Biomass-Bioenergy* **2018**, *118*, 172–179. [CrossRef]
2. Saxena, R.C.; Adhikari, D.K.; Goyal, H.B. Biomass-based energy fuel through biochemical routes: A review. *Renew. Sustain. Energy Rev.* **2009**, *13*, 167–178. [CrossRef]
3. Wafiq, A.; Reichel, D.; Hanafy, M. Pressure influence on pyrolysis product properties of raw and torrefied Miscanthus: Role of particle structure. *Fuel* **2016**, *179*, 156–167. [CrossRef]
4. Wilk, M.; Magdziarz, A. Hydrothermal carbonization, torrefaction and slow pyrolysis of Miscanthus giganteus. *Energy* **2017**, *140*, 1292–1304. [CrossRef]
5. Lewandowski, I.; Clifton-Brown, J.; Trindade, L.M.; Van Der Linden, G.C.; Schwarz, K.-U.; Müller-Sämann, K.; Anisimov, A.; Chen, C.-L.; Dolstra, O.; Donnison, I.S.; et al. Progress on Optimizing Miscanthus Biomass Production for the European Bioeconomy: Results of the EU FP7 Project OPTIMISC. *Front. Plant Sci.* **2016**, *7*, 1–23. [CrossRef]
6. Parveen, I.; Threadgill, M.D.; Hauck, B.; Donnison, I.; Winters, A. Isolation, identification and quantitation of hydroxycinnamic acid conjugates, potential platform chemicals, in the leaves and stems of Miscanthus×giganteus using LC–ESI-MSn. *Phytochemistry* **2011**, *72*, 2376–2384. [CrossRef]
7. Tew, T.L.; Cobill, R.M. Genetic Improvement of Sugarcane as an Energy Crop. In *Genetic Improvement of Bioenergy Crops*; Vermerris, W., Ed.; Springer: New York, NY, USA, 2008. [CrossRef]
8. Da Costa, R.M.F.; Lee, S.J.; Allison, G.G.; Hazen, S.P.; Winters, A.; Bosch, M. Genotype, development and tissue-derived variation of cell-wall properties in the lignocellulosic energy crop Miscanthus. *Ann. Bot.* **2014**, *114*, 1265–1277. [CrossRef]
9. Nowicki, L.; Siuta, D.; Markowski, M. Pyrolysis of Rapeseed Oil Press Cake and Steam Gasification of Solid Residues. *Energies* **2020**, *13*, 4472. [CrossRef]

10. Lehmann, J.; Joseph, S. *Biochar for Environmental Management: Science and Technology*, 2nd ed.; Earthscan Routlegde: New York, NY, USA, 2015.
11. Kim, J.; Hyun, S. Sorption of ionic and nonionic organic solutes onto giant Miscanthus-derived biochar from methanol-water mixtures. *Sci. Total Environ.* **2018**, *615*, 805–813. [CrossRef] [PubMed]
12. He, K.; He, G.; Wang, C.; Zhang, H.; Xu, Y.; Wang, S.; Kong, Y.; Zhou, G.; Hu, R. Biochar amendment ameliorates soil properties and promotes Miscanthus growth in a coastal saline-alkali soil. *Appl. Soil Ecol.* **2019**, *155*, 103674. [CrossRef]
13. Mimmo, T.; Panzacchi, P.; Baratieri, M.; Davies, C.A.; Tonon, G. Effect of pyrolysis temperature on miscanthus (Miscanthus × giganteus) biochar physical, chemical and functional properties. *Biomass-Bioenergy* **2014**, *62*, 149–157. [CrossRef]
14. Cheng, J.; Lee, X.; Tang, Y.; Zhang, Q. Long-term effects of biochar amendment on rhizosphere and bulk soil microbial communities in a karst region, southwest China. *Appl. Soil Ecol.* **2019**, *140*, 126–134. [CrossRef]
15. Novak, J.M.; Ippolito, J.A.; Ducey, T.F.; Watts, D.W.; Spokas, K.; Trippe, K.M.; Sigua, G.C.; Johnson, M.G. Remediation of an acidic mine spoil: Miscanthus biochar and lime amendment affects metal availability, plant growth, and soil enzyme activity. *Chemosphere* **2018**, *205*, 709–718. [CrossRef] [PubMed]
16. Khan, W.-U.D.; Ramzani, P.M.A.; Anjum, S.; Abbas, F.; Iqbal, M.; Yasar, A.; Ihsan, M.Z.; Anwar, M.N.; Baqar, M.; Tauqeer, H.M.; et al. Potential of miscanthus biochar to improve sandy soil health, in situ nickel immobilization in soil and nutritional quality of spinach. *Chemosphere* **2017**, *185*, 1144–1156. [CrossRef]
17. Mete, F.Z.; Mia, S.; Dijkstra, F.A.; Abuyusuf, M.; Hossain, A.S.M.I. Synergistic Effects of Biochar and NPK Fertilizer on Soybean Yield in an Alkaline Soil. *Pedosphere* **2015**, *25*, 713–719. [CrossRef]
18. Godlewska, P.; Ok, Y.S.; Oleszczuk, P. The dark side of black gold: Ecotoxicological aspects of biochar and biochar-amended soils. *J. Hazard. Mater.* **2021**, *403*, 123833. [CrossRef]
19. Assil, Z.; Esegbue, O.; Mašek, O.; Gutierrez, T.; Free, A. Specific enrichment of hydrocarbonclastic bacteria from diesel-amended soil on biochar particles. *Sci. Total Environ.* **2020**, *762*, 143084. [CrossRef]
20. Wang, C.; Lv, H.; Yang, W.; Li, T.; Fang, T.; Lv, G.; Han, Q.; Dong, L.; Jiang, T.; Jiang, B.; et al. SVCT-2 determines the sensitivity to ascorbate-induced cell death in cholangiocarcinoma cell lines and patient derived xenografts. *Cancer Lett.* **2017**, *398*, 1–11. [CrossRef]
21. Hilber, I.; Bastos, A.C.; Loureiro, S.; Soja, G.; Marsz, A.; Cornelissen, G.; Bucheli, T.D. The different faces of biochar: Contamination risk versus remediation tool. *J. Environ. Eng. Landsc. Manag.* **2017**, *25*, 86–104. [CrossRef]
22. Palansooriya, K.N.; Wong, J.T.F.; Hashimoto, Y.; Huang, L.; Rinklebe, J.; Chang, S.X.; Bolan, N.; Wang, H.; Ok, Y.S. Response of microbial communities to biochar-amended soils: A critical review. *Biochar* **2019**, *1*, 3–22. [CrossRef]
23. Lyu, H.; He, H.; Tang, J.; Hecker, M.; Liu, Q.; Jones, P.D.; Codling, G.; Giesy, J.P. Effect of pyrolysis temperature on potential toxicity of biochar if applied to the environment. *Environ. Pollut.* **2016**, *218*, 1–7. [CrossRef] [PubMed]
24. Wang, C.; Wang, Y.; Herath, H.M.S.K. Polycyclic aromatic hydrocarbons (PAHs) in biochar—Their formation, occurrence and analysis: A review. *Org. Geochem.* **2017**, *114*, 1–11. [CrossRef]
25. Cipullo, S.; Snapir, B.; Tardif, S.; Campo, P.; Prpich, G.; Coulon, F. Insights into mixed contaminants interactions and its implication for heavy metals and metalloids mobility, bioavailability and risk assessment. *Sci. Total Environ.* **2018**, *645*, 662–673. [CrossRef]
26. Zadel, U.; Nesme, J.; Michalke, B.; Vestergaard, G.; Płaza, G.A.; Schröder, P.; Radl, V.; Schloter, M. Changes induced by heavy metals in the plant-associated microbiome of Miscanthus x giganteus. *Sci. Total Environ.* **2020**, *711*, 134433. [CrossRef]
27. Arduini, I.; Masoni, A.; Mariotti, M.; Ercoli, L. Low cadmium application increase miscanthus growth and cadmium translocation. *Environ. Exp. Bot.* **2004**, *52*, 89–100. [CrossRef]
28. Nsanganwimana, F.; Pourrut, B.; Mench, M.; Douay, F. Suitability of Miscanthus species for managing inorganic and organic contaminated land and restoring ecosystem services. A review. *J. Environ. Manag.* **2014**, *143*, 123–134. [CrossRef]
29. Grycova, B.; Pryszcz, A.; Lestinsky, P.; Chamradova, K. Preparation and characterization of sorbents from food waste. *Green Process. Synth.* **2017**, *6*, 287–293. [CrossRef]
30. Lakshman, V.; Brassard, P.; Hamelin, L.; Raghavan, V.; Godbout, S. Pyrolysis of Miscanthus: Developing the mass balance of a biorefinery through experimental tests in an auger reactor. *Bioresour. Technol. Rep.* **2021**, *14*, 100687. [CrossRef]
31. Yan, Y.; Meng, Y.; Zhao, H.; Lester, E.; Wu, T.; Pang, C.H. Miscanthus as a carbon precursor for graphene oxide: A possibility influenced by pyrolysis temperature. *Bioresour. Technol.* **2021**, *331*, 124934. [CrossRef]
32. Yang, H.; Yan, R.; Chen, H.; Zheng, C.; Lee, A.D.H.; Liang, D.T. In-Depth Investigation of Biomass Pyrolysis Based on Three Major Components: Hemicellulose, Cellulose and Lignin. *Energy Fuels* **2006**, *20*, 388–393. [CrossRef]
33. Budai, A.; Wang, L.; Grønli, M.G.; Strand, L.T.; Antal, M.J., Jr.; Abiven, S.; Dieguez-Alonso, A.; Anca-Couce, A.; Rasse, D.P. Surface Properties and Chemical Composition of Corncob and Miscanthus Biochars: Effects of Production Temperature and Method. *J. Agric. Food Chem.* **2014**, *62*, 3791–3799. [CrossRef]
34. Bergs, M.; Völkering, G.; Kraska, T.; Pude, R.; Do, X.T.; Kusch, P.; Monakhova, Y.; Konow, C.; Schulze, M. Miscanthus x giganteus Stem Versus Leaf-Derived Lignins Differing in Monolignol Ratio and Linkage. *Int. J. Mol. Sci.* **2019**, *20*, 1200. [CrossRef]
35. Yan, Y.; Meng, Y.; Tang, L.; Kostas, E.T.; Lester, E.H.; Wu, T.; Pang, C.H. Ignition and Kinetic Studies: The Influence of Lignin on Biomass Combustion. *Energy Fuels* **2019**, *33*, 6463–6472. [CrossRef]
36. Kim, J.-Y.; Oh, S.; Hwang, H.; Moon, Y.-H.; Choi, J.W. Assessment of miscanthus biomass (Miscanthus sacchariflorus) for conversion and utilization of bio-oil by fluidized bed type fast pyrolysis. *Energy* **2014**, *76*, 284–291. [CrossRef]

37. Huang, C.-W.; Li, Y.-H.; Xiao, K.-L.; Lasek, J. Cofiring characteristics of coal blended with torrefied Miscanthus biochar optimized with three Taguchi indexes. *Energy* **2019**, *172*, 566–579. [CrossRef]
38. Schimmelpfennig, S.; Glaser, B. One Step Forward toward Characterization: Some Important Material Properties to Distinguish Biochars. *J. Environ. Qual.* **2012**, *41*, 1001–1013. [CrossRef]
39. Spokas, K.A.; Cantrell, K.B.; Novak, J.M.; Archer, D.W.; Ippolito, J.A.; Collins, H.P.; Boateng, A.A.; Lima, I.M.; Lamb, M.C.; McAloon, A.J.; et al. Biochar: A Synthesis of Its Agronomic Impact beyond Carbon Sequestration. *J. Environ. Qual.* **2012**, *41*, 973–989. [CrossRef]
40. Yang, C.; Liu, J.; Lu, S. Pyrolysis temperature affects pore characteristics of rice straw and canola stalk biochars and biochar-amended soils. *Geoderma* **2021**, *397*, 115097. [CrossRef]
41. Quilliam, R.S.; Rangecroft, S.; Emmett, B.A.; DeLuca, T.H.; Jones, D.L. Is biochar a source or sink for polycyclic aromatic hydrocarbon (PAH) compounds in agricultural soils? *GCB Bioenergy* **2013**, *5*, 96–103. [CrossRef]
42. Dutta, T.; Kwon, E.; Bhattacharya, S.S.; Jeon, B.H.; Deep, A.; Uchimiya, M.; Kim, K.-H. Polycyclic aromatic hydrocarbons and volatile organic compounds in biochar and biochar-amended soil: A review. *GCB Bioenergy* **2017**, *9*, 990–1004. [CrossRef]
43. Odinga, E.S.; Gudda, F.O.; Waigi, M.G.; Wang, J.; Gao, Y. Occurrence, formation and environmental fate of polycyclic aromatic hydrocarbons in biochars. *Fundam. Res.* **2021**, *1*, 296–305. [CrossRef]
44. IBI. International Biochar Initiative. International Biochar Initiative. Copyright © 2018. Available online: https://biochar-international.org (accessed on 17 February 2022).
45. Cho, D.-W.; Cho, S.-H.; Song, H.; Kwon, E.E. Carbon dioxide assisted sustainability enhancement of pyrolysis of waste biomass: A case study with spent coffee ground. *Bioresour. Technol.* **2015**, *189*, 1–6. [CrossRef] [PubMed]
46. Tian, H.; Hu, Q.; Wang, J.; Chen, D.; Yang, Y.; Bridgwater, A.V. Kinetic study on the CO2 gasification of biochar derived from Miscanthus at different processing conditions. *Energy* **2021**, *217*, 119341. [CrossRef]

Příloha [P6]

GRYCOVA, B., PRYSZCZ, A., CHAMRADOVA, K. & **LESTINSKY, P.** 2018. Influence of potassium hydroxide and method of carbonization treatment in garden and corn waste microwave pyrolysis. *Biomass & Bioenergy*, 118, 40-45. IF_{2018} = 3,537 (5 year IF 5.5). Autorský podíl 25 %. Počet citací dle WoS 15.

Role uchazeče:

- návrh postupu prací, vyhodnocení výsledků, vyvození závěrů z dosažených výsledků

Biomass and Bioenergy 118 (2018) 40–45

Contents lists available at ScienceDirect

Biomass and Bioenergy

journal homepage: www.elsevier.com/locate/biombioe

Research paper

Influence of potassium hydroxide and method of carbonization treatment in garden and corn waste microwave pyrolysis

B. Grycova*, A. Pryszcz, P. Lestinsky, K. Chamradova

VSB – Technical University of Ostrava, Institute of Environmental Technology, 17.listopadu 15/2172, Ostrava – Poruba, 708 33, Czech Republic

ARTICLE INFO

Keywords:
Microwave pyrolysis
Garden waste
Hydrogen
Activation

ABSTRACT

After initial selection, the samples of garden and corn waste were activated by potassium hydroxide and processed by microwave pyrolysis using both single-step and double-step methods. Experiments were carried out in a self-made microwave reactor for 20 min at the power of 440 W. The distribution and quality of the resulting products were evaluated. The gaseous components were analysed discontinuously by gas chromatography. The concentration of measured hydrogen (activated corn waste 54.4 vol %, non-activated corn waste 18.8 vol %) was strongly influenced by activation and material selection. The char with a heating value of 33.3 MJ kg^{-1} suggested the direction of its further use as fuel. Optimum conditions of sorbents production from garden waste material with a surface area of 530 $m^2 g^{-1}$ with regard to the influence of the activation were determined.

1. Introduction

Biomass has recently caught considerable interest as a low-cost renewable and sustainable raw material and a new option for worldwide alternative energy production. An increase in the production of unused garden waste can be seen over the past years and indicates the general tendency over the long-term [1]. Cut grass from housing estates, parks and gardens make up the largest part of the bio-waste that has been bundled from the surrounding villages and towns and processed on composting sites at the Depos Horní Suchá a.s. According to the company's information, production of bio-waste is increasing. In 2004, a total of 472 tonnes were recorded, while last year it was already ten times more. Green power will definitely be playing an important part as an available renewable resource to play a role in energy generation and production of chemicals, in order to mitigate climate change and replace fossil resources. Most of this waste is dealt with by biochemical processes [2]. Pyrolysis could be an attractive method to facilitate efficient conversion of the above mentioned waste to upper-class products with the help of process optimization. In recent years, microwave irradiation has brought some really promising results as a substitute heating method [3], and great attention has been paid to its advantages over the conventional electric heating processes [4]. The main characteristics of microwave heating place ensure both selectivity and efficiency, all of which contribute to desired results. Electromagnetic waves ranging from 300 MHz to 300 GHz form the basis of microwaves, which means that corresponding wave lengths are between 1 m and 1 mm [5] and can pass through the material to cause uniform temperature change [6]. The main advantage is that the microwave heating is direct - the energy is absorbed only by the sample and is not wasted on the container in which the sample is placed. Direct heating is also highly controllable and efficient, and in many cases this efficiency will make up for the relatively high cost of microwave energy. Microwaves can generate microplasma and hot spots, which promote heterogeneous catalytic reactions and produce a greater concentration of hydrogen in the resulting gas than convectional pyrolysis. Nevertheless, it suffers from a number of drawbacks. The monitored and controlled temperature is very hard to manage, because conventional thermometers cannot be used as thermocouples.

A variety of biomass materials, such as wood [7], coffee hulls [8], sugarcane bagasse [9], wheat straw [10], or corn stalk [11] have been processed by microwave heating. As a result of the ever growing interest in microwave pyrolysis, it is possible to find a wide range of complete reviews available in scientific literature [12], focused on biochar [13], with regard to pyrolysis conditions [14] and based on global fossil energy scenario [15].

It is generally known that biomass is not typically a good microwave absorber. The presence of fairly high moisture and inorganic substances can progress absorption capacity. Carbonaceous materials such as char or activated carbon are well-intentioned applicants for microwave absorbers to stimulate process of biomass pyrolysis [16]. Carbon

* Corresponding author.
E-mail addresses: barbora.grycova@vsb.cz (B. Grycova), adrian.pryszcz@vsb.cz (A. Pryszcz), pavel.lestinsky@vsb.cz (P. Lestinsky), katerina.chamradova@vsb.cz (K. Chamradova).

https://doi.org/10.1016/j.biombioe.2018.07.022
Received 6 February 2018; Received in revised form 29 June 2018; Accepted 30 July 2018
Available online 24 August 2018
0961-9534/

absorption is up to 8 times larger than water absorption. Microwave absorbers and some catalysts added to biomass can adjust products distribution, increase process energy efficiency, or improve the characteristics of resulting products [13].

Product distribution of microwave and conventional pyrolysis is described as being quite different. This could be attributed to a number of different factors such as biomass properties, microwave values, reaction conditions, etc. Based on published analysis focused on corn waste material, the average gas, liquid, and solid yields were assessed as being approximately 35–41, 33–37, and 26–29 wt. % [3]. Practically half of the biomass can be converted into permanent gases by using microwave pyrolysis. The effects of reaction time and temperature on the yield of gas, bio-oil and biochar from a Douglas fir sawdust pellet using a microwave pyrolysis method were reported by Ren et al. [17]. It was found out that increasing reaction time and temperature led to an increase in the yield of volatiles. Zhao et al. [10] published on the influence of temperature on the microwave-induced pyrolysis of wheat straw. Increasing temperature from 400 °C to 600 °C initiated a progression in the yield of gas products. Catalytic effect as well as the effect of temperature on the pyrolysis process, the cracking of tars and phenolic compounds to the permanent gases (H_2 and CO) was studied by Lestinsky et al. [18]. The catalytic active elements, namely nickel, cobalt or iron were added to the char to become the basis for improved hydrogen production.

The composition of gas product from microwave pyrolysis of rice husks [19], coffee hulls [20] and pine sawdust [21] were evaluated. Based on data taken from above mentioned references the main components of the gas such as hydrogen and carbon monoxide can be observed in the range of 22–42 and 23–43 vol %. Methane and carbon dioxide have also occurred. Contribution of light hydrocarbons would have amounted to only 3 vol %. All this makes microwave pyrolysis a promising method for the production of hydrogen rich fuel gas [22].

The possibility of using microwave induced pyrolysis to recover energy from rice straw was discussed [23]. Rich flue gas was the product of this process with H_2 (55 vol %), CO_2 (17 vol %), CO (13 vol %), and CH_4 (10 vol %). Domingues et al. [24] investigated the microwave assisted pyrolysis of sewage sludge with regard to maximizing the gas yield and quality. The experiments were carried out by means of both single mode and multimode microwave reactors. Graphite and char were applied as absorbers while helium was used as carrier gas. It was concluded that microwave irradiation improved the proportion of gases produced (up to 38 vol % for H_2 and 66 vol % for $H_2 + CO$). In addition, it was proven that microwave irradiation decreased reaction time by 14 min compared to the conventional process. Therefore, microwave radiation becomes a common source of energy in accelerating chemical reactions.

Pyrolysis has also been proved as a technology to produce biochar [25]. Data demonstrate that biochar and its activated derivatives have the capacity to eliminate different contaminants [26]. Microwave irradiation has yielded hopeful results, significantly lowering energy consumption in the production of low-cost adsorbents [27] with auspicious pore characteristics [7]. A high BET and Langmuir surface area of 972 and 1519 $m^2 g^{-1}$ was reached by microwave-induced KOH activation of rambutan peel, within a short activation time of only 12 min [28].

Microwave-assisted pyrolysis with chemical activation to convert orange peel into activated carbon was reported by Lam et al. [29]. The orange peel was first carbonized via microwave-assisted pyrolysis to produce biochar, which was then activated and converted into activated carbon by means of chemical impregnation coupled with microwave-assisted pyrolysis with high BET surface area (1350 $m^2 g^{-1}$). It was found that the higher temperature and retention time enhanced the pore structure of biochar from microwave pyrolysis of corn stalk [30]. Li et al. [31] and Sharma et al. [32] stated influence of temperature on the BET surface area and micropore volume.

The biochar produced by rice straw microwave pyrolysis under a power of 300, 400, and 500 W was tested for surface area analysis [23]. The BET surface area was 165.74–274.49 $m^2 g^{-1}$. Increasing microwave power from 300 W to 500 W caused an increase of ~1.6 times. By direct activation of hay with the use of microwave radiation were obtained microporous bio-carbons of a surface area ranging from 88 to 265 $m^2 g^{-1}$ [33]. Microwave assisted potassium hydroxide activation of fibers of oil palm empty fruit bunches was reported by Farma et al. [34]. Microwave irradiation time of 15 min resulted in the production of activated carbon with a surface area of 320 $m^2 g^{-1}$. According to different scientific sources, KOH is defined as one of the most efficient activation agents [35]. A study was carried out to investigate the activation qualities of different activation agents, including KOH, NaOH, K_2CO_3 and Na_2CO_3. The S_{BET} results ($1835 > 1579 > 1559 > 660\ m^2 g^{-1}$ for KOH, K_2CO_3, NaOH, Na_2CO_3) indicated that KOH was the most suitable activation agent of all. Potassium added to biomass promoted the decomposition process, also known as catalytic effect of potassium [36]. Also the impregnation ratio of KOH had a strong effect on the characteristics of activated char as it was clarified by Khezami et al. [37]. The two-step process was chosen for the preparation of activated carbons from peach stones, with the use of a conventional reactor [38].

Microwaves represent a new way to perform heating, and the effects are promising. A continuous microwave pyrolysis system can provide solutions to many problems commonly found in other methods [14]. Reactions run in record time, and what is more, the reactions that normally lead to incomplete mixtures of chemicals can sometimes be an improvement for the desired product. To our knowledge, there are no available reports on garden waste processing by microwave pyrolysis. This article is focused on the possibility of garden waste processing including corn silage in a non-conventional manner, especially because of the necessity to reduce landfilling in the Czech Republic in the coming years under Directive 1999/31/EC on Landfills. Even though the above mentioned waste is commonly used for biogas and compost production, it is collected as a mixture also containing substances which do not yield a good compost quality and are difficultl to degrade under composting conditions, and whose separation would be difficult. For this reason, biochemical processing could be unstable with a questionable suitability and the waste has to be subsequently deposited in landfills. Therefore, the objective of this study is to experimentally investigate the microwave pyrolysis of the original samples as well as activated samples. According to our data, this waste may be effectively converted to higher quality syngas and biochar.

2. Materials and methods

2.1. Material

The samples of garden waste (named GW) and corn waste (named CW) were taken from the Depos Horní Suchá a.s. to process them via microwave pyrolysis. GW could be described as a mixture of grass, foliage, weeds, flowers, small twigs, tulips, clay with stones etc. This type of waste is often processed by biochemical processes or just landfilled. In theory, it should be an excellent material, but actually this is not true. Based on our experimental data, it contains too much lignocellulose, waxes and other hardly anaerobically degradable substances. However, in a mesophilic reactor with 800 l of cattle manure and a daily dose of 4 kg per day, the production of 1 m^3 of biogas was determined with an amount of CH_4 60–66 vol %.

CW is a waste material of KWS Atletico cultivar corn silage from biogas station Pustejov. This material was experimentally tested in a lab-scale model in our laboratory of anaerobic digestion designed of a partially mixed bioreactor made of a triple-layer plastic bag of PVC-PES-PVC foil. The volume of the anaerobic batch was set to 0.5 m^3. Mesophilic anaerobic digestion was conducted in the semi-continuous mode for 120 days. The average organic loading rate achieved 4.27 $kg_{VS}\ m^{-3}\ d^{-1}$. The average methane content in raw biogas was 52.5 vol

%. The specific methane production stabilized at 0.123 m_N^3 kg^{-1} and the specific biogas production was 0.234 m_N^3 kg^{-1} [39].

For pyrolysis experiments, both samples of waste were milled by laboratory knife mill Testchem LMN-100, to adjust the size to the required 8 × 8 mm. Analytically determined waste parameters (content of water, ash and volatile, carbon, hydrogen, nitrogen, sulfur, oxygen, heating values) were carried out according to the standards ASTM D3172 - 13 and D5373 – 16. For this purpose, the LECO TGA 701 thermogravimetric analyser, the LECO AC 350 calorimeter and the elemental analyser LECO CHNS 628 were used.

Density was measured by Thermo Scientific Pycnomatic ATC semiautomatic pycnometer. Acidity was detected in an aqueous extract according to the EN 15933:2012 standard. The higher heating value HHV was measured based on ISO 1928 and lower heating value was calculated based on measured data.

2.2. KOH activation

The original non-activated samples (named GWn and CWn) were further activated (named GWa and CWa) with the use of potassium hydroxide. The testers were mixed with KOH, in a ratio of 1:4, which is the optimum value cited in literature [40]. Approx. 20 g of sample were mixed with 80 g KOH dissolved in 100 ml of water. Then the mixture was stirred for 15 min. The mixture stayed for 8 h, afterwards it was dried and pyrolyzed. The activated samples were neutralized with diluted hydrochloric acid, after that they were filtered and rinsed with hot water and pH was checked. The samples were further subjected to the one-step method (activation before carbonization) and only for S_{BET} measurement to the double-step method (carbonization, activation, carbonization).

2.3. Laboratory devices

The laboratory apparatus used to perform the series of experiments is shown in Fig. 1. The original dried samples as well as activated samples were thermal treated in the self-made microwave reactor for 20 min at the power of 440 W. This power generates temperature of 800 °C depending on the composition of the batch. Temperature was checked by the thermocouple. On the upper part of the microwave PANASONIC NN-SD271 a hole was cut out for placing a flask with the sample (50 g of sample with 10 g of char obtained from the pyrolysis process of the sawdust) into the microwave. The flask was connected with a glass tube with cooler. Five impinge bottles with water and acetone were used to purify gaseous and vapours products. This purified pyrolysis gas flowed through the gasometer to the point, where samples were taken into 20 dm^3 Tedlar gas sampling bags. Experiments were carried out under nitrogen atmosphere (100 cm^3 min^{-1}).

2.4. Analysis of gaseous products

After the pyrolysis process off-line analysis of the pyrolysis gas was carried out. The gaseous components, namely methane, ethene, ethane, propane, propene, hydrogen, carbon monoxide and carbon dioxide were examined with the use of gas chromatography. Agilent 7890A gas chromatograph equipped with a flame ionization detector (FID) with hydrogen flow rate of 30 ml min^{-1} and helium flow rate of 25 ml min^{-1} was used. Helium flow rate of 5 ml min^{-1} was set up in case of thermal conductivity detector (TCD). The Micropacked column with following properties 2 m × 0.53 mm was used to separate the components on the basis of different capabilities of different strengths of attachment to the stationary phase.

2.5. Characterization of solid residues

Ultimate analysis of pyrolysed solid residues was done. The density was measured by Thermo Scientific Pycnomatic ATC semiautomatic pycnometer by using helium as a carrier gas. Final characterization of the resulting solid residues was carried out by nitrogen sorption at 77 K. 3Flex Surface Characterization Analyser (Micromeritics) was used for the characterization. Before the nitrogen physisorption measurements, the activated samples were degassed at 300 °C for 24 h under vacuum less than 1 Pa. BET surface area (specific surface area) determined by ten-point BET method for relative pressure range p/p0 = 0.05–0.30 was used. Mesopore/external surface area was determined by the t-plot method using the Broekhoff-DeBoer standard isotherm. Micropore volume was determined by the t-plot method using the Broekhoff-DeBoer standard isotherm. Net pore volume was determined at p/p0 ~ 0.99.

2.6. Determination of water content

The condensates from pyrolysis were subjected to the determination of water content by the Karl-Fischer method on TitroLine 7500 KF.

3. Results and discussion

3.1. Feedstock analysis

In this part, the properties of samples and the effect of conditions were examined. For the samples analyses listed in Table 1 (proximate and ultimate analysis, true density ρ_{TS}, bulk density ρ_b, acidity pH and ratio C:N) were performed.

3.2. Product distribution

A very high volatile content (78.5 wt. %) can be observed at CW, nevertheless low ash content and a reasonable amount of carbon makes it an appropriate precursor for such processing. A high ash content in case of GW is probably caused by soil that is a part of the mixture and whose separation would be difficult. Samples were subjected to TGA analysis for the purpose of identification of their thermal behaviour. The total mass change of approx. 85 wt. % was detected at the temperature of 800 °C in case of CW and 65 wt. % in case of GW (see Fig. 2).

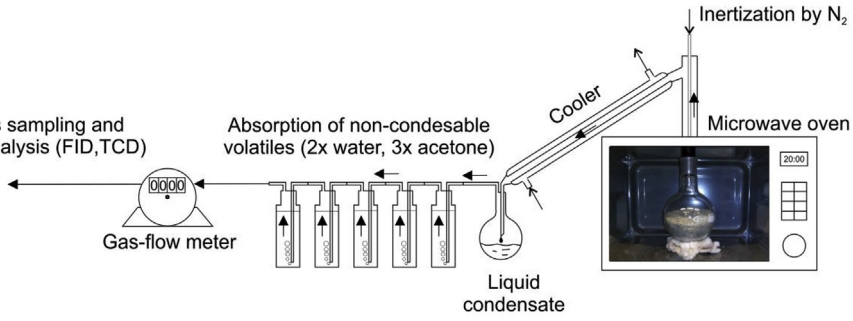

Fig. 1. Microwave apparatus.

Table 1
Content of water, ash and volatile, carbon, hydrogen, nitrogen, sulfur, oxygen, density, acidity and heating values of input materials.

Sample	W^r (wt. %)	A^r (wt. %)	V^r (wt. %)	C^r (wt. %)	H^r (wt. %)	N^r (wt.%)	S^r (wt.%)
GW	5.2	23.9	57.3	37.1	4.5	1.7	0.2
CW	2.3	1.8	78.5	45.9	6.4	2.1	0.1
Sample	**Or (wt. %)**	ρ_{TS} (kg m^{-3})	ρ_b (kg m^{-3})	pH (wt. %)	**C:N** (wt. %)	**HHV^r** ($MJkg^{-1}$)	**LHV^r** ($MJkg^{-1}$)
GW	27.4	1676	0.5	5.7	21.8	15.1	13.3
CW	41.4	1419	nd	4.1	21.9	18.9	17.1

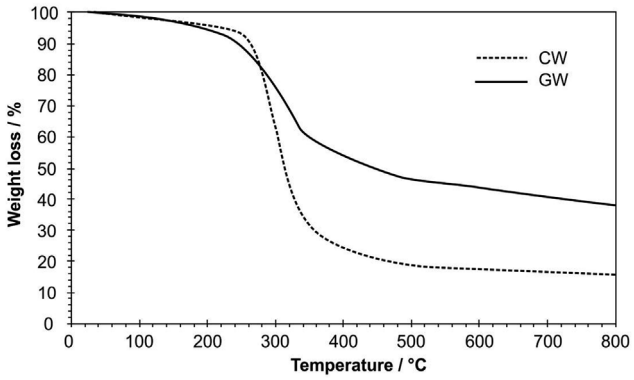

Fig. 2. Total mass change of input materials.

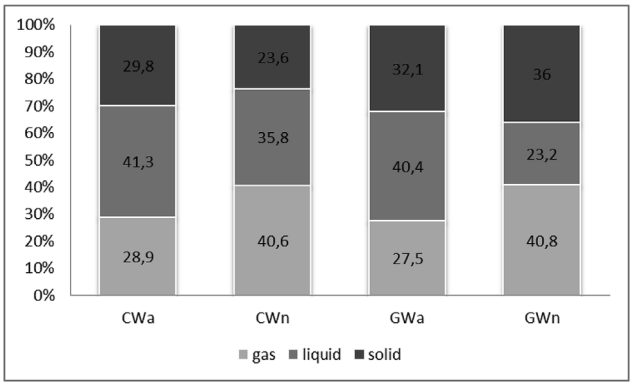

Fig. 3. Product distribution of activated and non-activated samples.

The highest weight loss was observed in the temperature range from 280 to 350 °C. The distribution of final products is presented in Fig. 3. Liquid yields increased in case of the activated samples while the amount of gases decreased noticeably.

3.3. Analysis of gaseous products

Hydrogen production has been dealt with in a number of scientific reports [41]. The concentration of measured hydrogen was strongly influenced by activation and selection of the input materials as shown in Fig. 4, especially for corn grain waste material (GWa 42.4 vol %, GWn 41.6 vol %; CWa 54.4 vol %, CWn 18.8 vol %). The highest hydrogen concentration conforms to Huang et al. [23]. H_2, CO, and CO_2 were the major gases. The sum of hydrogen and carbon monoxide accounted for about 85 vol % of the total volume of pyrolytic gas of CWa, which can be further used to produce fuels with numerous uses, such as for the production of hydrogen, syngas or natural gas. Methane concentration ranged from 5 to 10 vol %. Besides the main components mentioned above, there were some minor molecules in the samples, especially C_2H_6. For that reason, pyrolytic gases originating under microwave radiation show possibility and economic value in purification and upgrading of hydrogen. In addition, the residual hydrocarbon gases are not suggested for extraction and separation due to their low quantity, but their high calorific value may lead to their use as fuel. Another point of view can be the comparison of yields as shown in Fig. 5. Gas formation gradually increased at the beginning of the process.

3.4. Evaluation of solid residues in terms of adsorption properties

Activated carbons were prepared by direct activation before carbonization (single-step) and also by the double-step method which contains firstly carbonization and secondly activation and carbonization. Table 2 demonstrates the values of ultimate and proximate analysis, density ρ, mesopore/external surface area, micropore volume, net pore volume for samples excluding double-step and BET surface area of single-step, double-step and non-activated samples after microwave pyrolysis. In the case of non-activated samples, a lower value of the surface area was achieved in comparison with activated samples. The porosity as well as elemental composition of solid residues depends mainly on final temperature and precursor nature. The porous properties were also compared to study the influence of the carbonization treatment. The S_{BET} values after the double-step method tend to be slightly higher in case of corn waste material but visibly higher in case of garden waste material. On the other hand, it must be mentioned that the single-step method is simpler, energetically and environmentally more suitable than the double-step method. However, activated samples did not reach the values such as commercial activated carbons, or as some authors reported [29,30]. These values suggest an opportunity for using this waste in “single-use sorbents” production. Higher heating value of CWn reached a value which deserves attention from the point of view of its further use as fuel.

3.5. Rating condensates

The condensates from microwave pyrolysis were subjected to the determination of water content by the Karl-Fischer method on TitroLine 7500 KF. The measured values are shown in Table 3. Different reactions dominated during heat treatment should be taken into account. Based on the results it can be stated that activation, especially OH^- contained in the activating agent, also influenced water content in liquid residues.

4. Conclusion

The selected waste materials were activated and processed via microwave reactor. The resulting products were evaluated subsequently. From the results it could be concluded that activation of samples and method of carbonization treatment affected quality and quantity of final products. KOH activation has resulted in BET surface area and hydrogen increasing. On the other hand, KOH activation caused a heating value degreasing of corn waste solid residue from 33.3 to 31.6 MJ kg^{-1}. However, the use of modified solid residues produced by microwave pyrolysis may be an effective method from the perspective of industrial application. The maximum BET surface area of 530 $m^2 g^{-1}$ was analysed.

Acknowledgements

This work was supported by EU structural funding in Operational Programme Research, Development and Education, project No. CZ.02.1.01/0.0/0.0/16_019/0000853 “IET-ER”.

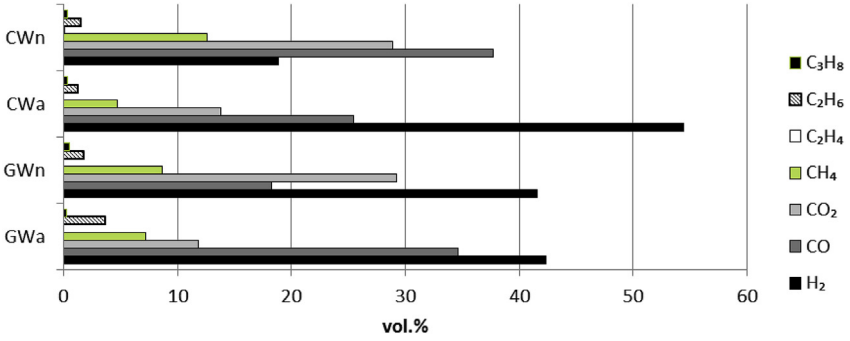

Fig. 4. Gas composition after microwave pyrolysis.

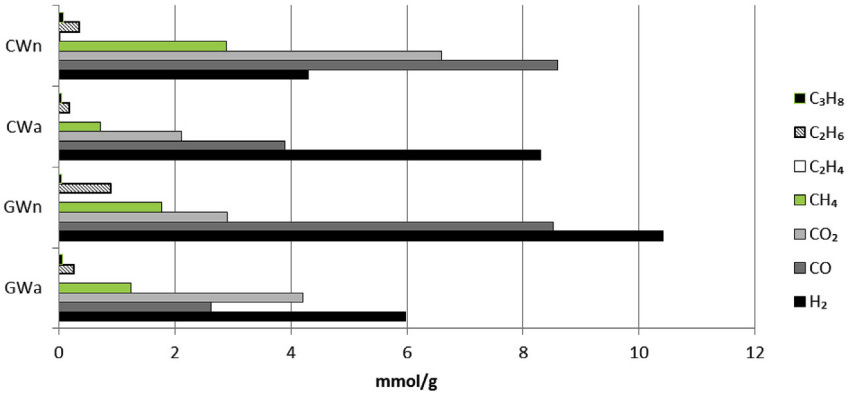

Fig. 5. Gas yields after microwave pyrolysis.

Table 2
Proximate analysis, S_{BET}, S_{meso}, V_{micro}, V_{net}, density and higher heating value of samples after microwave pyrolysis.

Sample	A^d (wt.%)	V^d (wt.%)	FC^d (wt.%)	$S_{BET\ single\text{-}step}$ (m^2g^{-1})	$S_{BET\ double\text{-}step}$ (m^2g^{-1})	S_{meso} (m^2g^{-1})	V_{micro} ($mm^3_{liq}\ g^{-1}$)	Vnet ($mm^3_{liq}\ g^{-1}$)	ρ (gcm^{-3})	HHV^d ($MJkg^1$)
GWa	34.8	9.8	55.4	307	530	n.d.	n.d.	318	1.90	22.7
GWn	39.0	6.4	54.6	298	–	63	113	198	1.89	20.3
CWa	8.1	11.8	80.1	420	430	55	174	232	1.80	31.6
CWn	4.9	6.9	88.3	138	–	n.d.	n.d.	156	1.79	33.3

Table 3
Water content of condensates.

	GWa	GWn	CWa	CWn
Water content (wt.%)	84.5	79.3	71.0	67.2

References

[1] ISOH (ONLINE) (CIT. 2018-06-20). Available from: https://isoh.mzp.cz/VISOH/?fillFilter=True.
[2] L.J. Wu, T. Kobayashi, H. Kuramochi, Y.Y. Li, K.Q. Xu, Improved biogas production from food waste by co-digestion with de-oiled grease trap waste, Bioresour. Technol. 201 (2016) 237–244.
[3] J. Huang, P. Chiueh, S. Lo, A review on microwave pyrolysis of lignocellulosic biomass, Sustainable Environ. Res. 26 (2016) 103–109.
[4] Huang Yu-Fong, Chiueh Pei-Te, Kuan Wen-Hui, Lo Shang-Lien, Microwave pyrolysis of lignocellulosic biomass: heating performance and reaction kinetics, Energy 100 (2016) 137–144.
[5] K.E. Haque, Microwave energy for mineral treatment processes a brief review, Int. J. Miner. Process. 57 (1999) 1–24.
[6] Z. Song, Y. Yang, X. Zhao, J. Sun, W. Wang, Y. Mao, Ch. Ma, Microwave pyrolysis of tire powders: evolution of yields and composition of products, J. Anal. Appl. Pyrolysis 123 (2017) 152–159.
[7] M. Miura, H. Kaga, A. Sakurai, T. Kakuchi, K. Takahashi, Rapid pyrolysis of wood block by microwave heating, J. Anal. Appl. Pyrolysis 71 (2004) 187–199.
[8] J.A. Menendez, A. Dominguez, Y. Fernandez, J.J. Pis, Evidence of self-gasification during the microwave-induced pyrolysis of coffee hulls, Energy Fuels 21 (2007) 373–378.
[9] W.H. Chen, S.C. Ye, H.K. Sheen, Hydrothermal carbonization of sugarcane bagasse via wet torrefaction in association with microwave heating, Bioresour. Technol. 118 (2012) 195–203.
[10] X.Q. Zhao, M. Wang, H.Z. Liu, L.Z. Li, C.Y. Ma, Z.L. Song, A microwave reactor for characterization of pyrolyzed biomass, Bioresour. Technol. 104 (2012) 673–678.
[11] X. Wang, W. Morrison, Z. Du, Y. Wan, X. Lin, P. Chen, et al., Biomass temperature profile development and its implications under the microwave-assisted pyrolysis condition, Appl. Energy 99 (2012) 386–392.
[12] Y. Zhang, P. Chen, S. Liu, P. Peng, M. Min, Y. Cheng, E. Anderson, et al., Effects of feedstock characteristics on microwave-assisted pyrolysis – a review, Bioresour. Technol. 230 (2017) 143–151.
[13] J. Li, J. Dai, G. Liu, H. Zhang, Z. Gao, J. Fu, Y. He, Y. Huang, Biochar from microwave pyrolysis of biomass: a review, Biomass Bioenergy 94 (2016) 228–244.
[14] F. Motasemi, T. Muhammad, A. Afzal, A review on the microwave-assisted pyrolysis technique, Renew. Sustain. Energy Rev. 28 (2013) 317–330.
[15] F. Mushtaq, R. Mat, F.N. Ani, A review on microwave assisted pyrolysis of coal and biomass for fuel production, Renew. Sustain. Energy Rev. 39 (2014) 555–574.
[16] A. Menendez, A. Arenillas, B. Fidalgo, Y. Fernendez, L. Zubizarreta, E.G. Calvo, et al., Microwave heating processes involving carbon materials, Fuel Process. Technol. 91 (2010) 1–8.
[17] S. Ren, H. Lei, L. Wang, Q. Bu, S. Chen, J. Wu, et al., Biofuel production and kinetics analysis for microwave pyrolysis of Douglas fir sawdust pellet, J. Anal. Appl. Pyrolysis 94 (2012) 163–169.
[18] P. Lestinsky, B. Grycova, A. Pryszcz, A. Martaus, L. Matejova, Hydrogen production from microwave catalytic pyrolysis of spruce sawdust, J. Anal. Appl. Pyrolysis 124 (2017) 175–179.
[19] S.P. Zhang, Q. Dong, L. Zhang, Y.Q. Xiong, High quality syngas production from microwave pyrolysis of rice husk with char-supported metallic catalysts, Bioresour. Technol. 191 (2015) 17–23.
[20] A. Dominguez, J.A. Menendez, Y. Fernandez, J.J. Pis, J.M. Valente Nabais, P.J.M. Carrott, et al., Conventional and microwave induced pyrolysis of coffee hulls

for the production of a hydrogen rich fuel gas, J. Anal. Appl. Pyrolysis 79 (2007) 128–135.
[21] X.H. Wang, H.P. Chen, X.J. Ding, H.P. Yang, S.H. Zhang, Y.Q. Shen, Properties of gas and char from microwave pyrolysis of pine sawdust, BioResources 4 (2009) 946–959.
[22] Y.F. Huang, W.H. Kuan, S.L. Lo, C.F. Lin, Hydrogen-rich fuel gas from rice straw via microwave-induced pyrolysis, Bioresour. Technol. 101 (2010) 1968–1973.
[23] Y.F. Huang, W.H. Kuan, S.L. Lo, C.F. Lin, Total recovery of resources and energy from rice straw using microwave induced pyrolysis, Bioresour. Technol. 99 (2008) 8252–8258.
[24] A. Dominguez, J.A. Menendez, M. Inguanzo, J.J. Pís, Production of bio-fuels by high temperature pyrolysis of sewage sludge using conventional and microwave heating, Bioresour. Technol. 97 (2006) 1185–1193.
[25] M. Tripathi, J.N. Sahu, P. Ganesan, Effect of process parameters on production of biochar from biomass waste through pyrolysis: a review, Renew. Sustain. Energy Rev. 55 (2016) 467–481.
[26] W. Gwenzi, N. ChaukurA, C. Noubactep, F.N.D. Mukome, Biochar-based water treatment systems as a potential low-cost and sustainable technology for clean water provision, J. Environ. Manag. 197 (2017) 732–749.
[27] R.H. Hesas, et al., Preparation and characterization of activated carbon from apple waste by microwave assisted phosphoric acid activation: application in methylene blue adsorption, BioResources 8 (2) (2013) 2950–2966.
[28] V.O. Njoku, K.Y. Foo, M. Asif, B.H. Hameed, Preparation of activated carbons from rambutan (Nephelium lappaceum) peel by microwave-induced KOH activation for acid yellow 17 dye adsorption, Chem. Eng. J. 250 (2014) 198–204.
[29] S.S. Lam, R.K. Liew, Y.M. Wong, P.N.Y. Yek, N.L. Ma, C.L. Lee, H.A. Chase, Microwave-assisted pyrolysis with chemical activation, an innovative method to convert orange peel into activated carbon with improved properties as dye adsorbent, J. Clean. Prod. 162 (2017) 1376–1387.
[30] L. Zhu, H. Lei, L. Wang, G. Yadavalli, X. Zhang, Y. Wei, et al., Biochar of corn stover: microwave-assisted pyrolysis condition induced changes in surface functional groups and characteristics, J. Anal. Appl. Pyrolysis 115 (2015) 149–156.
[31] W. Li, K. Yang, J. Peng, L. Zhang, S. Guo, H. Xia, Effects of carbonization temperatures on characteristics of porosity in coconut shell chars and activated carbons derived from carbonized coconut shell chars, Ind. Crop. Prod. 28 (2008) 190–198.
[32] R.K. Sharma, J.B. Wooten, V.L. Baliga, P.A. Martoglio-Smith, M.R. Hajaligol, Characterization of char from the pyrolysis of tobacco, J. Agric. Food Chem. 50 (2002) 771–783.
[33] J. Kazmierczak-Razna, P. Nowicki, R. Pietrzak, Characterization and application of bio-activated carbons prepared by direct activation of hay with the use of microwave radiation, Powder Technol. 319 (2017) 302–312.
[34] R. Farma, D. Fatjrin, M. Awitdrus, Deraman, Physical properties of activated carbon from fibers of oil palm empty fruit bunches by microwave assisted potassium hydroxide activation, 6th International Conference on Theoretical and Applied Physics (ICTAP) Location: Hasanuddin Univ, Makassar, INDONESIA Date: SEP 19-21, 2016, https://doi.org/10.1063/1.4973090.
[35] X. Hongying, Ch. Song, Z. Libo, P. Jinnhui, Utilization of walnut shell as a feedstock for preparing high surface area activated carbon by microwave induced activation: effect of activation agents, Green Process. Synth. 5 (2016) 7–14.
[36] F. Guo, Y. Liu, Y. Wang, X. Li, T. Li, Ch. Guo, Pyrolysis kinetics and behavior of potassium-impregnated pine wood in TGA and a fixed-bed reactor, Energy Convers. Manag. 130 (2016) 184–191.
[37] L. Khezami, A. Chetouani, B. Taouk, R. Capart, Production and characterisation of activated carbon from wood components in powder: cellulose, lignin, xylan, Powder Technol. 157 (2005) 48–56.
[38] T. Tsoncheva, A. Mileva, B. Tsynsarski, et al., Activated carbon from Bulgarian peach stones as a support of catalysts for methanol decomposition, Biomass Bioenergy 109 (2018) 135–146.
[39] J. Rusin, K. Kasakova, K. Chamradova, K. Obroucka, B. Stanek, High-solids semi-continuous anaerobic digestion of corn silage in bag-type digester, Green Process. Synth. 6 (2018) 268–276.
[40] Gyu Hwan Oh, Park Chong Rae, Preparation and characteristics of rice-straw-based porous carbons with high adsorption capacity, Fuel 81 (2002) 327–336.
[41] O. Bičáková, P. Straka, Production of hydrogen from renewable resources and its effectiveness, Int. J. Hydrogen Energy 37 (2012) 11563–11578.

Příloha [P7]

LESTINSKY, P., ZIKMUND, Z., GRYCOVA, B., RYCZKOWSKI, R., GRAMS, J. & INAYAT, A. 2020. Production of hydrogen over Ni/carbonaceous catalyst. *Fuel*, 278. IF_{2020} = 6,609 (5 year IF 7.621). Autorský podíl 45 %. Počet citací dle WoS 15.

Role uchazeče:

- návrh tématu, návrh postupu prací, experimentální práce, vyhodnocení výsledků, vyvození závěrů z dosažených výsledků

Fuel 278 (2020) 118398

Contents lists available at ScienceDirect

Fuel

journal homepage: www.elsevier.com/locate/fuel

Full Length Article

Production of hydrogen over Ni/carbonaceous catalyst

P. Lestinsky[a,*], Z. Zikmund[a,b], B. Grycova[a], R. Ryczkowski[c], J. Grams[c], A. Inayat[a]

[a] Institute of Environmental Technology, VSB-Technical University of Ostrava, 17. Listopadu 2172/15, Ostrava-Poruba 70800, Czech Republic
[b] Faculty of Materials and Technology, VSB-Technical University of Ostrava, 17. Listopadu 2172/15, Ostrava-Poruba 70800, Czech Republic
[c] Institute of General and Ecological Chemistry, Faculty of Chemistry, Lodz University of Technology, Zeromskiego 116, 90-924 Lodz, Poland

ARTICLE INFO

Keywords:
Dry reforming
Pyrolysis
Biomass
Steam reforming
Carbonaceous materials
Microwave pyrolysis

ABSTRACT

Catalytic materials for hydrogen production were synthesized by impregnating waste spruce sawdust with nickel nitrate followed by microwave pyrolysis. Ni/carbonaceous materials thus obtained were tested as catalyst for dry reforming of methane as well as for upgrading of organic vapours from biomass pyrolysis. Among five samples synthesized with different amount of Ni on carbonaceous support, the sample with 13.2 wt% Ni showed the highest CH_4 and CO_2 conversion for dry reforming at 800 °C. The yields of 31.4 vol% for H_2 and 39.0 vol% for CO were recorded. The catalyst sample exhibited only a small decrease in activity after 6 h of time-on-stream. The same sample was applied as catalyst for upgrading of organic vapours from thermal pyrolysis of spruce sawdust and cellulose. A considerable increase in H_2 content (i.e. from 1.2 to 14.1 mmol g^{-1}) in the product mixture was observed. The main advantage of using carbonaceous support is its resistance towards rapid deactivation due to coke deposition. This advantage can be exploited by using it as catalyst support in reactions that suffer from such catalyst deactivation. Furthermore, the honeycomb-like structure and morphology of carbonaceous materials can promote mass transfer around catalytically active sites that can be beneficial in reactions involving large molecules.

1. Introduction

Hydrogen is one of the most important gases in the chemical industry. It is not only essential in the refining industry and organic synthesis, but also in the production of methanol and ammonia [1]. Nowadays, hydrogen is mainly produced by steam reforming of methane, partial oxidation processes or coal gasification [2]. The vast reserves of hydrogen are present in sea water, but an enormous amount of energy would be required to set free hydrogen from the water molecules. In recent years, several hydrogen production methods have been explored and developed. They include dry reforming reaction, or thermo catalytic decomposition of methane or other organic compounds, namely VOCs (volatile organic compounds). Along with VOCs (that contain a considerable amount of CH_4), industries also produce large amounts of CO_2 which is a well-known greenhouse gas and its emission is steadily increasing every year. Both harmful gases i.e. CH_4 and CO_2 could be utilized and hence abated simultaneously, thanks to dry reforming reaction. This is the reason why dry reforming reaction has been intensively studied focusing on the utilization of CO_2 and its conversion into useful products, such as syngas which is a gas mixture of CO and H_2 [3–5].

In past years, growing interest in the use of supported nickel catalyst for the dry reforming reaction was observed. In this regard, one of the most popular supports is alumina, which is also commercially used as a support for industrial catalysts for steam reforming of methane [3]. Commercial Ni/Al_2O_3 has the disadvantage of low fouling resistance, due to the absence of steam, which when dosed in stoichiometric excess, can suppress the formation of carbon deposits in steam reforming [6]. Besides Ni/Al_2O_3, bimetallic (NiCo) catalysts deposited on silicon carbide [7], or natural material such as Olivine [8] or Dolomite [9] were also used.

Dry reforming of methane is strongly endothermic reaction, which in fact consists of more than twenty intermediate reactions steps [10], but for easy understanding it could be described by three intermediate stages (Eq. 2–4):

$$CH_4 + CO_2 \rightarrow 2CO + 2H_2,\ \Delta H_{298} = +247 kJ \cdot mol^{-1} \quad (1)$$

$$CH_4 \rightarrow C^* + 2H_2 \quad (2)$$

$$CO_2 \rightarrow CO + O^* \quad (3)$$

$$C^* + O^* \rightarrow CO \quad (4)$$

The major problem related with dry reforming of methane is the quick deactivation of catalyst due to carbon deposition caused by the

* Corresponding author.
E-mail address: pavel.lestinsky@vsb.cz (P. Lestinsky).

https://doi.org/10.1016/j.fuel.2020.118398
Received 3 March 2020; Received in revised form 8 May 2020; Accepted 11 June 2020
Available online 20 June 2020
0016-2361/

Nomenclature

Symbols

S_{BET}	Specific surface area ($m^2\ g^{-1}$)
S_{meso}	Specific mesopore surface area ($m^2\ g^{-1}$)
V_{micro}	Specific micropore volume ($cm^3\ g^{-1}$)
V_{net}	Specific total pore volume ($cm^3\ g^{-1}$)

Greek symbolsAbbreviations

GHSV	Gas hourly space velocity (h^{-1})
SEM	Scanning electron microscopy
XRD	X-Ray Diffraction

active carbon species(C*). The active carbon species are created during decomposition or dissociation of methane or hydrocarbons and are necessary for CO production. However, when these species do not take part in the decomposition of CO_2 molecules to produce CO, they stay on the surface of metal catalyst and produce coke. The formation of carbon deposit can be limited using higher reaction temperature (above 900 °C), but such high temperature may result in sintering of metal particles on the catalysts surface. Also, conducting the reaction at such conditions is energy inefficient [11,12]. In addition to increase in reaction temperature, another way of inhibiting carbon deposit is modification of Ni catalyst by a suitable promoter. One of the most popular promoters for reforming catalysts is Ceria. Ceria has redox property thanks to the highly mobile oxygen vacancies in its structure that in this case provide oxygen which reduces the degree of carbon deposit [13].

Besides dry reforming of methane, hydrogen can also be produced by upgrading of organic vapours obtained from biomass pyrolysis [14]. Pyrolysis of biomass results in the formation of different products such as solid residue, liquids, and gaseous compounds. The gaseous fraction mainly consists of volatile organic compounds (VOCs), oxides of carbon and steam [15]. These gaseous compounds can be subjected to secondary reactions as follows:

$$C_xH_y + xCO_2 \rightarrow \left(\frac{y}{2}\right)H_2 + 2xCO \quad (5)$$

$$CH_4 + 2H_2O \rightarrow CO_2 + 4H_2 \quad (6)$$

$$CO_2 + H_2 \rightarrow CO + H_2O \quad (7)$$

$$2CO \rightarrow C + CO_2 \quad (8)$$

It corresponds to steam reforming, reverse water–gas shift and Boudouard reaction. The carbonaceous material as carbon structure of biomass may also undergo a water gas reaction, thereby reducing the amount of solid residue and further amount of the hydrogen is produced:

$$C + H_2O \rightarrow CO + H_2 \quad (9)$$

The contribution of each of these reactions in the reaction mechanism strongly depends on the reaction conditions and the type of used catalysts [16]. Despite the relatively high temperature of the process, thermal conversion of biomass and further upgrading of volatile products is an interesting possibility of producing bio hydrogen in the future.

Recent works have shown a new way of developing coke-resistant catalysts which can be achieved by the application of carbonaceous support. The carbonaceous supports can be produced by controlled formation of carbon e.g. Carbon Black, Carbon Nanotubes [1]. The advantages of carbonaceous support are low cost, high temperature resistance, tolerance to sulphur and other poisoning compounds and of course decrease of overall CO_2 emissions from the process of preparation [17]. Fildago et al. [18] prepared catalyst for dry reforming by depositing metallic Ni on commercial activated carbon. Metallic Nickel is usually prepared by the reduction of nickel oxide, which is created by applying wet impregnation of aqueous solution of nickel compounds (nitrate, acetate) [5]. This route involves an extra step for the reduction of nickel oxide to metallic nickel using hydrogen. Zhang et al. [19] came up with the idea of using the carbonaceous surface of biomass to reduce metal oxides during pyrolysis. Here the main role in reducing nickel oxide to metallic from is played by the high amount of hydrogen, which is produced during microwave pyrolysis, as reported in our previous work [14]. The presence of nickel doped carbonaceous material in microwave pyrolysis process leads to more than twice the amount of hydrogen produced than without Ni. In this regard, the aim of the present work is to develop an efficient and versatile Ni/carbonaceous catalyst for the potential application in high temperature hydrogen production processes. A further aim is to test the synthesized catalyst for dry reforming of methane as well as for upgrading of organic vapours derived from thermal pyrolysis of biomass.

2. Materials and methods

2.1. Materials

For the catalyst preparation, nickel nitrate hexahydrate (Sigma-Aldrich) with a purity of 99.99% was used as Ni precursor. As a precursor for carbonaceous support material, raw spruce sawdust with a size fraction 0.63 – 1.25 mm was utilized. In addition, biochar previously obtained from pyrolysis of the same spruce sawdust was employed as radiation absorbent during microwave pyrolysis.

2.2. Catalyst preparation

In a first step, raw spruce sawdust was dried at 110 °C for 24 h. The dry sawdust was then mixed with different concentrations (0.05, 0.1, 0.5, 1 and 2 mol l^{-1}) of aqueous solution of nickel nitrate hexahydrate, stirred for 12 h and filtered. The wet impregnated sawdust samples thus obtained were then mixed with biochar, in the ratio of 1/20. The final mixture was then placed in a flask and inserted into a microwave reactor for pyrolysis under nitrogen atmosphere. The microwave pyrolysis was performed for 20 min, during which the power of the microwave oven was kept at 440 W for the first 5 min and then increased to 950 W for the next 15 min. During this process, the sawdust was pyrolyzed to produce carbonaceous materials whereas; nickel nitrate was decomposed to nickel oxide which was then reduced in situ to Ni^0 using hydrogen that was produced during the pyrolysis of sawdust used. In situ reduction of Ni is possible due to the presence of hydrogen produced by the pyrolysis of sawdust [14]. About 10 wt% of biochar remained in Ni/carbonaceous since it was not possible to separate the microwave absorbent from it. Catalyst samples were marked from Ni-C1 to Ni-C5 thus from the lowest concentration of nickel nitrate to a higher concentration.

2.3. Catalyst characterization

The Ni content in the synthesized catalysts was determined through X-ray fluorescence (XRF) analysis, performed on SPECTRO XEPOS (Spectro Analytical) using powder method. The samples were analysed by using one-off cuvette and 1 g of sample was used for each experiment. For the elemental analysis of the samples, ultimate analysis was performed on LECO CHSN628 analyser.

Phase composition of synthesized catalysts was determined using powder X-ray diffraction (XRD) analysis conducted on Rigaku SmartLab diffractometer equipped with D/teX Ultra 250 detector. The source of irradiation was a cobalt lamp (CoKα, 0.15418 nm) operated at 40 mA and 40 kV.

To determine the textural properties of biochar and synthesized catalysts, physisorption of nitrogen was performed. For this purpose, a

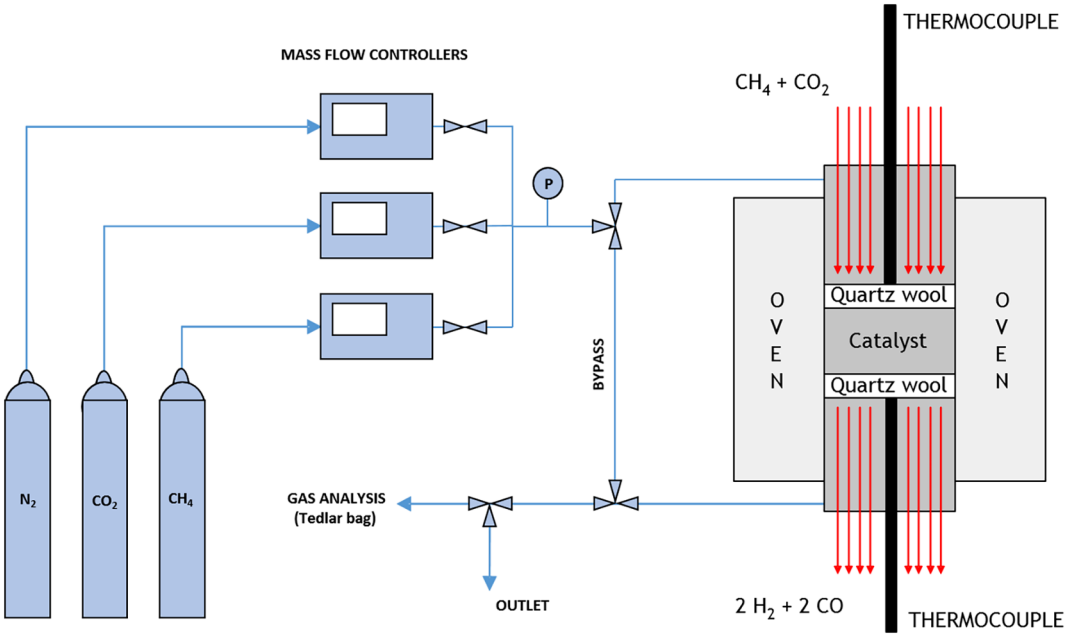

Fig. 1. Schematic diagram of the setup used for dry reforming reaction.

Micrometrics 3Flex analyser was used. The specific surface area (S_{BET}) was calculated using Brunauer-Emmett-Teller (BET) theory [20]. The mesopore surface area (S_{meso}) and the micropore volume (V_{micro}) were also evaluated based on the t-plot method using the Carbon Black STSA standard isotherm. The net pore volume (V_{net}) was determined from the nitrogen adsorption isotherm.

The scanning electron microscopy technique was applied for the study and analysis of the samples surface. For this purpose, a Quanta 450 FEG electron microscope was used. The imaging was performed in secondary and backscattered electron mode using an accelerating voltage of 20 keV.

2.4. Catalytic activity measurement

The catalytic activity measurements of the synthesized Ni/carbonaceous catalysts were performed using two test reactions, namely dry reforming of methane and upgrading of vapours from thermal pyrolysis of biomass. For this purpose, two lab-scale catalyst test rigs were used. The details of the test rigs and the measurement methods are given in detail in the following sections.

2.4.1. Dry reforming of methane

The catalytic dry reforming of methane was performed in a lab-scale fixed bed reactor setup for which a quartz glass tube with an internal diameter of 4 mm was used as reactor. The catalyst particles with an average diameter of 0.388 mm were packed in the tube to give a bed length of 20 mm. The catalyst particle size was chosen to ensure the plug flow conditions.

For each experiment, 0.1 g of catalyst was packed in the quartz reactor tube. The tube was pre heated to reach the desired temperature using a LAC LT 50/300/13 oven. During the pre-heating step the reactor was kept under constant nitrogen flow with a flow rate of 24 cm^3 min^{-1}. Once the desired temperature had reached, nitrogen flow was turned off and the flow of gaseous mixture, CH_4:CO_2 (1:1) for dry reforming reaction was started. The flow rate of each gas was regulated by using Aalborg GF17 mass flow controllers. The pressure at the reactor inlet was monitored by a manometer and the gas volume at the reactor outlet was measure by a rotameter. The gases at the reactor outlet were collected every 30 min using Tedlar® gas sampling bags and the GC analysis was performed immediately after the sampling. The schematic diagram of the setup is given in Fig. 1. The temperatures before and after the catalyst bed were measured to determine the true reactor temperature for dry reforming reaction. The decrease in temperature (10 to 20 °C) after the catalyst bed indicated the occurrence of reforming (strongly endothermic) reaction.

2.4.1.1. Catalytic upgrading of biomass pyrolysis vapours. The most active catalyst in dry reforming reaction was further tested in catalytic upgrading of vapours produced during pyrolysis of biomass. Here, the experiments were performed in a lab-scale test rig as shown schematically in Fig. 2. The rig comprised of two reactors connected in series. In the first reactor (diameter – 10 mm, length – 200 mm, power – 1500 W, heating rate about 100 °C/min), biomass (spruce sawdust or cellulose) was thermally pyrolyzed at 500 °C. The pyrolysis vapours produced in the first reactor were then led to the second reactor (diameter – 10 mm, length – 150 mm, power – 700 W, heating rate about 100 °C/min) that contained the catalyst and were heated to

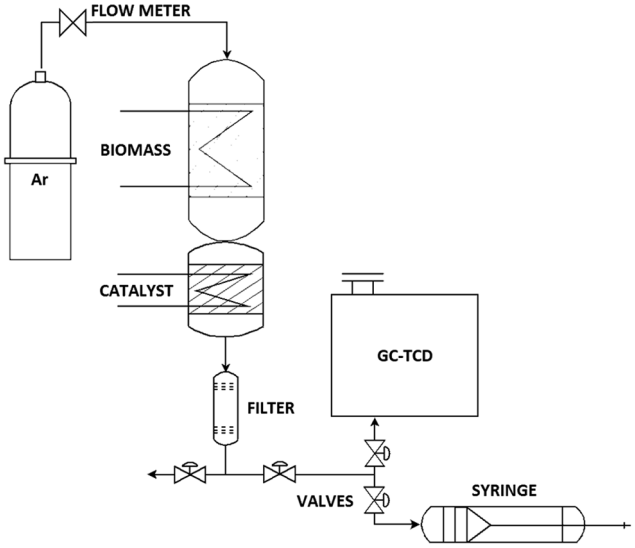

Fig. 2. Scheme of the test rig used for catalytic upgrading of biomass pyrolysis vapours.

700 °C, where upgrading of pyrolysis intermediates occurred. During each experiment, argon with a flow rate of 15 cm3 min-1 was used as carrier gas. For each experiment, 0.4 g of the feedstock and 0.1 g of catalyst were employed. The gases at the outlet of the second reactor were collected in a gas capture syringe for the GC analysis.

2.5. Analysis of gaseous products

2.5.0.1. Dry reforming of methane

The analysis of the gaseous products from dry reforming experiments, collected in gas sampling bags, was performed using an Agilent 7890A GC. The GC was equipped with a thermal conductivity detector (TCD), a flame ionization detector (FID) and a micropacked column of the dimensions of 2 m × 0.53 mm. During the analysis, the amounts of CH_4, CO, CO_2 and H_2 were determined.

2.5.0.2. Catalytic upgrading of vapours from biomass pyrolysis

The gaseous products formed in pyrolysis as well as in catalytic upgrading of biomass decomposition vapours were collected in scaled metal syringe for the GC analysis. The GC analysis was performed using an Agilent 7820A GC, equipped with a TCD and a packed column of the type Agilent 6Ft 1/8 2 mm Molsieve 5A 60/80 SS. The amounts of H_2, CO, CO_2 and CH_4 were determined.

3. Results and discussion

3.1. Ni/Carbonaceous materials

The results from XRF and elemental analysis are summarized in Table 1. It was observed that increasing concentration of the Ni precursor resulted in higher amount of Ni that was introduced into carbonaceous materials. Consequently, the content of carbon and other elements decreased. It was noted that the carbonaceous support contained not only carbon but also small amount of nitrogen, hydrogen, and oxygen. Here, oxygen content for individual samples was calculated to 100 wt%.

The XRD spectra of Ni/carbonaceous materials are shown in Fig. 3. The main phases detected included metallic nickel (Ni^0) at 52° and 60.9° and carbon as graphite (C^0) at 30.2°. In addition, small refluxes of NiO were also observed. The small peaks at 47° and 55° were K_β from metallic nickel. Furthermore, magnesium calcite ($Mg_{0.03}Ca_{0.97}CO_3$), which is a common component of biomass ash, was also detected. The Ni crystallite size was estimated using Scherrer equation and the results are given in Table 2. It was noted that Ni crystallite size in Ni/carbonaceous materials synthesized in the present work is bigger than those reported in literature [21–23].

The XRD results confirmed the observations from XRF analysis. In Fig. 3, it is evident that the intensity of metallic nickel peak increased with increasing nickel content in the carbonaceous support. At the same time, the intensity of graphite decreased. From the peak intensities as depicted in Fig. 3, it is also clear that Ni was present mostly as Ni^0 phase, as the peaks corresponding to NiO showed very small intensities. From these observations, it seems that most NiO produced from the decomposition of nickel nitrate was reduced using the hydrogen

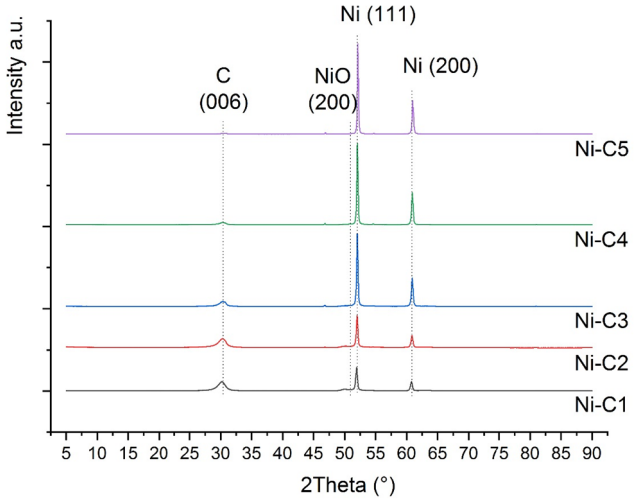

Fig. 3. XRD diffractograms of Ni/carbonaceous catalysts.

generated during microwave pyrolysis. This is very interesting for the catalytic application of Ni/Carbonaceous materials in dry reforming or steam reforming reactions, as in these reactions Ni^0 plays the role of catalytically active material.

For determining the textural properties, the Ni/Carbonaceous and biochar samples were analysed using nitrogen physisorption. The results as shown in Table 3 demonstrate that the fresh biochar (parent carbonaceous material - CM) had large S_{BET} i.e., around 300 $m^2\ g^{-1}$. However, this value was considerably decreased after wet impregnation with nickel nitrate and subsequent microwave pyrolysis. Also, a trend of decrease in surface area with increasing Ni content was observed. Furthermore, a decrease in the S_{meso} was also noted. Nevertheless, it was not as strong as in the case of S_{BET}. The presence of mesopores in catalytic materials is very important for certain applications, as they promote mass transfer around the catalyst surface and allow the penetration of large molecules to active sites on the surface [24]. Also, in Table 3, a decrease in micropore volume with increasing Ni content can be observed. A possible explanation for this effect could be the increased loading of nickel on the surface of carbonaceous material that can lead to pore blocking resulting in decrease of the overall pore volume of the carbonaceous materials.

The amount of Ni is relevant for the catalytic applications, but even more important is a uniform distribution of nickel particles on the

Table 1
Content of Nickel on the catalyst surface and composition of carbonaceous support.

	Ni (wt. %)	C (wt. %)	H (wt. %)	N (wt. %)	O* (wt. %)	ash (wt.%)
Ni-C1	7.5	85.5	1.4	0.6	2.6	2.4
Ni-C2	13.2	80.2	1.3	0.6	2.4	2.3
Ni-C3	32.3	62.6	1.0	0.5	1.9	1.7
Ni-C4	37.9	57.4	0.9	0.4	1.7	1.7
Ni-C5	63.7	33.5	0.5	0.3	1.0	1

* oxygen was calculated to 100%

Table 2
Size of Nickel crystallite on the catalyst surface.

Sample	Crystallite size (nm)
Ni-C1	33.8
Ni-C2	39.1
Ni-C3	54.0
Ni-C4	60.3
Ni-C5	94.9

Table 3
BET analysis of parent carbonaceous material and Ni-C catalysts.

	S_{BET}($m^2\ g^{-1}$)	S_{meso}($m^2\ g^{-1}$)	V_{micro}(cm^3liq g^{-1})	V_{net}(cm^3liq g^{-1})
CM	334	133	0.099	0.192
Ni-C1	123	89	0.038	0.184
Ni-C2	118	85	0.025	0.178
Ni-C3	89	73	0.018	0.149
Ni-C4	80	46	0.018	0.110
Ni-C5	25	18	0.004	0.037

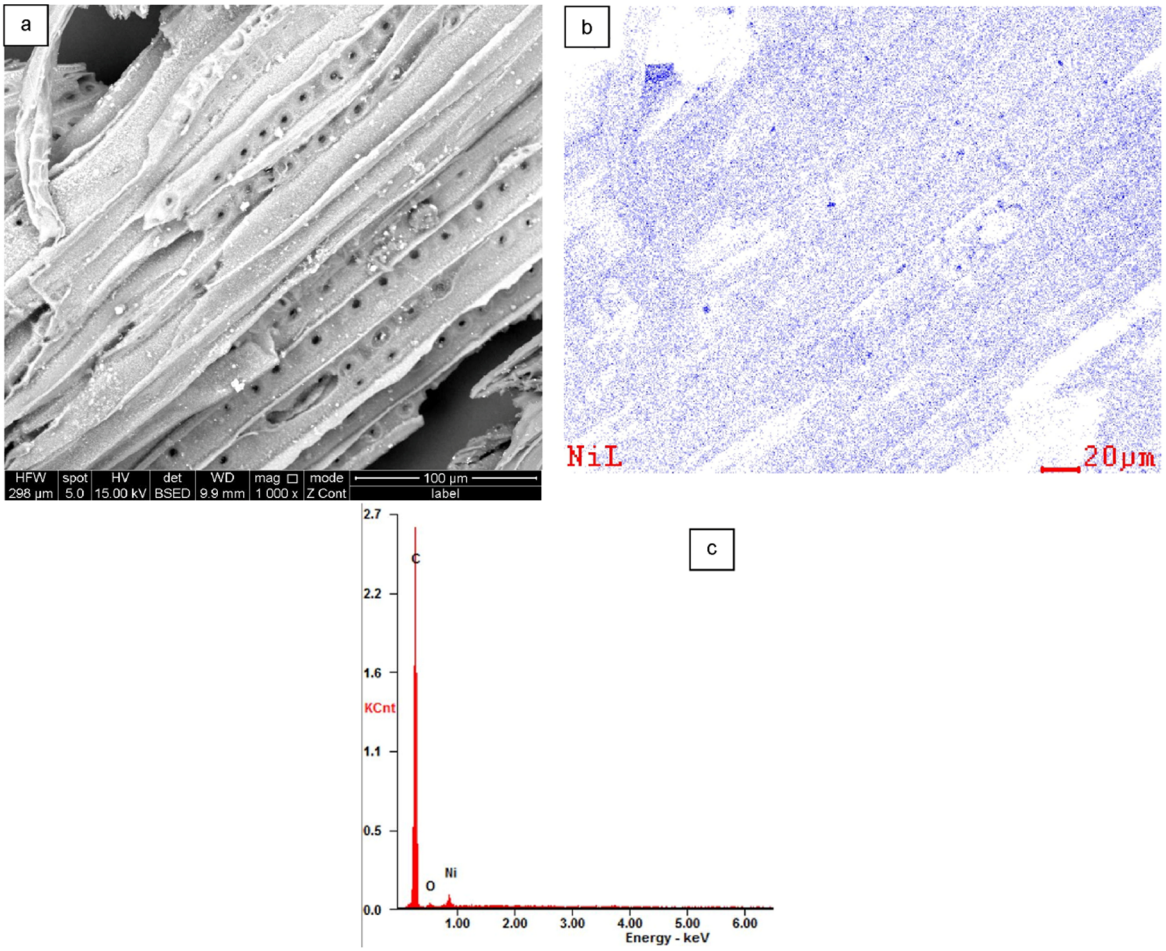

Fig. 4. (a) SEM image of Ni-C2 surface with (b) EDX distribution maps of Nickel and (c) distribution of element on the surface.

support surface. Therefore, the synthesized catalysts were analysed using SEM and EDX to determinate the surface distribution of Ni particles. The results obtained for Ni-C2 sample are shown in Fig. 4. From the figure, it can be seen that Ni particles were well distributed on the surface. However, few large white spots were also visible, indicating the presence of some Ni clusters. Furthermore, the presence of C and O on the surface was observed, which corresponds to the results of elemental analysis as shown in Table 1.

The carbonaceous support in Ni/carbonaceous catalyst system showed a very interesting structure and morphology. In Fig. 5, SEM image of a catalyst particle from the sample Ni-C2 is shown. A highly porous monolithic or honeycomb-like structure can be seen. During the microwave pyrolysis, the removal of volatile organic matter from the saw dust particles led to a porous structure with straight channels. As discussed above, catalytic materials with such a porous structure are good candidates for the reactions which involve large molecules and/or suffer from high mass transfer limitations. On the other side, higher nickel content (Ni-C5) covered the honeycomb-like structure of the carbonaceous catalyst (see Fig. A1) that led to lower conversion as compared to the sample Ni-C2.

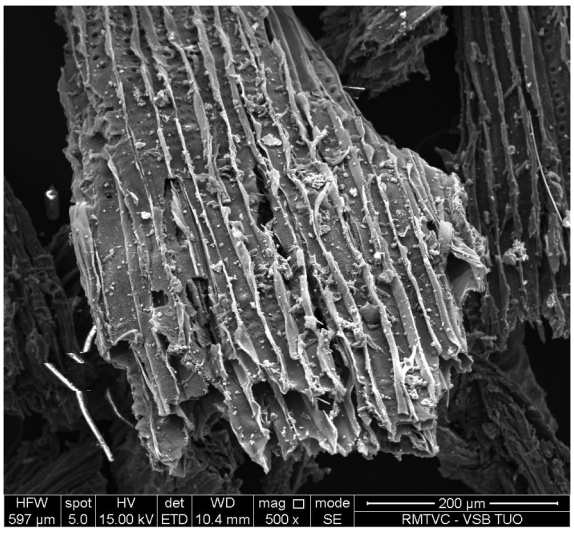

Fig. 5. SEM image of fresh Ni-C2 catalyst.

3.2. Dry reforming reaction

All samples of synthesized catalysts were tested in dry reforming of methane. The experiments were performed at 800 °C, which is considered to be an appropriate temperature for dry reforming [2]. As at this temperature, the side reactions, such as reverse water–gas shift reactions, are thermodynamically suppressed. Each experiment was carried out for 6 h of time-on-stream and average values of methane and carbon dioxide conversions thus obtained are listed in Table 4.

Based on these results, among five samples, the Ni-C2 (with approx. 13 wt% of Ni) was identified as the most active catalyst which allowed for the highest CH_4 and CO_2 conversion in comparison with others. The composition of the gaseous mixture (CH_4, CO_2, H_2 and CO) as a function of time-on-stream for dry reforming using Ni-C2 is given in Fig. 6.

The results show that during first 60 min, considering the CH_4

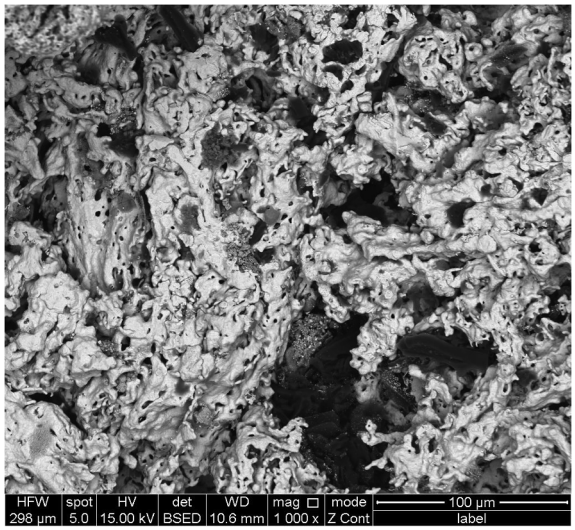

Fig. A1. SEM image of the fresh Ni-C5.

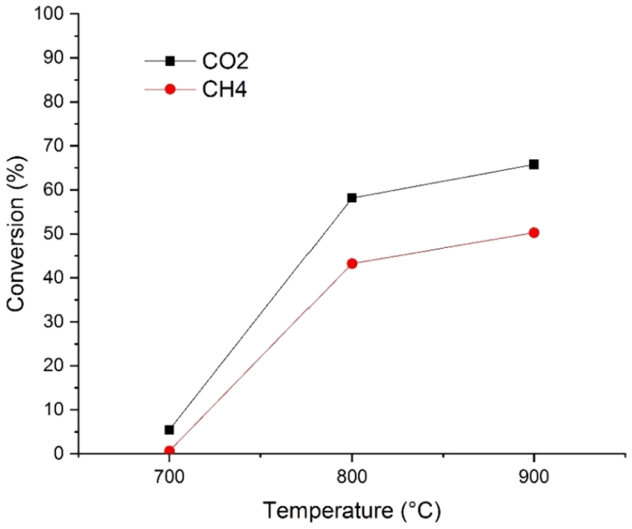

Fig. 7. Conversion of CH_4 and CO_2 on Ni-C2 catalyst at different temperatures.

Table 4
Average conversion of methane and carbon dioxide and average reaction products during 6 h experiment at 800 °C.

Catalyst	Conversion (%)		Reaction products (vol.%)	
	CH_4	CO_2	H_2	CO
Ni-C1	23*	57*	15.0*	38.8*
Ni-C2	43	58	26.6	40.0
Ni-C3	26	41	20.1	29.4
Ni-C4	23	38	18.8	29.6
Ni-C5	18	38	13.7	29.7

* Experiment with Ni-C1 was stopped after 2 h due to decrease in methane conversion from 56% to almost zero.

conversion, a lower H_2 content was obtained. On the other hand, increase in CO content was according to the decrease in CO_2. This can be attributed to the reduction of remaining NiO on the catalyst surface that used some of the hydrogen produced during this time period. It is worth noting that for the next approximately 3 h, the contents of H_2 and CO remained almost constant, thus indicating very little or no deactivation of the catalyst. Only during the last 60 min, a slight decrease in methane and carbon dioxide conversions was observed. Also, from 240 to 300 min, the amount of CO decreased but H_2 content remained stable.

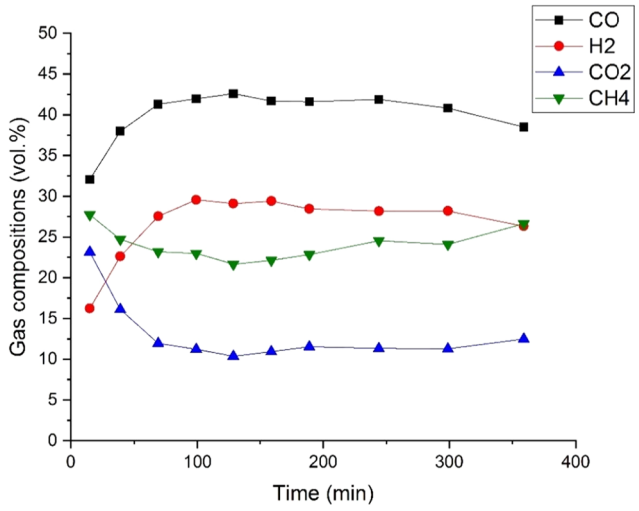

Fig. 6. Gas composition produced on Ni-C2 catalyst at 800 °C.

This indicates that during this period of time, hydrogen produced could leave the catalyst surface; however, the carbon atom remained on the catalyst surface and did not take part in the reaction for CO production. According to the literature [25], this fact is related with the formation of carbon deposits on Nickel surface.

Furthermore, in Table 4 it can be seen the conversion of both CH_4, and CO_2 decreased as the Ni content exceeded 14 wt%. This is probably due to a lower global surface of Ni content due to the formation of larger clusters. This is also clear in the case of Ni-C1 with lower Ni content (hence higher surface area due to less Ni clusters) gives higher conversion i.e. 56% of CH_4 and 78% of CO_2. However, this was only for a short period of time of approximately 1 h. After that the conversion was dropped dramatically almost to zero. This may be ascribed to the fact that the higher initial methane conversion produced high amount of active carbon species (Eq. (2)) that did not to react with CO_2 (Eq. 3–4) and deposited on the catalyst surface, thus clogging the active centres and leading to a rapid deactivation of the catalyst.

The influence of the reaction temperature on the catalytic performance of Ni-C2 was also studied. For this purpose, catalytic test at 700, 800 and 900 °C were carried out and the results obtained are presented in Fig. 7. From the results it seems that the highest conversions of CH_4 (50%) and CO_2 (66%) were achieved at 900 °C. However, increasing the conversion of 7% over a temperature increase of 100 °C is not very energetic. On the opposite, the dry reforming reaction did not occur at 700 °C, they were probably suppressed by the water gas-shift reaction or other reaction. The higher reaction temperature e.g. 1000 °C was not used, because the high energy intensity (at such high temperatures) brings only a small increase in conversion. Li et al. [26] performed dry reforming on Fe rich biomass derived char and conversion at 800 °C was around 90%, but only for 120 min., after that the conversion was drastically decreased. But these high conversions were probably connected with 10 times lower gas hourly space velocity (GHSV) in the reactor as compared to the present studies. Fidalgo et al. [18] used a carbon-supported nickel catalysts and conversion was a little higher as compared to the present study, but again in this case the GHSV significantly lower. Izhab et al. [27] studied dry reforming at low temperatures around 650–750 °C, their conversion was a little higher (approximately 11–17%) at the half of GHSV as compared to the present study. Based on these comparisons with the literature studies that used carbonaceous support, Ni-C2 catalysts seems to be quite competitive.

During all experiments, the CO_2 conversion was higher than that of CH_4. This fact has been reported by other authors too [28,29]. It is mainly explained on the basis of basic centres present on the catalyst

Table 5
Main products formed in the upgrading of biomass/cellulose pyrolysis vapours.

Feedstock/Catalyst	Yield (mmol g^{-1})			
	H_2	CO	CH_4	CO_2
cellulose	1.3	1.2	0.9	6.2
spruce sawdust	1.2	0.9	1.2	6.3
cellulose/Ni-C2	17.1	3.1	1.1	11.9
spruce sawdust/Ni-C2	14.1	2.6	1.3	10.2
cellulose/20%Ni/ZrO_2 [36]	11.2	4.4	1.5	5.0
cellulose/10% $NiCo_2$/SBA-15[38]	13.4	16.6	2.1	12.4

surface, where adsorption of CO_2 takes place faster than that of CH_4. Excess CO_2 at active sites could participate in reactions such as the reverse-Boudouard and reverse-water gas shift, consequently higher CO_2 conversion is achieved, and higher amount of CO is produced.

Please note that the conversions of CH_4 and CO_2 in the present study are smaller as compared to the ones on Ni-based catalysts reported in literatures [10,30–33]. This is may be attributed to bigger Ni crystallite size on the support surface (approximately from 30 to 90 nm) compared to the literature studies (approximately from 8 to 30 nm)[29]. However, the main advantage of the Ni/carbonaceous catalyst system presented in the present study is its enhanced stability towards deactivation. Furthermore, it benefits from naturally occurring material for its synthesis. To synthesized Ni/carbonaceous catalyst with smaller Ni particle and high Ni content, additional work will be performed in the future.

3.3. Catalytic upgrading of vapours from biomass pyrolysis

The composition of gaseous products formed in non-catalytic and catalytic pyrolysis of biomass (spruce sawdust) and cellulose is presented in Table 5. The efficiency of thermal conversion of both types of the feedstock was low and allowed for production of similar amounts of hydrogen (1.3 and 1.2 mmol g^{-1} in the case of cellulose and spruce sawdust, respectively). However, the application of Ni-C2 catalyst (which was the most active in dry reforming reaction) resulted in considerable (more than 10 times) increase in H_2 content in comparison to non-catalytic process (17.1 and 14.1 mmol g^{-1} in the case of cellulose and spruce sawdust, respectively). Simultaneously, carbon dioxide and carbon oxide yields increased 2–3 times, while CH_4 content remained on the same level.

The obtained results indicate that the presence of Ni allows for the production of higher amount of gaseous compounds, which is connected with facilitation of the cleavage of C–C and C-O bonds present in the liquid products of lignocellulosic feedstock decomposition by pyrolysis (i.e. alcohols, phenols, creosols, organic acids). The molecules of hydrocarbons with oxygen derivatives can be easier converted into permanent gas such as H_2, CO, CO_2 and CH_4 [34]. An increase in the hydrogen yield in the case of catalytic process results also from contribution of both steam reforming and water–gas shift reaction, which can proceed in the presence of water molecules formed in the first step of thermal decomposition of biomass [35].

It is worth to mention that an application of Ni/carbonaceous material catalyst allowed to obtain higher hydrogen yield than that observed in the case of the use of Ni supported on a commercial silica, alumina, ceria, Ni/$CaAlO_x$ or even bimetallic Ni-Co/SBA-15 [36–38].

4. Summary and conclusion

Supported Ni based catalysts were synthesized by using naturally occurring material (raw spruce sawdust) used as precursor for carbonaceous support. Wet impregnation of sawdust with nickel nitrate followed by microwave pyrolysis resulted in Ni/carbonaceous materials that were used as catalyst. During microwave pyrolysis the removal of organic vapours from sawdust led to a honeycomb-like structure of carbonaceous support material in Ni/carbonaceous catalyst system. Thus, adding an advantageous feature to the catalyst that can improve its performance in applications that involve large molecules and/or suffer from mass transfer limitation.

The synthesized catalysts were employed in dry reforming of methane as well as in catalytic upgrading of vapours from pyrolysis of biomass. It was demonstrated that the catalyst sample with 13.4 wt% Ni showed good catalytic activity in dry reforming of CH_4, giving average conversions of 43 and 58% for CH_4 and CO_2, respectively.

Furthermore, it exhibited good resistance towards deactivation by showing only a slight decrease in conversion after 6 h of time-on-stream. It was shown that the use of catalyst in upgrading of vapours derived from biomass pyrolysis allowed for considerable increase in H_2 content in the mixture of gaseous products in comparison to non-catalytic process.

CRediT authorship contribution statement

P. Lestinsky: Conceptualization, Supervision, Writing - original draft, Writing - review & editing. **Z. Zikmund:** Investigation, Validation. **B. Grycova:** Resources, Investigation. **R. Ryczkowski:** Investigation, Validation. **J. Grams:** Supervision, Writing - original draft. **A. Inayat:** Writing - review & editing.

Declaration of Competing Interest

The authors declare that they have no known competing financial interests or personal relationships that could have appeared to influence the work reported in this paper.

Acknowledgements

The work was supported from ERDF “Institute of Environmental Technology – Excellent Research” (No. CZ.02.1.01/0.0/0.0/16_019/0000853) and Student grant projects SP2019/91. Experimental results were accomplished by using Large Research Infrastructure ENREGAT supported by the Ministry of Education, Youth and Sports of the Czech Republic under project No. LM2018098.

References

[1] Guil-Lopez R, Botas JA, Fierro JLG, Serrano DP. Comparison of metal and carbon catalysts for hydrogen production by methane decomposition. Applied Catalysis a-General 2011;396(1–2):40–51.
[2] Usman M, Daud W, Abbas HF. Dry reforming of methane: Influence of process parameters-A review. Renew Sustain Energy Rev 2015;45:710–44.
[3] Bermudez JM, Fidalgo B, Arenillas A, Menendez JA. Dry reforming of coke oven gases over activated carbon to produce syngas for methanol synthesis. Fuel 2010;89(10):2897–902.
[4] Akri M, Chafik T, Granger P, Ayrault P, Batiot-Dupeyrat C. Novel nickel promoted illite clay based catalyst for autothermal dry reforming of methane. Fuel 2016;178:139–47.
[5] Qian K, Kumar A. Catalytic reforming of toluene and naphthalene (model tar) by char supported nickel catalyst. Fuel 2017;187:128–36.
[6] Tribalis A, Panagiotou GD, Bourikas K, Sygellou L, Kennou S, Ladas S, et al. Ni Catalysts Supported on Modified Alumina for Diesel Steam Reforming. Catalysts 2016;6(1).
[7] Djinovic P, Pintar A. Stable and selective syngas production from dry CH4-CO2 streams over supported bimetallic transition metal catalysts. Appl Catal B-Environ 2017;206:675–82.
[8] Courson C, Makaga E, Petit C, Kiennemann A. Development of Ni catalysts for gas production from biomass gasification. Reactivity in steam- and dry-reforming. Catal Today 2000;63(2–4):427–37.
[9] Haydary J, Susa D, Dudas J. Pyrolysis of aseptic packages (tetrapak) in a laboratory screw type reactor and secondary thermal/catalytic tar decomposition. Waste Manage 2013;33(5):1136–41.
[10] Abdulrasheed A, Jalil AA, Gambo Y, Ibrahim M, Hambali HU, Hamill MYS. A review on catalyst development for dry reforming of methane to syngas: Recent advances. Renew Sustain Energy Rev 2019;108:175–93.
[11] Bermudez JM, Fidalgo B, Arenillas A, Menendez JA. CO2 reforming of coke oven gas over a Ni/gamma Al2O3 catalyst to produce syngas for methanol synthesis. Fuel 2012;94(1):197–203.
[12] Guo J, Lou H, Zheng X. The deposition of coke from methane on a Ni/MgAl2O4

catalyst. Carbon 2007;45(6):1314–21.
[13] Xu X, Jiang E, Wang M, Xu Y. Dry and steam reforming of biomass pyrolysis gas for rich hydrogen gas. Biomass Bioenergy 2015;78:6–16.
[14] Lestinsky P, Grycova B, Pryszcz A, Martaus A, Matejova L. Hydrogen production from microwave catalytic pyrolysis of spruce sawdust. J Anal Appl Pyrol 2017;124:175–9.
[15] Chen X, Che Q, Li S, Liu Z, Yang H, Chen Y, et al. Recent developments in lignocellulosic biomass catalytic fast pyrolysis: Strategies for the optimization of bio-oil quality and yield. Fuel Process Technol 2019;196:106180.
[16] Grams J, Ruppert AM. Development of Heterogeneous Catalysts for Thermo-Chemical Conversion of Lignocellulosic Biomass. Energies 2017;10(4).
[17] Ashik UPM, Wan Daud WMA, Abbas HF. Production of greenhouse gas free hydrogen by thermocatalytic decomposition of methane – A review. Renew Sustain Energy Rev 2015;44:221–56.
[18] Fidalgo B, Zubizarreta L, Bermudez JM, Arenillas A, Menendez JA. Synthesis of carbon-supported nickel catalysts for the dry reforming of CH4. Fuel Process Technol 2010;91(7):765–9.
[19] Zhang SP, Dong Q, Zhang L, Xiong YQ. High quality syngas production from microwave pyrolysis of rice husk with char-supported metallic catalysts. Bioresour Technol 2015;191:17–23.
[20] Gregg SJ, Sing KSW. Adsorption, surface area, and porosity. London; New York: Academic Press; 1982.
[21] Srilatha K, Viditha V, Srinivasulu D, Ramakrishna SUB, Himabindu V. Hydrogen production using thermocatalytic decomposition of methane on Ni-30/activated carbon and Ni-30/carbon black. Environ Sci Pollut Res 2016;23(10):9303–11.
[22] Xu BQ, Wei JM, Wang HY, Sun KQ, Zhu QM. Nano-MgO: novel preparation and application as support of Ni catalyst for CO2 reforming of methane. Catal Today 2001;68(1–3):217–25.
[23] Li WZ, Zhao ZK, Wang GR. Modulating morphology and textural properties of ZrO2 for supported Ni catalysts toward dry reforming of methane. AIChE J 2017;63(7):2900–15.
[24] Zhao J, Wang G, Qin L, Li H, Chen Y, Liu B. Synthesis and catalytic cracking performance of mesoporous zeolite Y. Catal Commun 2016;73:98–102.
[25] Zhang GJ, Liu JW, Xu Y, Sun YH. Ordered mesoporous Ni/Silica-carbon as an efficient and stable catalyst for CO2 reforming of methane. Int J Hydrogen Energy 2019;44(10):4809–20.
[26] Li LZ, Yan KS, Chen J, Feng T, Wang FM, Wang JW, et al. Fe-rich biomass derived char for microwave-assisted methane reforming with carbon dioxide. Sci Total Environ 2019;657:1357–67.
[27] Izhab I, Amin NAS, Asmadi M. Dry reforming of methane over oil palm shell activated carbon and ZSM-5 supported cobalt catalysts. Int J Green Energy 2017;14(10):831–8.
[28] Sato K, FujiMoto K. Development of new nickel based catalyst for tar reforming with superior resistance to sulfur poisoning and coking in biomass gasification. Catal Commun 2007;8(11):1697–701.
[29] Ayodele BV, Hossain SS, Lam SS, Osazuwa OU, Khan MR, Cheng CK. Syngas production from CO2 reforming of methane over neodymium sesquioxide supported cobalt catalyst. J Nat Gas Sci Eng 2016;34:873–85.
[30] Guo JJ, Lou H, Zhao H, Chai DF, Zheng XM. Dry reforming of methane over nickel catalysts supported on magnesium aluminate spinels. Applied Catalysis a-General 2004;273(1–2):75–82.
[31] Jang WJ, Shim JO, Kim HM, Yoo SY, Roh HS. A review on dry reforming of methane in aspect of catalytic properties. Catal Today 2019;324:15–26.
[32] Zhang G, Liu J, Xu Y, Sun Y. A review of CH4CO2 reforming to synthesis gas over Ni-based catalysts in recent years (2010–2017). Int J Hydrogen Energy 2018;43(32):15030–54.
[33] Aramouni NAK, Touma JG, Abu Tarboush B, Zeaiter J, Ahmad MN. Catalyst design for dry reforming of methane: Analysis review. Renew Sustain Energy Rev 2018;82:2570–85.
[34] Chen D, He L. Towards an Efficient Hydrogen Production from Biomass: A Review of Processes and Materials. ChemCatChem 2011;3(3):490–511.
[35] Swierczynski D, Libs S, Courson C, Kiennemann A. Steam reforming of tar from a biomass gasification process over Ni/olivine catalyst using toluene as a model compound. Appl Catal B-Environ 2007;74(3–4):211–22.
[36] Matras J, Niewiadomski M, Ruppert A, Grams J. Activity of Ni catalysts for hydrogen production via biomass pyrolysis. Kinet Catal 2012;53(5):565–9.
[37] Chen FY, Wu CF, Dong LS, Vassallo A, Williams PT, Huang J. Characteristics and catalytic properties of Ni/CaAlOx catalyst for hydrogen-enriched syngas production from pyrolysis-steam reforming of biomass sawdust. Appl Catal B-Environ 2016;183:168–75.
[38] Zhao M, Church TL, Harris AT. SBA-15 supported Ni-Co bimetallic catalysts for enhanced hydrogen production during cellulose decomposition. Appl Catal B-Environ 2011;101(3–4):522–30.

Příloha [P8]

LESTINSKY, P. & PALIT, A. 2016. Wood Pyrolysis Using Aspen Plus Simulation and Industrially Applicable Model. *GeoScience Engineering*, 62, 11-16. Bez IF. Autorský podíl 90 %. Počet citací dle Google Scholar 35.

Role uchazeče:

- návrh tématu, návrh postupu prací, modelování v AspenPlus, vyhodnocení výsledků, vyvození závěrů z dosažených výsledků

DE GRUYTER
OPEN
DOI: 10.1515/gse-2016-0003

WOOD PYROLYSIS USING ASPEN PLUS SIMULATION AND INDUSTRIALLY APPLICABLE MODEL

Pavel Lestinsky[1], Aloy Palit[1,2]
1 Institute of Environmental Technology, VSB-TU Ostrava, Czech Republic,
e-mail: pavel.lestinsky@vsb.cz
2 Department of Chemical Engineering, DCRUST, Haryana, India,
e-mail: aloy920@gmail.com

Abstract

Over the past decades, a great deal of experimental work has been carried out on the development of pyrolysis processes for wood and waste materials. Pyrolysis is an important phenomenon in thermal treatment of wood, therefore, the successful modelling of pyrolysis to predict the rate of volatile evolution is also of great importance. Pyrolysis experiments of waste spruce sawdust were carried out. During the experiment, gaseous products were analysed to determine a change in the gas composition with increasing temperature. Furthermore, the model of pyrolysis was created using Aspen Plus software. Aspects of pyrolysis are discussed with a description of how various temperatures affect the overall reaction rate and the yield of volatile components. The pyrolysis Aspen plus model was compared with the experimental data. It was discovered that the Aspen Plus model, being used by several authors, is not good enough for pyrolysis process description, but it can be used for gasification modelling.

Keywords: Pyrolysis, Spruce sawdust, Modelling, Aspen Plus

1 INTRODUCTION

Pyrolysis is a thermochemical decomposition process at elevated temperature in absence of oxygen. The pyrolysis gas contains mainly H_2, CO, CO_2, CH_4, and others light hydrocarbons such as C_2H_2, C_2H_4, C_2H_6, C_3H_6, C_3H_8. Pyrolysis of biomass yields gases, liquids (so-called bio-oils), and a carbonaceous residue (so-called bio-char). The obtained yields depend on the feedstock composition and pyrolysis conditions. There are three types of pyrolysis: fast pyrolysis with a typical maximum bio-oil yield of around 60-80 wt. % at very short residence times, convectional pyrolysis with equal yields of product at middle residence time (minutes), and as the last, slow pyrolysis with a maximum solid yield of around 60-80 wt. % at very long residence time (hours) [1]. Cellulose, hemicelluloses, and lignin are typical main compounds of wood. The amounts of these compounds are dependent on the type of wood. Water and inorganic elements are further components of wood.

The pyrolysis of wood is typically initiated at 200 °C (so-called torrefaction) and lasts till the temperature of 450-550°C is achieved, depending on the species of wood and required product [2]. Pyrolysis plays an important role in the thermal treatment of wood sawdust, since the products of this stage, namely gas and char combustion, respectively, release thermal energy. The sawdust is not combustible directly, because its particle size distribution is not suitable. Therefore, it is necessary to use the briquetting, but that is another input energy and loss of money. The next possibility is to use it as a build material in OSB tables. Recently, the market is oversaturated with sawdust and thus its use for pyrolysis can be acceptable. In order to design a sawdust treatment process, a techno-economical model can bring interesting information [3]. The primary objectives of these models are to provide a diagnostic tool for evaluating the importance of various system parameters and identify system characteristics useful for experimentalists and comparisons between them. The pyrolytic decomposition of wood involves a complex series of reactions, and consequently, changes in experimental heating conditions or sample composition, and preparation may affect not only the rate of reaction, but also the actual course of reactions. The conversions of wood materials to liquids and gaseous products were the processes of great interest in many experiments [4]. Second-generation biofuels are seen as a solution for further increasing the share of renewable energies in the transport sector while reducing the negative impacts associated with conventional biofuels. In fact, there is an important potential of lignocellulosic biomass from forest residue, agricultural waste, and energy crops which is still unused and potentially suitable for bioenergy production with low environmental impact. Maximizing the use of residual biomass is necessary in order to fulfil the targets for biofuel share and greenhouse gas emission reduction set up in the proposal for renewable energy directive. Nevertheless, converting wood and biomass into liquid fuels is not an easy task and adequate technologies are needed [5].

2 EXPERIMENTAL PART

The spruce sawdust was used as a pyrolysis material. The ultimate and proximate analyses were made based on the elemental analysis and thermogravimetric analysis. The results of the analyses are listed in Table 1.

DE GRUYTER
OPEN
DOI: 10.1515/gse-2016-0003

Table 1: Ultimate analysis and proximate analysis of spruce sawdust

Ultimate analysis	
component	wt. %
C	51.75
H	6.09
N	0.96
O*	40.60

Proximate analysis	
component	wt. %
Moisture	17.30
Volatiles	77.51
Fixed C	21.89
Ash	0.60

* oxygen was calculated to 100 wt. %

A stainless steel reactor was used for thermal treatment of the waste spruce sawdust. The schema of the experimental apparatus is shown in Figure 1. The sawdust sample, 100 g in weight, was used as FEED in the reactor which was heated at a heating rate of 5 °C/min, and samples of gases were collected between 20 °C and 800 °C at an interval of approximately of 50 °C. The liquid phase is collected in the cylindrical container in the middle of the equipment and a continuous flow of cold water is passed through to maintain the heating effect of the equipment. Acetone and Water are used as absorbents of volatile products, which were not collected in the container after the cooler. While the gas is passing through these samples, the colour of the absorbent changes with a change in the composition of gases. The solid residue remained in the reactor (stainless retort) and was removed and weighed after cooling the reactor to laboratory temperature.

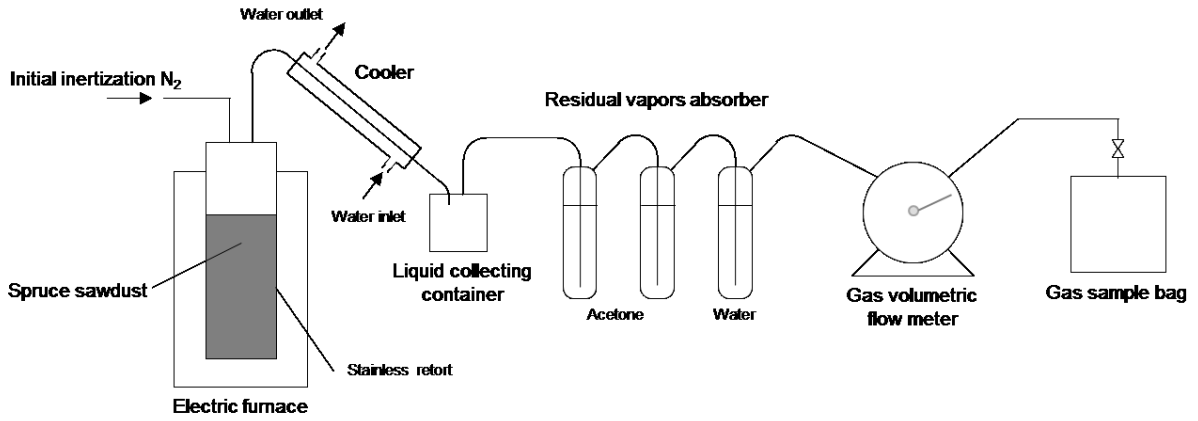

Figure 1: Flow sheet of Experimental Setup

The samples of gases were collected in the Tedlar bags and analysed on chromatography to find the composition of CH_4, CO, H_2, and CO_2. The compositions of gas samples were determined by the gas Chromatography Agilent 7890A with a flame ionization detector and a thermal conductivity detector. A Micropacked column (2 m x 0.53 mm) was used in the chromatograph to separate gaseous components. The result of all the sampling is elaborated in the graphs below (Figures 2 and 3). The gas composition was measured at different intervals of temperatures. The liquid and solid products were weighed, and the mass balance of pyrolysis was created.

DE GRUYTER
OPEN
DOI: 10.1515/gse-2016-0003

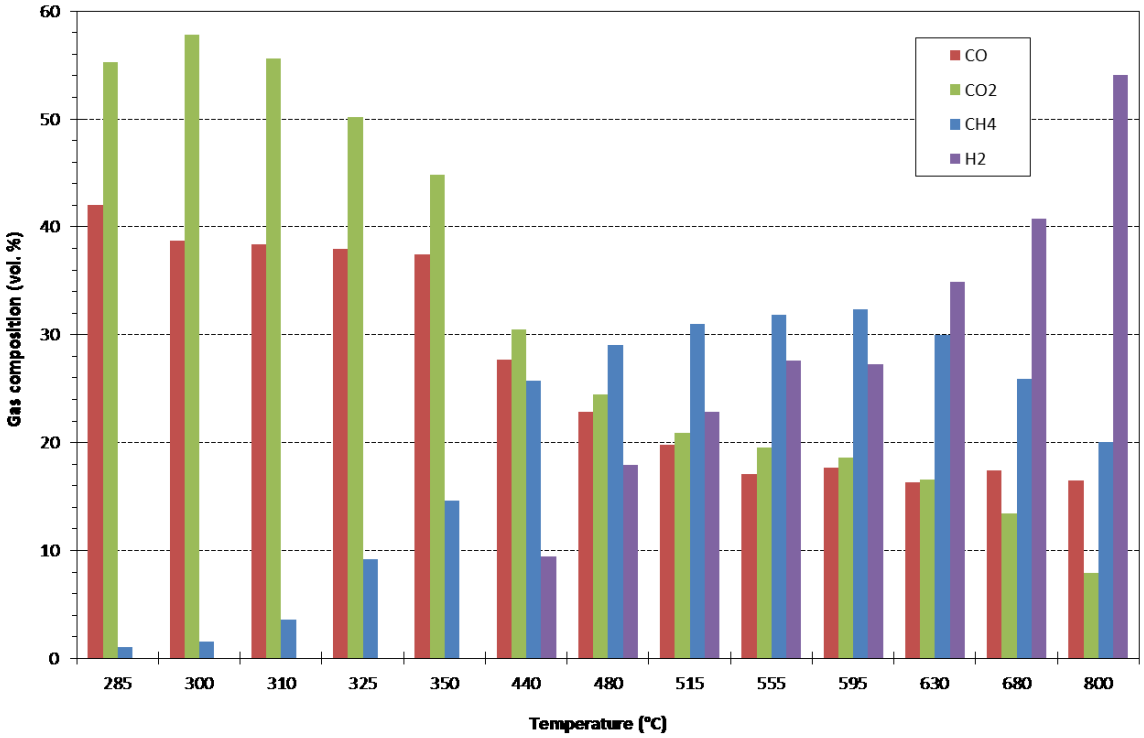

Figure 2: Change in gas composition (CO, CO_2, CH_4, and H_2) during pyrolysis

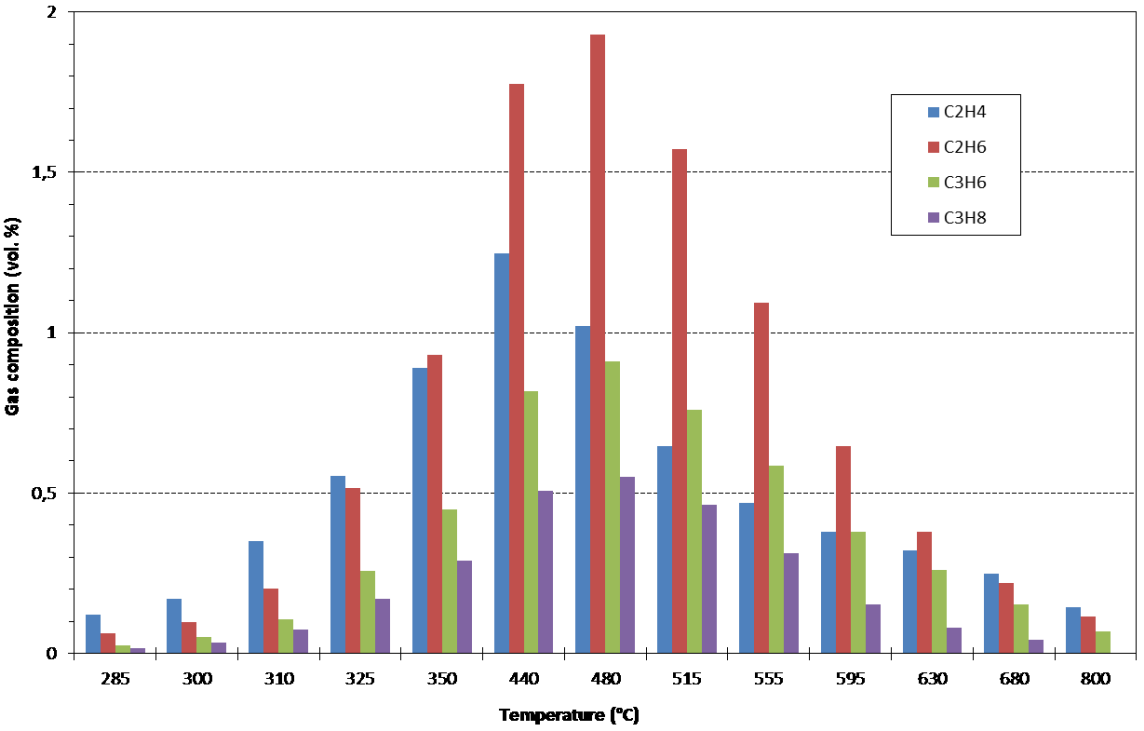

Figure 3: Change in gas composition (light hydrocarbons) during pyrolysis

3 SIMULATION OF PYROLISIS

This work presents a model of a pyrolysis reactor based on an equilibrium model approach implemented in Aspen Plus®. Unlike other works, which implement the pyrolysis reactor as a black box unit giving an a priori defined pyrolysis product composition, the use of an equilibrium approach permits a really predictive simulation, which estimates yields and compositions of pyrolysis products depending on reactor conditions. Aspen Plus® has advanced and dedicated functionalities, such as detailed heat exchanger design, dynamic simulation, batch and reactor process modelling. It also provides the option to use an equation-based approach in some of its routines,

DE GRUYTER
OPEN
DOI: 10.1515/gse-2016-0003

which permits convenient use of design. External FORTRAN files are used in the Aspen Plus® user subroutine for the description of complex mechanisms. Property methods: PENG-ROB is used as a base property method for the whole system. Spruce sawdust and char components were defined as non-conventional components based on their ultimate analysis including C, H, O, N, S; Cl and Ash elements, and proximate analysis (see Table 1). The syngas production from the spruce sawdust was done at temperatures in a range of 300-800 °C and atmospheric pressure (101325 Pa) was used.

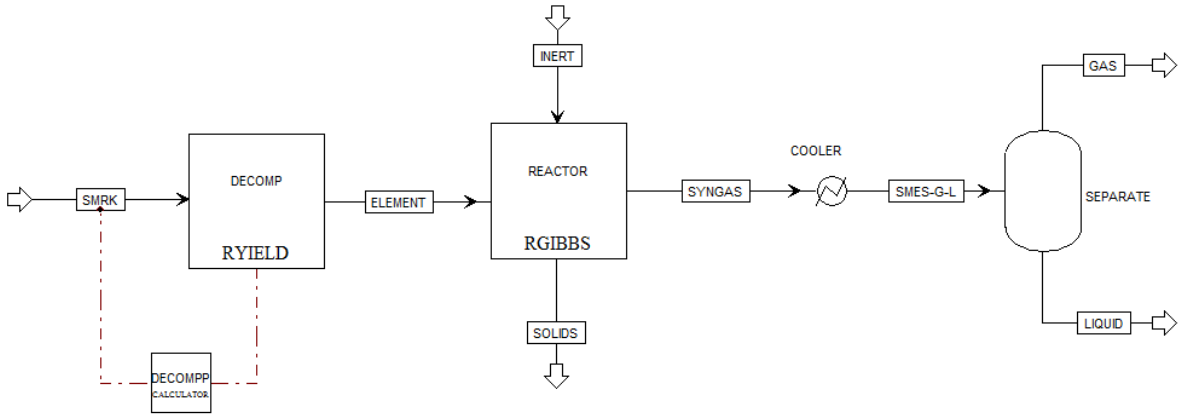

Figure 4: Flowsheet of decomposition and pyrolysis of spruce wood

The flowsheet of syngas production is shown in Figure 4. The spruce wood was decomposed in the RYIELD reactor (a reactor where stoichiometry and kinetics are unknown parameters) to the elements by the ultimate analysis. These elements passed to the RGIBBS reactor (a reactor with a phase equilibrium or simultaneous phase, and a chemical equilibrium in vapour-liquid-solid systems) where syngas was created by thermodynamics equilibrium for a given temperature and pressure. The solid residue was divided in the RGIBBS reactor. The vapour mixture was cooled to 20 °C by a cooler and divided in a separator (FLASH2) to gases and liquid (represented by water only). The gas composition produced by pyrolysis was important as those gases are created from elements by the thermodynamic equilibrium at given temperature and pressure.

4 RESULTS

The yields of pyrolysis products (gas, liquid, and solid) are shown in Figure 5. The amount of solid residue was around 25 wt. % at 600 °C, and relates to the content of fixed carbon. At higher temperatures, the water gas shift reaction started, carbon monoxide and hydrogen were created, and the amount of carbon began to decrease. This part significantly differs from the experimental one. Water was evaporated below 200 °C and collected after the cooler in a condensate container, so it could not react with carbon in the reactor at higher temperature. The amount of gas product increased with increasing temperature, which was observed by many authors [6, 7]. The gas composition of pyrolysis product is shown in Figure 6. The concentration of CO and H_2 increased with increasing temperature. The increases in the CO, H_2 content relate to the decreasing concentrations of CO_2, H_2O, and CH_4. The concentrations of light hydrocarbons were in a range on 400-500 °C, after that, light hydrocarbons were decomposing, which resulted in increases of H_2 concentrations. On the other hand, a half of the volume of produced gas was created below 400 °C that means without H_2.

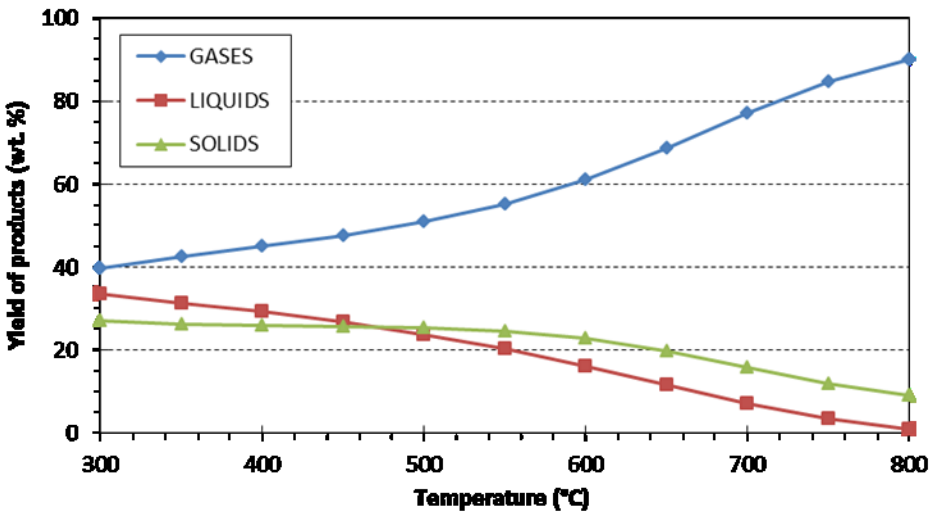

Figure 5: Yields of products from simulation of spruce sawdust pyrolysis

DE GRUYTER
OPEN
DOI: 10.1515/gse-2016-0003

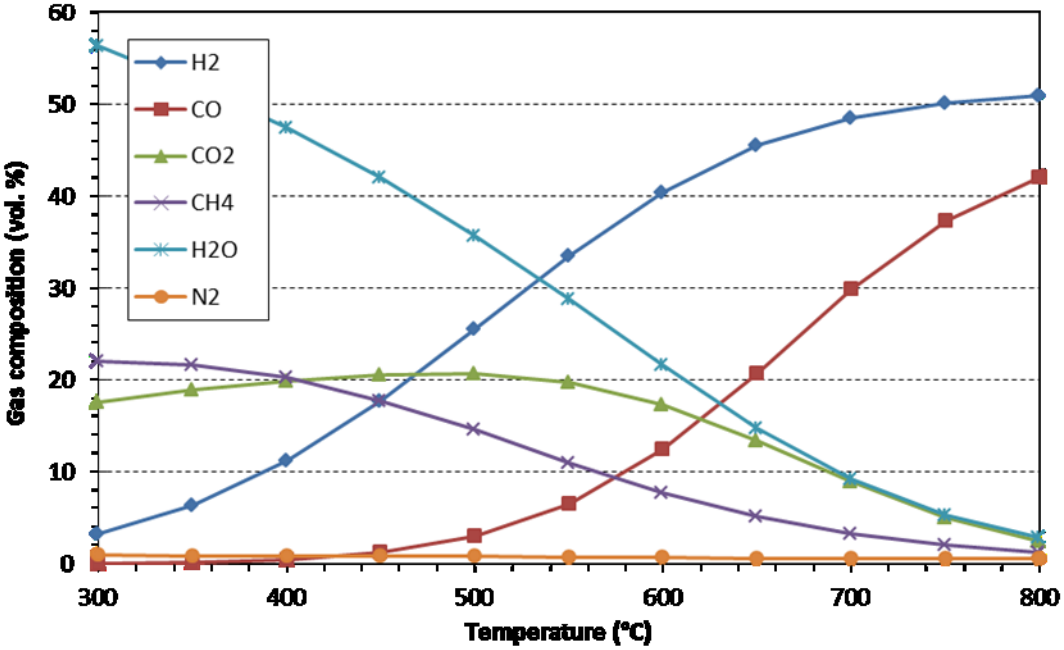

Figure 6: Gas compositions from simulation of spruce sawdust pyrolysis

This increasing content of CO, H_2 had a huge effect on the low heating value of the produced syngas (shown in Figure 7). When multiplying the low heating value and the volume of produced syngas, we will get the energetic potential of produced syngas related to 1 kg feed of spruce sawdust; it is more energy than in the raw wood (approximately 14 MJ/kg). The heating value of solid residue was not calculated, because the biochar is better to use as bio-fertilizer then the solid fuel.

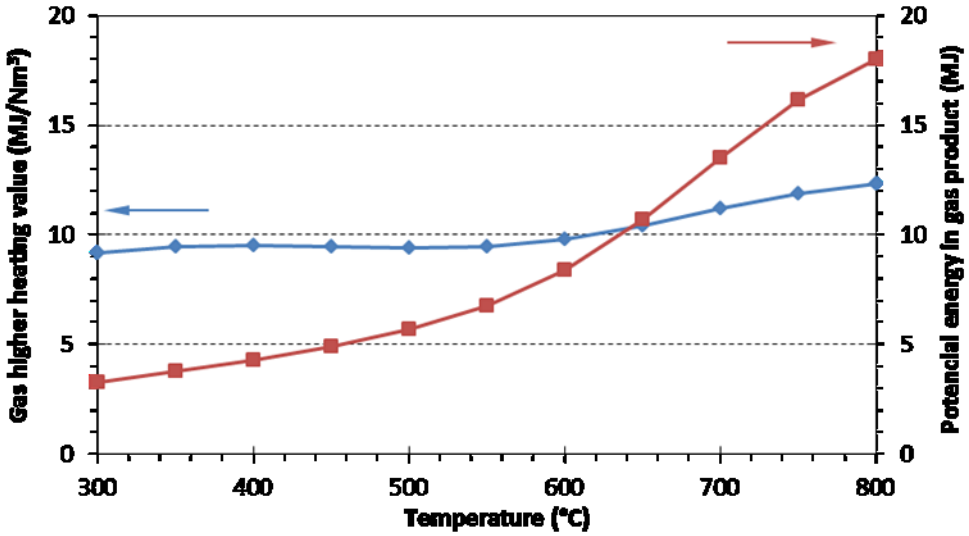

Figure 7: Gas lower heating value and total amount of energy in produced syngas

5 CONCLUSION

The process of spruce sawdust pyrolysis in the laboratory was compared with the model created in the AspenPlus software. Figures 2, 3 and Figure 5 show great differences between the aspen plus model and experiments. It is obvious that the modelling through the decomposition and subsequent formation of gas based on the thermodynamics equilibrium is not appropriate for the modelling of pyrolysis process. There are articles where authors [8] used only a model without comparative experiments, and those results are misleading. The industrial application of the spruce sawdust pyrolysis model can be used, but only for the gasification process, not for the pyrolysis process. The pyrolysis model must contain a chemical reaction of individual wood compounds (cellulose, hemicellulose, and lignin) which is highly dependent on temperature and chemical composition of ash (catalytic effect). One of pyrolysis products is a liquid condensate, which contains hundred organic oxygenate compounds (phenol, cresols, organic acids, etc.), and creating these products is impossible to model without knowledge of chemical reactions kinetics.

DOI: 10.1515/gse-2016-0003

Aspen Plus is a suitable tool for creating a techno-economic performance analysis of the pyrolysis or gasification processes [9, 10]. However, it is necessary to create a suitable model, which will reflect the experimental conditions, duration and progress of process.

ACKNOWLEDGEMENT

This work was financially supported by the Ministry of Education, Youth and Sports of the Czech Republic in the "National Feasibility Program I", project No. LO1208 "Theoretical Aspects of Energetic Treatment of Waste and Environment Protection against Negative Impacts", and by the EU structural funding Operational Programme Research and Development for Innovation, project No. CZ.1.05/2.1.00/19.0388.

REFERENCES

[1] Yang S. I., Wu M. S., Wu C. Y. Application of biomass fast pyrolysis part I: Pyrolysis characteristics and products. *Energy*. 2014, 66, 162-171.

[2] Strandberg M., Olofsson I., Pommer L., Wiklund-Lindström S., Åberg K., Nordin A. Effects of temperature and residence time on continuous torrefaction of spruce wood. *Fuel Processing Technology*. 2015, **134**, 387-398.

[3] Zhang Y., Brown T. R., Hu G., Brown R.C. Techno-economic analysis of two bio-oil upgrading pathways. *Chemical Engineering Journal*. 2013, **225**, 895-904.

[4] Yaman S. Pyrolysis of biomass to produce fuels and chemical feedstocks. *Energy Conversion and Management*. 2004, **45**(5), 651-671.

[5] Tanneru S.K., Steele P.H. Direct hydrocracking of oxidized bio-oil to hydrocarbons. *Fuel*. 2015, **154**, 268-274.

[6] Calonaci M., Grana R., Barker H. E., Bozzano G., Dente M., Ranzi E. Comprehensive Kinetic Modelling Study of Bio-oil Formation from Fast Pyrolysis of Biomass. *Energy & Fuels*. 2010, **24**(10), 5727-5734.

[7] Xianjun X., Zongkang S., Peiyong M., Jin Y., Zhaobin W. Establishment of Three Components of Biomass Pyrolysis Yield Model. *Energy Procedia*. 2015, **66**, 293-396.

[8] Visconti A., Miccio M., Juchelkova D. Equilibrium-based simulation of lignocellulosic biomass pyrolysis via Aspen Plus. In: *Recent Advances in Applied Mathematics, Modelling and Simulation*: Proceedings of the 8th International Conference on Applied Mathematics, Simulation, Modelling: November 22-24, 2014, Florence, Italy. WSEAS Press, 2014, 242-252. ISBN: 978-960-474-398-8.

[9] Shemfe M.B., Gu S., Ranganathan P. Techno-economic performance analysis of biofuel production and miniature electric power generation from biomass fast pyrolysis and bio-oil upgrading. *Fuel*. 2015, **143**, 361-372.

[10] Fan Y., Yi Q., Li F., Yi L., Li W. Tech-economic assessment of a coproduction system integrated with lignite pyrolysis and Fischer–Tropsch synthesis to produce liquid fuels and electricity. *Fuel Processing Technology*. 2015, **135**, 180-186.